# Structure and Physiological Function of the Vacuolar Anion Channel ALMT9 in *Arabidopsis thaliana* and *Vitis Vinifera*

## Dissertation

zur

Erlangung der naturwissenschaftlichen Doktorwürde

(Dr. sc. nat.)

vorgelegt der

Mathematisch-naturwissenschaftlichen Fakultät

der

Universität Zürich

von

**Ulrike Bätz**

aus Deutschland

**Promotionskomitee**

Prof. Dr. Enrico Martinoia (Leitung der Dissertation)

Prof. Dr. Beat Keller

Dr. Alexis De Angeli

Dr. Cornelia Eisenach

**Zürich, 2016**

# Table of Contents

# Summary

The vacuolar function in plants is diverse, and so is the physiological role of transporters and channels at the vacuolar membrane that catalyze the uptake or release of solutes. One member of the *Arabidopsis thaliana* Aluminum-activated Malate Transporter (AtALMT) family, AtALMT9, has been previously demonstrated to be localized at the vacuolar membrane, the tonoplast. *AtALMT9* encodes a channel protein that is capable of mediating malate and $Cl^-$ inward rectifying currents corresponding to an uptake of these anions into the vacuole.

In this thesis ALMT9 proteins of Arabidopsis and *Vitis Vinifera* are characterized at the molecular, structural and functional level. In the first chapter a large-scale mutagenesis is presented that aimed at determining the structure-function relations in AtALMT9. Using the patch-clamp technique the putative conduction pathway as well as residues that are crucial for AtALMT9 structure, functionality and regulation were identified. Moreover, citrate was found to act as an open channel blocker of AtALMT9, and a point-mutated channel in which this inhibition is abolished was characterized. The differences in inhibition sensitivity of the channel variants were used to provide evidence that AtALMT9 is composed of several subunits. In chapter II, it is additionally demonstrated that other AtALMT channels are also localized to the tonoplast, and are capable of forming heteromeric channel complexes with AtALMT9. Chapter III deals with the physiological relevance of AtALMT9-mediated vacuolar $Cl^-$ uptake during salinity. It is shown that the capacity of vacuolar ion uptake affects whole-plant accumulation and distribution of $Na^+$ and $Cl^-$. Genetic and physiological approaches as well as expression analyses suggested that these differences in $Na^+$ and $Cl^-$ contents during salinity are based on altered transcript levels of plasma-membrane localized transport proteins in the vasculature of *atalmt9* mutant plants. In chapter IV, it is shown that AtALMT9 has a physiological function in seed germination in particular under salt stress. It is demonstrated that AtALMT9 is highly expressed in seeds, and that knock-out mutant seeds lacking the channel are more sensitive to the application of high NaCl concentrations. Finally, it is shown in Chapter V that a homolog of AtALMT9 is

expressed in fruits of *Vitis vinifera* throughout ripening and maturation. VvALMT9 is targeted to the tonoplast and mediates malate fluxes into grape berry vacuoles. In addition, VvALMT9 is shown to catalyze significant tartrate uptake, an organic acid that is highly accumulated in grape berries.

In summary, in this thesis I present novel insights into the structural and compositional organization of AtALMT channels, the physiological role of AtALMT9-mediated vacuolar ion uptake under salinity and during seed germination, and the function of VvALMT9 in berries of *Vitis vinifera*. The multiple cellular and physiological processes in which ALMT9 channels are shown to be involved demonstrate the necessity of anion and osmotic homeostasis in plant cells.

# Zusammenfassung

Die Funktion der Vakuole in Pflanzen ist facettenreich, und daher ist auch die physiologische Rolle von Transportern und Kanälen welche die Aufnahme oder die Abgabe von Substraten über die vakuoläre Membrane katalysieren verschieden. Ein Mitglied von der Aluminium-aktivierten Malat Transporter (ALMT) Protein Familie in *Arabidopsis thaliana*, AtALMT9, ist in der vakuolären Membran, dem Tonoplast, lokalisiert. Es wurde zuvor gezeigt, dass AtALMT9 ein spannungsabhängiger einwärts gleichrichtender Kanal ist, welcher die Aufnahme von Malat und $Cl^-$ in die Vakuole katalysiert.

In dieser Dissertation werden ALMT9 Homologe von *Arabidopsis thaliana* und *Vitis Vinifera* auf der molekularen, strukturellen und funktionalen Ebene charakterisiert. Im ersten Kapitel wird eine umfassende Mutagenese beschrieben, in welcher die Beziehungen zwischen Struktur und Funktionalität von AtALMT Kanälen untersucht werden. Mit Hilfe der Patch-Clamp-Technik wurden die potenzielle zentrale Pore des Kanals sowie Aminosäure Reste identifiziert, die für die Struktur, die Funktionalität und die Regulation des Kanals wichtig sind. Ausserdem wurde aufgezeigt, dass Citrat den AtALMT9 Kanal blockiert, und es wird ein mutierter Kanal identifiziert, welcher nicht mehr von Citrat inhibiert werden kann. Die Unterschiede in der Sensitivität zu Citrate wurden ausgenutzt um zu zeigen, dass AtALMT9 aus mehreren Untereinheiten besteht. In Kapitel II wird zudem gezeigt, dass weitere AtALMT Kanäle im Tonoplast lokalisiert sind, und dass diese Kanäle mit AtALMT9 heteromere Kanalkomplexe formen können. Das dritte Kapitel handelt von der physiologischen Relevanz von $Cl^-$ Strömen durch AtALMT9 während die Pflanze einem Salzstress ausgesetzt ist. Es wird gezeigt, dass die Kapazität der vakuolären Ionenaufnahme die Akkumulation und Verteilung von $Na^+$ und $Cl^-$ in der kompletten Pflanze beeinflusst. Genetische und physiologische Methoden sowie Expressionsanalysen haben Ausschluss darüber gegeben, dass die unterschiedlichen $Na^+$ und $Cl^-$ Gehalte während des Salzstresses vermutlich auf Unterschiede in der Transkription von Transportern in der Plasmamembran im vaskulären System von *atalmt9* Mutanten zurückzuführen sind. Im

vierten Kapitel wird gezeigt, dass AtALMT9 eine physiologische Funktion während der Samenkeimung insbesondere unter Salzstress aufweist. Es wird gezeigt, dass AtALMT9 in Samen exprimiert ist, und dass mutierte Samen, in welchen der Kanal fehlt, sensitiver auf hohe externe NaCl Konzentrationen reagieren. Abschliessend wird in Kapitel V gezeigt, dass ein Homolog von AtALMT9 auch in Früchten von *Vitis Vinifera* während des Reifeprozesses exprimiert ist. VvALMT9 ist ebenfalls im Tonoplast lokalisiert, und katalysiert die Malataufnahme in die Vakuolen der Weintrauben. Darüber hinaus wird gezeigt, dass auch Tartrat von VvALMT9 transportiert wird, welche eine organische Säure darstellt die wesentlich in Weintrauben akkumuliert.

Zusammenfassend werden in dieser Dissertation neue Einblicke in die strukturelle und kompositionelle Organisation von AtALMT Kanälen, in die Rolle von AtALMT9 Strömen unter Salzstress und während der Samenkeimung, und in die Funktion von VvALMT9 in Weintrauben gegeben. Die verschiedenartigen zellulären und physiologischen Prozesse, in denen ALMT9 Kanäle eine Rolle spielen, zeigen deutlich auf, dass Anionen und osmotische Homöostasen in Pflanzenzellen von essentieller Bedeutung sind.

# 1. Introduction

## 1.1. The Vacuole – A Compartment with a Multitude of Functions

Plants are sessile organisms that frequently encounter fluctuations in their environment. These fluctuations range from differences in nutrient supply, water and $CO_2$ availability, and light conditions, to exposure to toxic compounds or biotic stressors, and many more. The vacuole is a compartment that serves a fundamental role in adaptation mechanisms towards such fluctuations. The vacuole can occupy up to 90 % of the cellular volume in mature cells and its content comprises, amongst others, toxic and nutritive inorganic ions, organic acids, soluble carbohydrates, amino acids, enzymes, secondary metabolites and xenobiotics. As the vacuole buffers large variations of environmental conditions, the solute composition is highly dynamic and reflects changes in the environment. In addition, the composition is also dependent on other factors, such as the type of organ, the cell-type, the time of the day, the metabolic state, the developmental stage of the plant and the cell, and the plant species (Isayenkov et al., 2010, Martinoia et al., 2012, Matile, 1987, Conn and Gilliham, 2010). For instance, leaf mesophyll vacuoles act as temporal carbohydrate storage, whereas sugar cane or tuber vacuoles predominantly accumulate sugars for a prolonged period (Martinoia et al., 2007). Also, toxic ions are preferentially sequestered in vacuoles of leaf epidermal cells to reduce damage in the more susceptible mesophyll cells (Martinoia et al., 2007, Munns and Tester, 2008). In addition, two types of vacuoles can be found in plants, the lytic vacuole and the protein storage vacuole (Paris et al., 1996), that contain different proportions of a given solute. In most cells, these two types of vacuoles are not clearly distinguishable (Martinoia et al., 2012, Frigerio et al., 2008).

Collectively, decades of research revealed a tremendous diversity and a dynamic adaptation of the vacuolar solute composition within plants. To guarantee rapid exchange of the huge variety of molecules across the vacuolar membrane, the tonoplast,

plants are equipped with a battery of transport systems. The tightly regulated and directed vacuolar solute passage mediated by these transport processes build the basis of the multitude of functions performed by the large central vacuole. In the following, key functions of the plant vacuoles will be introduced.

### 1.1.1 Cell Elongation, Seed Germination and Stomatal Movement

The turgor pressure of plant cells pushes the cell membrane against the cell wall to maintain rigidity. The turgor is achieved by water influx into the vacuole that is driven by the accumulation of osmotically active solutes. Since vacuoles store the majority of cellular solutes and water, they constitute the main compartment of turgor generation. The differences in turgor pressure are accompanied by local loosening of the cell wall (Cosgrove, 1996). Together, these are in turn the driving forces for cell expansion and plant growth, and thereby optimize the surface for absorption of sunlight during photosynthesis.

Rapid changes in vacuolar volume and, hence, cell size can only occur since bidirectional water flow across the tonoplast is catalyzed by aquaporins (Reisen et al., 2003, Lin et al., 2007). Aquaporins have been identified in almost all organisms but are particularly abundant and diverse in plants (Kaldenhoff and Fischer, 2006). They belong to the large superfamily of Major Intrinsic Proteins (MIP) of integral membrane proteins (Maeshima, 1992). Dependent on their subcellular localization and phylogeny MIPs are divided into four subfamilies. Aquaporins that integrate into the vacuolar membrane belong to the so called Tonoplast Intrinsic Proteins (TIP) subfamily and are encoded by 10 genes in *Arabidopsis thaliana* (Arabidopsis) (Weig et al., 1997, Johanson et al., 2001). They act as water-permeable transmembrane channels and play a fundamental role in plant water balance and osmoregulation. Of note, since the late 1990s functional analyses have revealed that aquaporins facilitate the transporter of other substrates than $H_2O$, such as urea, $NH_3$/ $NH_4^+$, $CO_2$, or hydrogen peroxide (Kaldenhoff and Fischer, 2006, Bienert et al., 2007).

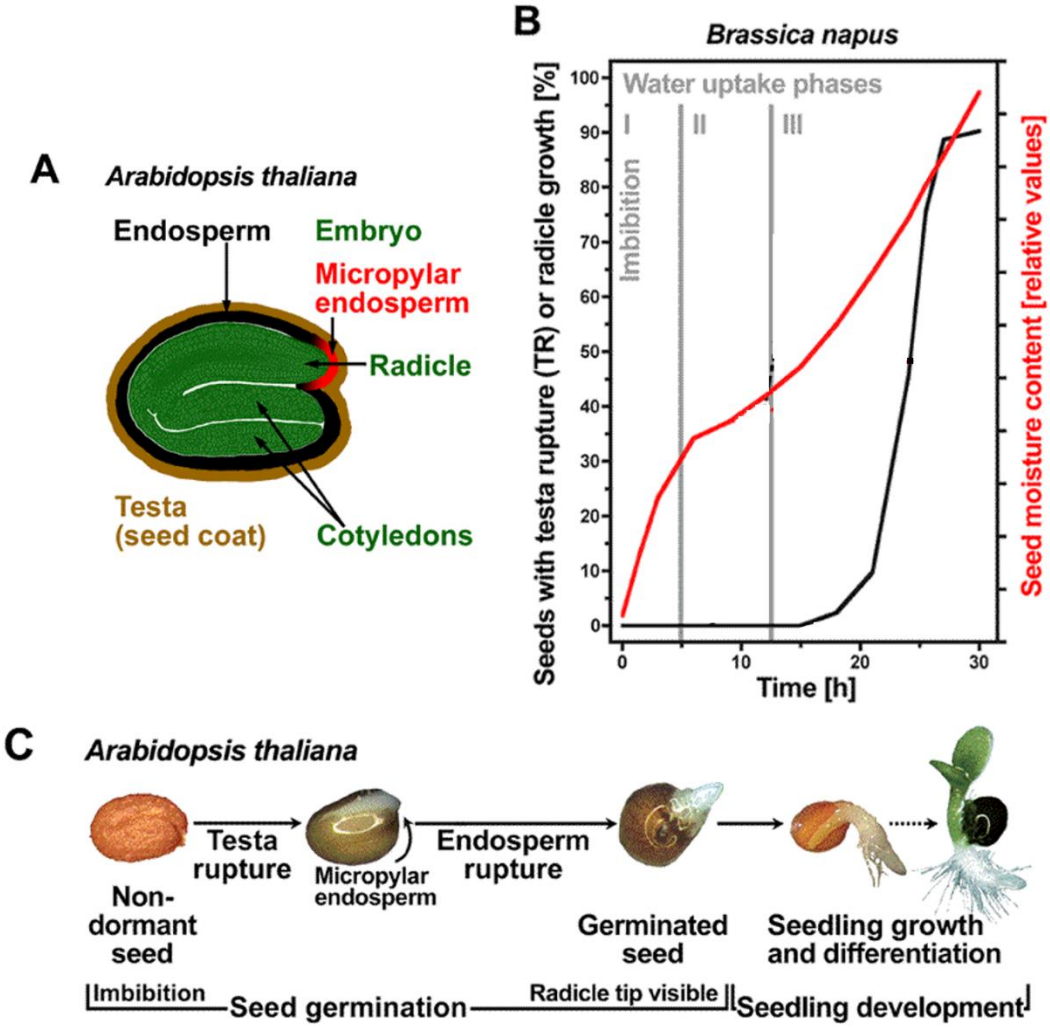


**Figure 1. Early Stages of Seed Germination are Dependent on Rapid Water Uptake.**

**(A)** Morphology of a mature Arabidopsis seed.

**(B)** Seeds (here: *Brassica napus*) rapidly take up water in the early stages of seed germination (designated imbibition) that cumulates in testa rupture and, upon endosperm rupture, in radicle emergence.

**(C)** Visible events during seed germination and the following seedling development in Arabidopsis. Adapted from Weitbrecht et al., 2011.

Solute uptake and the accompanied water influx into the vacuole mediated by TIPs is particularly important during seed germination (Figure 1). In many plant species, the embryo in the seed is covered by a seed coat (testa) and an endosperm layer, which need to be ruptured in order to facilitate embryo outgrowth by radicle emergence. One of the first steps during germination is designated imbibition, a rehydration process in which seeds rapidly take up water. The subsequent volume change of the vacuole and therefore the embryo culminates in testa rupture, endosperm rupture and radicle emergence (Weitbrecht et al., 2011). In accordance, TIPs have been found to be expressed in seeds (Johnson et al., 1990), and are suggested to play a critical role in these early steps of germination (Maurel, 1997, Maurel et al., 1997, Vander Willigen et al., 2006, Maurel et al., 1995).

In addition to the importance of turgor regulation for cell expansion and seed germination, the reversible volume change mediated by vacuolar swelling and shrinking is also fundamental for stomatal movement. Stomata are microscopic pores at the leaf surface. Each stomatal pore is surrounded by a pair of specialized epidermal cells designated guard cells. Due to differential thickening of the cell walls of guard cells, alterations in turgor result in bending and differential opening of the pore that is surrounded by the guard cells (Blatt, 2000). Stomatal pores and their tightly controlled opening and closing are a prerequisite for plant performance since gas exchange, water loss and leaf temperature are regulated by this mean (MacRobbie, 1998, Hetherington, 2001, Nilson and Assmann, 2007, Kim et al., 2010). Thereby, photosynthesis and plant metabolism can be optimally balanced.

Vacuolar solute fluxes in guard cells are predominantly based on potassium ($K^+$) ions (Fischer, 1968, Andrés et al., 2014), and on anions such as malate ($mal^{2-}$), chloride ($Cl^-$) and nitrate ($NO_3^-$), as well as on other metabolites such as sugars (Poffenroth et al., 1992, Talbott and Zeiger, 1996, Guo et al., 2003). The relative contribution of each anion to stomatal movement is dependent on the plant species, the time of the day and the environmental conditions (Schnabl and Raschke, 1980, Talbott and Zeiger, 1996). Ion fluxes that are directed from the apoplast to the vacuole are responsible for stomatal opening, fluxes from the vacuole to the apoplast for stomatal closure. Hence, the coordinated action of transport systems at the vacuolar as well as at the plasma

membrane rapidly change the water potential of guard cells and thereby the direction of water fluxes, and contribute to the dynamic movement of stomatal pores (Blatt et al., 2014, Chen et al., 2012, Wang et al., 2014, Roelfsema and Hedrich, 2005). During dark-induced stomatal closure, the volume of Arabidopsis guard cell vacuoles reduces 20 % compared to the open state (Tanaka et al., 2007). Interestingly, besides changes in volume also modifications in the tonoplast morphology have been observed. During stomatal closure the guard cell vacuole fragments into many small vacuole (Gao et al., 2005, Gao et al., 2009, Andrés et al., 2014) that might be able to fuse again when opening is required. The fragmentation was suggested to be an elegant strategy to reduce vacuolar volume while maintaining the total membrane surface area, in order to facilitate rapid re-opening (Figure 2). The changes in volume and morphology during stomatal movement demonstrate impressively the plasticity of the vacuole.

Transport processes in guard cells that contribute to the opening and closure of stomatal pores are majorly controlled by environmental stimuli such as light, water availability, $CO_2$ and relative humidity (Hetherington and Woodward, 2003, Kim et al., 2010, Shimazaki et al., 2007). The phytohormone ABA (abscisic acid) serves as link between the environmental status and transport activities since it initiates and regulates intracellular processes in the guard cells that result in stomatal closure. The presence of ABA influences regulatory factors, including the phosphorylation status of proteins (Lee et al., 2009, Geiger et al., 2009, Geiger et al., 2010, Imes et al., 2013) or the membrane potential (Ache et al., 2000, Hosy et al., 2003, Kim et al., 2010), which directly modulate the activity of transport processes across the plasma and vacuolar membrane. The mode of action and transduction of ABA-mediated signals in guard cells is well studied and reviewed in Joshi-Saha et al. (2011) and Munemasa et al. (2015), but will not be further discussed in this thesis.

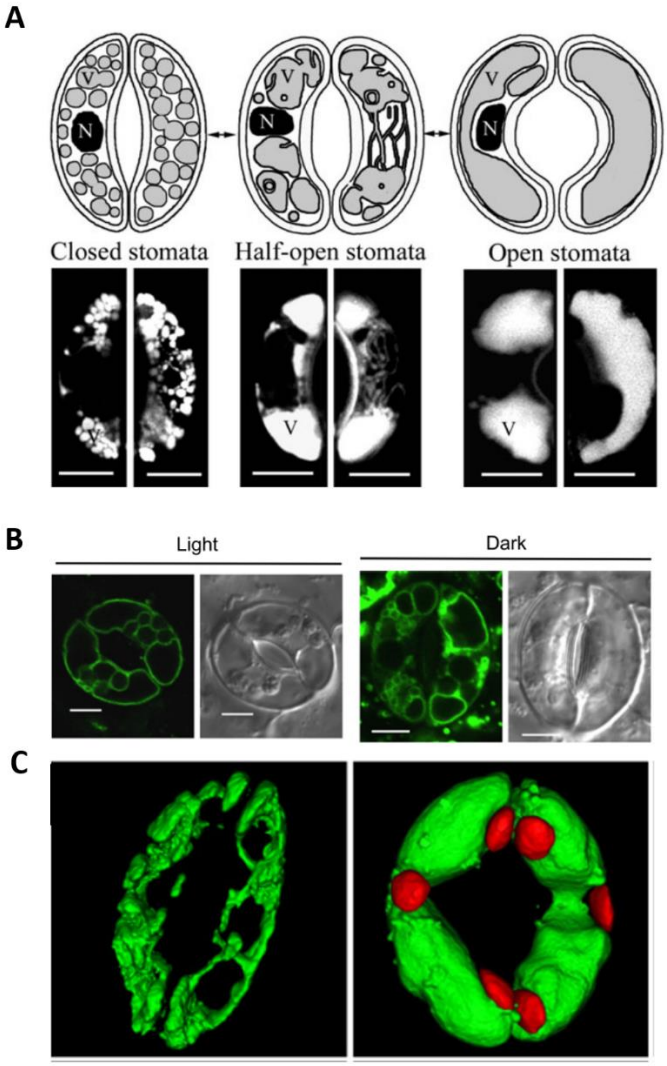


**Figure 2. Guard Cell Vacuole Dynamics during Stomatal Movement.**

**(A)** Model (upper panel) and confocal laser scanning microscopy (lower panel) of *Vicia faba* guard cell vacuolar organization during stomatal opening and closure. The vacuoles are labeled using acridine organge. N, nucleus; V, vacuole. Bars = 10 µm. Adapted from Gao et. al., 2009. **(B)** Vacuolar morphology in Arabidopsis guard cells visualized with the aquaporin AtTIP1;1:GFP during opening (light) and closure (dark). Depicted are bright-field (right panels) and GFP images (left panels). Scale bars = 5 µm.
**(C)** Three-dimensional projection of vacuolar morphology in Arabidopsis guard cells. Vacuoles are loaded with the vacuolar dye 2',7'-bis-(2-carboxyethyl)-5-(and-6)-carboxyfluorescein acetoxymethyl (BCECF-AM) in closed (left panel) and open (right panel) state. The auto-fluorescence signal of chloroplasts is shown in red. (B) and (C) are adapted from Andrés et al. (2014).

## 1.1.2. Storage of Nutrients, Metabolites and Signaling Compounds

A major function of the vacuole is to maintain optimal conditions in the cytosol and guarantee plant metabolism. The storage of nutrients and metabolic intermediates in the vacuole regulates cellular metabolism and assists continuous plant growth under fluctuating environmental conditions. Besides, signaling compounds are reversibly stored in vacuoles to fine-tune cytosolic concentrations. In the following, the functional role of vacuolar storage is discussed, and $NO_3^-$, malate and calcium ($Ca^{2+}$) fluxes were selected as examples.

The vacuole serves as a temporal storage reservoir for nutrients to buffer fluctuations in availability. Nutrients can be accumulated to safe in times of plenty and remobilized by vacuolar release during scarcity. Hence, directed nutrient fluxes into or out of the vacuole allow adaptation to cytosolic nutrient levels according to the current physiological requirement and specific cellular demands. Nitrogen availability is a major limiting factor for plant growth and crop production (Frink et al., 1999). Nitrogen is a key structural component of macromolecules in plants and can act as signal that impacts on many aspects of plant biology. The nutrient $NO_3^-$ is the primary nitrogen source for most plants (Dechorgnat et al., 2011). To guarantee nitrogen use efficiency and high accumulation of $NO_3^-$, plants need to possess an antiporter at the tonoplast with $NO_3^-$-selectivity (De Angeli et al., 2006). This is because a $NO_3^-$-selective channel would only account for concentration gradients of 3-fold between cytosol and vacuolar lumen, whereas secondary active transporters allow an accumulation factor of up to 100 (De Angeli et al., 2006, Cookson et al., 2005). Interestingly, it is only common for land plants to store $NO_3^-$ as a nitrogen reserve in the vacuole, whereas aquatic photosynthetic organisms such as the algae *Chara* do not accumulate $NO_3^-$ above passive transport levels, even upon exposure to high $NO_3^-$ concentrations for several month (Miller and Zhen, 1991).

The relative importance of storing the metabolite malate is also dependent on the plant species and the organ type. Malate is the most predominant carboxylate in most plants and an intermediate of the tricarboxylic acid cycle in all plant species (Fernie et al., 2004). Malate can accumulate to concentrations up to 350 mM (Martinoia and Rentsch,

1994). In general, in vacuoles malate serves as an important charge-balancing anion (largely for $K^+$), regulates cell turgor and cytoplasmic pH, and contributes to stomatal movement and microbe interaction as a root exudate in the rhizosphere (Martinoia et al., 2007, Fernie and Martinoia, 2009, Martinoia and Rentsch, 1994). In addition, in plants that exhibit Crassulacean Acid Metabolism (CAM) and $C_4$ photosynthesis (Black and Osmond, 2003) malate plays a fundamental role as central intermediary in the process of photosynthetic carbon assimilation. CAM is an adaptation of photosynthesis to heat and limited availability of water (Cushman and Bohnert, 1999). In plants that can perform CAM, such as *Mesembryanthemum crystallinum*, $CO_2$ is fixed during the night by malic acid synthesis via the cytosolic enzyme phosphoenolpyruvate carboxylase (PEPC) and malate dehydrogenase (MDH), and large amounts of this temporary carbon storage molecule are accumulated in mesophyll cell vacuoles. During the light period, stomata close and malic acid is released into the cytosol and subsequently decarboxylated into pyruvate and $CO_2$ via NADP- and/or NAD-malic enzyme, or via pyruvate $P_i$ dikinase, depending on the species (Cheffings et al., 1997). $CO_2$ in turn is re-assimilated in the Calvin Cycle in chloroplasts by ribulose-1,5-bisphosphate carboxylase (RUBISCO) (Cushman and Bohnert, 1999). Taken together, day-night fluxes of malate across the vacuolar membrane are a prerequisite of CAM plants to limit water loss during the hot day period.

Besides its major role as counter-anion and in CAM plants, malate is also highly accumulated in fruits of various plant species (Etienne et al., 2013, Etienne et al., 2014, Lobit et al., 2006). The accumulation of malic acid and other organic acids such as citric acid (Etienne et al., 2013) majorly influences the titratable acidity of fruits and thereby determines their quality. Malic acid is the predominant organic acid in ripe apple, peach loquat and pear fruits, whereas citric acid is dominant in citrus fruits (Etienne et al., 2013, Etienne et al., 2014), and tartaric acid contributes highly to the acidity of grape berries (Terrier et al., 2001). The malate concentration undergoes great changes during fruit growth and ripening (Etienne et al., 2014, Conde et al., 2007, Terrier et al., 2001), and several studies have suggested that the level of malate accumulation in fruits is controlled at the level of vacuolar storage (Etienne et al., 2013, Lobit et al., 2006, Berüter, 2004, Schauer et al., 2006). Uptake of malate into the fruit vacuole has been proposed to occur through facilitated diffusion (Maeshima, 2001). Therefore, it has

been speculated that the Aluminum-activated Malate Transporter (ALMT) family (see below) which encompasses channels that mediate malate uptake could play a role in organic acid accumulation in fruits (Etienne et al., 2013). Nevertheless, the regulation mechanisms and factors that influence fruit acidity and malate metabolism, transport and accumulation in mesocarp cells are still obscure, since these processes are dependent on complex genetic, developmental and environmental factors (Etienne et al., 2013, Etienne et al., 2014).

Vacuoles form a major intracellular store of $Ca^{2+}$ ions which exhibit profound signaling function in plant cells. In response to a number of abiotic and biotic stresses (e.g. light, touch, low or high temperature, oxidative stress, or elicitors), as well as hormonal stimuli, $Ca^{2+}$ is released from the vacuole which causes changes in free cytosolic $Ca^{2+}$ concentrations (Kudla et al., 2010). Thus, to guarantee appropriate signal transduction, $Ca^{2+}$ storage in intracellular reservoirs such as the vacuole are tightly regulated, and concentrations in the cytosol must be kept constant and low. $Ca^{2+}$ accumulates into the vacuole by both, ATP-driven $Ca^{2+}$ pumps (Sanders et al., 2002) and $H^+$-coupled $Ca^{2+}$ antiporters (Williams et al., 2000, Shigaki and Hirschi, 2000), and is released by ion channels at the tonoplast (Pottosin and Schönknecht, 2007, Peiter, 2011). The efflux from intracellular stores can be activated by second messengers such as inositol 1,4,5-triphosphate ($InsP_3$) (Schumaker and Sze, 1986, Alexander et al., 1990), inositol hexakiphosphate ($InsP_6$) (Lemtiri-Chlieh et al., 2000, Lemtiri-Chlieh et al., 2003), or cyclic ADP-ribose (cADPR) (Allen et al., 1995). However, the genetic basis of the corresponding genes that code for vacuolar $Ca^{2+}$ channels are still under debate (Peiter, 2011, Isayenkov et al., 2010, Martinoia et al., 2012).

### 1.1.3. Sequestration of Toxic Ions

The vacuole does not only take up beneficial ions and serves as a temporal storage reservoir. Many ions display toxicity, especially when accumulated to high concentrations, and need to be sequestered into the vacuole to keep the cytosolic conditions optimal for metabolism. For instance, $Cl^-$ is an essential micronutrient for higher plants acting as a co-factor for photosynthesis, as a counter anion to stabilize

membrane potentials, and as a regulator for pH gradients, turgor, the osmotic homeostasis and enzyme activity in the cytosol (White and Broadley, 2001, Teakle and Tyerman, 2010). Yet, when accumulated excessively in the cytosol $Cl^-$ ions turn harmful for the plant. The critical concentration at which $Cl^-$ becomes toxic is dependent on the plant species, and is estimated to be 4-7 mg $g^{-1}$ dry weight (DW) for $Cl^-$ sensitive species such as alfalfa (*Medicago sativa*) or citrus (*Citrus sp*.) and 15-50 mg $g^{-1}$ DW for tolerant species such as corn (*zea mays*), cotton (*Gossypium hirsutum*) or lettuce (*Lactuca sativa*) (Teakle and Tyerman, 2010, Xu et al., 1999). $Cl^-$ interferes with metabolic processes such as the photosynthetic capacity by initiating chlorophyll degradation in the chloroplasts, and thus limits plant growth (Tavakkoli et al., 2010, Tavakkoli et al., 2011). In addition, $Cl^-$ ions might build up in the apoplast and dehydrate cells, and in the cytoplasm where they might inhibit enzymes involved in carbohydrate metabolism (Munns and Tester, 2008). $Cl^-$ toxicity mainly occurs during salinity (NaCl) stress, and is therefore accompanied by a simultaneous toxic effect of sodium ($Na^+$) accumulation. In contrast to the micronutrient $Cl^-$, $Na^+$ is non-essential for plants. High $Na^+$ concentrations interfere *inter alia* with $K^+$ and $Ca^{2+}$ nutrition, which results in the inhibition of enzymatic processes and protein synthesis in the cytosol (Munns and Tester, 2008), and disturb efficient stomatal conductance resulting in a depression of photosynthesis and plant growth (Tavakkoli et al., 2010, Tavakkoli et al., 2011, James et al., 2006, Munns and Tester, 2008). Salinity tolerance strategies and adaptation mechanisms for both, excessive $Na^+$ and $Cl^-$ ions, are discussed in detail in Section 1.3.

Besides $Cl^-$ and $Na^+$, many other ions such as heavy metals can exhibit detrimental effects on plants, and are sequestered into the vacuole to counteract their toxicity in the cytosol (Martinoia et al., 2012). Again, some of them are essential mineral nutrients (iron, zinc, copper, manganese, nickel and molybdenum), yet become toxic at a certain concentration. For instance, iron is engaged in redox reactions, zinc is associated with numerous proteins, and copper is involved in plastidic electron transport and is crucial for the protection against oxidative stress (Wintz et al., 2003, Martinoia et al., 2012, Briat et al., 2007); yet the concentration of these free metals must be kept extremely low in the cytosol in order to avoid toxic symptoms such as oxidative stress or enzyme deactivation (Martinoia et al., 2007). Other heavy metals including cadmium, arsenic,

lead, chromium and mercury are not required for plant physiology and metabolism (Peng and Gong, 2014), and are taken up by plants owing to the indiscriminate nature of some transporters. These metal(loid)s cause oxidative injury and competitive inhibition of essential mineral nutrients. To detoxify heavy metals and maintain low but essential concentrations of them in the cytosol, plants have evolved several transporter proteins at the tonoplast to sequester (and release) these ions into the vacuole in a highly controlled manner (Peng and Gong, 2014, Martinoia et al., 2007, Martinoia et al., 2012). Besides the sequestration of the heavy metal ions in the vacuole, another detoxification strategy is the uptake of chelated heavy metals across the tonoplast. Chelators such as the so called phytochelatins (PC) (reviewed in Mendoza-Cózatl et al., 2011), glutathione or nicotianamine (reviewed in Curie et al., 2009), form stable metal complexes that are subsequently sequestered into vacuoles for detoxification (Mendoza-Cózatl et al., 2011, Cobbett and Goldsbrough, 2002).

# 1.2. Transporters at the Vacuolar Membrane

The vacuolar membrane is a hydrophobic barrier composed of a lipid bilayer that cannot be freely passed by water-soluble molecules (e.g. ions and carbohydrates) via diffusion. Therefore, the tonoplast is equipped with complex transport proteins that catalyze the selective fluxes of diverse molecules with distinct size, chemical properties and origins into and out of the vacuole. To fine-tune and constantly control and adapt vacuolar fluxes, the transport protein composition and activity at the tonoplast is impressively dynamic: proteins can be regulated by changes in protein abundance through differential gene expression or by modifications in protein activity (e.g. by post-translational modification or by interacting proteins) (reviewed in Neuhaus and Trentmann, 2014).

Three classes of membrane-embedded transport proteins can be found at the tonoplast. Primary active transporters directly utilize energy to catalyze the transport of compounds. An example are vacuolar proton ($H^+$) pumps which use the energy gained from ATP or $PP_i$ hydrolysis to translocate $H^+$ against the electrochemical gradient into the vacuolar lumen and store potential energy by establishing a pH gradient ($\Delta pH$) and transmembrane potential difference, the membrane potential ($\Delta\Psi$) (Gaxiola et al., 2007). Secondary active transporters also translocate compounds against their concentration or electrochemical gradient. This kind of transport is dependent on $\Delta pH$ and $\Delta\Psi$ generated and maintained by pumps, and uses the energy dissipated by a downhill movement of a molecule across the tonoplast to catalyze the concurrent movement of a molecule uphill the electrochemical gradient. The two substrates can be translocated in the same or opposite direction across the membrane, defining the two classes of secondary active transporters, the symporters and antiporters (Etxeberria et al., 2012). In contrast to active transporters, ion channels belong to a third class of tonoplast transport proteins that function as selective pores (Gouaux and Mackinnon, 2005) and permit fluxes down the electrochemical potential of the permeating ion. The diffusion of solutes through ion channels is rapid, allowing fluxes of $10^8$ ions per second. Due to the thermodynamics, channel-mediated ion fluxes are considered dissipative, passive transporter processes (Gadsby, 2009).

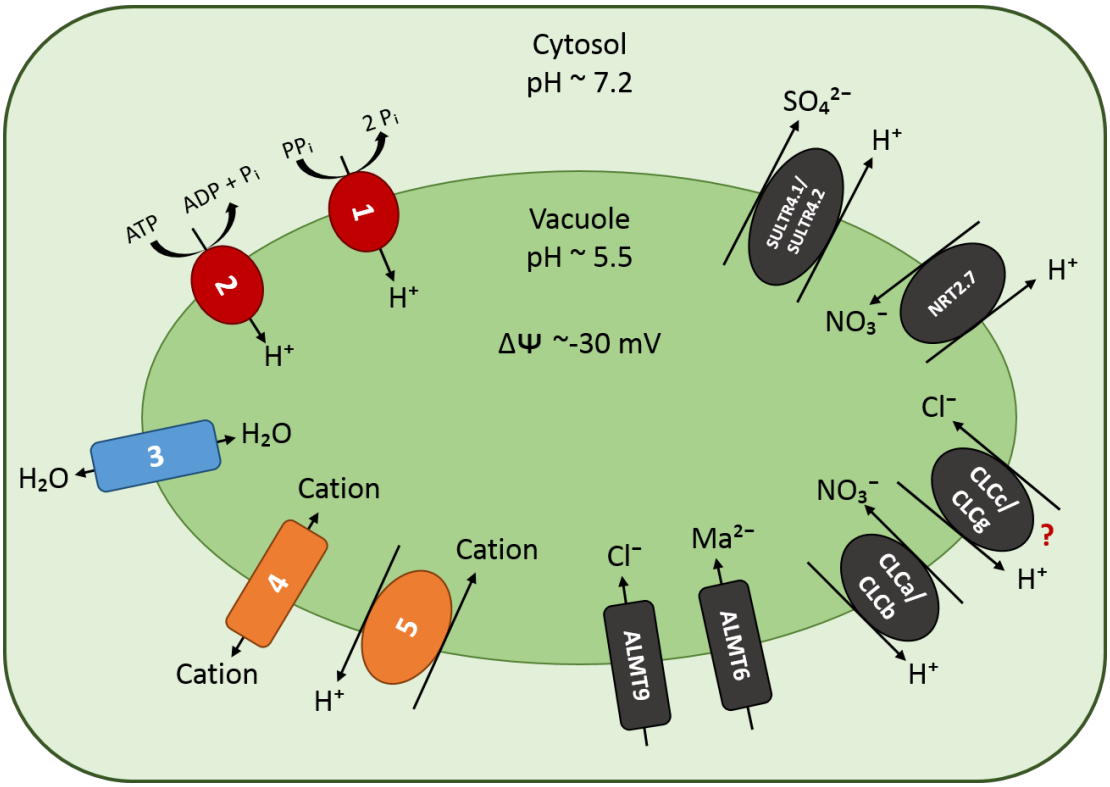


**Figure 3. Selected Transport Proteins at the Tonoplast of *Arabidopsis thaliana*.**

Transport of solutes and accumulation across the tonoplast is an energy consuming process. The plant vacuolar membrane is energized by primary active transporters that use energy out of the hydrolysis of ATP or $PP_i$ to acidify the vacuolar lumen and establish a membrane potential across the tonoplast. Depicted are the responsible vacuolar proton pumps, the V-PPase (1) and the V-ATPase (2). Secondary active transporters (symporters and antiporters) translocate substrates such as cations (5) and various anions against their electrochemical gradient. Channels catalyze the thermodynamic downhill transport of substrates such as cations (4) and several anions. Aquaporins (TIPs; 3) are pores that facilitate water fluxes across the tonoplast. Identified and characterized transport proteins that mediate anion fluxes across the tonoplast are depicted, and described in the text in more detail. Note: ion coupling ratios of secondary active transporters are not indicated. Additionally, it has not been shown whether CLCc and CLCg function as channels or transporters, and their ion flux direction has not been determined.

The combined and concerted action of these three classes of transport facilitate the variety of fluxes across the tonoplast. Nowadays, transporter proteins implicated in several aspects of vacuolar function have been started to be identified and characterized. Here, the transport proteins and protein families that energize the vacuolar membrane as well as secondary active transporters and channels that selectively catalyze the movement of organic and inorganic anions across the tonoplast will be discussed in more detail (Figure 3).

### 1.2.1. Energizing Ion Transport across the Tonoplast

The tonoplast is energized by two types of $H^+$-translocating pumps: the vacuolar $H^+$-ATPase (V-ATPase), which is fueled by ATP, and the $H^+$-pyrophosphatase (V-PPase), which makes use of the chemical energy of the phosphoanhydride bond of pyrophosphate ($PP_i$) (Gaxiola et al., 2007, Hedrich et al., 1989). The $H^+$-pump activity of both enzymes generates the so called proton motif force (pmf) that consists of a steep $\Delta pH$ across the tonoplast (2-4 pH units) and a rather small tonoplast membrane potential gradient ($\Delta\Psi$; -10 to -30 mV) (Martinoia et al., 2007, Walker et al., 1996, Pottosin and Schönknecht, 2007). The pmf can energize secondary activate transport to translocate compounds against their concentration or electrochemical gradient. In addition, ion diffusion through channel proteins depends not only on the concentration gradient of the permeating ion, but can also be regulated through $\Delta\Psi$ that is generated by the activity of the $H^+$-pumps, highlighting the necessity of the V-ATPase and the V-PPase in facilitating secondary active and passive trans-tonoplast solute fluxes (Figure 3).

In the vacuolar membrane the V-ATPase is the major pump and can account for up to 35 % of the total proteins (Klink et al., 1990). However, both the V-ATPase and the V-PPase are highly abundant in the tonoplast (Carter et al., 2004, Jaquinod et al., 2007, Shimaoka et al., 2004) and can be found in all types of vacuoles (Hedrich et al., 1989). It is assumed that only the combined action of both pumps enables plants to maintain transport across the tonoplast in various tissues, developmental stages and even under stressful conditions (Kriegel et al., 2015, Maeshima, 2000).

The V-PPase consists of a homodimer (two 71-80 kDa subunits) of a single polypeptide chain (Maeshima, 2000, Gaxiola et al., 2007). Its substrate, PPi, is a by-product of several biosynthetic processes, such as DNA and RNA synthesis or sucrose and cellulose synthesis (Martinoia et al., 2007). In contrast to the V-PPase, the V-ATPase is an enormous enzyme complex with a molecular weight of more than 700 kDa that is highly conserved in all eukaryotes (Stevens and Forgac, 1997, Nishi and Forgac, 2002, Schumacher and Krebs, 2010). In Arabidopsis at least 26 genes encode for the multiple subunits, the expression of which is subject to intense regulations under various environmental stress conditions (Dietz et al., 2001, Sze et al., 2002). The holoenzyme can be subdivided into two major functional domains, $V_1$ and $V_0$. The membrane peripheral cytoplasmic $V_1$ sector with its eight subunits is required for ATP binding and hydrolysis, and $H^+$-translocation across the tonoplast occurs through the multi-subunit $V_0$ complex that is membrane-intrinsic (Sze et al., 1999, Schumacher and Krebs, 2010). Interestingly, many subunits are encoded by several isogenes (Sze et al., 2002), and the number of isoforms can differ between species (Kluge et al., 2003). In addition, different isoforms can exhibit distinct intracellular localizations not only in the vacuolar membrane, but also in the *trans*-Golgi network/ early endosomes (TGN/EE) (Brüx et al., 2008, Krebs et al., 2010, Kawasaki-Nishi et al., 2001, Dettmer et al., 2006, Schumacher and Krebs, 2010), increasing the complexity of the pump, and the challenge to study its different physiological functions. The functional relation and relative contribution of V-ATPases at the tonoplast and the TGN/EE and the V-PPase to the acidification of the vacuolar lumen is still not fully understood (Krebs et al., 2010, Kriegel et al., 2015).

Besides these two proton pumps, some plant species contain also P-type $H^+$-ATPases at the tonoplast that are expressed in specific cell-types or tissues such as petal epidermis cells of petunia (*Petunia hybrida*) and that are involved in vacuolar hyperacidification (Müller et al., 1996, Faraco et al., 2014, Verweij et al., 2008, Eisenach et al., 2014).

## 1.2.2. Anion Channels and Transporters at the Tonoplast

The vacuolar functions discussed above, including turgor establishment and cell volume change, and nutrient storage and detoxification, are highly dependent on anion fluxes across the tonoplast. In the following, gene families encoding for transporter or channel proteins that mediate the fluxes of inorganic anions such as $Cl^-$ and $NO_3^-$ and organic anions such as malate across the vacuolar membrane will be discussed with respect to knowledge mainly gained from the model plant Arabidopsis (Figure 3). It will become apparent that during the last decades, tremendous progress has been made in deciphering the properties of these vacuolar transport proteins regarding (i) their molecular identity, (ii) their thermodynamic properties (e.g. passive or active transport, flux direction, coupling ratio where applicable); (iii) their substrate specificity; (iv) their regulation (e.g. transcriptional or post-translational); (v) their tissue-specific expression pattern; and (vi) their functional role in plants.

### 1.2.2.1. AtCLCs

The ubiquitous Chloride Channel (CLC) gene family is present in most organisms including bacteria, yeast, animals and plants (Jentsch, 2008). The first CLC that was characterized is the voltage-gated channel CLC-0 that mediates $Cl^-$ currents in the electric organ of Torpedo fish (White and Miller, 1979, Jentsch et al., 1990). CLCs were originally described to act as channels, whereas others have been found to function as anion/ $H^+$ antiporters (Accardi and Miller, 2004, Picollo and Pusch, 2005, De Angeli et al., 2006, Zifarelli and Pusch, 2010). Astonishingly, the mutation of one amino acid, the so called 'gating glutamate', into an uncharged residue has been suggested to abolish the coupling between anions and $H^+$ and converts an CLC antiporter into a protein with channel characteristics (Bergsdorf et al., 2009).

In Arabidopsis, the CLC family is composed of seven members named AtCLCa to AtCLCg. Among them, the four members AtCLCa-c and AtCLCg are localized at the tonoplast or prevacuolar compartements, while AtCLCd and AtCLCf reside in Golgi vesicles and AtCLCe was shown to be localized in the thylakoid membrane of chloroplasts (Marmagne et al., 2007, Zifarelli and Pusch, 2010, Lv et al., 2009, von der

Fecht-Bartenbach et al., 2007). The first characterized CLC in plants was the vacuolar transporter AtCLCa in Arabidopsis. Geelen and co-workers observed that a loss-of-function mutant of AtCLCa exhibits reduced $NO_3^-$ contents in shoots and roots compared to the wild-type (Geelen et al., 2000). A subsequent study revealed that AtCLCa is a substrate-specific antiporter that couples $NO_3^-$ transport to the export of $H^+$ across the tonoplast with a stoichiometry of 2:1 to drive $NO_3^-$ accumulation into the vacuole (De Angeli et al., 2006). Thereby, AtCLCa activity accounts for up to 50 % of the $NO_3^-$ storage in Arabidopsis (Geelen et al., 2000, Monachello et al., 2009, Wege et al., 2010). Its substrate-specificity for $NO_3^-$ over $Cl^-$ is dependent on a single amino acid, proline 160 (Bergsdorf et al., 2009, Wege et al., 2010, Dutzler et al., 2002). Interestingly, substituting this residue with a serine (P160S), which occurs at the corresponding position in most CLCs, abolishes the preferential $NO_3^-$ selectivity of AtCLCa and results in similar $Cl^-$ and $NO_3^-$ transport rates. The importance of this residue for vacuolar $NO_3^-$ uptake is substantiated by the fact that the expression of the native AtCLCa-P160 in *atclca* knock-out mutants, but not the expression of the AtCLCa-P160S transporter mutant variant, complements the reduction in $NO_3^-$ accumulation (Wege et al., 2010).

Besides its importance in vacuolar $NO_3^-$ storage, AtCLCa is expressed in guard cells and has a functional role in stomatal movement (Wege et al., 2014). As expected from previous studies, AtCLCa has been shown to be involved in stomatal opening through vacuolar $NO_3^-$ uptake. However, it has also been uncovered that AtCLCa fulfills a role in stomatal closure in response to ABA, indicating that the transporter mediates bidirectional fluxes that are physiologically relevant. The outward current of AtCLCa was found to be enhanced by the phosphorylation of threonine 38 at the amino-terminal cytoplasmic domain. Apart from providing new insights into the physiological function of AtCLCa, this study disclosed a central regulatory mechanisms of the electrophysiological properties of AtCLC transporters (Wege et al., 2014).

Among all CLCs in Arabidopsis, AtCLCa and AtCLCb share the highest degree of homology and are approximately 80 % identical (Barbier-Brygoo et al., 2010). As observed in *Xenopus leavis* (Xenopus) oocytes, AtCLCb also functions as a $NO_3^-/ H^+$ exchanger, and is also localized at the tonoplast in plants (von der Fecht-Bartenbach et

al., 2010). However, knock-out mutants did not uncover a clear phenotype, retaining its physiological function *in planta* undetermined.

The two other AtCLCs that reside in (pre)vacuolar membranes, AtCLCc and AtCLCg, are assigned a functional role in $Cl^-$ transport in Arabidopsis. Accordingly, and in contrast to AtCLCa (Bergsdorf et al., 2009, Wege et al., 2010, Dutzler et al., 2002), both proteins display the sequence motif in favor of a transporter with $Cl^-$ selectivity (Zifarelli and Pusch, 2010). AtCLCc is localized to the tonoplast and highly expressed in pollen and stomata (Jossier et al., 2010). Knock-out mutants showed impaired light-dependent stomatal opening and ABA-insensitivity during stomatal closure. The wild-type stomatal movement was restored upon exchanging KCl with $KNO_3$ in the opening buffer bath solution, indicating that the phenotype of *atclcc* mutants is based on impaired $Cl^-$ translocation across the tonoplast of guard cells. Another set of experiments revealed that *atclcc* mutants have higher sensitivity to NaCl and KCl stress, substantiating an implication of the transport protein in transmembrane $Cl^-$ fluxes (Jossier et al., 2010). Similarly, mutants lacking the vacuolar AtCLCg showed reduced biomass production under NaCl and KCl exposure, but not under osmotic stress upon mannitol application (Nguyen et al., 2015). In the presence of NaCl, *atclcg* mutant plants over-accumulated $Cl^-$ in shoots compared to the wild-type, pointing towards a role of AtCLCg in $Cl^-$ homeostasis during salt stress. *AtCLCg* is expressed in mesophyll cells, hydathodes and the phloem, and double mutants of *atclcc atclcg* revealed that both transport proteins do not act redundantly (Nguyen et al., 2015). Nevertheless, further research is required to determine the electrophysiological characteristics of AtCLCc and AtCLCg, i.e. the selectivity, the flux direction, and the thermodynamics of the transport.

#### 1.2.2.2. AtNRT2.7

Another protein family in which members have been shown to facilitate anion transport across biological membranes is the NRT (Nitrate Transporter) family of Arabidopsis, which is divided into NRT1s and NRT2s (Tsay et al., 2007). In Arabidopsis, there are 53 *NRT1* genes and 7 *NRT2* genes. NRT2 are high-affinity $NO_3^-$ transporters, while

most members of the NRT1 family are predominantly low-affinity $NO_3^-$ transporters. NRT1 transporters belong to the same family as Peptide Transporters (PTR) which transport a broad spectrum of substrates (Tsay et al., 2007) including $Cl^-$ (Li et al., 2015). Recently a unified nomenclature for NRT1/PTR has been proposed. Members of this family should be named NPF (NRT1/PTR Family) (Léran et al., 2014).

AtNPFs and most AtNRT2 family members have been shown to be localized to the plasma membrane. The only vacuolar AtNRT protein characterized to date is AtNRT2.7 (Chopin et al., 2007). The gene is specifically expressed at the final stage of seed maturation. Interestingly, the seed is an organ in which AtCLCa is not expressed (Martinoia et al., 2012). $NO_3^-$ transport activity of AtNRT2.7 has been demonstrated in Xenopus oocytes and in mutant plants deficient in $NO_3^-$ transport by ectopic expression. Accordingly, knock-out mutants of the vacuolar $NO_3^-$ transporter showed reduced $NO_3^-$ contents in mature seeds, suggesting that AtNRT2.7 is involved in the loading of $NO_3^-$ into embryo vacuoles.

#### 1.2.2.3. AtSULTR4-1 and AtSULTR4-2

Sulphur is one of the essential macronutrient for growth of higher plants. Excessive sulphate ($SO_4^{2-}$) accumulates mainly in the vacuoles and constitutes a large internal sulphur reserve (Martinoia et al., 2000). The access of internal $SO_4^{2-}$ pools by vacuolar release is fundamental for plant growth and development (Martinoia et al., 2007). Two vacuolar $SO_4^{2-}$ transporters, AtSULTR4-1 and AtSULTR4-2, have been identified in Arabidopsis (Kataoka et al., 2004). They function as $SO_4^{2-}$ exporter upon $SO_4^{2-}$ limitation in xylem parenchyma cells. In accordance, AtSULTR4-1 is transcriptionally up-regulated in shoots, and AtSULTR4-2 expression is induced in both shoots and roots under $SO_4^{2-}$ starvation. Vacuoles isolated from plants lacking both transport proteins (*atsultr4-1 atsultr4-2*) contained higher amounts of $SO_4^{2-}$ compared to the wild-type. On the whole-tissue level, double knock-out mutants exhibited higher $SO_4^{2-}$ contents in roots, whereby shoot accumulation was not affected (Kataoka et al., 2004). Remarkably, no protein has been described that mediates $SO_4^{2-}$ uptake into the vacuole,

and the same is true for the import of phosphate, another nutrient that is temporary stored in plant vacuoles (Massonneau et al., 2000).

#### 1.2.2.4. AttDT

The Arabidopsis tonoplast dicarboxylate transporter AttDT (Emmerlich et al., 2003) is orthologous to the animal $Na^+$/dicarboxylate transporter (NaDC1-3). In the Arabidopsis genome AttDT is the only homolog of the human NaDC family. While vertebrate $Na^+$/dicarboxylate transporter are located at the plasma membrane and their activity is regulated by $Na^+$ (Markovich and Murer, 2004), AttDT is targeted to the tonoplast and its activity displays $Na^+$-independency (Emmerlich et al., 2003). It is proposed that AttDT drives the accumulation of dicarboxylic acids such as malate by the electrochemical gradient that exists across the tonoplast (Meyer et al., 2010a). In addition, it has been suggested that this transporter catalyzes both, vacuolar import and export of malate (Hurth et al., 2005). Mutant analysis of plants deficient in AttDT revealed no visible phenotype, but a significant reduction of malate accumulation in leaves compared to the wild-type (Hurth et al., 2005). Furthermore, mesophyll protoplasts of *attdt* knock-out mutants are more sensitive to cytosolic acidification, substantiating a role of vacuolar malate uptake in cytosolic pH regulation. Interestingly, patch-clamp measurement revealed that *attdt* vacuoles still exhibit strong inward-rectifying vacuolar malate currents (Emmerlich et al., 2003, Hurth et al., 2005), highly suggesting that two translocations systems, vacuolar malate transporters and vacuolar malate channels, are implicated in its accumulation in the vacuole that show partially functional redundancy. The corresponding channel proteins have been demonstrated to be encoded by genes belonging to the Aluminum-activated Malate Transporter (ALMT) family which will be discussed in the next paragraph.

#### 1.2.2.5. AtALMTs

ALMTs belong to a gene family that is exclusive to plants. In Arabidopsis, the family is composed of 14 members (Kovermann et al., 2007). Based on the amino acid sequence similarities three clades can be distinguished: clade I harbors the members

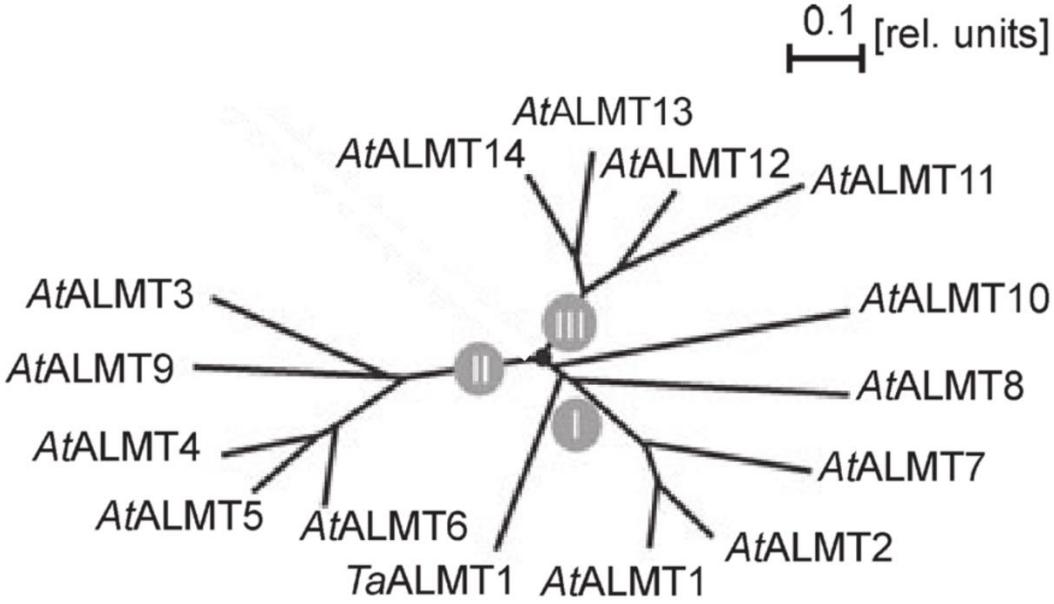


**Figure 4. Dendogram of the AtALMT family of *Arabidopsis thaliana*.**

Based on amino acid sequence similarities, the Aluminum-activated Malate Transporter (AtALMT) protein family in Arabidopsis can be subdivided into three clades. The wheat ALMT1 homolog (TaALMT1) clusters in the same clade as AtALMT1. Branch length are proportional to the level of interfered evolutionary change, and are given in relative units. Adapted from Kovermann et al., 2007.

AtALMT1, AtALMT2, AtALMT7, AtALMT8 and AtALMT10; clade II encompasses the members AtALMT3, AtALMT4, AtALMT5, AtALMT6 and AtALMT9; and clade III is composed of the members AtALMT11-14 (Figure 4). However, the first identified and characterized ALMT was not an Arabidopsis protein, but TaALMT1 of bread wheat (*Triticum aestivum*).

Molecular comparison of a pair of near-isogenic wheat lines that differed in their sensitivity to aluminum ions identified TaALMT1 as a component of aluminum tolerance in wheat (Sasaki et al., 2004). In addition, mapping of *TaALMT1* revealed that the gene correlates with a major QTL for aluminum resistance (Raman et al., 2005). Aluminum is toxic for plants due to the solubilization of $Al^{3+}$ cations in acidic soils. In order to counteract toxicity, most plants excrete carboxylates such as malate in response

to $Al^{3+}$ into the soil to chelate the trivalent cation and form non-toxic complexes. In accordance, in wheat the capacity of aluminum to stimulate carboxylate efflux into the rhizosphere co-segregates with aluminum tolerance (Delhaize et al., 1993a), and the involvement of an aluminum-activated anion channel in roots in this process has been suggested (Ryan et al., 1997, Delhaize et al., 1993b). TaALMT1, the long-sought-after carboxylate channel, has been shown to be constitutively expressed in root apices and to be localized at the plasma membrane (Yamaguchi et al., 2005). Detailed electrophysiological studies in Xenopus oocytes revealed that TaALMT1 is a channel that mediates malate efflux into the rhizosphere, and that its activity is increased in response to $Al^{3+}$ ions (Piñeros et al., 2008a). TaALMT1 clusters in the same clade as AtALMT1, and both proteins share a 44 % sequence identity (Barbier-Brygoo et al., 2010; Figure 4). As its counterpart in wheat, AtALMT1 localizes to the tonoplast of root cells and shows similar channel properties by mediating $Al^{3+}$-activated malate extrusion (Hoekenga et al., 2006, Kobayashi et al., 2007). Studies of ALMT1 in several species indicated that its functionality is highly (Hoekenga et al., 2006, Kobayashi et al., 2007, Ligaba et al., 2006, Fontecha et al., 2007) but not fully (Piñeros et al., 2008b) conserved within plants. Indeed, for instance the *Brassica napus* homolog, BnALMT1, is involved in conferring aluminum tolerance through facilitating the efflux of carboxylates into the rhizosphere (Ligaba et al., 2006), but the *Zea mays* homolog, ZmALMT1, is not activated by extracellular $Al^{3+}$ and is more permeable for inorganic anions such as $Cl^-$ and $NO_3^-$ than for malate (Piñeros et al., 2008b). In addition to its function in aluminum tolerance, malate extrusion mediated by AtALMT1 has been shown to recruit beneficial bacteria in the rhizosphere and stimulate plant-microbe interaction (Rudrappa et al., 2008).

Although the aluminum activation of ALMT1 activity gave the family its name, the abbreviation is misleading since not all members are aluminum activated, and in fact the proteins display characteristics of channels and not transporters. For instance, the channel activity of AtALMT12, another characterized member that is localized to the plasma membrane in Arabidopsis, is independent of the presence of $Al^{3+}$ ions (Meyer et al., 2010b, Sasaki et al., 2010). AtALMT12 was reported to be highly expressed in guard cells and a loss-of-function mutant is impaired in ABA-induced stomatal closure, darkness, elevated $CO_2$ and external $Ca^{2+}$ (Meyer et al., 2010b, Sasaki et al., 2010).

Electrophysiological studies in Xenopus oocytes that express AtALMT12 showed a fast, strongly voltage-dependent inward current that corresponds to a depolarization-activated anion efflux out of the cell. These properties are reminiscent of the rapid-type (R-type) anion currents observed in guard cells (Schroeder and Keller, 1992). Interestingly, malate has been suggested to be a potent regulator of these R-type anion currents (Hedrich and Marten, 1993), and AtALMT12 voltage-dependency is shifted by extracellular malate (Meyer et al., 2010b). In addition, *atalmt12* knock-out mutant and wild-type vacuoles showed no differences in anion current density in the absence of malate (Sasaki et al., 2010), but a 40 % reduction in the presence of external (apoplastic-side) malate (Meyer et al., 2010b). Together, these results provide strong evidence that AtALMT12 is a component of the malate-activated R-type anion currents in guard cells which are crucial for stomatal closure.

AtALMT proteins do not exclusively reside at the plasma membrane. Two members of clade II, AtALMT6 and AtALMT9, have been demonstrated to be tonoplast-localized channels (Kovermann et al., 2007, Meyer et al., 2011). AtALMT6 is predominantly expressed in guard cells and mediates inward-rectifying malate currents corresponding to an influx of malate into the vacuole, but is also capable of mediating malate efflux (Meyer et al., 2011). Using patch-clamp analyses, the activity of AtALMT6 was found to be regulated by cytosolic $Ca^{2+}$, cytosolic malate and vacuolar pH. Vacuoles released from guard cell protoplasts of *atalmt6* knock-out mutants showed reduced malate currents compared to wild-type vacuoles (Meyer et al., 2011). Nevertheless, no stomatal phenotype was observed in *atalmt6* plants, pointing towards a functional redundancy of malate channels in the vacuoles of guard cells.

The vacuolar anion channel AtALMT9 has been shown to be expressed in mesophyll and guard cells (Kovermann et al., 2007). Patch-clamp analyses of vacuoles released from mesophyll protoplasts of *Nicotiana benthamiana* (tobacco) that transiently overexpress AtALMT9 and of Xenopus oocytes that express AtALMT9 showed that the protein functions as an inward-rectifying channel that is permeable for malate. Similar to *atalmt6*, vacuoles of *atalmt9* knock-out mutants exhibited slightly reduced malate currents, but no visible phenotype was observed in early studies (Kovermann et al., 2007).

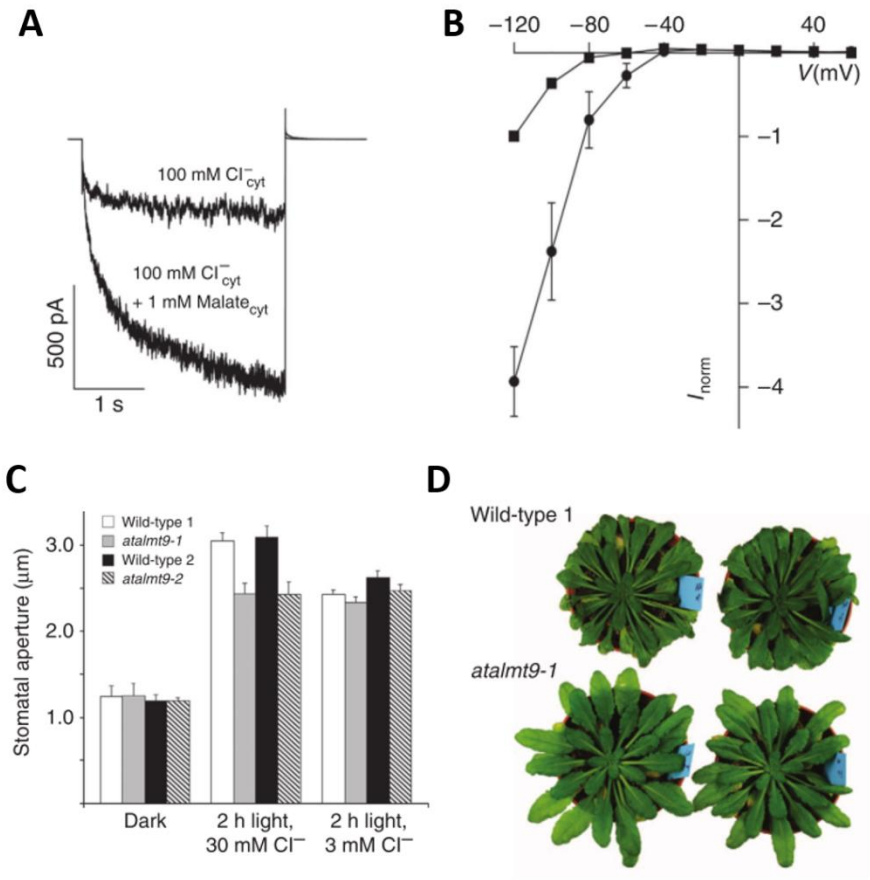


**Figure 5. AtALMT9 is a Malate-Activated Vacuolar $Cl^-$ Channel Required for Stomatal Opening.**

**(A)** and **(B)** Patch-clamp analyses of AtALMT9-mediated $Cl^-$ currents and malate-activated $Cl^-$ currents in vacuoles of tobacco mesophyll protoplasts that transiently overexpress AtALMT9-GFP. Experiments were performed under symmetrical $Cl^-$ conditions (100mM $Cl^-_{cyt}$/ 100mM $Cl^-_{vac}$) at -120 mV in an excised cytosolic-side-out patching configuration. The cytosolic solution was subsequently exchanged and 1mM malate was added. (A) Representative currents elicited before (upper trace) and after the addition of 1mM malate (lower trace). (B) Normalized I–V curves in absence (squares) or in presence of 1 mM malate (circles) in the cytosolic solution.

**(C)** Stomatal aperture measurements on epidermal peels revealed that *atalmt9* mutants show an impaired light-dependent stomatal opening that is dependent on the presence of $Cl^-$ ions in the opening buffer.

**(D)** *atalmt9* knock-out mutants showed less sensitivity to drought stress. Results are from De Angeli et al., 2013.

Since AtALMT9 is highly expressed in guard cells, in a subsequent study the stomatal movement of two independent *atalmt9* knock-out mutants was investigated (De Angeli et al., 2013b). Compared to the corresponding wild-types, *atalmt9* mutants showed a reduction in stomatal opening in response to light, whereas the stomatal closure in response to darkness and ABA was not impaired. The lower stomatal aperture resulted in reduced wilting and reduced sensitivity during drought stress (De Angeli et al., 2013b; Figure 5). However, the impaired light-dependent stomatal opening and enhanced drought resistance was not attributed to the malate permeability of the channel. De Angeli and co-workers demonstrated in elaborate patch-clamp analyses that AtALMT9 is permeable for $Cl^-$, and this $Cl^-$ inward current can be activated by physiological concentrations (1 mM) of cytosolic malate (Figure 5). Stomata assays on epidermal peels of *atalmt9* and wild-type plants with opening buffers based on KCl revealed that AtALMT9 mediates physiologically relevant $Cl^-$ currents. This finding was substantiated by electrophysiological studies on *ataltm9* knock-out vacuoles isolated from mesophyll protoplasts which exhibited reduced overall $Cl^-$ currents compared to wild-type vacuoles (De Angeli et al., 2013b). To date, AtALMT9 is the only member of the ALMT family of which the physiological function was clearly attributed to its capability of mediating $Cl^-$ fluxes.

Members of the AtALMT family have been characterized with respect to their intracellular localization and tissue expression, to their electrophysiological properties, and to their physiological function. However, the membrane topology and structural and compositional organization of ALMT channels remain largely ambiguous.

Upon preliminary *in silico* topology analyses (Kovermann et al., 2007), two studies attempted to unravel the topology of ALMT channels in more detail (Motoda et al., 2007, Dreyer et al., 2012).

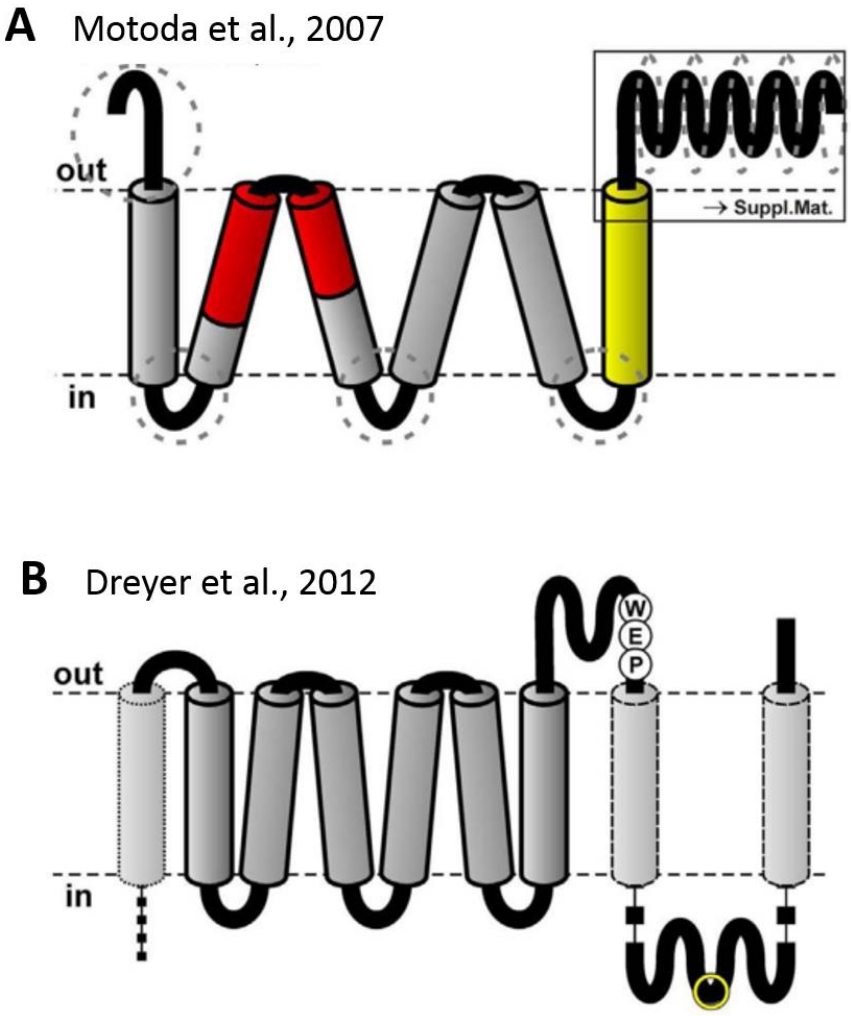


**Figure 6. Model Proposing the Topology of ALMT Channels.**

**(A)** Motoda and co-workers (2007) proposed a model in which the protein TaALMT1 exhibits six transmembrane-spanning domains and both, N- and C- terminus, are located extracellularly. **(B)** In contrast, Dreyer and co-workers (2012) suggest a topology for ALMTs with nine transmembrane domains and the N-terminal end being cytosolic. Adapted from Dreyer et al., 2012.

Motoda and co-workers made use of computer-predictions and immunocytochemical techniques to propose a model of the secondary structure of TaALMT1 (Motoda et al., 2007). The model suggests that TaALMT1 contains six transmembrane domains with the amino (N)- and carboxyl (C)- terminal ends located on the extracellular side of the

plasma membrane (Figure 6). Using sequence information of the genome of 32 fully sequenced plant species a modified topology was suggested a few years later (Dreyer et al., 2012). In this model, the C-terminal half of ALMTs is spanning the membrane twice resulting in extracellular and intracellular C-terminal regions. Furthermore, it was speculated that the larger N-terminal extension may exhibit another membrane spanning region (Figure 6). The discrepancy between both models hampers interpretations and conclusions. More detailed structural analyses of ALMTs would be valuable to address some open questions: The identification of the conduction pathway might add to the understanding of the different substrate specificities, and the determination of the cellular localization of N- and C-termini might enlighten putative regulatory domains. Besides characterizing structural features and the topology, studies on the compositional organization of ALMT channels (i.e. potential homo- and heteromerization) might provide insights into the functional redundancy and regulation of these anion channels.

# 1.3. Salinity as a Tool to Study Transport Processes in Plants

Soil salinity is a central issue for future food production since a quarter to one third of all agricultural land on earth are affected and crop yield is severely comprised (Rengasamy, 2006, Kronzucker and Britto, 2011). Salt accumulation in arable soils is mainly derived from sea water, and from irrigation water that contain salts (Tester and Davenport, 2003), and the predominant salt in saline soil is NaCl (Munns and Tester, 2008).

Salinity tolerance differs widely between plant species and is defined as the ability of plants to maintain growth under saline conditions relative to the growth under non-saline conditions (Møller and Tester, 2007). Salinity tolerance research is therefore particularly important for applied researchers aiming at improving crop productivity under challenging environmental conditions. However, the application of salt stress and studying its effects on plants is also a valuable approach to understand transport processes since many salinity adaptation mechanisms are based on differences in ion movement and controlled ion accumulation and distribution. Although Arabidopsis is a glycophyte species sensitive to moderate levels of NaCl and results on salinity tolerance obtained from Arabidopsis can only be extrapolated to crop species with caution, it is a valuable model plant to study and discover transport processes during salinity (Møller and Tester, 2007). For that purpose, transcriptomics and proteomics are strong tools to identify candidate genes and proteins (Deyholos, 2010, Tester and Davenport, 2003), and Arabidopsis provides unique benefits to understand the role of them using genetic and molecular approaches.

When dealing with salinity (high NaCl concentrations), plants encounter two stress components, the osmotic and the ionic. The osmotic stress is based on the decrease of water potential in the soil surrounding the roots during salinity, which hinders the plant to take up water. The osmotic stress starts immediately and affects stomatal conductance and plant growth. Mechanisms that reduce water loss and increase cellular water uptake such as the production of compatible solutes account for osmotic tolerance (Munns and Tester, 2008). Ionic stress is based on the accumulation of $Na^+$ and $Cl^-$ in

the cytosol, the chloroplasts and the apoplast, where toxic ions interfere with metabolic processes, inhibit photosynthetic processes and dehydrate cells (reviewed in: Teakle and Tyerman, 2010, Munns and Tester, 2008). Although $Na^+$ and $Cl^-$ impact plant physiology differently, both ions exhibit toxic effects on plants simultaneously and their cellular damage is additive (Tavakkoli et al., 2010, Tavakkoli et al., 2011, Geilfus et al., 2015, Munns and Tester, 2008, Teakle and Tyerman, 2010). Ionic tolerance is mainly achieved by two key mechanisms: at the whole-plant level, plants have evolved transport mechanisms that prevent the accumulation of excessive toxic ions in the tissue where they are most detrimental, in the photosynthetically active mesophyll cells. And at the cellular level plants have evolved mechanisms to withstand the toxicity of ions once accumulated to high concentrations, mainly through the sequestration into the vacuole. In the next paragraphs, these salinity adaptation mechanisms will be discussed, and identified and characterized transport proteins involved in these processes will be introduced.

### 1.3.1. Salinity Adaptation Mechanisms at the Whole-Plant Level

The photosynthetically active shoot tissue is more sensitive to the accumulation of $Na^+$ and $Cl^-$ ions during salinity than roots. Hence, a crucial salinity adaptation mechanism on the whole-plant level is the reduction of ion accumulation in the aerial part of the plant. This shoot $Na^+$ and $Cl^-$ exclusion is facilitated at three main control points that are associated with regulated ion transport processes: (i) net uptake at the soil-root interface; (ii) radial transport across the root; and (iii) xylem loading (Figure 6). Notably, the root-to-shoot transfer of ions is not only dependent on regulated transport processes that control net uptake, radial transport and xylem loading, but also on transpiration rates. Transpiration rates have a major influence on $Na^+$ and $Cl^-$ transport and shoot accumulation (Møller and Tester, 2007, Munns and Tester, 2008) and controlled transpiring conditions are therefore a crucial factor when investigating the transport processes that confer adaptation towards saline conditions.

Shoot ion exclusion of $Na^+$ highly correlates with the ability of plants to withstand salt stress (Munns and Tester, 2008). However, also the limitation of $Cl^-$ accumulation has been reported to contribute to salinity tolerance in many plant species (Tavakkoli et al., 2011, Teakle and Tyerman, 2010, Gong et al., 2011, Teakle et al., 2007, Brumós et al., 2010, White and Broadley, 2001, Läuchli et al., 2008, Moya et al., 2003), whereby the genes and proteins that underpin the $Cl^-$ exclusion trait during salinity are less studied than their $Na^+$ counterparts (Teakle and Tyerman, 2010, Henderson et al., 2014, Brumós et al., 2009). The relative importance and efficiency of the exclusion of each ion species dependents on the plant species. For instance, genetic variation in salinity tolerance in some plant species such as wheat correlates with leaf $Na^+$ accumulation but not with $Cl^-$ accumulation (Møller and Tester, 2007, Gorham et al., 1987, Gorham et al., 1990). By contrast, salinity tolerance correlates with $Cl^-$ exclusion in some other plant species (Teakle and Tyerman, 2010, Munns and Tester, 2008), including soybean (Luo et al., 2005) and lotus (Teakle et al., 2007). However, in many plant species, $Na^+$ and $Cl^-$ fluxes and accumulation are thermodynamically coupled (Teakle and Tyerman, 2010).

Besides limiting the accumulation of toxic ions in the shoots by controlling transport processes at the root, plants distribute $Na^+$ and $Cl^-$ within the shoots once they have been translocated in order to minimize the damage in more sensitive cell types. In the following, the transport processes that underpin shoot ion exclusion as well as intercellular ion partitioning within the shoots during salinity will be discussed in more detail.

#### 1.3.1.1. Net Uptake of $Na^+$ and $Cl^-$ Ions at the Soil-Root Interface

The reduction of net ion uptake into root epidermal cells during salinity belongs to the major components of salinity tolerance (Figure 7). The main challenge for plants is thereby the selectivity of ion transport, i.e. excluding toxic ions while maintaining the uptake of beneficial macronutrients such as $K^+$, $Ca^{2+}$ and $NO_3^-$. The net uptake at the soil-root interface is a function of initial ion entry and efflux of ions back into the soil.

Both, the concentration gradient and membrane potential at the plasma membrane favor the passive uptake of $Na^+$ into root cells (Munns and Tester, 2008). This influx is likely

to occur through non-selective cation channels (NSCCs) (reviewed by Demidchik and Maathuis, 2007), including cyclic nucleotide-gated channels (CNGCs) (reviewed by Kaplan et al., 2007) and glutamate-activated channels (GLRs) (reviewed by Davenport, 2002), and possibly also via members of the high-affinity $K^+$ transporter (HKT) family and other $K^+$ transport proteins (Haro et al., 2005, Laurie et al., 2002, Craig Plett and Møller, 2010, Kronzucker and Britto, 2011). Most of the $Na^+$ that enters root cells is likely transported back out of the cell into the soil via plasma membrane $Na^+/H^+$ antiporters (Tester and Davenport, 2003, Blumwald et al., 2000, Pardo et al., 2006). However, the active $Na^+$ efflux is insufficient to entirely counteract the passive unidirectional influx (Jacoby and Hanson, 1985). Efflux to the soil and apoplast is presumably facilitated by active transport (Sun et al., 2009). AtSOS1, a $Na^+/H^+$ antiporter at the plasma membrane in the root stele and epidermal cells of the root tip was identified by mapping of a salt overly sensitive phenotype in Arabidopsis and is a candidate for $Na^+$ root exclusion (Wu et al., 1996, Ding and Zhu, 1997, Shi et al., 2000, Shi et al., 2002). Knock-out mutants that lack AtSOS1 over-accumulate $Na^+$ in shoots and roots (Shi et al., 2000), whereas plants that overexpress the transporter have reduced levels of $Na^+$ in the roots and the xylem (Shi et al., 2003). AtSOS1 is regulated by the protein kinase AtSOS2, which is in turn regulated by the $Ca^{2+}$ binding protein AtSOS3 (Qiu et al., 2002); together, these proteins constitute a crucial component of salinity tolerance, the so called SOS pathway.

$Cl^-$ enters the root by active $H^+$-dependent transport at low concentrations (Beilby and Walker, 1981, Felle, 1994) and passively by channels at high $Cl^-$ concentrations (Skerrett and Tyerman, 1994). Efflux of $Cl^-$ from the roots has also been observed in several plant species and appears to contribute to salinity tolerance (Teakle and Tyerman, 2010, Britto et al., 2004, Lorenzen et al., 2004).

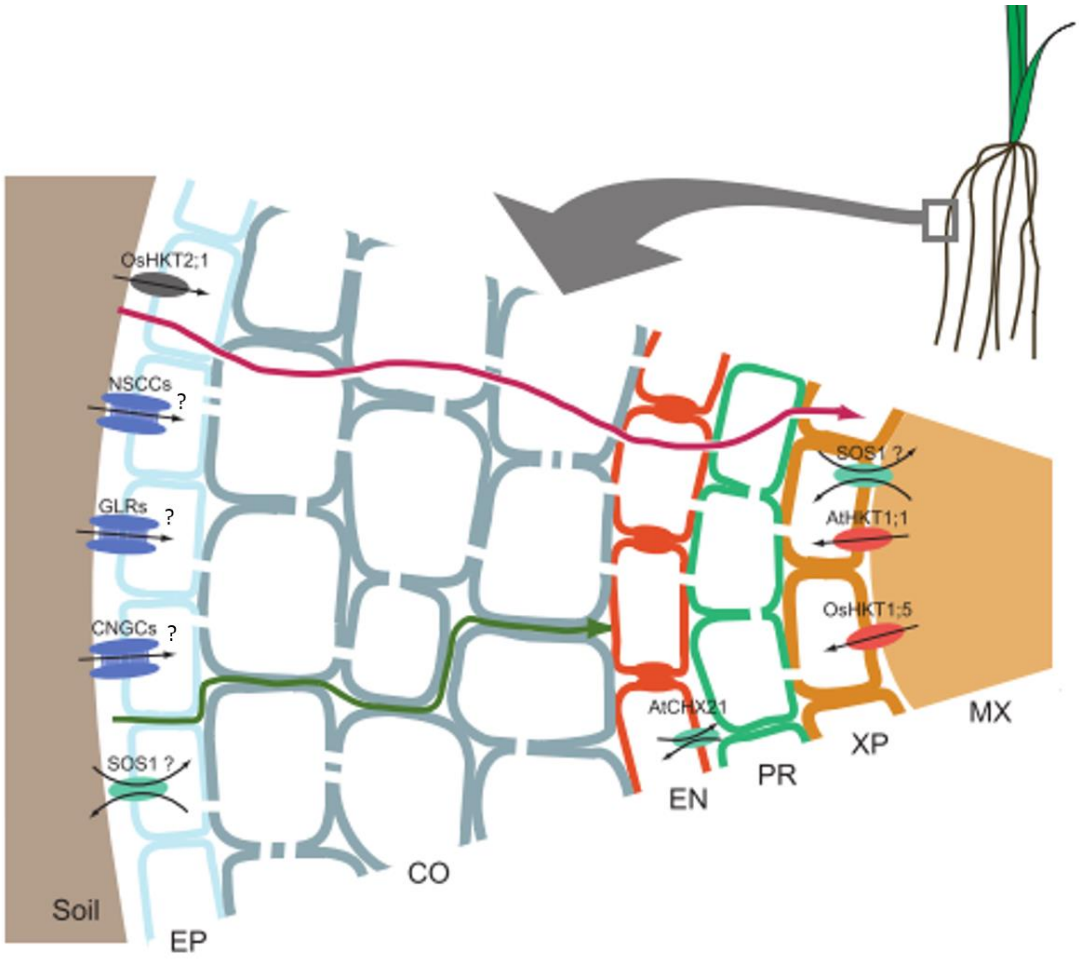


**Figure 7. Transport of $Na^+$ across the Root during Salinity.**

Depicted are transport proteins that are putatively involved in the transport of $Na^+$ in roots during salt stress. Initial entry of $Na^+$ from the soil to the epidermal cells was suggested to be passively mediated by NSCCs (non-selective cation channels), GLRs (glutamate-activated channels) and CNGCs (cyclic nucleotide-gated channels) as well as by antiporters of the HKT family. Efflux might be catalyzed by $Na^+/H^+$ antiporters such as SOS1at the epidermal plasma membrane. Radial $Na^+$ fluxes across the root might be partially apoplastic (green route), but ions might take predominantly the symplastic pathway (purple route). In the endodermis, trans-plasma membrane transport of $Na^+$ might be controlled by AtCHX21. Once reached the stele, loading of $Na^+$ into the xylem vessels is potentially catalyzed by SOS1, while xylem retrieval into the xylem parenchyma cells is mediated by AtHKT1;1 and OsHKT1;5 in rice (*Oryza sativa*). EP, epidermis; CO, cortex; EN, endodermis; PR, pericycle; XP, xylem parenchyma; MX, metaxylem. Adapted from Plett and Møller, 2010.

1.3.1.2. Radial Ion Transport across the Roots

After initial entry, the ions pass several cell layers (the epidermis, the cortex, the endodermis, and the stele including pericycle and xylem parenchyma cells) before reaching the xylem vessels in the center of the root (Figure 7). This process is called radial transport across the root and ions can follow a symplastic and transcellular or an apoplastic route (Pitman, 1982). In general, apoplastic ion flow could occur up to the endodermis, at which point transport across the plasma membrane for entry into the symplast is required for further radial movement. However, in Arabidopsis apoplastic radial transport of $Na^+$ was shown to be minimal (Essah et al., 2003). Symplastic transport denotes the translocation of molecules within the cytoplasm of nonvascular cells and the movement of these molecules from cell to cell via plasmodesmata (Pickard, 2003). Ions are not uniformly distributed along the different cell layers of the root, providing evidence for symplastic radial transport, and suggesting that mechanisms exists that control the accumulation of ions in specific cell types (Läuchli et al., 2008, Craig Plett and Møller, 2010, Storey et al., 2003). In the endodermis of Arabidopsis, AtCHX21, a member of the cation/$H^+$ exchanger (CHX) family, has been suggested to contribute to the control of radial $Na^+$ transport towards the xylem (Hall et al., 2006). However, its mode of action remains to be elucidated.

1.3.1.3. Net Loading of $Na^+$ and $Cl^-$ into the Root Xylem

Similar to net uptake of ions at the root surface, the amount of $Na^+$ and $Cl^-$ in the root xylem is dependent on xylem loading and retrieval from the xylem vessels into the xylem parenchyma cells (Figure 7). Controlling this process is crucial since following the transport in the xylem vessels $Na^+$ and $Cl^-$ ions are moved with the transpiration stream to the shoots.

The loading of $Na^+$ might be an active process, as supported by the fact that AtSOS1 is expressed in the plasma membrane of stelar cells and *atsos1* mutants accumulate less shoot $Na^+$ than wild-type plants (Shi et al., 2002). However, the function of AtSOS1 in xylem loading has not been fully elucidated (Craig Plett and Møller, 2010). The retrieval of $Na^+$ back to the xylem parenchyma cells before it reaches the shoots is better

understood. In Arabidopsis, AtHKT1;1, that belong to the HKT family, plays a fundamental role in this process (Davenport et al., 2007). AtHKT1;1 is a $Na^+$-selective uniporter that is highly expressed in the plasma membrane of root stelar cells and that catalyzes the influx of $Na^+$ from the xylem vessels back into xylem parenchyma cells. Thereby, AtHKT1;1 reduces root-to-shoot ion transfer and $Na^+$ accumulation in shoots. Based on its function it is intuitive that *hkt1;1* knock-out mutants show elevated xylem (Sunarpi et al., 2005) and shoot $Na^+$ levels during salinity (Mäser et al., 2002). In contrast, cell type-specific overexpression of *HKT1;1* in stelar root cells reduces shoot $Na^+$ contents by 37 to 64 % (Møller et al., 2009). Interestingly, also natural variations of *HKT1;1* expression correlate inversely with shoot $Na^+$ accumulation in several Arabidopsis accessions (Rus et al., 2006, Jha et al., 2010). In addition, mutant plants of the transcription factor ABI4 (Shkolnik-Inbar et al., 2013) and ARR1 and ARR12 (Mason et al., 2010) exhibit elevated expression levels of *HKT1;1* that result in reduced shoot $Na^+$ accumulation. Hence, in several studies it became apparent that the transcriptional regulation of *HKT1;1* is sufficient to manipulate whole-plant $Na^+$ accumulation.

Less is known about the candidate transport proteins that mediate net xylem loading of $Cl^-$. In stelar root cells different types of anion conductance were identified by patch-clamping that might contribute to the passive delivery of $Cl^-$ to the xylem through channels (Köhler and Raschke, 2000, Gilliham and Tester, 2005). However, the molecular identity of the corresponding genes remains to be discovered. Recently, a member of the AtNPF family, AtNPF2.4, has been found to be localized at the plasma membrane of the root stele and to facilitate electrochemically passive $Cl^-$-selective transport (Li et al., 2015). AtNPF2.4 was suggested to be involved in $Cl^-$ loading into the root xylem and therefore to putatively contribute to the regulation of root-to-shoot transfer of $Cl^-$ during salt stress (Li et al., 2015).

#### 1.3.1.3. Partitioning of $Na^+$ and $Cl^-$ within the Shoots

The capacity of plants to prevent the transport of toxic ions to the shoots is limited. In addition, the majority of $Na^+$ and $Cl^-$ that is delivered to the shoots remain in the shoots,

because for most plant species the recirculation of these ions to the roots via phloem transport is negligible (Davenport et al., 2007, Munns, 2002, Munns and Tester, 2008, Tester and Davenport, 2003). Therefore, once delivered to the aerial part, plants allocate toxic ions within the shoot. In fact, $Na^+$ and $Cl^-$ accumulation was observed preferentially in old leaves (Craig Plett and Møller, 2010 and references therein), in the leaf margins (Shapira et al., 2009), and in the epidermal cells (Huang and Van Steveninck, 1989, James et al., 2006, Karley et al., 2000), to avoid toxicity in more photosynthetically active cells such as mesophyll cells. The genetic basis of the partitioning of $Na^+$ and $Cl^-$ within the shoots is not known.

### 1.3.2. Salinity Adaptation Mechanisms at the Cellular Level

When having reached the shoots, $Na^+$ and $Cl^-$ must be kept at low concentrations in the cytosol to not interfere with cellular metabolism. For that purpose plants load large quantities of both ions into the vacuole. The importance of this removal of toxic ions from the cytosol becomes apparent when determining whole-leaf $Na^+$ concentrations that might commonly reach 200 mM while the leaf is still physiologically functional (Munns and Tester, 2008). At these concentrations enzyme activity would be completely repressed, if the ions and enzymes are not spatially separated (Munns and Tester, 2008). Notwithstanding, *in vitro* experiments showed that enzymes in halophytic plants are not less sensitive to salt exposure than the corresponding enzymes of glycophytes. This observation suggests that salinity adaptation mechanisms are not based on the evolution of tolerance of enzymatic functions in plants from saline environments; however, the capacity of intracellular ion compartmentation in shoots partially determines salinity tolerance. Next, the functional role of vacuolar ion sequestration during salinity will be discussed, and thereby some questions regarding its contribution to salt stress tolerance will be raised (Figure 8).

1.3.2.1. Intracellular Ion Sequestration- The Vacuole, Who Else?!

Numerous studies attempted to increase the ion sequestration efficiency of a broad variety of plant species during salinity in order to enhance performance and productivity under these unfavorable conditions. Since many vacuolar transport processes are driven by the electrochemical gradient established by $H^+$-pumps, one strategy to enhance vacuolar sequestration is the manipulation of the $H^+$-pumping activity across the tonoplast. When overexpressing the V-PPase gene *AtAVP1* of Arabidopsis, transgenic plants were more resistant to high concentrations of NaCl, presumably through increased sequestration of toxic ions into the vacuole (Gaxiola et al., 2001). In accordance, based on the enhanced vacuolar $H^+$-gradient, isolated vacuolar membrane vesicles derived from transgenic plants showed enhanced cation uptake, and on the whole-plant level leafs accumulated higher $Na^+$ concentrations (Gaxiola et al., 2001). This study opened a new avenue to engineer salt-tolerant crop plants. Therefore, ever since, the *AtAVP1* gene or corresponding V-PPase genes from other plant species were used to manipulate salinity tolerance in numerous plant species, including sugar cane (Kumar et al., 2014), cotton (Pasapula et al., 2011, Zhang et al., 2011), creeping bentgrass (Li et al., 2010), tomato (Bhaskaran and Savithramma, 2011), tobacco (Arif et al., 2013, Li et al., 2014, Dong et al., 2011, Duan et al., 2007), barley (Schilling et al., 2014), apple (Dong et al., 2011), sugar beet (Wu et al., 2015), and Arabidopsis that overexpressed the V-PPase gene of Eucalyptus (Gamboa et al., 2013), or the halophytes *Suaeda corniculata* (Liu et al., 2011) or *Kalidium foliatum* (Yao et al., 2012).

A similar approach is the overexpression of antiporters at the tonoplast that catalyze $H^+$-dependent cation uptake into the vacuole. Members of the NHX ($Na^+/H^+$ antiporter) family, which has eight isoforms in Arabidopsis (Yokoi et al., 2002), have been shown to facilitate cation/$H^+$ exchange at various cellular membranes in plants (Figure 8). For instance AtNHX7, also known as AtSOS1, catalyzes the efflux of $Na^+$ across the plasma membrane (Shi et al., 2000). By contrast, the isoforms AtNHX1 to AtNHX4 are located at the vacuolar membrane and AtNHX1 (and AtNHX2) were subject to intense research with respect to its implication in salinity tolerance acting as a vacuolar $Na^+/H^+$ antiporter. Overexpression of *AtNHX1* and *AtNHX2* has been shown to confer halotolerance in several plant species (Apse et al., 1999, Munns and Tester, 2008, Leidi

et al., 2010, Craig Plett and Møller, 2010 and references therein). Yet, some studies indicated that the improved performance during salinity is due to an ameliorated $K^+$ compartmentation (Jiang et al., 2010, Leidi et al., 2010, Rodriguez-Rosales et al., 2008), challenging the widespread consensus of NHX1 being the major player in vacuolar $Na^+$ sequestration to avert ion toxicity. Likewise, the analysis of *atnhx1 atnhx2* mutants in Arabidopsis revealed defects in leaf development in the absence of $Na^+$ (Apse et al., 2003), and provided evidence for a role of AtNHX1 and AtNHX2 in vacuolar $K^+$ accumulation during cell expansion and stomatal movement (Bassil et al., 2011b, Barragán et al., 2012, Andrés et al., 2014). By contrast, the double mutant showed similar sensitivity to salinity and enhanced shoot $Na^+$ accumulation (Barragán et al., 2012). Of note, cellular metabolism is highly dependent on $K^+$, since this cation is as an essential co-factor for numerous enzymes which can be displaced but not substituted by $Na^+$ (Serrano, 1996). Hence, not only $Na^+$ sequestration, but also the maintenance of a favorable $K^+/Na^+$ ratio in the cytosol contributes to salt tolerance.

With respect to intracellular $Cl^-$ uptake, CLCc and CLCg have been suggested to be involved in salinity tolerance (Jossier et al., 2010, Nguyen et al., 2015). Both are vacuolar $Cl^-$ transport proteins, and *clcc* and *clcg* mutant plants as well as the double knock-out show sensitivity to salt stress. However, their distinct physiological mode of action during the response to salinity remains elusive.

In 2010, Krebs and coworkers provided evidence for a new piece in the salinity tolerance puzzle (Krebs et al., 2010). Astonishingly, in that study it was shown that not only the regulated transport across the tonoplast contributes to intracellular ion sequestration during salt stress. They made use of two transgenic Arabidopsis lines, one that lacked the vacuolar V-ATPase at the tonoplast, and one that lacked the V-ATPase at the TGN/EE. Mutant plants deficient in the tonoplast-localized V-ATPase were impaired in nutrient uptake, while no differences in salinity tolerance were observed. Yet, mutants lacking the V-ATPase at the TGN/EE showed reduced tolerance to salt stress (Krebs et al., 2010), indicating that the $H^+$-pump activity at this organelle contributes to intracellular ion sequestration and hence to cellular tolerance during salinity (Figure 8).

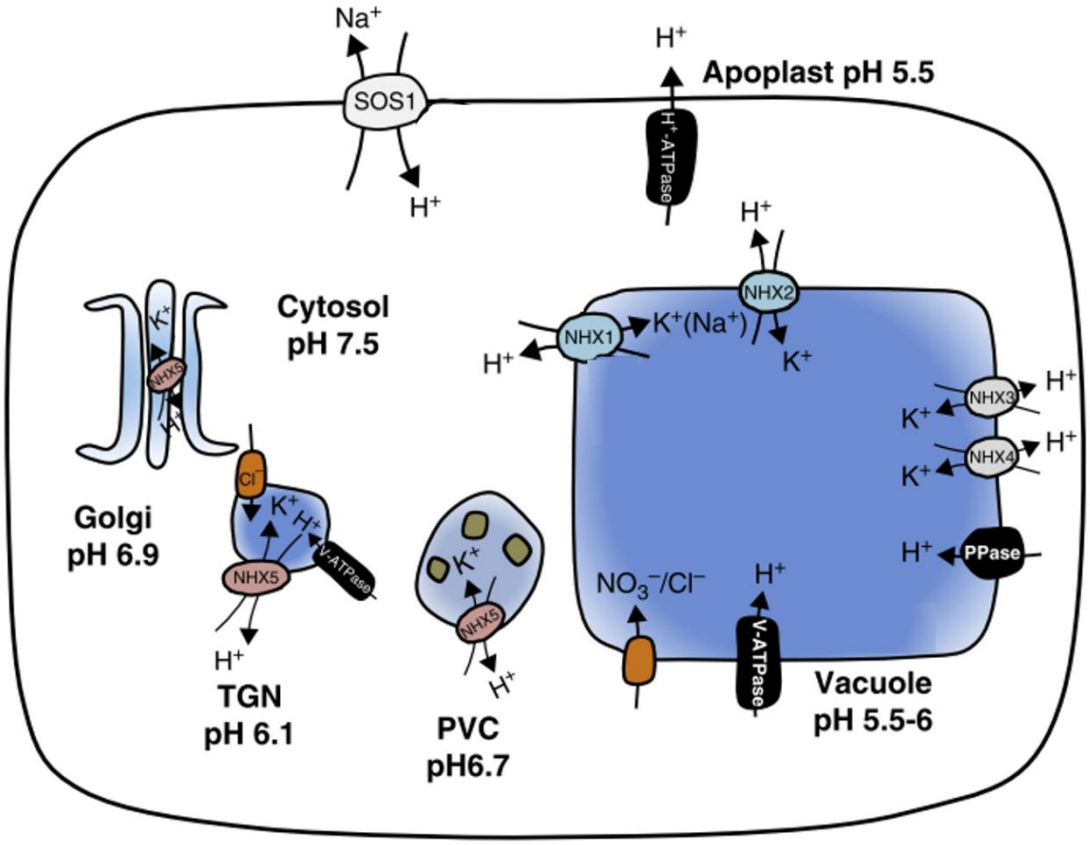


**Figure 8. Mechanisms of Intracellular $Na^+$ Compartmentation and $K^+$ Homeostasis upon Salt Exposure.**

Schematic diagram of transport proteins involved in intracellular $Na^+$ sequestration and $K^+$ homeostasis during salinity in Arabidopsis. The pH gradient and membrane potential required for secondary active transport of cations across endomembranes is established by the V-PPase (tonoplast) and the V-ATPase (TGN, *trans*-golgi network; and tonoplast). Cation/$H^+$ exchanger that belong to the AtNHX family have been proposed to mediate $Na^+$ and $K^+$ transport across the plasma membrane (AtNHX7/AtSOS1), the tonoplast (AtNHX1 to AtNHX4) and across the membrane of the Golgi, the TGN and pre-vacuolar compartments (PVC; AtNHX5, and also AtNHX6 which is not shown). AtNHX proteins localized at endomembranes were demonstrated to contribute to intracellular cation homeostasis during salinity. Note that transporters and channels that mediate $Cl^-$ sequestration as well as the cation/$Cl^-$ cotransporter (CCC) that is localized at the TGN are not depicted. Adapted from Bassil and Blumwald (2014).

This observation was substantiated by studies on two endosomal AtNHX antiporters in Arabidopsis. AtNHX5 and AtNHX6 localize to the Golgi and the TGN and were shown to be crucial for controlling organelle pH and cation homeostasis (Bassil et al., 2011a, Reguera et al., 2015). In addition, *atnhx5 atnhx6* double mutants were more sensitive to salinity (Bassil et al., 2011a; Figure 8). Overexpressing isoforms of endosomal NHX antiporters such as NHX5 enhanced salt stress tolerance in several plant species which is putatively based on altered endosomal cation homeostasis (Rodriguez-Rosales et al., 2008, Bassil et al., 2012). Recently, the cation/$Cl^-$ cotransporter (CCC) of Arabidopsis and *Vitis vinifera* was shown to localize to the TGN/EE and was also attributed a role in salinity tolerance (Henderson et al., 2015). Nevertheless, it has not been elucidated yet how endosomal pH and/or ion homeostasis influence salinity tolerance. Endosomal trafficking and vesicle fusion to the vacuole has been suggested to be crucial for cellular responses to abiotic stresses (Mazel et al., 2004, Leshem et al., 2006, Hamaji et al., 2009). Therefore, it has been proposed that excessive $Na^+$ might be sequestered within vesicles that subsequently fuse with the vacuole to contribute to the reduction of cytosolic $Na^+$ (Bassil et al., 2012).

#### 1.3.2.2. Vacuolar Ion Uptake during Salinity- More than a Waste Storage?

The role of the vacuole in ion sequestration during salinity is still not well understood. In recent years, fluxes across endosomal membranes were attributed an increasing role in intracellular ion sequestration, and the transport proteins that mediate $Na^+$ and $Cl^-$ uptake across the tonoplast are ambiguous. In addition, the functional role of vacuolar ion uptake during salinity other than the detoxification of toxic ions into mesophyll vacuoles has not been intensively considered to date. For example, questions about the functional significance of vacuolar ion uptake rapidly after onset of salinity or in other tissues than mesophyll cells has not been studied. However, studies have indicated that the vacuolar function might go beyond the role of a trash bin for toxic ions. For instance, the vacuolar storage capacity in the vasculature of roots has been shown to influence whole-plant ion accumulation and long-distance transport of heavy metals (Peng and Gong, 2014), and durum wheat genotypes that differed in root-to-shoot ion translocation and shoot ion exclusion capacity during salinity showed differences in

vacuolar ion storage along the radial root (Läuchli et al., 2008). A potential role of vacuolar ion uptake on whole-plant ion movement under salt stress has not been investigated. It will be of interest to study the link and coordination of vacuolar and plasma membrane fluxes under high NaCl concentrations. Hence, the identification of further vacuolar transport proteins that are involved in the storage of $Na^+$ or $Cl^-$ would tremendously add to our understanding of the role of vacuolar ion uptake and its relative contribution to the adaptation mechanisms in response to salinity. For instance, the Arabidopsis AtALMT9 has been recently identified as the first vacuolar $Cl^-$ channel in plants. Investigating *atalmt9* mutant plants under high salinity could be valuable to understand the consequences of impaired vacuolar $Cl^-$ uptake on whole-plant transport processes including ion accumulation and distribution.

# 1.4. Aims of this Thesis

Vacuolar ion uptake into the vacuole is of tremendous importance for a multitude of physiological processes in plants. The identification and characterization of transport proteins that catalyze solute fluxes across the tonoplast add to our understanding of the role of vacuolar ion uptake in plant physiology.

*AtALMT9* belongs to a gene family in Arabidopsis that encodes for anion channels that mediate inward rectification across the vacuolar and the plasma membrane, corresponding to anion efflux out of the cytosol. Specifically, AtALMT9 is located at the tonoplast, is permeable for malate, and clusters in a subfamily (clade II) that encompasses four more AtALMT members which are all putatively vacuolar anion channel. However, the topology, structural organization and potential multimerization status of ALMT channels remains ambiguous, which constricts studies on their regulation and physiological function.

Besides being permeable for malate, AtALMT9 has been recently identified as the first genuine vacuolar channel that mediates the uptake of $Cl^-$ into the vacuole. Based on its high expression in guard cells, mutant plants lacking AtALMT9 exhibit impaired stomatal opening. The functional role of AtALMT9 was thereby studied under physiological $Cl^-$ concentrations, but it has not been investigated whether this $Cl^-$ channel might be also involved in anion uptake under excessive $Cl^-$ concentrations such as under salinity.

Notably, AtALMT9 is not solely expressed in guard cells, and its putative physiological roles in vacuolar anion uptake in other tissues and organs as well as the function of ALMT9 homologs in other plant species have not been characterized to date.

The goal of this thesis was to address the following five research questions to better understand the structural organization of ALMT9 and its physiological function as vacuolar anion channel.

Regarding the structure and composition of AtALMT9:

(i) What is the topology and structure-function relation of AtALMT9? Is AtALMT9 a channel complex composed of several subunits?
(ii) Does AtALMT9 interact with other vacuolar AtALMT channels?

Regarding the role of AtALMT9 in vacuolar $Cl^-$ uptake upon salt exposure:

(iii) Is AtALMT9 involved in responses to salt stress? What is the role and relative contribution of vacuolar anion uptake to salinity adaptation mechanisms?

Regarding the physiological function of ALMT9 in specific organs:

(iv) Is AtALMT9 involved in rapid vacuolar solute uptake during seed germination? Is its role more pronounced under challenging environmental conditions such as salt stress?
(v) Does ALMT9 contribute to malate storage in fruits? As a model organisms the berries of grapevine (*Vitis vinifera*) have been investigated.

# 2. Chapter I:

## Identification of a Probable Pore-Forming Domain in the Multimeric Vacuolar Anion Channel AtALMT9

Jingbo Zhang*[12], Ulrike Baetz*[1], Undine Krügel[1], Enrico Martinoia[1] and Alexis De Angeli[13]

[1] Department of Plant and Microbial Biology, University of Zurich, 8008 Zurich, Switzerland

[2] Current address: Division of Biological Sciences, Cell and Developmental Biology Section, University of California, San Diego, CA 92093-0116, USA

[3] Current address: Institut de Biologie Intégrative de la Cellule, CNRS, 91190 Gif-Sur-Yvette, France

* These authors contributed equally to this work

Published in *Plant Physiology* 2013 Oct; 163 (2):830-843

Author Contributions:

J.Z. and U.B. performed cloning, subcellular localization and expression analysis. Electrophysiological characterization of the citrate block and the mutant channels was done by J.Z., U.B. and A.D.A. U.K. conducted biochemical characterization of AtALMT9 multimers. E.M. and A.D.A. supervised the project. The manuscript was written by J.Z., U.B. and A.D.A.

# Identification of a Probable Pore-Forming Domain in the Multimeric Vacuolar Anion Channel AtALMT9[1][W][OPEN]

**Jingbo Zhang[2], Ulrike Baetz[2], Undine Krügel, Enrico Martinoia, and Alexis De Angeli***

Institute of Plant Biology, University of Zürich, CH–8008 Zurich, Switzerland

Aluminum-**a**ctivated malate transporters (ALMTs) form an important family of anion channels involved in fundamental physiological processes in plants. Because of their importance, the role of ALMTs in plant physiology is studied extensively. In contrast, the structural basis of their functional properties is largely unknown. This lack of information limits the understanding of the functional and physiological differences between ALMTs and their impact on anion transport in plants. This study aimed at investigating the structural organization of the transmembrane domain of the Arabidopsis (*Arabidopsis thaliana*) vacuolar channel AtALMT9. For that purpose, we performed a large-scale mutagenesis analysis and found two residues that form a salt bridge between the first and second putative transmembrane $\alpha$-helices (TM$\alpha$1 and TM$\alpha$2). Furthermore, using a combination of pharmacological and mutagenesis approaches, we identified citrate as an "open channel blocker" of AtALMT9 and used this tool to examine the inhibition sensitivity of different point mutants of highly conserved amino acid residues. By this means, we found a stretch within the cytosolic moiety of the TM$\alpha$5 that is a probable pore-forming domain. Moreover, using a citrate-insensitive AtALMT9 mutant and biochemical approaches, we could demonstrate that AtALMT9 forms a multimeric complex that is supposedly composed of four subunits. In summary, our data provide, to our knowledge, the first evidence about the structural organization of an ion channel of the ALMT family. We suggest that AtALMT9 is a tetramer and that the TM$\alpha$5 domains of the subunits contribute to form the pore of this anion channel.

The transport of ions across cellular membranes is mediated by specialized proteins that catalyze the transfer of charged molecules across hydrophobic lipid bilayers. Based on the thermodynamics, two major classes of transport systems can be distinguished: (1) passive transporters such as ion channels, which catalyze the flux of solutes down the electrochemical gradient, and (2) active transporters like pumps and antiporters, which transport molecules against their electrochemical gradient. Independent of the nature of the transport system, the flux of ions across membranes is crucial for a wide range of physiological functions in plants. Among others, ion transport is involved in intracellular pH regulation, metal tolerance, stomatal movement, cellular signaling, plant nutrition, and cell expansion (Roelfsema and Hedrich, 2005; Kim et al., 2010; Barbier-Brygoo et al., 2011). Despite the importance of anion transport in plant physiology, only in the last decade has the molecular identity of anion transport proteins started to be unveiled by identifying the chloride channel (CLC), slow anion channel (SLAC), and aluminum-activated malate transporter (ALMT) families. Their discovery has been a fundamental breakthrough in understanding the molecular mechanisms of anion homeostasis and its roles in various aspects of plant cell physiology (Ward et al., 2009; Barbier-Brygoo et al., 2011; Hedrich, 2012; Martinoia et al., 2012).

The CLC family consists of both anion channels and secondary active transporters, which are ubiquitously expressed in all living organisms. In Arabidopsis (*Arabidopsis thaliana*), the first identified and characterized member of the family was AtCLCa (Hechenberger et al., 1996; Geelen et al., 2000). AtCLCa is targeted to the tonoplast and acts as a $2NO_3^-/H^+$ antiporter (De Angeli et al., 2006). In planta, AtCLCa represents a major vacuolar nitrate transporter driving the accumulation of this anion into the vacuole. Subsequent studies revealed that all other Arabidopsis CLCs are likewise localized in intracellular membranes but feature different cellular functions (Barbier-Brygoo et al., 2011).

The SLAC protein family was identified in the last decade (Negi et al., 2008; Vahisalu et al., 2008). Despite its recent discovery, the characterization of this plant anion transporter family proceeded rapidly (Negi et al., 2008; Vahisalu et al., 2008; Geiger et al., 2009, 2010; Brandt et al., 2012). SLAC1, the first identified member of the family, is involved in slow-type anion currents across the plasma membrane of plant cells (Negi et al., 2008; Vahisalu et al., 2008). This ion channel is expressed in guard cells, where it mediates the efflux of anions into the apoplast, a process that is

[1] This work was supported by the Chinese Scholarship Council (to J.Z.), by a long-term EMBO fellowship (to A.D.A.), and by the Swiss National Foundation (to U.B., E.M., and A.D.A.).

[2] These authors contributed equally to the article.

* Address correspondence to deangeli.alexis@gmail.com.

The author responsible for distribution of materials integral to the findings presented in this article in accordance with the policy described in the Instructions for Authors (www.plantphysiol.org) is: Alexis De Angeli (deangeli.alexis@gmail.com).

[W] The online version of this article contains Web-only data.

[OPEN] Articles can be viewed online without a subscription.

www.plantphysiol.org/cgi/doi/10.1104/pp.113.219832

 

fundamental for stomata closure. SLAC1 regulates the stomatal aperture in response to different stimuli such as abscisic acid and high $CO_2$ and ozone concentrations (Negi et al., 2008; Vahisalu et al., 2008). In addition, the activity of SLAC1 is controlled by different kinases (Geiger et al., 2009, 2010) that are part of various signaling pathways. This multiple regulation of SLAC1 suggests that it plays a critical role in the integration of different environmental stimuli.

ALMTs are membrane proteins exclusive to plants. In Arabidopsis, this family consists of 14 members that can be grouped into three clades (Kovermann et al., 2007). The first member of the ALMT family, TaALMT1, was identified in wheat (*Triticum aestivum*) by Sasaki et al. (2004) when screening for genes associated with aluminum resistance. They provided evidence that TaALMT1 as well as AtALMT1, its homolog in Arabidopsis, are channels that catalyze the efflux of malate across the plasma membrane of root cells (Yamaguchi et al., 2005; Hoekenga et al., 2006). This exudation of organic acids into the soil facilitates the detoxification of environmental $Al^{3+}$. Besides contributing to $Al^{3+}$ tolerance, ALMTs have been found to exhibit other important physiological functions. AtALMT12 has been proposed to mediate rapid anion currents across the plasma membrane of guard cells in order to induce stomata closure (Meyer et al., 2010). AtALMT9 and AtALMT6 have been shown to be channels localized in the tonoplast that mediate the export of malate into the vacuole (Kovermann et al., 2007; Meyer et al., 2011). AtALMT6 is predominantly expressed in guard cells, where its activity is regulated by cytosolic $Ca^{2+}$ and vacuolar pH (Meyer et al., 2011). In contrast, AtALMT9 is widely expressed in several plant tissues, such as the mesophyll and guard cells. Recently, AtALMT9 was shown to play a crucial role in stomata movement, where it functions as a malate-activated chloride channel (De Angeli et al., 2013).

The knowledge about ion channel structures has expanded considerably in the last 20 years. Notably, various three-dimensional structures of such proteins have been solved (Choe, 2002; Jentsch, 2008; Traynelis et al., 2010). This has boosted the research into and the understanding of structure-function relations in transport systems. Among the anion channel families described above, the structure has been determined for CLCs (Dutzler et al., 2002) and SLACs (Chen et al., 2010). Additionally, large structure-function analyses have been conducted, providing detailed knowledge on the molecular basis underlying the ion channel functionality of these families. In contrast, little information was revealed about the structure of ALMTs by describing an important phosphorylation site (Ligaba et al., 2009; Furuichi et al., 2010) and by providing data on the topology (Motoda et al., 2007; Dreyer et al., 2012). However, the proposed models in these studies do not entirely coincide regarding the number of transmembrane-spanning domains, the cellular orientation of the N terminus, and the organization of the C-terminal domain. Therefore, the structural organization of ALMTs is still ambiguous.

In this study, we performed a large-scale mutagenesis analysis of the transmembrane domain (TMD) of Arabidopsis ALMTs using the vacuolar channel AtALMT9 as a model. The aim was to identify regions of the TMD that potentially exhibit functional relevance by forming the pore or the voltage sensor. For that purpose, we took advantage of citrate, which we identified as an open channel blocker of AtALMT9. The use of this blocker allowed elucidation of the structural details of ion channels, such as the quaternary organization and pore-forming domains, when no crystal structure was available (MacKinnon, 1991; Yellen et al., 1991; Ferrer-Montiel and Montal, 1996; Linsdell, 2005). By this means, it is possible to show, for instance, that potassium channels are tetramers and to identify their "selectivity filter" domain (MacKinnon and Yellen, 1990; MacKinnon, 1991). Thus, by using citrate, we pharmacologically investigated structure-function relations in AtALMT9. We identified a region adjacent to and within the fifth putative TMD that is supposedly involved in forming the permeation pathway of AtALMT9. Moreover, we demonstrated that AtALMT9 is a multimeric channel of probably four subunits in which the monomers participate in forming the pore.

## RESULTS

### Citrate Inhibits AtALMT9-Mediated Malate Currents

Blocking agents represent a common tool as reporter molecules to analyze functional and structural features of ion channels. In an attempt to disclose a blocker of the vacuolar channel AtALMT9, we were guided by a previous finding in which citrate was suggested to competitively inhibit malate uptake across the tonoplast (Rentsch and Martinoia, 1991). In order to test whether citrate is a blocker of AtALMT9, we isolated vacuoles from transiently transformed tobacco (*Nicotiana benthamiana*) protoplasts that overexpressed AtALMT9-GFP (OE AtALMT9). We used the patch-clamp technique to measure macroscopic currents mediated by AtALMT9 in the cytosolic-side-out excised patch configuration (Fig. 1). To avoid rectification due to ion concentration gradients between the two sides of the patched membrane, we performed experiments in symmetric ionic conditions (100 mM $malate_{vac}$/100 mM $malate_{cyt}$). Patches obtained from OE AtALMT9 tobacco vacuoles displayed inward-rectifying malate currents with time-dependent relaxations and a mean amplitude of $-1.44 \pm 0.51$ nA at $-120$ mV, as reported in previous studies (Fig. 1A; Table I; Kovermann et al., 2007; for convention details regarding the applied voltage, see "Materials and Methods"). Even though citric acid is to 97% a tricarboxylate at pH 7.5 and exhibits similarities to the dicarboxylate malate (Fig. 1B), we could not detect a

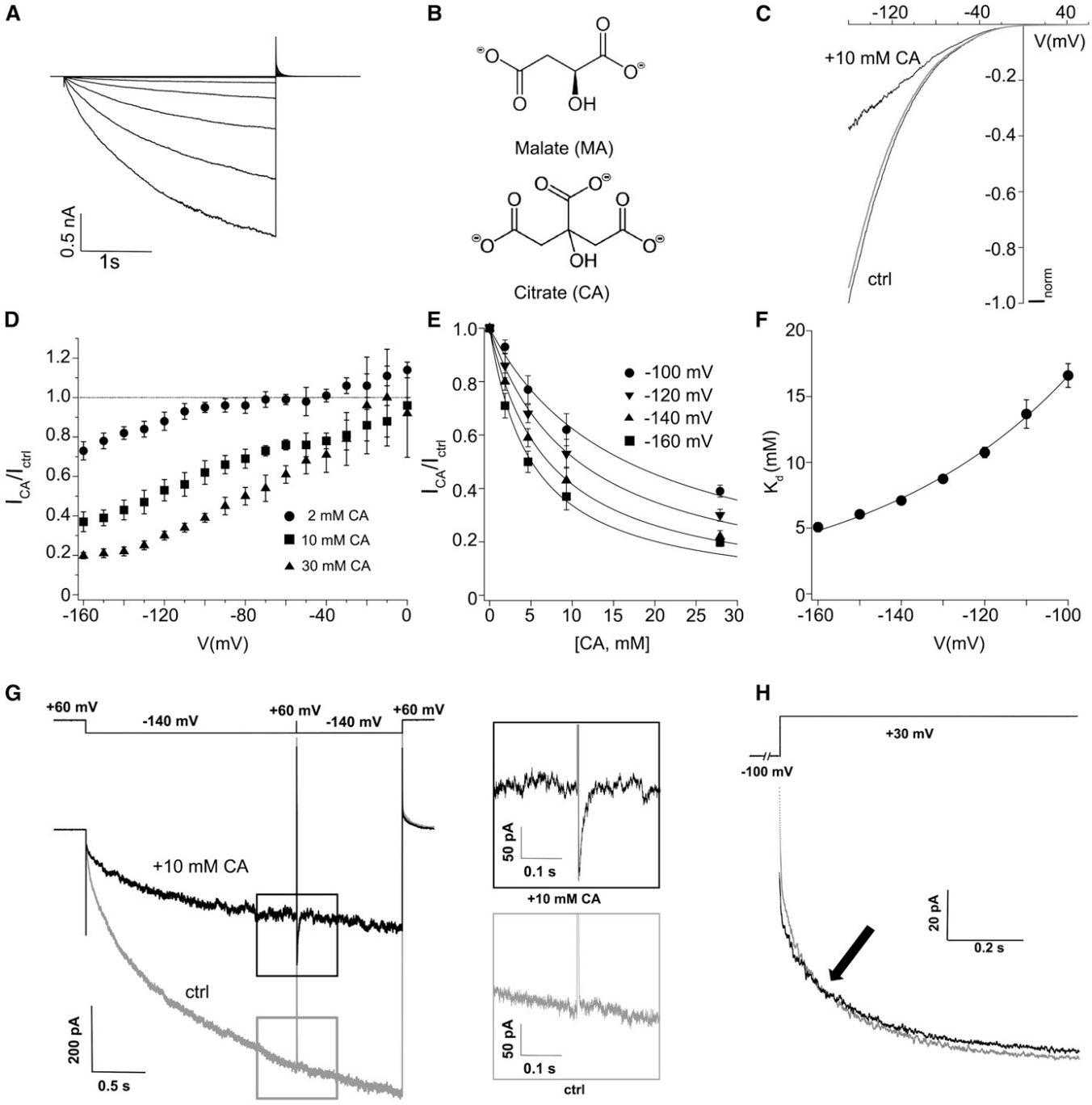


**Figure 1.** Citrate is a blocker of AtALMT9-mediated malate currents. A, Typical time-dependent currents from excised cytosolic-side-out patches obtained from AtALMT9-overexpressing tobacco vacuoles in symmetric malate conditions (100 mM $malate_{vac}$/100 mM $malate_{cyt}$). Currents were evoked in response to 3-s voltage pulses ranging from +60 mV to −120 mV in 20-mV steps, followed by a tail pulse at +60 mV, with a holding potential at +60 mV. B, Molecular structure of L-malate (MA) and citrate (CA) acids. C, Reversible inhibition of $AtALMT9_{WT}$ currents by 10 mM $citrate_{cyt}$. Normalized current-voltage curves were obtained with a voltage ramp (from +60 to −160 mV in 1.5 s) in cytosolic control solution (ctrl; 100 mM $malate_{cyt}$) and after adding 10 mM $citrate_{cyt}$ (100 mM $malate_{cyt}$ + 10 mM $citrate_{cyt}$). The gray line indicates the recovery in control cytosolic solution. D and E, Ratios between currents recorded in control and $citrate_{cyt}$-containing solutions ($I_{CA}/I_{ctrl}$) when using different $citrate_{cyt}$ concentrations ($n$ = 4–5). E, Dose-response curves for $citrate_{cyt}$ at different potentials. Solid lines are fits obtained with Equation 1. F, Voltage dependency of the $K_d^{citrate}$. Solid lines correspond to data fitted with Equation 3. G, Representative current recording of a kick-out experiment on AtALMT9-meditated current. The currents were evoked using the voltage pulse protocol shown above the current traces. After the 3-ms pulse at +60 mV, a transient decrease of the current is observable in the presence of 10 mM $citrate_{cyt}$ (black trace inset). In contrast, in cytosolic control solution (gray trace inset), no transient decrease is

**Table I.** *Properties of wild-type and mutant AtALMT9 channels expressed in tobacco*

Data are presented as means ± SD.

| chunK-Sample | I(nA) at −120 mV[a] | No. of Experiments | Conductive | $I_{citrate}/I_{ctrl}$ at −160 mV[b] | $K_d^{citrate}$ at −160 mV[c] | Rectification Rate[d] |
|---|---|---|---|---|---|---|
| | | | | | mM | |
| Untransformed | −0.06 ± 0.03 | 3 | No | – | – | – |
| $AtALMT9_{WT}$ | −1.44 ± 0.51**** | 11 | Yes | 0.37 ± 0.05 | 5.1 ± 0.3 | 0.19 ± 0.03 |
| K87E | −1.52 ± 0.30** | 4 | Yes | 0.59 ± 0.03**** | 16.2 ± 2.3 | 0.22 ± 0.02 |
| K87R | −0.92 ± 0.06*** | 3 | Yes | 0.39 ± 0.04 | – | – |
| K93E | −0.11 ± 0.04 | 5 | No | – | – | – |
| K93A | −0.07 ± 0.03 | 4 | No | – | – | – |
| K93N | −0.09 ± 0.04 | 3 | No | – | – | – |
| K93R | −0.80 ± 0.42* | 4 | Yes | – | – | – |
| E130A | −0.07 ± 0.01 | 3 | No | – | – | – |
| E130D | −1.28 ± 0.15**** | 5 | Yes | – | – | – |
| E130K | −0.13 ± 0.07 | 4 | No | – | – | – |
| K139E | −1.1 ± 0.15** | 3 | Yes | 0.42 ± 0.04 | – | 0.16 ± 0.01 |
| R143E | −0.10 ± 0.07 | 3 | No | – | – | – |
| R143N | −0.09 ± 0.06 | 3 | No | – | – | – |
| K187E | −0.09 ± 0.08 | 3 | No | – | – | – |
| K187N | −0.07 ± 0.04 | 4 | No | – | – | – |
| K193E | −1.46 ± 0.62** | 7 | Yes | 0.99 ± 0.02**** | – | 0.50 ± 0.09*** |
| K193A | −1.75 ± 0.25**** | 5 | Yes | 0.82 ± 0.02**** | – | 0.24 ± 0.03* |
| K193N | −0.63 ± 0.14* | 3 | Yes | 0.83 ± 0.03**** | – | 0.29 ± 0.06* |
| K193R | −0.94 ± 0.43* | 4 | Yes | 0.39 ± 0.04 | – | 0.16 ± 0.04 |
| E196A | −0.87 ± 0.26*** | 6 | Yes | 0.39 ± 0.06 | – | – |
| R200N | −1.43 ± 0.58** | 5 | Yes | 0.86 ± 0.04**** | – | 0.18 ± 0.05 |
| R200E | −0.12 ± 0.05 | 3 | No | – | – | – |
| R200K | −0.62 ± 0.12* | 3 | Yes | 0.38 ± 0.03 | – | 0.21 ± 0.02 |
| R215E | −0.07 ± 0.03 | 3 | No | – | – | – |
| R215N | −0.69 ± 0.27* | 4 | Yes | 0.37 ± 0.04 | – | 0.14 ± 0.01** |
| R226E | −0.09 ± 0.06 | 3 | No | – | – | – |
| R226N | −0.14 ± 0.08 | 4 | No | – | – | – |
| K93E/E130K | −1.30 ± 0.27* | 3 | Yes | 0.37 ± 0.02 | – | – |

[a]Current measured in 100 mM $malate_{cyt}$/100 mM $malate_{vac}$. Asterisks indicate statistically significant differences from untransformed tobacco (*$P < 0.05$, **$P < 0.01$, ***$P < 0.001$, ****$P < 0.0001$; two-tailed Student's *t* test). [b]Ratio between the current measured in 100 mM $malate_{cyt}$ + 10 mM $citrate_{cyt}$ and the current measured in 100 mM $malate_{cyt}$. Asterisks indicate statistically significant differences from $AtALMT9_{WT}$ (****$P < 0.0001$; two-tailed Student's *t* test). [c]$K_d^{citrate}$ determined with Equation 1. [d]Rectification rate measured as described in the text. Asterisks indicate statistically significant differences from $AtALMT9_{WT}$ (*$P < 0.05$, **$P < 0.01$, ***$P < 0.001$; two-tailed Student's *t* test).

significant permeation of citrate through AtALMT9 ($I_{citrate}/I_{malate}$ = 5% ± 5%; Supplemental Fig. S1A), as shown for BnALMT1 and BnALMT2 (Ligaba et al., 2006). However, when 10 mM citrate was applied at the cytosolic side (100 mM $malate_{vac}$/100 mM $malate_{cyt}$ + 10 mM $citrate_{cyt}$), AtALMT9 malate currents were reversibly inhibited to residual 37% ± 5% of the original current at −160 mV (Fig. 1C). The inhibition of the ion flux induced by $citrate_{cyt}$ was dose and voltage dependent (Fig. 1, D and E). Notably, the inhibitory effect of $citrate_{cyt}$ on AtALMT9-mediated currents occurred more pronouncedly at more negative membrane potentials (Fig. 1, C and D). However, the inhibition by $citrate_{cyt}$ did not change the voltage dependency of the relative open probability of the channel (Supplemental Fig. S1B). This implies that $citrate_{cyt}$ inhibition does not originate from a shift in channel gating toward more negative membrane potentials. When further analyzing the dose response of $citrate_{cyt}$ inhibition at different applied potentials, we found that the dissociation constant of $citrate_{cyt}$ ($K_d^{citrate}$; 5.1 ± 0.3 mM at −160 mV) was voltage dependent (Fig. 1, E and F). This finding indicates that the inhibiting anion citrate experiences the applied transmembrane electrical field. Consequently, we could estimate that citrate penetrates approximately 17% of the applied transmembrane electrical field (Woodhull, 1973). This, in turn, suggests that the interaction between citrate and the channel occurs within the membrane-spanning domain of AtALMT9 and possibly within the conduction pathway.

**Figure 1**. (*Continued.*)
observable. H, Crossing of the tail currents at +30 mV in control conditions (gray trace) and in the presence of 10 mM $citrate_{cyt}$ (black trace). AtALMT9 currents were elicited by an activating prepulse at −100 mV for 2 s followed by a tail pulse at +30 mV (1 s), as depicted above the current traces. The holding potential was set to +60 mV. Error bars represent SD.

To obtain direct evidence that citrate acts as an open channel blocker by interacting with the pore of AtALMT9, we investigated whether citrate binds to the activated channel. In a first step, we performed "kick-out experiments" (Becker et al., 1996; Fig. 1G). This approach is based on the reversible dissociation of citrate from its binding site when applying a short voltage pulse to the activated AtALMT9 channel at which $citrate_{cyt}$ was shown to no longer effectively block AtALMT9 (i.e. $V_m \geq 0$ mV; Fig. 1C). The "kick-out pulse" was transient and adjusted in order to not influence the voltage-dependent gating of the channel (Fig. 1G). Consequently, the proportion of channels in an open configuration was stable during and after the kick-out pulse. Therefore, effects on the current after the kick-out pulse did not originate from effects on the channel gating but from reversible pore blocking. During the kick-out experiments, we first activated the channels with a voltage pulse at −140 mV for 2 s. Subsequently, we stepped for 3 ms to a positive membrane potential (+60 mV) and then restored the membrane potential to −140 mV again (Fig. 1G). When this protocol was applied in the presence of the cytosolic control buffer (100 mM $malate_{cyt}$), the 3-ms pulse to +60 mV did not induce any significant channel closure, since the current levels before and immediately after the pulse were indistinguishable (Fig. 1G, gray trace inset). Differently, when applying the same protocol in the presence of 10 mM $citrate_{cyt}$, the 3-ms pulse at +60 mV was followed by a transient increase of the current that relaxed rapidly to the prepulse current amplitude (the time constant of the current relaxation is $\tau = 11.5 \pm 0.4$ ms at −140 mV; Fig. 1G, black trace inset). This fast relaxation after the kick-out pulse reflected the reversible binding kinetic of citrate to the channel. Thus, the results confirmed that citrate is capable of blocking AtALMT9 by binding to the open channel configuration. Concurrently, as expected for channels blocked in the open configuration, deactivating tail currents relaxed more slowly in the presence of $citrate_{cyt}$ than in its absence because of the dissociation of the blocking agent prior to closure of the channel. Hence, the application of an open channel blocker like citrate generates a typical crossover of the tail currents (Clay, 1995; Fig. 1H). Taken together, these data strongly indicate that citrate is an open channel blocker and that its inhibitory effect is likely due to a block of the conduction pathway of AtALMT9.

### Effects of Positively and Negatively Charged Amino Acid Residues on Pore Conductivity

Despite the fact that ALMT proteins are known and have been studied for many years, few experimental data are available on the structure-function level (Motoda et al., 2007; Furuichi et al., 2010; Mumm et al., 2013). In particular, no study was conducted to investigate the TMD of ALMTs so far. Based on in silico analyses (http://aramemnon.botanik.uni-koeln.de), AtALMT9 is predicted to consist of a TMD at the N terminus and a soluble C-terminal domain encompassing roughly half of the protein. The TMD is predicted to be formed by six putative transmembrane $\alpha$-helices, whereby the N terminus exhibits an intracellular orientation (TM$\alpha$1–TM$\alpha$6; Fig. 2A). However, other arrangements, such as an inverse inside-outside structure or more $\alpha$-helices, were also proposed (Motoda et al., 2007; Dreyer et al., 2012). We performed a multiple alignment throughout all members of the ALMT family in Arabidopsis and identified several conserved or partially conserved amino acids within the TMD (Fig. 2B; Supplemental Fig. S2). We focused predominantly on positively charged residues, since they were often found to be relevant for functional elements of ion channels (pore and voltage sensor; Linsdell, 2005; Catterall, 2010). Interestingly, in line with the positive-inside rule (von Heijne and Gavel, 1988), the cytosolic-facing moiety of AtALMT9 exhibits a higher number of positively charged residues compared with the vacuolar moiety. While eight positively charged residues (three Arg and five Lys residues) are located at the cytosolic moiety, only three conserved positive residues face the vacuolar side (Fig. 2, A and B). To analyze the role of these residues in the TMD of AtALMT9, we substituted them by site-directed mutagenesis and monitored the effects of the mutation at a functional level (Fig. 2, D and E; Table I).

We transiently expressed the AtALMT9-GFP mutant channels in tobacco and first analyzed their intracellular localization by confocal laser scanning microscopy to verify whether the introduced point mutations resulted in a mistargeting of the protein. Interestingly, none of the mutations had an effect on the vacuolar targeting of the AtALMT9 channel (Fig. 2C; Supplemental Fig. S3). Subsequently, we analyzed the functionality of the mutated derivatives of AtALMT9 by performing patch-clamp analysis under the same experimental conditions as described above (Fig. 1A). The analysis revealed that the individual residues impacted differently on channel functionality. The removal of the positive charge of conserved Lys and Arg residues and the negative charge of the conserved Glu predicted to be inside the TMD$\alpha$s (Lys-93, Glu-130, Arg-143, Lys-187, and Arg-226) resulted in a loss of conductivity (Fig. 2, D and E; Table I). On the contrary, substituting other conserved positively and negatively charged residues predicted to be in the loops between the TMD$\alpha$s (Lys-87, Lys-139, Lys-193, and Glu-196) apparently did not affect the functionality of AtALMT9. In fact, patches from vacuoles transformed with these mutants presented time-dependent inward-rectifying currents with amplitudes that are reminiscent of those observed for $AtALMT9_{WT}$ (Figs. 1A and 2, D and E; Table I). Interestingly, the mutation of the two amino acids Arg-200 and Arg-215, the charge of which is not entirely conserved among the Arabidopsis ALMTs, affected the functionality of AtALMT9 dependent on the introduced residue. When

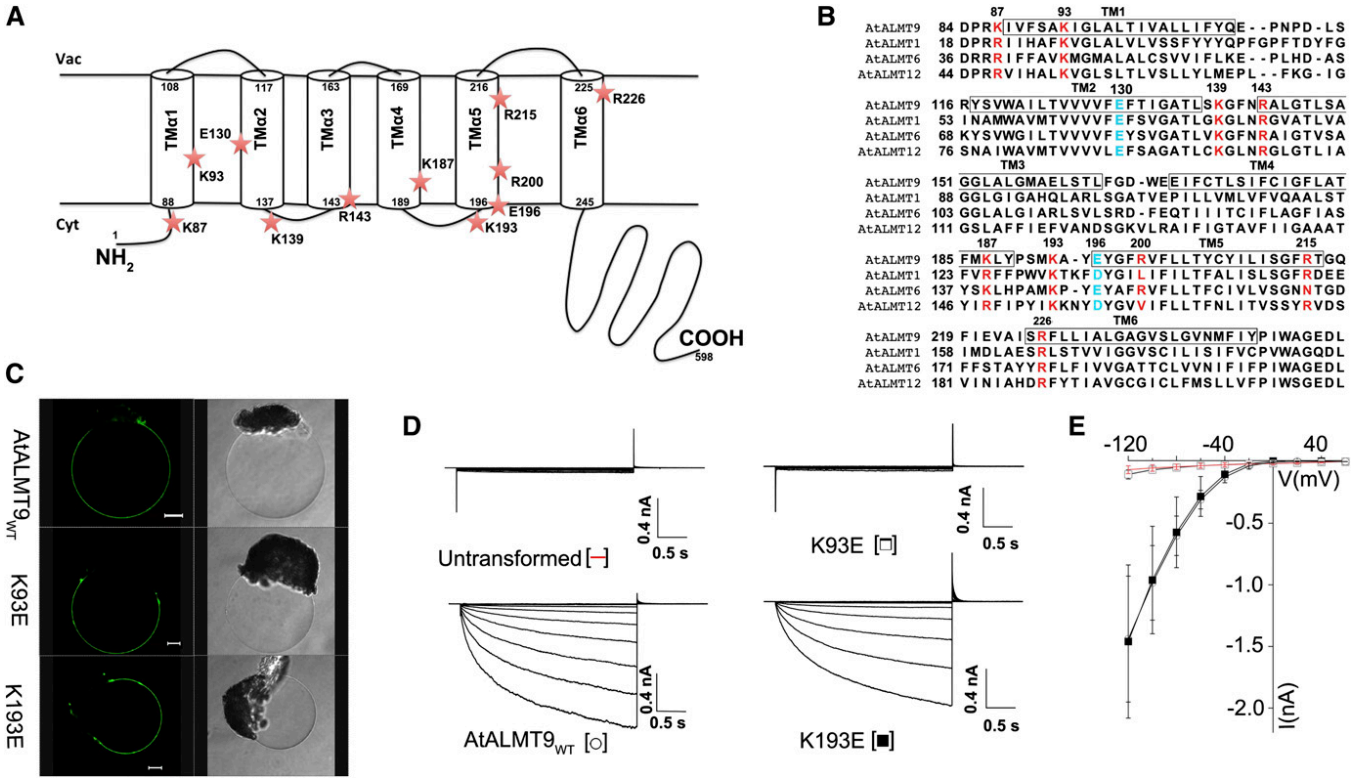


**Figure 2.** Impact of the mutation of conserved residues on AtALMT9 functionality. A, The TMD of AtALMT9 is predicted to be formed by six putative transmembrane $\alpha$-helices (TM$\alpha$1–TM$\alpha$6) with the N terminus being located in the cytosol. The model illustrates the location of the amino acids targeted by site-directed mutagenesis (red stars). B, Multiple alignment of AtALMT9 with representative AtALMT proteins (AtALMT1, AtALMT6, and AtALMT12). The alignment was conducted with the Jalview software (Waterhouse et al., 2009). The black boxes indicate the predicted TM$\alpha$s of AtALMT9. The conserved amino acids used for mutagenesis are displayed in red (positively charged residues) and in blue (negatively charged residues). C, Fluorescence and transmission images of vacuoles released from lysed tobacco mesophyll protoplasts transiently overexpressing AtALMT9$_{WT}$-GFP, AtALMT9$_{K93E}$-GFP, and AtALMT9$_{K193E}$-GFP imaged by confocal laser scanning microscopy. Bars = 10 $\mu$m. D, Representative current recordings of excised cytosolic-side-out patches of untransformed vacuoles as well as vacuoles overexpressing AtALMT9$_{WT}$, AtALMT9$_{K93E}$, and AtALMT9$_{K193E}$. Currents were evoked in response to 3-s voltage pulses ranging from +60 to −120 mV in 20-mV steps followed by a tail pulse at +60 mV. E, Mean current-voltage curves of untransformed vacuoles (red bars; $n$ = 3), AtALMT9$_{WT}$ (white circles; $n$ = 11), AtALMT9$_{K93E}$ (white squares; $n$ = 5), and AtALMT9$_{K193E}$ (black squares; $n$ = 7). In D and E, AtALMT9 currents were recorded in symmetric ionic conditions (100 mM malate$_{vac}$/100 mM malate$_{cyt}$). The holding potential was set to +60 mV. Error bars denote SD.

Arg-200 and Arg-215 were substituted with an Asn (AtALMT9$_{R200N}$ and AtALMT9$_{R215N}$), we observed time-dependent inward-rectifying currents comparable to AtALMT9$_{WT}$ (Table I; Supplemental Fig. S4, A and C). However, the introduction of a negatively charged residue like Glu (AtALMT9$_{R200E}$ and AtALMT9$_{R215E}$) led to nonfunctional channels (Table I; Supplemental Fig. S4, A and C). In summary, we observed three different effects on AtALMT9 channel functionality when mutating conserved charged residues. Four of the mutations we introduced induced a loss of conductivity, indicating that these residues were essential for the functionality of the channel. Furthermore, mutation of the cytosolic-facing residues did not influence channel functionality, whereas a third set of mutations resulted in a phenotype that was dependent on the introduced charge.

### TM$\alpha$1 and TM$\alpha$2 Are Connected by a Salt Bridge

The analysis of the primary sequence alignment revealed two conserved charged residues arousing our interest. Lys-93 and Glu-130 are located within TM$\alpha$1 and TM$\alpha$2, respectively (Fig. 2, A and B). In the hydrophobic environment of membranes, unitary charges need to be stabilized by an interaction with a solvent and/or with an opposite charge (Perutz, 1978). When Glu-130 was replaced by an Ala or a Lys (AtALMT9$_{E130A}$ or AtALMT9$_{E130K}$), the channel was nonconductive, similar to AtALMT9$_{K93A}$ and AtALMT9$_{K93E}$ (Fig. 3; Table I). However, channels harboring conservative mutations in which the respective charge was kept (AtALMT9$_{K93R}$ and AtALMT9$_{E130D}$) displayed inward currents comparable to AtALMT9$_{WT}$ (Table I). Thus, we hypothesized that the two charged residues

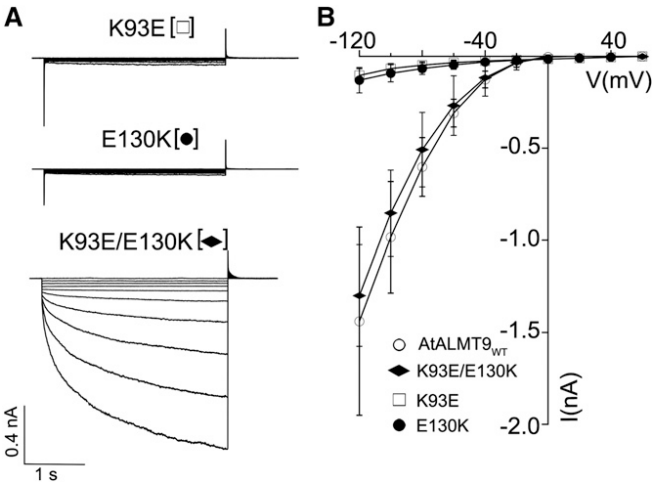


**Figure 3.** The conserved residues Lys-93 and Glu-130 form a salt bridge within the TMD of AtALMT9. A, Excised cytosolic-side-out current recordings from tobacco vacuoles overexpressing $AtALMT9_{K93E}$, $AtALMT9_{E130K}$, and the double mutant $AtALMT9_{K93E/E130K}$. Currents were evoked in response to 3-s voltage pulses ranging from +60 to −120 mV in 20-mV steps followed by a tail pulse at +60 mV. B, Mean current-voltage curves of malate currents mediated by $AtALMT9_{WT}$ (white circles; $n = 11$), $AtALMT9_{K93E/E130K}$ (black diamonds; $n = 3$), $AtALMT9_{K93E}$ (white squares; $n = 5$), and $AtALMT9_{E130K}$ (black circles; $n = 3$). Currents were recorded in symmetric conditions (100 mM $malate_{vac}$/100 mM $malate_{cyt}$). The holding potential was set to +60 mV. Error bars represent SD.

Lys-93 and Glu-130 could interact to form a salt bridge. To test this assumption, we generated a double mutant, $AtALMT9_{K93E/E130K}$, in which the charges of the amino acids Lys-93 and Glu-130 were exchanged. Astonishingly, the doubly mutated channel was functional and exhibited electrophysiological properties similar to $AtALMT9_{WT}$ (Fig. 3). $AtALMT9_{K93E/E130K}$ mediated currents with time-dependent relaxations and a mean amplitude of $-1.30 \pm 0.27$ nA at −120 mV (Fig. 3B; Table I). Moreover, the double mutant was inhibited by citrate, as demonstrated for the $AtALMT9_{WT}$ channel (Table I; Supplemental Fig. S5). These results indicate that the positively charged Lys-93 and the negatively charged Glu-130 connect TM$\alpha$1 and TM$\alpha$2 by a salt bridge that is essential for the functionality of the channel.

### Identification of Positively Charged Residues That Are Part of the Ion Conduction Pathway in AtALMT9

To investigate whether the mutated amino acids are possibly involved in forming the interaction site between citrate and the channel, we determined the sensitivity of the conductive AtALMT9 point mutants to citrate. The four charged residues Lys-87, Lys-139, Glu-196, and Arg-215 are located in the cytosolic loops next to TM$\alpha$1, TM$\alpha$2, and TM$\alpha$5 and at the vacuolar-facing moiety of TM$\alpha$5, respectively (Fig. 2, A and B). The channel derivatives $AtALMT9_{K87E}$, $AtALMT9_{K139E}$, $AtALMT9_{E196A}$, and $AtALMT9_{R215N}$ showed a moderate or no significant decrease in $citrate_{cyt}$ inhibition compared with $AtALMT9_{WT}$ $[(I_{citrate}/I_{ctrl})^{WT} = 0.37 \pm 0.05$, $(I_{citrate}/I_{ctrl})^{K87E} = 0.59 \pm 0.03$, $(I_{citrate}/I_{ctrl})^{K139E} = 0.42 \pm 0.04$, $(I_{citrate}/I_{ctrl})^{E196A} = 0.39 \pm 0.06$, and $(I_{citrate}/I_{ctrl})^{R215N} = 0.37 \pm 0.04$ at −160 mV; Fig. 4C; Table I]. In marked contrast, substitution of the residues Lys-193 and Arg-200, which reside at the cytosolic loop between TM$\alpha$4 and TM$\alpha$5 or within TM$\alpha$5, respectively, reduced the $citrate_{cyt}$ blockade efficiency dramatically $[(I_{citrate}/I_{ctrl})^{K193N} = 0.83 \pm 0.03$ at −160 mV and $(I_{citrate}/I_{ctrl})^{R200N} = 0.86 \pm 0.04$ at −160 mV; Fig. 4; Table I]. Since the substitution R200E resulted in a nonfunctional channel, the effect of a negatively charged residue at this amino acid position could not be investigated. Nevertheless, the mutation K193E, which introduced a Glu, provided a conductive channel but caused a complete loss of $citrate_{cyt}$ inhibition ($I_{citrate}/I_{ctrl} = 0.99 \pm 0.02$ at −160 mV; Fig. 4, A and C). In addition, when performing kick-out experiments with the citrate-insensitive mutants $AtALMT9_{K193E}$ and $AtALMT9_{R200N}$, the kick-out pulse was not followed by fast-relaxing current transients (Supplemental Figs. S1D and S4B). Since the transient current relaxation is due to the rapid dissociation and subsequent binding of $citrate_{cyt}$ to the open channel configuration of $AtALMT9_{WT}$, its absence provided evidence that $citrate_{cyt}$ was not able to interact with the $AtALMT9_{K193E}$ and $AtALMT9_{R200N}$ mutant channels and did not enter the TMD in these mutants. In contrast, the citrate-sensitive channel $AtALMT9_{R215N}$, which possesses a substitution at the vacuolar-facing part of the membrane, exhibited a transient current relaxation comparable to the wild-type channel after applying a kick-out pulse (Supplemental Fig. S4D).

Taken together, these results indicate that the positively charged residues Lys-193 and Arg-200, which are located adjacent to or within TM$\alpha$5, are involved in mediating the interaction of citrate with AtALMT9. Considering the fact that citrate acts as an open channel blocker, the data suggest that Lys-193 and Arg-200 are part of the ion conduction pathway of AtALMT9. To further confirm the pore-forming feature of the two residues and TM$\alpha$5, we explored the functional properties of the conductive AtALMT9 mutants by analyzing the "open channel rectification." This parameter directly reflects the properties of the conduction pathway itself, excluding rectification effects based on voltage-dependent gating. To quantify the open channel rectification of $AtALMT9_{WT}$ and its derivatives, we made used of the rectification rate coefficient (Linsdell, 2005). This coefficient is defined as the ratio between the conductance measured at the end of the activation pulse at −120 mV and the conductance measured at the beginning of the tail pulse at +60 mV (for details, see "Materials and Methods"). The rectification ratio of $AtALMT9_{WT}$ was $0.19 \pm 0.03$, indicating that the conduction pathway of this channel had intrinsic inward rectification properties. Strikingly, we observed that the citrate-insensitive channel

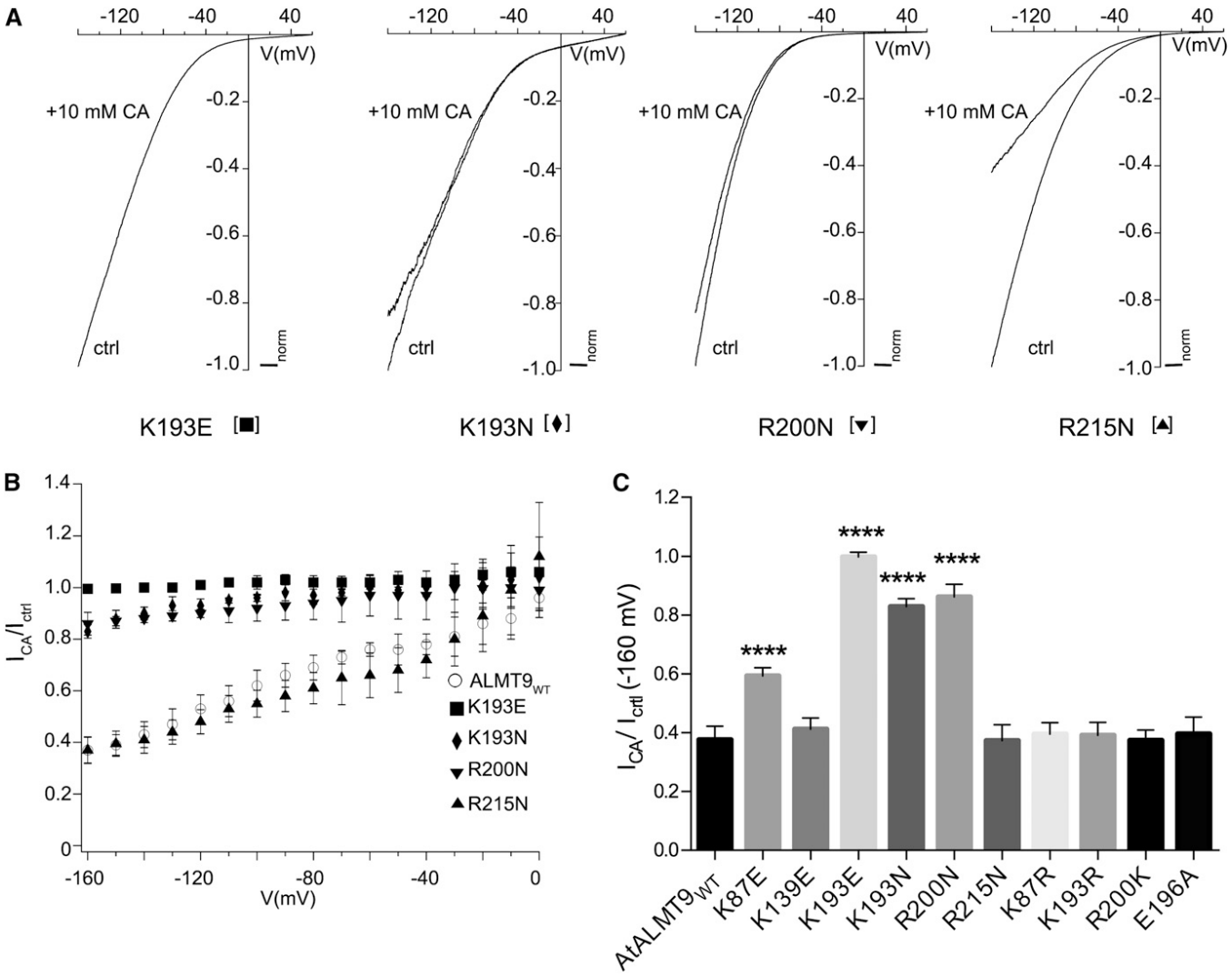


**Figure 4.** Variable effects of mutations of conserved AtALMT9 residues on citrate blockade. A, Normalized current-voltage curves of the mutants AtALMT9$_{K193E}$, AtALMT9$_{K193N}$, AtALMT9$_{R200N}$, and AtALMT9$_{R215N}$ in control conditions (ctrl) and in the presence of 10 mM citrate$_{cyt}$ (CA) obtained with a voltage ramp (from +60 mV to −160 mV in 1.5 s). B, Ratio between the control currents and the residual currents after inhibition with 10 mM citrate$_{cyt}$ ($I_{CA}/I_{ctrl}$). Depicted are AtALMT9$_{K193E}$ (squares; $n = 4$), AtALMT9$_{K193N}$ (diamonds; $n = 4$), AtALMT9$_{R200N}$ (inverted triangles; $n = 4$), AtALMT9$_{R215N}$ (triangles; $n = 3$), and AtALMT9$_{WT}$ (circles; $n = 4$). C, Ratios of the currents of different AtALMT9 mutants before and after the application of 10 mM citrate$_{cyt}$ ($I_{CA}/I_{ctrl}$; $n = 3$–5) at −160 mV. Currents were measured in symmetric conditions (100 mM malate$_{vac}$/100 mM malate$_{cyt}$). Asterisks indicate statistically significant differences from AtALMT9$_{WT}$ (****$P < 0.0001$; two-tailed Student's $t$ test). Error bars denote SD.

AtALMT9$_{K193E}$, which was mutated in an amino acid residue of the pore region, and AtALMT9$_{R215N}$, which harbors a mutation within TM$\alpha$5, exhibited an altered rectification ratio compared with AtALMT9$_{WT}$ (Table I). AtALMT9$_{K193E}$ showed a markedly increased rectification ratio of 0.50 ± 0.09, whereas AtALMT9$_{R215N}$ exhibited a lower rectification ratio (0.14 ± 0.01). The different rectification rates of AtALMT9$_{K193E}$ and AtALMT9$_{R215N}$ indicate that the mutated residues are involved in conferring rectification characteristics to the pore of AtALMT9. Hence, it is likely that Lys-193 and Arg-215 are involved in forming the conduction pathway. In summary, we could observe alterations in citrate block sensitivity and open channel rectification when analyzing the properties of the conductive mutant channels. We identified three positively charged residues preceding TM$\alpha$5 or within TM$\alpha$5 (Lys-193, Arg-200, and Arg-215) that fundamentally contribute to the functionality of the conduction pathway of AtALMT9.

### AtALMT9 Is a Multimeric Anion Channel Composed of Four Subunits

The discovery of the mutant channel AtALMT9$_{K193E}$, which is characterized by complete insensitivity to

citrate inhibition, provides the opportunity to investigate whether AtALMT9 is a monomeric or a multimeric channel (MacKinnon, 1991; Kosari et al., 1998). If AtALMT9 is a monomer, a co-overexpression of $AtALMT9_{WT}$ and $AtALMT9_{K193E}$ would not influence the $K_d^{citrate}$. In contrast, in case AtALMT9 functions as a multimeric complex, the heteromultimeric hybrids of $AtALMT9_{WT}$ and $AtALMT9_{K193E}$ would exhibit an altered sensitivity to $citrate_{cyt}$. Therefore, the presence of heteromultimers would result in a shift in $K_d^{citrate}$. We performed experiments in which we coinfiltrated tobacco leaves with a mixture of two *Agrobacterium tumefaciens* strains carrying plasmids with the sequence of either $AtALMT9_{WT}$ or $AtALMT9_{K193E}$ in different ratios (1:1 and 1:4). First, we verified the transcription levels of $AtALMT9_{WT}$ and $AtALMT9_{K193E}$ after coinfiltration. When infiltrating leaves with a 1:1 ratio of the two *A. tumefaciens* strains, we observed that 50.1% ± 9.2% of the *AtALMT9* transcripts were of wild-type origin and 49.9% ± 9.2% were the mutant sequence. Similarly, when coinfiltrating tobacco leaves with the two *A. tumefaciens* strains in a ratio of 1:4, we found that 15% ± 13% of the *AtALMT9* transcripts were the wild-type sequence and 85% ± 13% showed the sequence of $AtALMT9_{K193E}$ (Fig. 5A). Thus, using these *A. tumefaciens* mixtures, we were able to coexpress both AtALMT9 variants in tobacco in a ratio corresponding to that of the infiltration mix. Subsequently, we tested the citrate block sensitivity of vacuoles co-overexpressing $AtALMT9_{WT}$ and $AtALMT9_{K193E}$ in 1:1 and 1:4 ratios. As observed in OE $AtALMT9_{WT}$ patches, the coexpression displayed

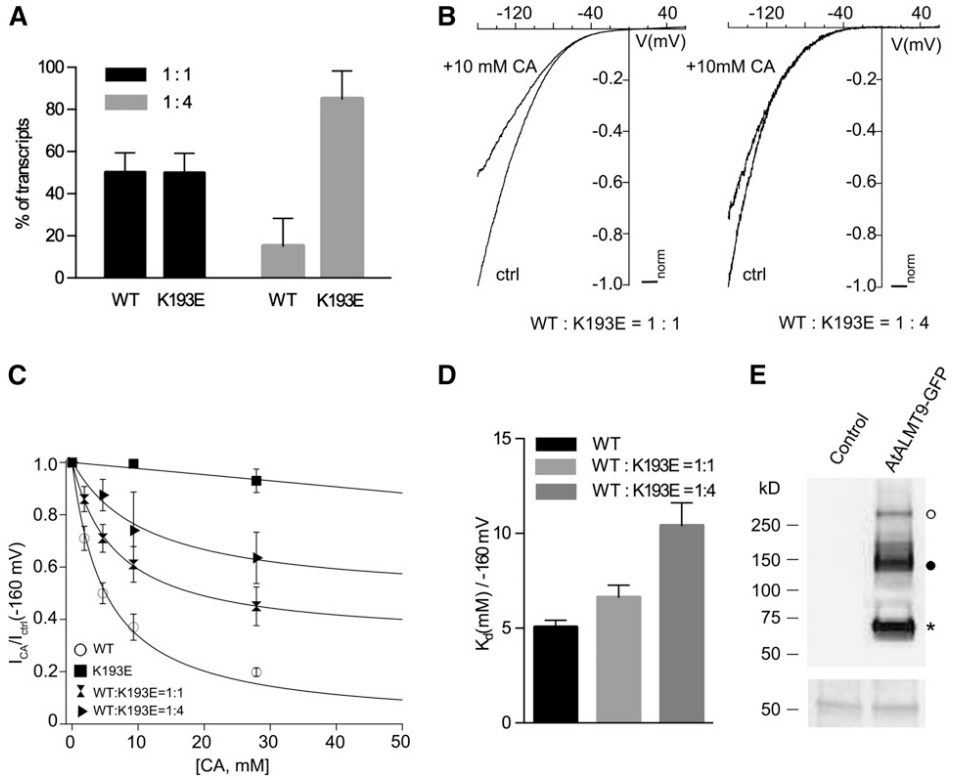


**Figure 5.** AtALMT9 forms homomultimeric complexes. A, Relative occurrence of $AtALMT9_{WT}$ and $AtALMT9_{K193E}$ transcripts in leaves of tobacco coinfiltrated with a 1:1 and a 1:4 mixture of *A. tumefaciens* strains each carrying plasmids with the sequence of one of the channel variants. Error bars represent SD of four biologically independent replicates (20 transcripts were analyzed for each replicate). B, Representative normalized current-voltage curves obtained with a voltage ramp (from +60 to −160 mV in 1.5 s; the holding potential was +60 mV) measured in excised cytosolic-side-out patches from vacuoles coexpressing $AtALMT9_{WT}$ and $AtALMT9_{K193E}$ at different ratios (left, $AtALMT9_{WT}$:$AtALMT9_{K193E}$ = 1:1; right, $AtALMT9_{WT}$:$AtALMT9_{K193E}$ = 1:4). Currents were recorded in control conditions (ctrl) and in the presence of 10 mM $citrate_{cyt}$ (CA). C, Dose-response curves for $citrate_{cyt}$ from vacuoles overexpressing $AtALMT9_{WT}$ (circles), $AtALMT9_{K193E}$ (squares), $AtALMT9_{WT}$:$AtALMT9_{K193E}$ = 1:4 (triangles), and $AtALMT9_{WT}$:$AtALMT9_{K193E}$ = 1:1 (hourglass; $n$ = 4–7). The data of $AtALMT9_{WT}$ were fitted with Equation 1. Data of the 1:1 and 1:4 ratios were fitted with Equation 2. Error bars denote SD. D, Values of the $K_d^{citrate}$ at $V_m$ = −160 mV derived from C. Currents were recorded in symmetric conditions (100 mM $malate_{vac}$/100 mM $malate_{cyt}$). Error bars display SD. E, Immunoblot analysis of microsomal proteins extracted from untransformed (control) and $AtALMT9_{WT}$-overexpressing (AtALMT9-GFP) leaves of tobacco using an anti-GFP antibody. In the top panel, the lane of protein extracts from AtALMT9-overexpressing leaves displays three bands corresponding to monomeric (star; approximately 70 kD), dimeric (black circle; approximately 140 kD), and tetrameric (white circle; approximately 280 kD) forms of the AtALMT9 protein complex. The bottom panel shows the corresponding Ponceau S staining. WT, Wild type.

malate currents that were blocked by citrate$_{cyt}$ (Fig. 5B). Notwithstanding, the currents in vacuolar patches co-overexpressing both AtALMT9 variants were less sensitive to citrate$_{cyt}$ than currents recorded in vacuoles only expressing AtALMT9$_{WT}$ and showed a shift in $K_d^{citrate}$ (Fig. 5C). The $K_d^{citrate}$ was 6.6 ± 0.6 mM and 10.4 ± 1.2 mM for the 1:1 and 1:4 ratios, respectively, thus representing 1.3- and 2.1-fold increases of $K_d^{citrate}$ compared with AtALMT9$_{WT}$ (Fig. 5D). This increase of $K_d^{citrate}$ in vacuoles simultaneously expressing AtALMT9$_{WT}$ and AtALMT9$_{K193E}$ is in agreement with a model in which both variants assemble to a hetero-multimeric channel and citrate interacts with multiple subunits. To further confirm this finding, we performed denaturing PAGE on microsomal proteins extracted from transiently transformed tobacco leaves that overexpressed AtALMT9-GFP (Fig. 5E). Using a GFP-specific antibody, we detected AtALMT9-GFP predominantly as an approximately 70-kD monomer. This band was smaller than predicted based solely on its formula molecular mass (93.5 kD) but was consistent with an apparent reduction in protein size observed under nonreducing conditions (Wittig and Schägger, 2008). We identified two higher order complexes in the absence of reducing agents and without heating up the samples (Fig. 5E). These complexes corresponded in size to an AtALMT9-GFP dimer (approximately 140 kD) and a tetramer (approximately 280 kD; Fig. 5E). Thus, these results provide evidence that AtALMT9-GFP functions as a multimer in which supposedly four subunits form the channel.

## DISCUSSION

The usage of blockers and the analysis of their effects on different site-specific mutants have allowed the development of structural models of ion channels when the crystal structures were not solved (MacKinnon, 1991; Yellen et al., 1991; Linsdell, 2005). Due to the absence of detailed data about the structure of ALMTs, the only available information comes from in silico predictions and a few structure-function studies (Motoda et al., 2007; Ligaba et al., 2009; Furuichi et al., 2010; Mumm et al., 2013). Hence, the exact topology of ALMT proteins is not yet unambiguously determined (Motoda et al., 2007; Dreyer et al., 2012). Nonetheless, on the basis of software predictions and the existing data, Arabidopsis ALMT channels are likely to be formed by an N-terminal TMD constituted of six membrane-spanning helices with the N-terminal and the C-terminal domains featuring an intracellular orientation (Fig. 2A; Kovermann et al., 2007; http://aramemnon.botanik.uni-koeln.de). Using in silico analysis, Piñeros et al. (2008) suggested that the TMD is involved in forming the permeation pathway. Nevertheless, the few structure-function studies focused on the C-terminal domain of ALMT proteins (Ligaba et al., 2009; Furuichi et al., 2010; Mumm et al., 2013). Because of the complete lack of experimental data on the N-terminal TMD of ALMTs, we performed a site-directed mutagenesis screen of this region using AtALMT9.

We could identify the three residues Lys-193, Arg-200, and Arg-215 as being important for channel functionality and possibly as being part of the anion conduction pathway. The mutation of Lys-193 and Arg-200, which are localized at the cytosolic face of AtALMT9, strongly impacted on both channel functionality and citrate blockade. The channel variants AtALMT9$_{K193N}$ and AtALMT9$_{K193E}$ display a strong and progressive effect on citrate inhibition sensitivity, resulting in a complete abolition of the open channel blockade in AtALMT9$_{K193E}$. Moreover, AtALMT9$_{K193E}$ features an impaired open channel rectification compared with AtALMT9$_{WT}$. Regarding position Arg-200, the substitution into a Glu results in a nonconductive channel (AtALMT9$_{R200E}$), while the channel variant AtALMT9$_{R200N}$ is functional but has strongly reduced citrate block sensitivity. Differently, mutation of the

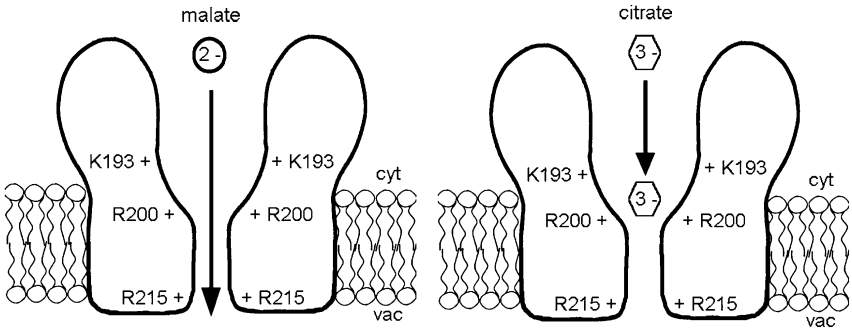


**Figure 6.** Model illustrating the block of AtALMT9 by cytosolic citrate. Cytosolic citrate inhibits AtALMT9 by acting as an open channel blocker. This indicates that citrate enters the permeation pathway to block AtALMT9 currents. To exert its blocking action, the trivalent anion citrate interacts electrostatically with the two positively charged residues Lys-193 and Arg-200. Lys-193 and Arg-200 are located at the cytosolic side of the channel and are likely to participate in forming the pore entrance. The vacuolar-facing Arg-215 is involved in the anion permeation process through AtALMT9 and, like Lys-193 and Arg-200, is part of the same putative transmembrane helix (TM$\alpha$5).

residue Arg-215, as expected by its predicted vacuolar-side localization, does not modify citrate inhibition. However, $AtALMT9_{R215N}$ is impaired in its rectification ratio, suggesting that the mutated residue is involved in the permeation process. Again, an exchange of the electrical charge of the residue (R215E) results in a nonconductive channel. Interestingly, the charge conservative mutant channels of these three positions ($AtALMT9_{K193R}$, $AtALMT9_{R200K}$, and $AtALMT9_{R215K}$) maintained the channel properties indistinguishable from $AtALMT9_{WT}$ (Fig. 4C). Therefore, the interaction of citrate with AtALMT9 is mainly electrostatic, and Lys-193 and Arg-200 are key residues in forming the citrate-binding site. When inhibiting AtALMT9 currents, citrate enters the TMD and penetrates 17% of the applied electrical field. Thus, combining this information with the predicted location of Lys-193 and Arg-200, it is likely that the binding site for citrate is placed at the cytosolic entrance of the conduction pathway of AtALMT9 (Fig. 6).

In addition, the results provided information about the topology of the AtALMT9 TMD. Our experimental data point toward an opposite orientation of ALMT proteins compared with the models proposed by Motoda et al. (2007) and Dreyer et al. (2012). Indeed, the fact that the mutation of the cytosolic-facing residues Lys-87, Lys-193, and Arg-200 impairs citrate block (Fig. 4; Supplemental Fig. S4) while the mutation of the vacuolar-facing Arg-215 does not is in agreement with the computer-based prediction of the topology of AtALMT9, with an intracellular localization of the N terminus and an orientation of the protein as depicted in Figure 2. Moreover, this study demonstrates that three residues (Lys-193, Arg-200, and Arg-215) that are important in the anion permeation process reside within TM$\alpha$5 or in the short loop preceding it. TM$\alpha$5 is predicted to span the entire membrane, whereby Lys-193 and Arg-200 are located on the opposite side of TM$\alpha$5 than Arg-215 (Fig. 2). Hence, it is tempting to speculate that TM$\alpha$5 lines the whole permeation pathway of AtALMT9, similar to what has been previously observed in other ion channels (Hilf and Dutzler, 2009; Hibbs and Gouaux, 2011).

Several introduced mutations of residues in the TMD result in major defects on AtALMT9 conductivity regardless of the chemical properties of the substitution (Table I). This nonfunctionality prevents further investigations but suggests an essential structural role of these residues. Nonetheless, we have identified the distinct structural role of the residue Lys-93. Lys-93 is located within TM$\alpha$1 and is strictly conserved among different ALMTs (Supplemental Fig. S2). We have demonstrated that Lys-93 forms a salt bridge with another strictly conserved residue in TM$\alpha$2, Glu-130. This proves that TM$\alpha$1 and TM$\alpha$2 are connected by a salt bridge that is crucial for channel functionality. Similar observations of a restored wild-type channel function when exchanging the residues of a salt bridge have been made in the cystic fibrosis transmembrane conductance regulators (Cotten and Welsh, 1999; Cui et al., 2013).

The concomitant finding of the pore blocker citrate and the mutant channel $AtALMT9_{K193E}$ that features abolished block sensitivity allowed investigation of the oligomeric state of AtALMT9 (MacKinnon, 1991). This is an intriguing opportunity, since, to our knowledge, it is not known whether ALMTs present a monomeric or multimeric architecture. To distinguish between these two possibilities, we coexpressed $AtALMT9_{WT}$ and $AtALMT9_{K193E}$ and found that the sensitivity to citrate was decreased and the $K_d^{citrate}$ was shifted. These results are consistent with a model in which AtALMT9 channels form a multimeric complex and citrate interacts with multiples of those subunits. Moreover, since citrate is an open channel blocker interacting with the pore-forming region, our data suggest that several AtALMT9 polypeptides participate in forming the anion conduction pathway. This type of multimeric organization is shared with several other families of ion channels like potassium channels (MacKinnon, 1991), Glu receptors (Rosenmund et al., 1998; Robert et al., 2001), and acid-sensing channels (Kosari et al., 1998, 2006; Snyder et al., 1998). However, due to the low affinity of citrate, it is not possible to apply saturating blocker concentrations that would have allowed determination of the exact stoichiometry of AtALMT9 complexes. Therefore, we used a biochemical approach to provide evidence that AtALMT9 features a multimeric organization. Our data suggest that AtALMT9 forms presumably tetrameric complexes, similar to what has been found for potassium channels (Daram et al., 1997; Doyle et al., 1998). These results are in line with recent findings on AtALMT9, where the induction of chloride conductance by malate was shown to exhibit a Hill coefficient of 2.5, indicating that more than two subunits are required to form a functional channel (De Angeli et al., 2013).

One question that arises from this ensemble of results is whether the structural characteristics we described for AtALMT9 are extendible to other members of the ALMT family. We predominantly investigated residues that are conserved among the family at least in their electrical charge. Moreover, based on secondary structure prediction, the N-terminal TMD has a remarkably conserved topology. Thus, it is probable that the results concerning the structure found for one ALMT are also valid for other members.

In conclusion, our work provides new molecular, biochemical, and biophysical details about the TMD of a member of the ALMT family. We identified a probable pore-forming region of ALMT anion channels and revealed that AtALMT9, and presumably also other ALMTs, are multimeric complexes formed by four subunits in which multiple subunits participate in the formation of the conduction pathway.

## MATERIALS AND METHODS

### Site-Directed Mutagenesis

Arabidopsis (*Arabidopsis thaliana*) AtALMT9 complementary DNA was cloned into the expression vector pART27 as described previously (Kovermann

et al., 2007). The site-directed mutants were generated following the manufacturer's instructions of the Quikchange Site-Directed Mutagenesis Kit (Agilent Technologies) with slight modifications. All point mutations were verified by sequencing.

## Overexpression of AtALMT9-GFP in Tobacco

*Agrobacterium tumefaciens* (GV3101) was transformed with plasmids containing the sequences of the $AtALMT9_{WT}$ channel and its point-mutated derivatives by electroporation. The *A. tumefaciens*-mediated infiltration of 4-week-old tobacco (*Nicotiana benthamiana*) leaves was performed as described previously with slight modifications (Yang et al., 2001). After transient transformation, tobacco plants were grown in the greenhouse (16 h of light/8 h of dark, 25°C/23°C, 100–200 $\mu$mol photons $m^{-2}$ $s^{-1}$, 60% relative humidity) for another 2 to 3 d and then used to isolate protoplasts for confocal laser scanning microscopy and patch-clamp experiments.

## Verification of $AtALMT9_{WT}$ and $AtALMT9_{K193E}$ Coexpression in Tobacco

*A. tumefaciens* strains harboring plasmids with either the sequence of $AtALMT9_{WT}$ or $AtALMT9_{K193E}$ were coinfiltrated into tobacco in a bacteria ratio of 1:1 and 1:4 after defining the optical density at 600 nm. Whole-leaf RNA was extracted 2 to 3 d after transient transformation, and complementary DNA was subsequently synthesized. We amplified *AtALMT9* via PCR using a 20-$\mu$L reaction volume and the Phusion High-Fidelity DNA Polymerase (Thermo Scientific). PCR conditions were set as follows: 98°C for 2 min in the first cycle; subsequently, 30 amplification cycles consisting of 10 s at 98°C, 20 s at 58°C, and 1.20 min at 72°C; the final extension was 5 min at 72°C. Subsequently, we cloned the PCR product into the pJet1.2/blunt cloning vector (CloneJet PCR Cloning Kit; Thermo Scientific) and determined the amount of $AtALMT9_{WT}$ and $AtALMT9_{K193E}$ transcripts by sequencing.

## Microscopy

Intracellular localization of AtALMT9-GFP mutants was determined by performing a lysis to release vacuoles of tobacco protoplasts overexpressing the appropriate mutant channel construct. Microscopy was conducted using a Leica DMIRE2 www.leica-microsystems.com laser scanning microscope that was equipped with a 63× glycerol objective. GFP fluorescence signal was imaged at an excitation wavelength of 488 nm, and the emission was detected between 500 and 530 nm. The appropriate Leica confocal software has been used for image acquisition. The images in Supplemental Figure S3 were obtained with an epifluorescence microscope (Nikon Eclipse TS100) and acquired with a digital camera (Nikon DS-Fi1).

## Electrophysiology

Mesophyll protoplasts from AtALMT9-GFP-overexpressing tobacco leaves were isolated by enzymatic digestion. The enzyme solution contained 0.3% (w/v) cellulase R-10, 0.03% (w/v) pectolyase Y-23, 1 mM $CaCl_2$, 500 mM sorbitol, and 10 mM MES, pH 5.3, 550 mosmol. Protoplasts were washed twice and resuspended in the same solution without enzymes. Vacuoles were released from mesophyll protoplast by the addition of 5 mM EDTA and a slight osmotic shock (500 mosmol; see medium below). Transformed vacuoles exhibiting an AtALMT9-GFP signal were selected using an epifluorescence microscope. Membrane currents from patches of the tonoplast were recorded using the excised cytosolic-side-out patch-clamp technique as described elsewhere (De Angeli et al., 2013). Briefly, currents were recorded with an EPC10 patch-clamp amplifier (HEKA Electronics) using Patchmaster software (HEKA Electronics). Data were analyzed with FitMaster software (HEKA Electronics). In experiments on macroscopic current recordings, the pipette resistance was 4 to 5 MΩ. Only patches presenting a seal resistance higher than 2 GΩ were used to perform experiments. Macroscopic current recordings were filtered at 300 Hz.

The pipette solution contained 112 mM malic acid and 5 mM HCl and was adjusted with BisTrisPropane (BTP) to pH 6. The osmolarity was adjusted with sorbitol to 550 mosmol. The bath solution contained (1) 100 mM malic acid, 3 mM $MgCl_2$, and 0.1 mM $CaCl_2$, adjusted to pH 7.5 with BTP; (2) 100 mM malic acid, citric acid (2, 5, 10, or 30 mM), 3 mM $MgCl_2$, and 0.1 mM $CaCl_2$, adjusted to pH 7.5 with BTP; and (3) 100 mM citric acid, 3 mM $MgCl_2$, and 0.1 mM $CaCl_2$, adjusted to pH 7.5 with BTP. The osmolarity was adjusted to 500 mosmol using sorbitol. All chemicals were purchased from Sigma-Aldrich. Liquid junction potentials were measured and corrected when higher than ±2 mV (Neher, 1992). Current-voltage characteristics were obtained by subtracting the current at time zero from the quasistationary currents (averaging the last 50 ms of the current trace) elicited by main voltage pulses. In all patch-clamp experiments, the applied membrane potential ($V_m$) is presented according to the convention for intracellular organelles of Bertl et al. (1992), namely $V_m = V_{cyt} - V_{vac}$, where $V_{cyt}$ and $V_{vac}$ are the cytosolic and vacuolar potentials, respectively.

The dose response for the $citrate_{cyt}$ inhibition of $AtALMT9_{WT}$ currents (Figs. 1 and 5; Supplemental Fig. S4) was fitted and analyzed with the Langmuir isotherm in the following form:

$$\frac{I}{I_0} = 1 - \frac{1}{1 + \frac{K_d^{CA}}{[CA]_{cyt}}} \quad (1)$$

where $I$ is the AtALMT9 current amplitude in the presence of $citrate_{cyt}$, $I_0$ is the AtALMT9 current under control solution, $[CA]_{cyt}$ is the cytosolic citrate concentration, and $K_d^{CA}$ is the dissociation constant of citrate.

The dose response for the $citrate_{cyt}$ inhibition of the co-overexpression of $AtALMT9_{WT}$ and $AtALMT9_{K193E}$ in 1:1 and 1:4 ratios (Fig. 5) was fitted with the Langmuir isotherm in the following form:

$$\frac{I}{I_0} = 1 - \frac{I_{inh}}{1 + \frac{K_d^{CA}}{[CA]_{cyt}}} \quad (2)$$

where $I$ is the current amplitude in the presence of $citrate_{cyt}$, $I_0$ is the current amplitude under control solution, $[CA]_{cyt}$ is the cytosolic citrate concentration, $K_d^{CA}$ is the dissociation constant of citrate, and $I_{inh}$ is the maximum fraction of current inhibited by $citrate_{cyt}$.

To estimate the fraction of the electrical field that citrate traverses to reach its binding site, the voltage-dependent dissociation constant relationship was fitted with the equation described by Woodhull (1973):

$$K_d^{CA}(V_m) = K_d^{CA}(0) \cdot e^{\frac{z\delta FV}{RT}} \quad (3)$$

in which $K_d^{CA}(V_m)$ is the voltage-dependent dissociation constant of citrate, $K_d^{CA}(0)$ is the dissociation constant of citrate at 0 mV, $V_m$ is the transmembrane potential, $z$ is the valence of the blocker, $\delta$ is the fraction of the electrical membrane field traversed by the blocker, and $F$, $R$, and $T$ are the Faraday constant, gas constant, and absolute temperature, respectively. Experiments were performed at room temperature (22°C–25°C).

For all calculations, the actual $citrate^{3-}$ concentration was determined with the Henderson-Hasselbach equation. The $citrate^{3-}$ concentration was estimated to be 93% of the different citric acid forms at pH 7.5.

The rectification rate coefficient was obtained by calculating the ratio between the conductance at the end of the activating pulse ($V_m$ = −120 mV) and the conductance at the very beginning of the deactivating pulse ($V_m$ = +60 mV). The conductance at the end of the activating pulse was estimated by using the ratio between the average current amplitude of the last 5 ms of the activation pulse and the applied activating potential. To calculate the conductance at the beginning of the deactivating pulse, the initial current was extrapolated from a monoexponential fit of the tail currents and divided by the applied deactivating potential of +60 mV.

## Microsomal Protein Extraction and Protein Gel-Blot Analysis

Leaf material from unfiltrated (or empty vector-expressing) tobacco plants (data not shown) and AtALMT9-GFP-expressing tobacco plants was homogenized by cryogenic grinding with mortar and pestle and mixed with 4°C ice-cold homogenization buffer (250 mM Tris-HCl, pH 8.5, 25 mM EDTA, 30% Suc, 5 mM dithiothreitol, and protease inhibitor cocktail tablet [Roche]). The debris was sedimented by centrifugation at 5,000 rpm in a table-top centrifuge (Biofuge fresco; Heraeus) for 10 min at 4°C. Afterward, the supernatant fraction was passed through Miracloth (Calbiochem), transferred into ultracentrifugation tubes, and spun down at 35,000 rpm in an ultracentrifuge for 45 min at 4°C (Beckman Optima, SW41Ti). The membranes were solubilized in 100 $\mu$L of solubilization buffer (15 mM MOPS, pH 7.0, 1 mM EDTA, 30% glycerol [v/v], 0.5% *n*-dodecyl-$\beta$-D-maltoside, and protease inhibitor cocktail tablet [Roche]) for 30 min on ice. Equal protein amounts (Quick Start Bradford

Protein Assay; Bio-Rad) were loaded on SDS-PAGE gels (4%–20% Mini PROTEAN TGX precast gradient gel; Bio-Rad) in the absence of dithiothreitol. Proteins were blotted on polyvinylidene difluoride membranes (0.45 $\mu$m; Millipore) using the tank approach (Mini Trans-Blot Electrophoretic Transfer Cell; Bio-Rad), and an anti-GFP antibody (Clontech; 1:1,000) was used for immunodetection.

Sequence data from this article can be found in the GenBank/EMBL data libraries under accession numbers NP_188473.1.

## Supplemental Data

The following materials are available in the online version of this article.

**Supplemental Figure S1.** $AtALMT9_{WT}$ and $AtALMT9_{K193E}$ are poorly permeable for citrate.

**Supplemental Figure S2.** Multiple alignment of the ALMT protein family of Arabidopsis.

**Supplemental Figure S3.** Intracellular localization of the different mutant channels of AtALMT9-GFP.

**Supplemental Figure S4.** AtALMT9 point mutants display different channel conductivity and sensitivity to citrate inhibition.

**Supplemental Figure S5.** The double mutant $AtALMT9_{K93E/E130K}$ is inhibited by intracellular citrate like $AtALMT9_{WT}$.

Received April 16, 2013; accepted August 5, 2013; published August 5, 2013.

## LITERATURE CITED

**Barbier-Brygoo H, De Angeli A, Filleur S, Frachisse JM, Gambale F, Thomine S, Wege S** (2011) Anion channels/transporters in plants: from molecular bases to regulatory networks. Annu Rev Plant Biol **62:** 25–51

**Becker D, Dreyer I, Hoth S, Reid JD, Busch H, Lehnen M, Palme K, Hedrich R** (1996) Changes in voltage activation, $Cs^+$ sensitivity, and ion permeability in H5 mutants of the plant $K^+$ channel KAT1. Proc Natl Acad Sci USA **93:** 8123–8128

**Bertl A, Blumwald E, Coronado R, Eisenberg R, Findlay G, Gradmann D, Hille B, Köhler K, Kolb HA, MacRobbie E, et al** (1992) Electrical measurements on endomembranes. Science **258:** 873–874

**Brandt B, Brodsky DE, Xue S, Negi J, Iba K, Kangasjärvi J, Ghassemian M, Stephan AB, Hu H, Schroeder JI** (2012) Reconstitution of abscisic acid activation of SLAC1 anion channel by CPK6 and OST1 kinases and branched ABI1 PP2C phosphatase action. Proc Natl Acad Sci USA **109:** 10593–10598

**Catterall WA** (2010) Ion channel voltage sensors: structure, function, and pathophysiology. Neuron **67:** 915–928

**Chen YH, Hu L, Punta M, Bruni R, Hillerich B, Kloss B, Rost B, Love J, Siegelbaum SA, Hendrickson WA** (2010) Homologue structure of the SLAC1 anion channel for closing stomata in leaves. Nature **467:** 1074–1080

**Choe S** (2002) Potassium channel structures. Nat Rev Neurosci **3:** 115–121

**Clay JR** (1995) Quaternary ammonium ion blockade of IK in nerve axons revisited: open channel block vs. state independent block. J Membr Biol **147:** 23–34

**Cotten JF, Welsh MJ** (1999) Cystic fibrosis-associated mutations at arginine 347 alter the pore architecture of CFTR: evidence for disruption of a salt bridge. J Biol Chem **274:** 5429–5435

**Cui G, Freeman CS, Knotts T, Prince CZ, Kuang C, McCarty NA** (2013) Two salt bridges differentially contribute to the maintenance of cystic fibrosis transmembrane conductance regulator (CFTR) channel function. J Biol Chem**288:** 20758–20767

**Daram P, Urbach S, Gaymard F, Sentenac H, Chérel I** (1997) Tetramerization of the AKT1 plant potassium channel involves its C-terminal cytoplasmic domain. EMBO J **16:** 3455–3463

**De Angeli A, Monachello D, Ephritikhine G, Frachisse JM, Thomine S, Gambale F, Barbier-Brygoo H** (2006) The nitrate/proton antiporter AtCLCa mediates nitrate accumulation in plant vacuoles. Nature **442:** 939–942

**De Angeli A, Zhang J, Meyer S, Martinoia E** (2013) AtALMT9 is a malate-activated vacuolar chloride channel required for stomatal opening in Arabidopsis. Nat Commun **4:** 1804

**Doyle DA, Morais Cabral J, Pfuetzner RA, Kuo A, Gulbis JM, Cohen SL, Chait BT, MacKinnon R** (1998) The structure of the potassium channel: molecular basis of $K^+$ conduction and selectivity. Science **280:** 69–77

**Dreyer I, Gomez-Porras JL, Riaño-Pachón DM, Hedrich R, Geiger D** (2012) Molecular evolution of slow and quick anion channels (SLACs and QUACs/ALMTs). Front Plant Sci **3:** 263

**Dutzler R, Campbell EB, Cadene M, Chait BT, MacKinnon R** (2002) X-ray structure of a ClC chloride channel at 3.0 A reveals the molecular basis of anion selectivity. Nature **415:** 287–294

**Ferrer-Montiel AV, Montal M** (1996) Pentameric subunit stoichiometry of a neuronal glutamate receptor. Proc Natl Acad Sci USA **93:** 2741–2744

**Furuichi T, Sasaki T, Tsuchiya Y, Ryan PR, Delhaize E, Yamamoto Y** (2010) An extracellular hydrophilic carboxy-terminal domain regulates the activity of TaALMT1, the aluminum-activated malate transport protein of wheat. Plant J **64:** 47–55

**Geelen D, Lurin C, Bouchez D, Frachisse JM, Lelièvre F, Courtial B, Barbier-Brygoo H, Maurel C** (2000) Disruption of putative anion channel gene AtCLC-a in Arabidopsis suggests a role in the regulation of nitrate content. Plant J **21:** 259–267

**Geiger D, Scherzer S, Mumm P, Marten I, Ache P, Matschi S, Liese A, Wellmann C, Al-Rasheid KAS, Grill E, et al** (2010) Guard cell anion channel SLAC1 is regulated by CDPK protein kinases with distinct $Ca^{2+}$ affinities. Proc Natl Acad Sci USA **107:** 8023–8028

**Geiger D, Scherzer S, Mumm P, Stange A, Marten I, Bauer H, Ache P, Matschi S, Liese A, Al-Rasheid KA, et al** (2009) Activity of guard cell anion channel SLAC1 is controlled by drought-stress signaling kinase-phosphatase pair. Proc Natl Acad Sci USA **106:** 21425–21430

**Hechenberger M, Schwappach B, Fischer WN, Frommer WB, Jentsch TJ, Steinmeyer K** (1996) A family of putative chloride channels from Arabidopsis and functional complementation of a yeast strain with a CLC gene disruption. J Biol Chem **271:** 33632–33638

**Hedrich R** (2012) Ion channels in plants. Physiol Rev **92:** 1777–1811

**Hibbs RE, Gouaux E** (2011) Principles of activation and permeation in an anion-selective Cys-loop receptor. Nature **474:** 54–60

**Hilf RJ, Dutzler R** (2009) Structure of a potentially open state of a proton-activated pentameric ligand-gated ion channel. Nature **457:** 115–118

**Hoekenga OA, Maron LG, Piñeros MA, Cançado GMA, Shaff J, Kobayashi Y, Ryan PR, Dong B, Delhaize E, Sasaki T, et al** (2006) AtALMT1, which encodes a malate transporter, is identified as one of several genes critical for aluminum tolerance in Arabidopsis. Proc Natl Acad Sci USA **103:** 9738–9743

**Jentsch TJ** (2008) CLC chloride channels and transporters: from genes to protein structure, pathology and physiology. Crit Rev Biochem Mol Biol **43:** 3–36

**Kim TH, Böhmer M, Hu H, Nishimura N, Schroeder JI** (2010) Guard cell signal transduction network: advances in understanding abscisic acid, $CO_2$, and $Ca^{2+}$ signaling. Annu Rev Plant Biol **61:** 561–591

**Kosari F, Sheng S, Kleyman TR** (2006) Biophysical approach to determine the subunit stoichiometry of the epithelial sodium channel using the Xenopus laevis oocyte expression system. Methods Mol Biol **337:** 53–63

**Kosari F, Sheng S, Li J, Mak DO, Foskett JK, Kleyman TR** (1998) Subunit stoichiometry of the epithelial sodium channel. J Biol Chem **273:** 13469–13474

**Kovermann P, Meyer S, Hörtensteiner S, Picco C, Scholz-Starke J, Ravera S, Lee Y, Martinoia E** (2007) The Arabidopsis vacuolar malate channel is a member of the ALMT family. Plant J **52:** 1169–1180

**Ligaba A, Katsuhara M, Ryan PR, Shibasaka M, Matsumoto H** (2006) The *BnALMT1* and *BnALMT2* genes from rape encode aluminum-activated malate transporters that enhance the aluminum resistance of plant cells. Plant Physiol **142:** 1294–1303

**Ligaba A, Kochian L, Piñeros M** (2009) Phosphorylation at S384 regulates the activity of the TaALMT1 malate transporter that underlies aluminum resistance in wheat. Plant J **60:** 411–423

**Linsdell P** (2005) Location of a common inhibitor binding site in the cytoplasmic vestibule of the cystic fibrosis transmembrane conductance regulator chloride channel pore. J Biol Chem **280:** 8945–8950

**MacKinnon R** (1991) Determination of the subunit stoichiometry of a voltage-activated potassium channel. Nature **350:** 232–235

**MacKinnon R, Yellen G** (1990) Mutations affecting TEA blockade and ion permeation in voltage-activated $K^+$ channels. Science **250:** 276–279

**Martinoia E, Meyer S, De Angeli A, Nagy R** (2012) Vacuolar transporters in their physiological context. Annu Rev Plant Biol **63:** 183–213

**Meyer S, Mumm P, Imes D, Endler A, Weder B, Al-Rasheid KAS, Geiger D, Marten I, Martinoia E, Hedrich R** (2010) AtALMT12 represents an R-type anion channel required for stomatal movement in Arabidopsis guard cells. Plant J **63:** 1054–1062

**Meyer S, Scholz-Starke J, De Angeli A, Kovermann P, Burla B, Gambale F, Martinoia E** (2011) Malate transport by the vacuolar AtALMT6 channel in guard cells is subject to multiple regulation. Plant J **67:** 247–257

**Motoda H, Sasaki T, Kano Y, Ryan PR, Delhaize E, Matsumoto H, Yamamoto Y** (2007) The membrane topology of ALMT1, an aluminum-activated malate transport protein in wheat (Triticum aestivum). Plant Signal Behav **2:** 467–472

**Mumm P, Imes D, Martinoia E, Al-Rasheid KA, Geiger D, Marten I, Hedrich R** (January 12, 2013) C-terminus mediated voltage gating of Arabidopsis guard cell anion channel QUAC1. Mol Plant http://dx.doi.org/10.1093/mp/sst008

**Negi J, Matsuda O, Nagasawa T, Oba Y, Takahashi H, Kawai-Yamada M, Uchimiya H, Hashimoto M, Iba K** (2008) $CO_2$ regulator SLAC1 and its homologues are essential for anion homeostasis in plant cells. Nature **452:** 483–486

**Neher E** (1992) Correction for liquid junction potentials in patch clamp experiments. Methods Enzymol **207:** 123–131

**Perutz MF** (1978) Electrostatic effects in proteins. Science **201:** 1187–1191

**Piñeros MA, Cançado GMA, Kochian LV** (2008) Novel properties of the wheat aluminum tolerance organic acid transporter (TaALMT1) revealed by electrophysiological characterization in *Xenopus* oocytes: functional and structural implications. Plant Physiol **147:** 2131–2146

**Rentsch D, Martinoia E** (1991) Citrate transport into barley mesophyll vacuoles: comparison with malate-uptake activity. Planta **184:** 532–537

**Robert A, Irizarry SN, Hughes TE, Howe JR** (2001) Subunit interactions and AMPA receptor desensitization. J Neurosci **21:** 5574–5586

**Roelfsema MRG, Hedrich R** (2005) In the light of stomatal opening: new insights into 'the Watergate'. New Phytol **167:** 665–691

**Rosenmund C, Stern-Bach Y, Stevens CF** (1998) The tetrameric structure of a glutamate receptor channel. Science **280:** 1596–1599

**Sasaki T, Yamamoto Y, Ezaki B, Katsuhara M, Ahn SJ, Ryan PR, Delhaize E, Matsumoto H** (2004) A wheat gene encoding an aluminum-activated malate transporter. Plant J **37:** 645–653

**Snyder PM, Cheng C, Prince LS, Rogers JC, Welsh MJ** (1998) Electrophysiological and biochemical evidence that DEG/ENaC cation channels are composed of nine subunits. J Biol Chem **273:** 681–684

**Traynelis SF, Wollmuth LP, McBain CJ, Menniti FS, Vance KM, Ogden KK, Hansen KB, Yuan H, Myers SJ, Dingledine R** (2010) Glutamate receptor ion channels: structure, regulation, and function. Pharmacol Rev **62:** 405–496

**Vahisalu T, Kollist H, Wang YF, Nishimura N, Chan WY, Valerio G, Lamminmäki A, Brosché M, Moldau H, Desikan R, et al** (2008) SLAC1 is required for plant guard cell S-type anion channel function in stomatal signalling. Nature **452:** 487–491

**von Heijne G, Gavel Y** (1988) Topogenic signals in integral membrane proteins. Eur J Biochem **174:** 671–678

**Ward JM, Mäser P, Schroeder JI** (2009) Plant ion channels: gene families, physiology, and functional genomics analyses. Annu Rev Physiol **71:** 59–82

**Waterhouse AM, Procter JB, Martin DM, Clamp M, Barton GJ** (2009) Jalview version 2: a multiple sequence alignment editor and analysis workbench. Bioinformatics **25:** 1189–1191

**Wittig I, Schägger H** (2008) Features and applications of blue-native and clear-native electrophoresis. Proteomics **8:** 3974–3990

**Woodhull AM** (1973) Ionic blockage of sodium channels in nerve. J Gen Physiol **61:** 687–708

**Yamaguchi M, Sasaki T, Sivaguru M, Yamamoto Y, Osawa H, Ahn SJ, Matsumoto H** (2005) Evidence for the plasma membrane localization of Al-activated malate transporter (ALMT1). Plant Cell Physiol **46:** 812–816

**Yang KY, Liu YD, Zhang SQ** (2001) Activation of a mitogen-activated protein kinase pathway is involved in disease resistance in tobacco. Proc Natl Acad Sci USA **98:** 741–746

**Yellen G, Jurman ME, Abramson T, MacKinnon R** (1991) Mutations affecting internal TEA blockade identify the probable pore-forming region of a $K^+$ channel. Science **251:** 939–942

**Identification of a probable pore forming domain in the multimeric vacuolar anion channel AtALMT9**

Jingbo Zhang, Ulrike Baetz, Undine Krügel, Enrico Martinoia and Alexis De Angeli

## Supplementary Figures

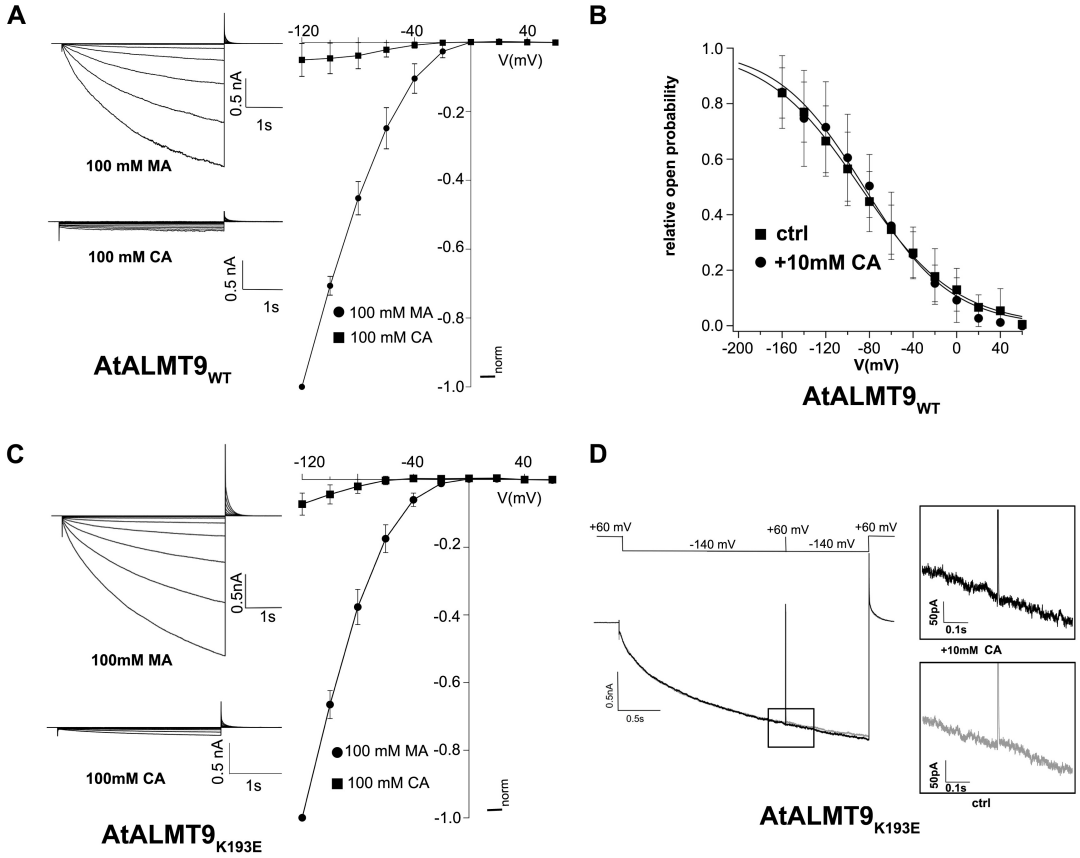


**Supplemental Figure S1. AtALMT9$_{WT}$ and AtALMT9$_{K193E}$ are poorly permeable for citrate.**

(A, C) Representative traces and normalized mean I-V curves of excised cytosolic-side out patches from *N. benthamiana* vacuoles overexpressing AtALMT9$_{WT}$ (A;

upper traces) and AtALMT9$_{K193E}$ (C; upper traces) displayed time dependent malate currents in symmetric ionic conditions (circles; 100 mM malate$_{vac}$/ 100 mM malate$_{cyt}$). When the cytosolic solution was replaced with 100 mM CA$_{cyt}$ (squares; 100 mM malate$_{vac}$/ 100 mM CA$_{cyt}$) the inward currents decreased and displayed only weak time dependent currents (A, C; lower traces). The current ratios $I_{CA}/I_{Malate}$(AtALMT9$_{WT}$) = 5 ± 5% and $I_{CA}/I_{Malate}$(AtALMT9$_{K193E}$) = 7 ± 3% show that CA is poorly permeable compared to malate. Currents were evoked in response to 3 s voltage pulses ranging from +60 mV to -120 mV in -20 mV steps followed by a tail pulse at +60 mV. The holding potential was set +60 mV. Error bars represent sd. Each data point corresponds to 4-11 patches. (B) Voltage dependency of the relative open probability of AtALMT9$_{WT}$ in control conditions (ctrl; 100 mM malate$_{vac}$/ 100 mM malate$_{cyt}$; circles) and in presence of 10 mM CA$_{cyt}$ (100 mM malate$_{vac}$/ 100 mM malate$_{cyt}$+10 mM CA$_{cyt}$; diamonds). The relative open probability was estimated from the initial current amplitude of the tail currents (derived from a mono-exponential fit of the current decay) which followed an activating pulse of various potentials. We were unable to reach the full activation of AtALMT9 channels as it is likely to occur at voltages more negatives than -160 mV, a value at which the vacuolar membrane becomes unstable. Therefore the data (n=8-10) was normalized to the $I_{max}$ value that was obtained by fitting each data set with the Boltzmann equation.

The solid lines represent the best fits of the mean relative open probability in control and in presence of 10 mM CA$_{cyt}$ with a Boltzmann equation in the following form:

$$P_O^{rel} = 1/(1 + e^{\left(\frac{zF(V-V_h)}{RT}\right)})$$

in which $P_O^{rel}$ is the relative open probability, z the gating charge, F the Faraday constant, R the universal gas constant, T the absolute temperature and $V_h$ the voltage of half activation. The fit shows that the presence of 10 mM CA$_{cyt}$ does not change significantly the voltage dependent gating of the channel since $V_h$ = -81 ± 1 mV and z = 0.6 ± 2 under control conditions and $V_h$ = -76 ± 3 mV and z = 0.7 ± 1 with 10 mM CA$_{cyt}$. (D) "Kick-out experiment" performed on the mutant AtALMT9$_{K193E}$. Grey traces were obtained under 100 mM malate$_{vac}$/ 100 mM malate$_{cyt}$ conditions and black traces in the presence of 10 mM CA$_{cyt}$ (100 mM malate$_{vac}$/ 100 mM malate$_{cyt}$+10 mM CA$_{cyt}$). The currents evoked in response to a 2 s voltage pulse at -140 mV. Subsequently, the membrane potential was transiently stepped for 3 ms to +60 mV and then restored to -140 mV for 1 s which was followed by a tail pulse at +60 mV. The holding potential was set to +60 mV. Error bars display sd.

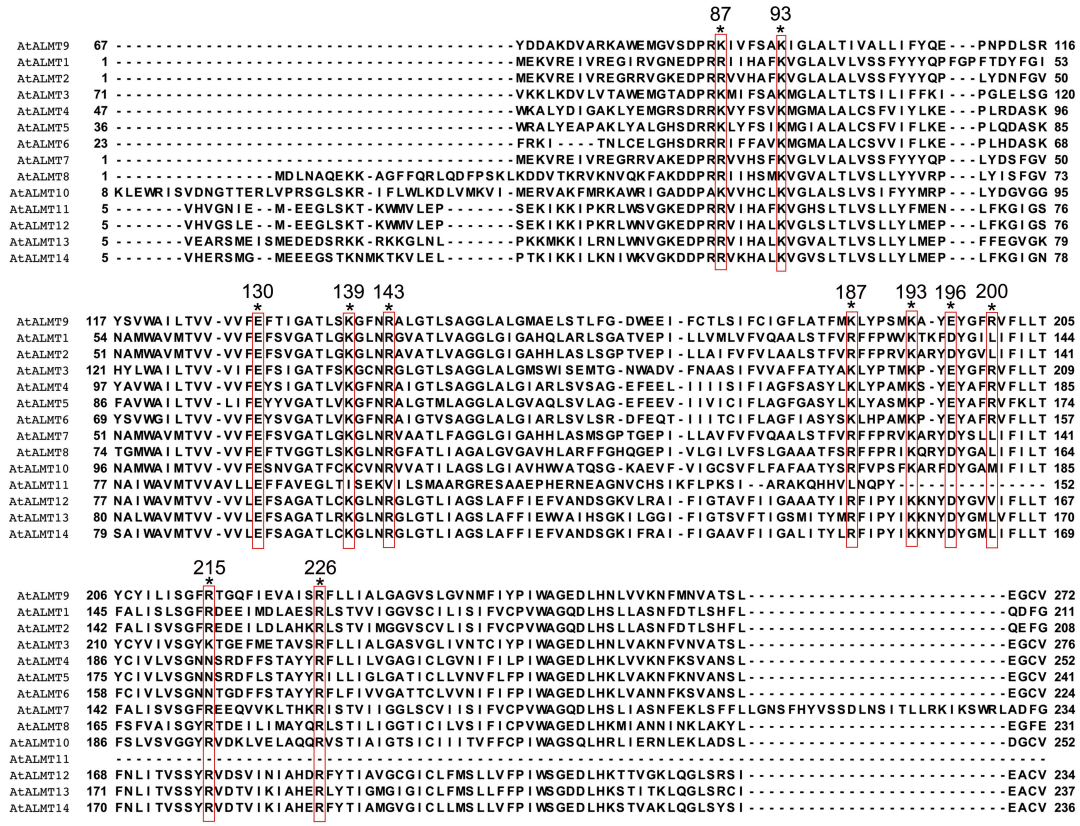

**Supplemental Figure S2. Multiple alignment of the ALMT protein family of *Arabidopsis thaliana*.**

The alignment was conducted with the Jalview software (Waterhouse *et al.,* 2009). Asterisks and red boxes indicate the residues that were targeted by site-directed mutagenesis in the present study.

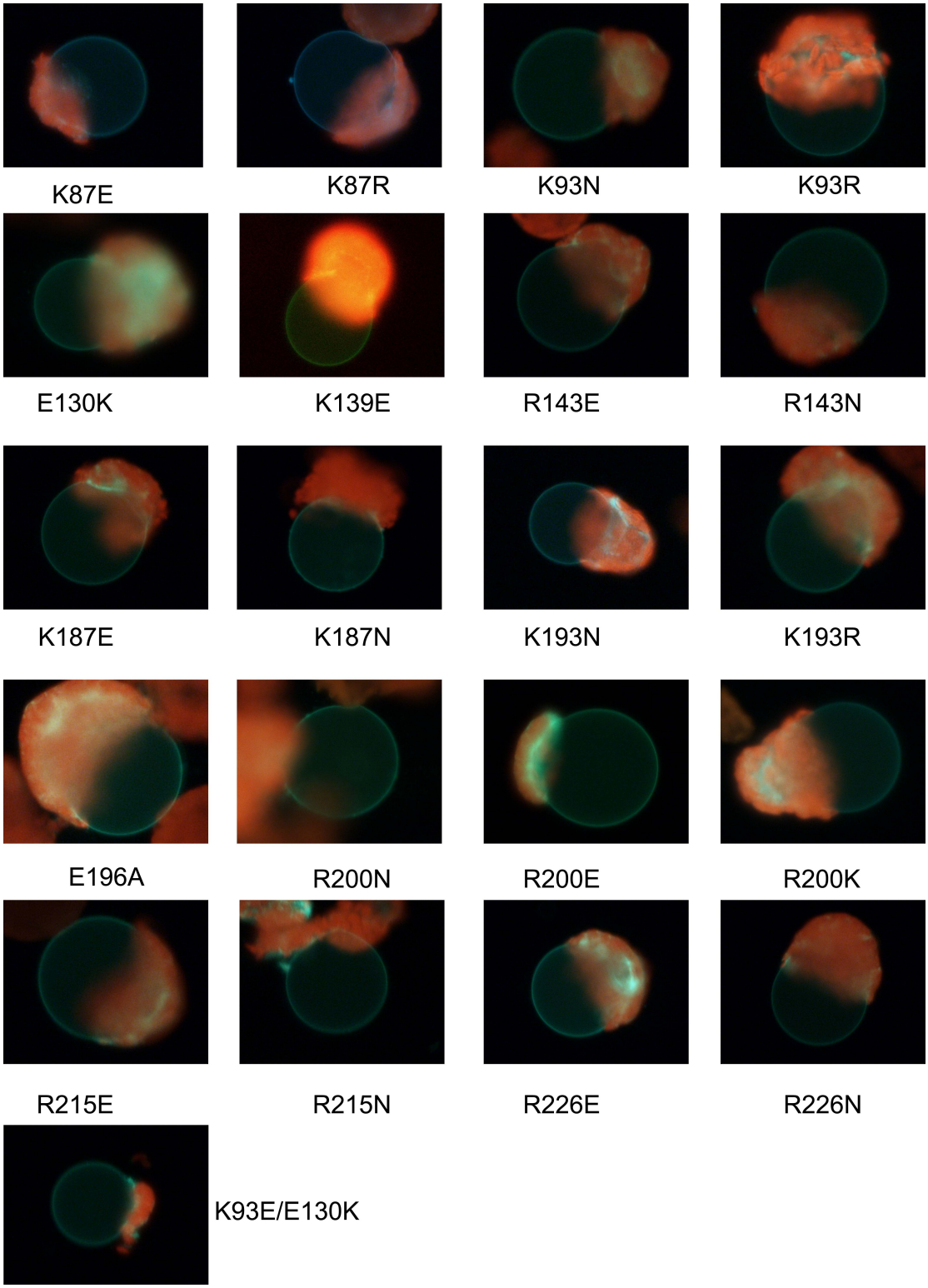


**Supplemental Figure S3. Intracellular localization of the different mutant channels of AtALMT9-GFP.**

Fluorescence images of vacuoles extracted from *N. benthamiana* protoplasts expressing the different AtALMT9-GFP mutants. None of the introduced mutations altered the tonoplastic localization of AtALMT9. The pictures were obtained with an

epifluorescence microscope (Nikon Eclipse TS100) and acquired with a digital camera (Nikon DS-Fi1).

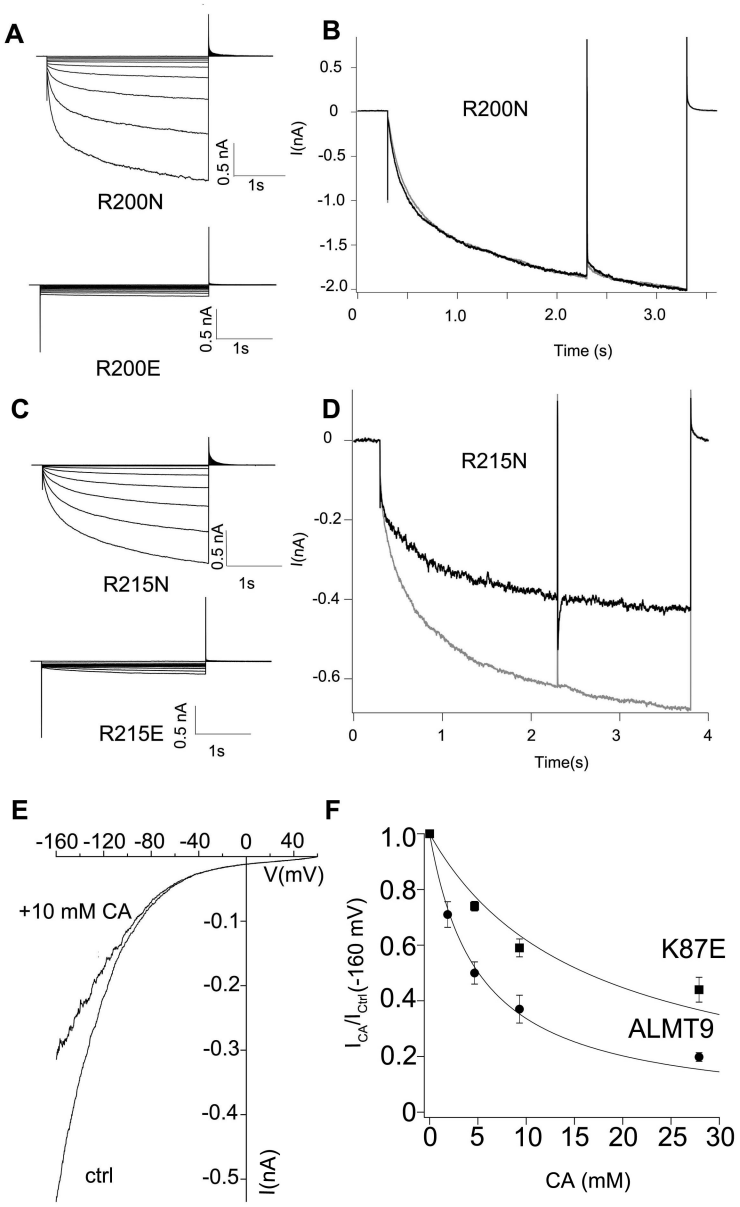


**Supplemental Figure S4. AtALMT9 point mutants display different channel conductivity and sensitivity to citrate inhibition**

Representative traces of current recordings from vacuoles overexpressing AtALMT9$_{R200N}$ and AtALMT9$_{R200E}$ (A), AtALMT9$_{R215N}$ and AtALMT9$_{R215E}$ (C) in symmetric malate conditions (100 mM malate$_{vac}$/ 100 mM malate$_{cyt}$). Currents were evoked in response to 3 s voltage pulses ranging from +60 mV to -120 mV in -20 mV steps followed by a tail pulse at +60 mV. The holding potential was +60 mV. "Kick-out experiments" were performed with the mutants AtALMT9$_{R200N}$ (B) and AtALMT9$_{R215N}$ (D). Grey traces were obtained in 100 mM malate$_{vac}$/ 100 mM malate$_{cyt}$ conditions and black traces in the presence of 10 mM CA$_{cyt}$ (100 mM

$malate_{vac}$/ 100 mM $malate_{cyt}$ + 10 mM $CA_{cyt}$). The currents evoked in response to a 2 s voltage pulse at -140 mV. Subsequently the membrane potential was transiently stepped for 3 ms to +60 mV and then restored to -140 mV for 1s which was followed by a tail pulse at +60 mV. The holding potential was set to +60 mV. (E) Representative I-V curves obtained with a voltage ramp (from +60 mV to -160 mV in 1.5 s; holding potential +60 mV) measured in excised cytosolic-side out patches from vacuoles expressing $AtALMT9_{K87E}$ in control conditions (ctrl) and in presence of 10 mM $CA_{cyt}$. (F) Dose-response of $CA_{cyt}$ concentration-dependent ratio of $AtALMT9_{WT}$ and $AtALMT9_{K87E}$ at -160 mV. To estimate the dissociation constant $K_d^{CA}$ the data points were fitted with a Langmuir isotherm (equation 1). The resulting $K_d^{CA}$ values were 5.1 ± 0.3 mM and 16.2 ± 2.3 mM for $AtALMT9_{WT}$ and $AtALMT9_{K87E}$, respectively. Error bars represent sd.

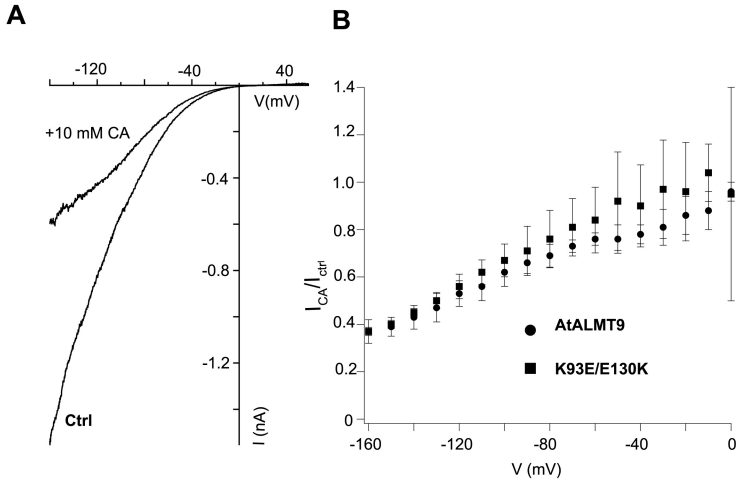


**Supplemental Figure S5. The double mutant $AtALMT9_{K93E/E130K}$ is inhibited by intracellular citrate comparable to $AtALMT9_{WT}$.**

(A) Representative I-V curves obtained with a voltage ramp (from +60 mV to -160 mV in 1.5 s; holding potential +60 mV) measured in excised cytosolic-side out patches from vacuoles expressing the double mutant $AtALMT9_{K93E/E130K}$ in control conditions (ctrl) and in presence of 10 mM $CA_{cyt}$. (B) Ratio between currents in presence of 10 mM $CA_{cyt}$ and in control conditions at different membrane potentials. Depicted are $AtALMT9_{WT}$ (circles; n = 4) and $AtALMT9_{K93E/E130K}$ (squares; n = 3). Error bars represent sd

# 3. Chapter II:

## Hetero-Multimerization of AtALMT Channels

Unpublished results.

Contributing Researchers:

AtALMT4-GFP was cloned and localized by Dr. Cornelia Eisenach. Kirsten Arens performed major parts of the ratiometric BiFC quantification. Ulrike Baetz conducted the cloning and subcellular localization of AtALMT5 and AtALMT3, patch-clamp analysis of AtALMT5-GFP, the cloning of the BiFC constructs, preliminary ratiomeric quantification of the different YFP-fusion constructs of AtALMT9, subcellular localization of the BiFC constructs in Arabidopsis protoplasts, and qRT-PCR. The project was designed and supervised by Prof. Enrico Martinoia, Dr. Alexis De Angeli, Dr. Cornelia Eisenach and Ulrike Baetz.

# 3.1. Introduction

In Arabidopsis, the *AtALMT* (Aluminum-activated Malate Transporter) gene family encodes for anion-permeable channel proteins that have been found to be located at the plasma and at the vacuolar membrane (Barbier-Brygoo et al., 2010, Meyer et al., 2010a). However, the membrane topology and structural and compositional organization of AtALMT channels remain largely ambiguous. Recently, detailed information about the structure-function relation and topology of AtALMT9, a vacuole-targeted member of the protein family, became available (Zhang et al., 2013; Chapter I). In that study it has been shown that the functional unit of the AtALMT9 channel is a homomer. The subunits of which AtALMT9 is composed each contributes to forming the conduction pathway (Zhang et al., 2013; Chapter I). Although the assembly of homomers has been shown to be required for AtALMT9 function, it remains elusive whether the channel is able to interact with other members of the AtALMT family to build heteromers that reside in the vacuolar membrane. Of note, at least one other member, AtALMT6 (Meyer et al., 2011), forms a functional channel at the tonoplast and is therefore a potential interaction partner of AtALMT9. Furthermore, heteromerization of plant channels has been observed before. For instance, plant $K^+$ channels are multimeric proteins built of four subunits (Daram et al., 1997, Gambale and Uozumi, 2006) that have been previously found to form homo- as well as heteromers with other proteins of the $K^+$ channel family (Lebaudy et al., 2008, Isacoff et al., 1990).

Several molecular approaches exist to investigate protein-protein interaction, such as yeast two-hybrid (Y2H) (Fields and Song, 1989), split-ubiquitin system (SUS) (Johnsson and Varshavsky, 1994), Förster resonance energy transfer (FRET) (Miyawaki et al., 1997), and bimolecular fluorescence complementation (BiFC) (Hu et al., 2002). BiFC is a powerful tool to study potential protein-protein interaction of membrane-spanning transporters or channels in living plant cells. Hence, here we make use of BiFC to investigate the putative heteromeric interaction of vacuolar AtALMT proteins. This method is based on the splitting of a fluorophore, such as eYFP (enhanced yellow fluorescent protein [Miyawaki et al., 1999]), into two non-fluorescent YFP

halves. The nYFP and the cYFP peptides are fused to one of the two potential interacting partners, respectively. Only if the putative protein interaction takes place, the two YFP peptides get in close proximity and the YFP fluorescence is complemented (Hu et al., 2002, Kerppola, 2006, Waadt and Kudla, 2008, Bracha-Drori et al., 2004, Walter et al., 2004). Hence, with this approach the detection of the YFP signal with Confocal Laser Scanning Microscopy (CLSM) indicates that the two proteins of interest are able to interact. The advantage over several other *in vivo* approaches is that interaction can be monitored in living plant cells. In addition, the intracellular localization can be determined using BiFC. Yet, this approach is based on the simultaneous expression of two constructs in the same cell, and co-transformation might lead to differences in copy number, expression levels or complete loss of one interacting partner. Additionally, negative results are difficult to interpret due to the lack of an internal expression and transformation control.

To overcome these drawbacks, Grefen and Blatt established a modified BiFC method, a 2in1 cloning system that enables ratiometric BiFC (rBiFC) and that is based on the introduction of multiple expression cassettes within a single vector backbone (Grefen and Blatt, 2012). The rBiFC approach does not rely on co-expression of several plasmids, since both candidate genes are simultaneously incorporated into the same vector backbone. Hence, variability in expression of the individual partners is overcome. In addition, this vector backbone harbors an internal fluorescent marker (soluble monomeric red fluorescent protein, mRFP) for expression and transformation control and ratiometric analysis, allowing comparison of different protein-protein interactions and thereby relative quantification of the interaction strength (Grefen and Blatt, 2012).

In this chapter of the thesis, I present evidence that, besides AtALMT9 (Kovermann et al., 2007) and AtALMT6 (Meyer et al., 2011), all other AtALMT proteins of clade II (Kovermann et al., 2007) are located at the vacuolar membrane. Moreover, it is shown that these vacuolar AtALMTs are able to form multi-heteromeric complexes. To obtain first insights into the physiological relevance of this interaction, I demonstrate that several vacuolar AtALMTs are expressed in parallel in the same tissues and organs.

## 3.2. Results

It has been shown in previous studies that AtALMT9 (Kovermann et al., 2007) and AtALMT6 (Meyer et al., 2011) reside at the vacuolar membrane. Since other members of the AtALMT family, namely clade II members, show high sequence similarities with AtALMT9 (Kovermann et al., 2007), the intracellular localization of these proteins was investigated. For that purpose, AtALMT5, AtALMT4 and AtALMT3 were fused to GFP and transiently transformed into tobacco (*Nicotiana benthamiana*) leaves by infiltration. Mesophyll protoplasts were obtained by enzymatic digestion and subsequently lysed in order to visualize the tonoplast.

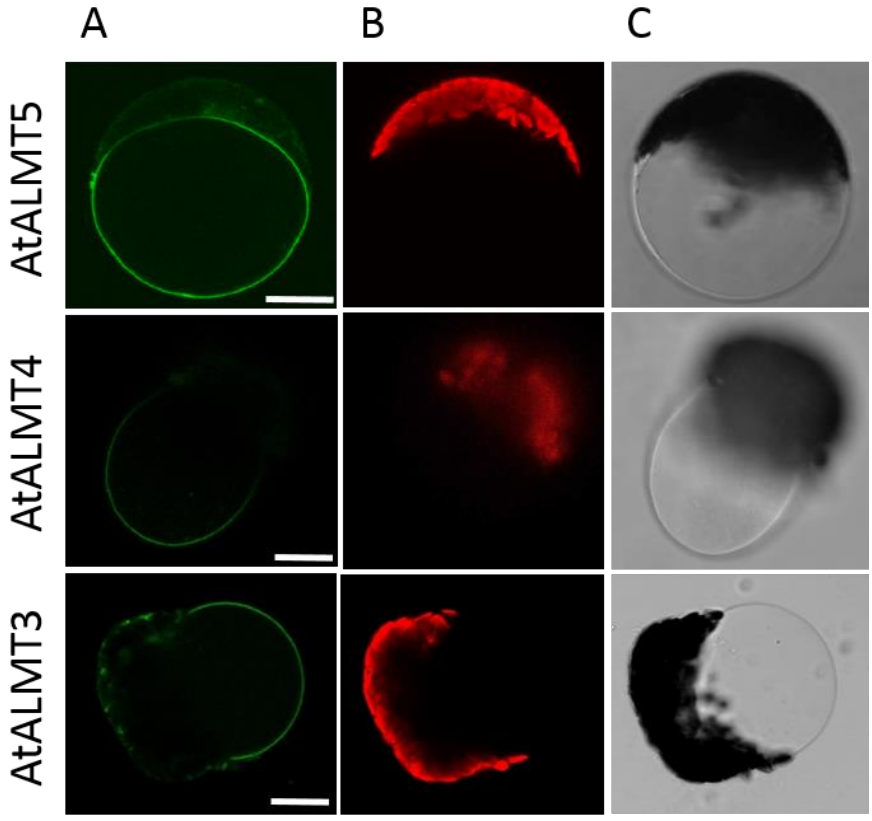


**Figure 1. Clade II AtALMT Members are Located at the Vacuolar Membrane.**

Confocal microscopy of AtALMT-GFP fusion proteins showing in panel **(A)** and **(B)** the fluorescent pictures and in **(C)** the bright fields. Tobacco leaves were transiently transformed, mesophyll protoplasts were obtained by digestion, and vacuoles were released. (A) The green signal represents the AtALMT-GFP fusion protein, (B) in red the auto-fluorescent signal of the chloroplasts are displayed. Scale bars = 25 µm.

The GFP signal was clearly detected at the vacuolar membrane, demonstrating that all clade II members of the AtALMT family are tonoplast-integral proteins (Figure 1). Patch-clamp analysis demonstrated that AtALMT4 (Eisenach et al., unpublished) and AtALMT5 proteins form functional channels. AtALMT5 was shown to be an inward rectifier that exhibits malate permeability (Figure 2).

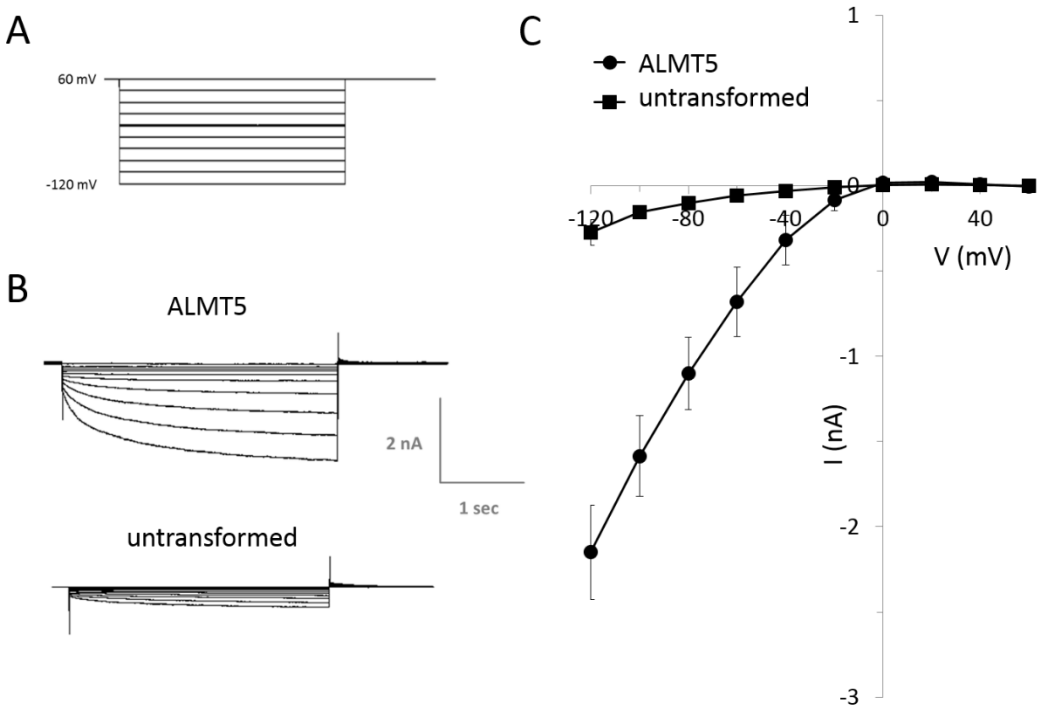


**Figure 2. AtALMT5 is an Inward Rectifying Malate Channel.**

Patch-clamp analyses of AtALMT5-GFP that is transiently overexpressed in tobacco mesophyll protoplasts. Protoplasts were obtained by digest and lysed to access the vacuolar membrane. Untransformed vacuoles served as a control for background malate currents. Both, the cytosolic and the vacuolar solutions contained 100 mM malate. Currents were recorded in the excised cytosolic-side-out configuration.

**(A)** The applied voltage pulses (3 sec) ranged from +60 mV to -120 mV and were recorded in 20 mV steps at a holding potential of +60 mV.

**(B)** Representative currents mediated by AtALMT5-GFP and by untransformed tobacco vacuoles.

**(C)** Mean currents mediated by AtALMT5-GFP (n=12) and untransformed vacuoles (n=5). Error bars denote S.E.M.

Since several AtALMT channels reside in the same membrane, and AtALMT9 has been shown to be composed of multiple subunits, the possibility arises that different vacuolar AtALMT channels interact to form heteromeric protein complexes. To test this hypothesis we made use of ratiometric bimolecular fluorescence complementation (rBiFC) (Grefen and Blatt, 2012). The modified rBiFC approach has several advantages: easier transformation (no need for co-transformation), transformation controls (constitutive RFP expression), more equal expression levels of interacting partners (expression from a single plasmid) and quantification of interaction (YFP/RFP ratio) (Grefen and Blatt, 2012).

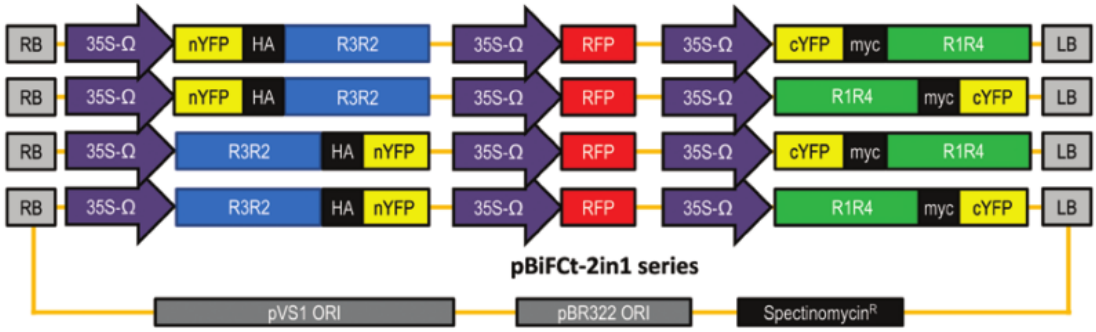


**Figure 3. Schematic Illustration of 2in1 BiFC Cloning System.**

Vector maps depicting the 2in1 BiFC vector series. The N- and C-terminal half of YFP (nYFP and cYFP) can be fused to the N-and C-terminal ends of the putative interacting candidate proteins (into the Gateway cassette R3R2 or R1R4, respectively), providing a total of four tag combinations. The constitutive expression of RFP under the control of the 35S promoter serves as a transformation and expression control as well as a tool for quantification. From Grefen and Blatt, 2012.

The approach is based on a single vector backbone that harbors multiple expression cassettes, both non-fluorescing YFP peptides as well as a constitutively expressed RFP (Figure 3). The N- and the C-terminal half of the YFP (nYFP and cYFP, respectively) can be fused to the N- or C-terminal end of the proteins of interest. Due to steric hindrance or differential localization of both termini at the other sites of membrane,

differences in interaction signal strength might arise dependent on the protein terminus at which the fluorophore halves are fused. Investigating all possible tag orientations for AtALMT9- AtALMT9 interaction allowed to determine which composition yields the strongest YFP signals (Figure 4). The constructs were transiently transformed into tobacco leaves by infiltration and emission of both, YFP and RFP, was monitored. The mean grey values of both fluorophores were calculated over a selected area. This representative area comprised the fluorescent signal of two adjacent cells. The mean fluorescence of YFP over RFP was plotted. As a control we made use of the proteins AtCBL1 and AtCIPK23 (YFP/RFP ratio of 2.6 ± 0.7), which have been previously demonstrated to exhibit strong interaction (Grefen and Blatt, 2012, Waadt et al., 2008).

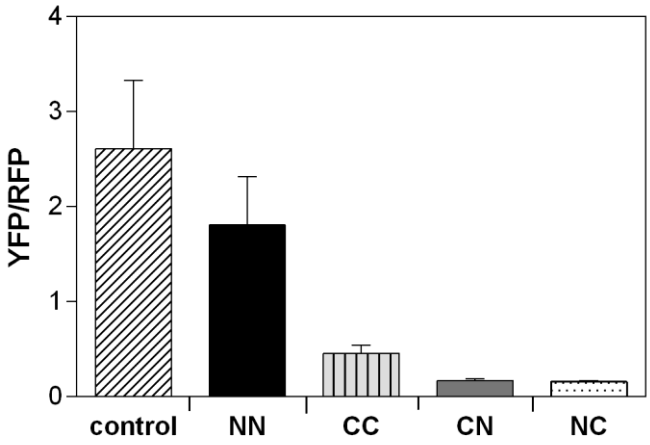


**Figure 4. AtALMT9 Interaction Detected with Different BiFC Fusion Constructs.**

Determination of YFP/RFP fluorescence signal ratio by confocal microscopy of tobacco epidermal leaf cells that overexpress different combinations of two AtALMT9 proteins that are tagged at either the N- or the C-terminal end to either half of YFP (nYFP or cYFP). NN, describes the constructs in which both, nYFP and cYFP peptides, are fused to the N-terminus of each AtALMT9; accordingly, CC represents the C-terminal fusion of nYFP and cYFP to each AtALMT9; CN, C-terminal fusion of nYFP and N-terminal fusion of cYFP; NC, N-terminal fusion of nYFP and C-terminal fusion of cYFP. N-terminal fusion of nYFP to AtCBL1 and a C-terminal fusion of cYFP to AtCIPK23 (Grefen and Blatt, 2012) served as positive control. Data were obtained from five independent transformations events in which $n \geq 5$ representative pictures were acquired and analyzed for each interaction construct. Results are shown as mean ± S.E.M.

Comparing the four different combinations at which the nYFP and cYFP can be fused to the two putatively interacting AtALMT9 subunits, we found that fusing the tag to the N-terminal end of both AtALMT9 proteins yields the highest interaction signal (Figure 4; 1.8 ± 0.5). The reason behind the different signal intensities might be a steric hindrance or differential localization of both termini in the other combinations, but cannot be concluded with this approach. In the following the interaction of vacuolar AtALMTs was investigated with constructs harboring N-terminally fused nYFP and cYFP peptides.

Next, we tested whether AtALMT9 interacts with any other vacuolar AtALMT. Again, the quantification was conducted using transiently transformed tobacco leaves (Figure 5A). Since BiFC is often associated with weak YFP background signal, we used the protein combination of AtVAMP711–AtALMT9 as a negative control. AtVAMP711 (vesicle-associated membrane proteins) is a SNARE protein (Uemura et al., 2005) that is not expected to interact with AtALMT9. Indeed, the YFP/RFP ratio in cells expressing the AtVAMP711–AtALMT9 was low (0.5 ± 0.1), representing the background signal when no specific interaction is expected to occur (Figure 5B). The YFP fluorescent signal over the RFP was significantly higher in leaves that expressed the AtALMT9-AtALMT9 construct (1.8 ± 0.2), confirming the previously obtained results that AtALMT9 forms homomeric channel complexes (Zhang et al., 2013; Chapter I). Interestingly, we show that AtALMT9 is also capable of forming hetero-multimeric complexes. The interaction capacity of AtALMT9 with AtALMT5 and AtALMT4 was confirmed by an YFP/RFP ratio of 2.0 ± 0.4 and 2.4 ± 0.2, respectively (Figure 5B). Yet, the fluorescent intensity of YFP does not support an interaction of AtALMT9 with AtALMT6 channel subunits, since the YFP/RFP ratio of 0.4 ± 0.1 for AtALMT9–AtALMT6 does not exceed the background signal of the negative control AtVAMP711–AtALMT9. Using this approach, we also showed that all other vacuolar AtALMTs are capable of forming homo- and heteromers (data not shown in this thesis). The subcellular localization of the interacting AtALMT channels in the vacuolar membrane was verified using protoplasts obtained from digested tobacco leaves (Figure 5C) and transiently transformed Arabidopsis protoplasts that were lysed to visualize the tonoplast (Figure 5D). By contrast, it was clearly observed that the soluble RFP was localized to the nucleus, the cytosol and possible other intracellular compartments.

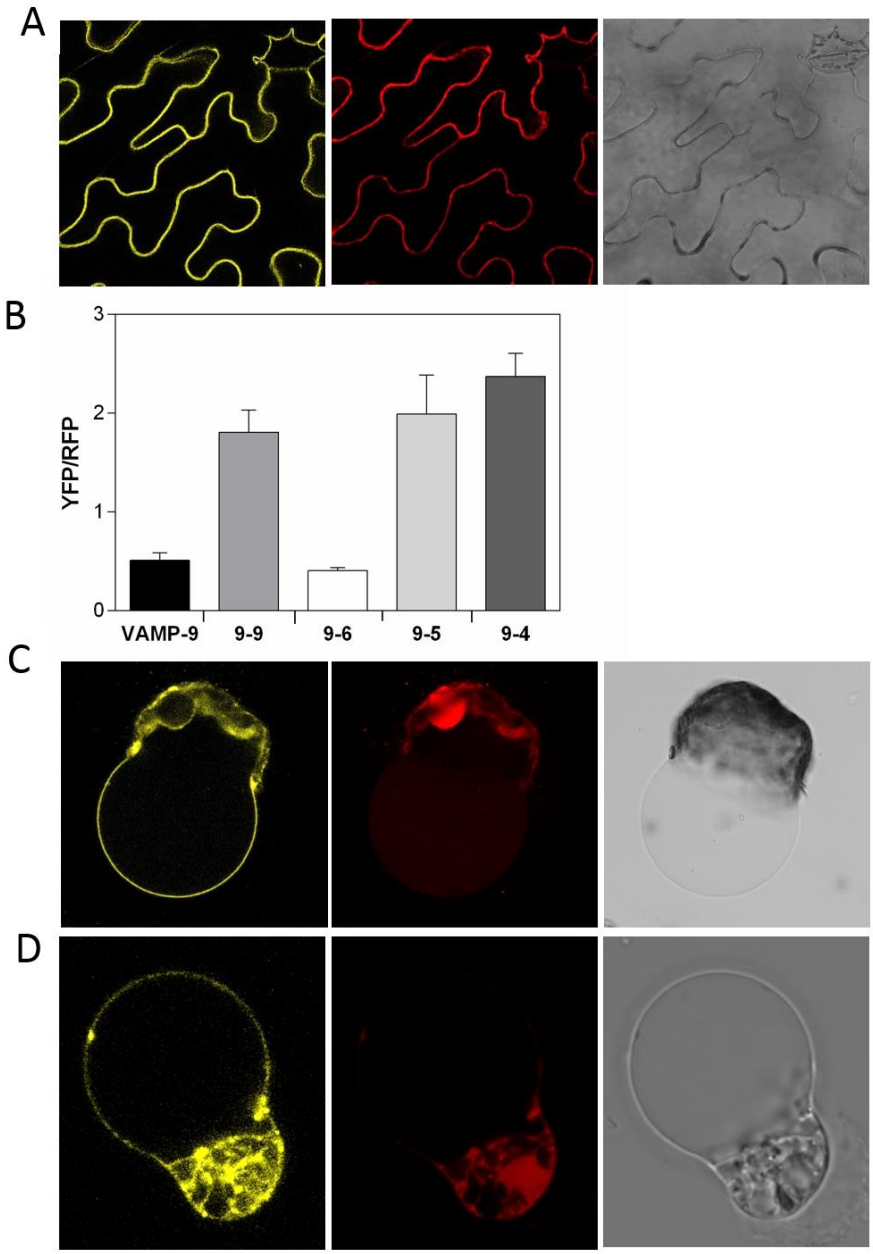


**Figure 5. AtALMT9 Forms Homo- and Heteromers with other Vacuolar AtALMTs.**

Confocal microscopy to determine the YFP/RFP fluorescent intensity signal ratio for the putative interaction of AtALMT9 (9) with AtVAMP711 (VAMP), AtALMT9 (9), AtALMT6 (6), AtALMT5 (5) and AtALMT4 (4). The position of the protein indicates whether it is fused to nYFP (protein named first) or to cYFP (second mentioned protein). All fluorescent peptides are fused to the N-terminal end of the respective interaction partner.

**(A)** Epidermal tobacco cells from leaves transiently overexpressing the different BiFC interaction constructs were used to quantify the intensity ratios shown on (B). Depicted is a representative picture of the interaction construct AtALMT9-AtALMT9.

(Figure legend 5 continued)

**(B)** Quantification of YFP/RFP fluorescence intensity ratios. Data were obtained from five independent transformations events in which n ≥ 5 representative pictures were acquired and analyzed for each interaction construct. Results are shown as mean ± S.E.M.

**(C)** and **(D)** Transient expression of rBiFC constructs carrying the interaction construct AtALMT9-AtALMT9 in tobacco (C) and (D) Arabidopsis protoplast. Vacuoles were released to uncover the subcellular localization of the protein complexes in the tonoplast.

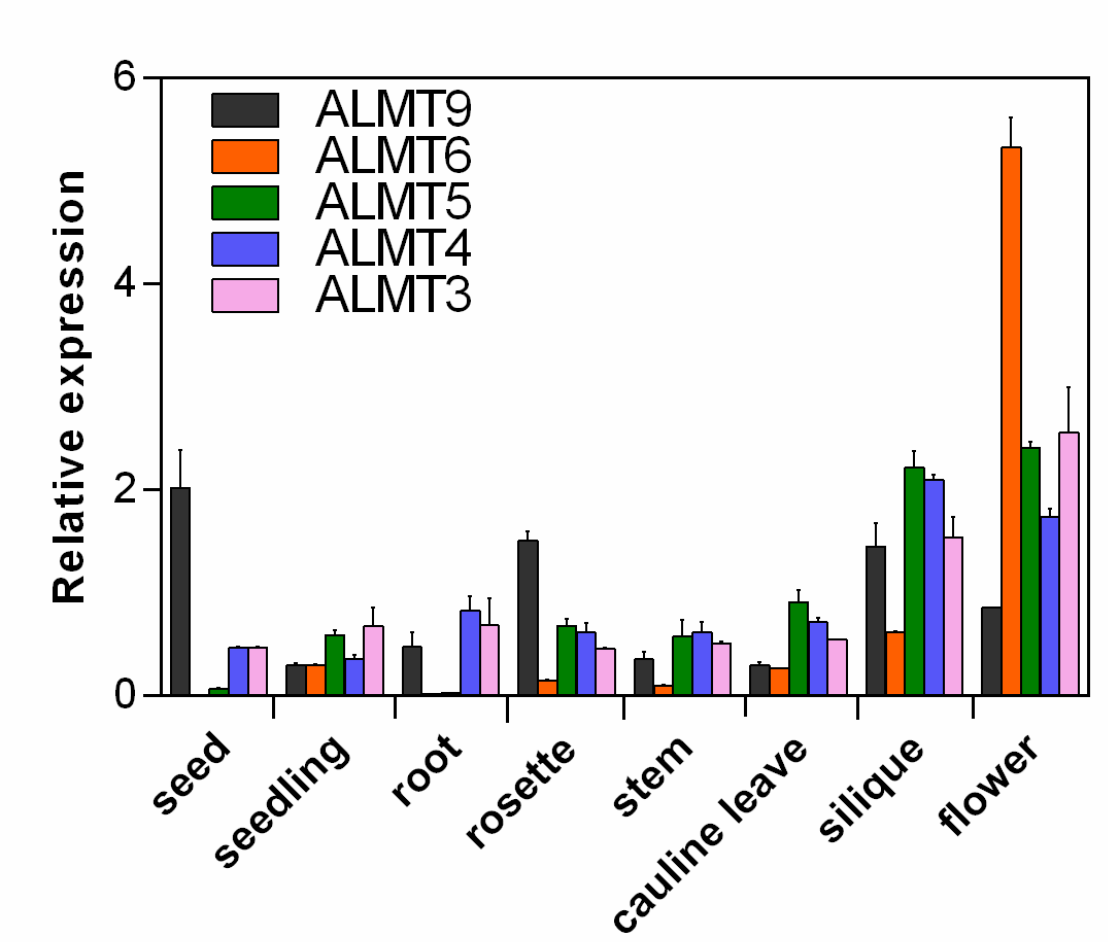


**Figure 6. Tissue Expression of Clade II *AtALMT* Members.**

qRT-PCR demonstrating the relative expression of *AtALMT* clade II members in different tissues and organs throughout the Arabidopsis life cycle. The data was normalized to the expression of *AtACT2* that served as a reference gene. Data are means ± SD of n = 2 biological replicates.

To gain first insights whether this interaction might appear *in planta* under physiological conditions, I investigated the tissue and organ expression of all vacuolar AtALMTs by quantitative real-time PCR (qRT-PCR; Figure 6). Plants were grown on plates and in sterile cylinders to assess expression during the complete life cycle. Although not all of the vacuolar *AtALMTs* are ubiquitously expressed in each of the investigated tissues and organs, e.g. *AtALMT5* and *AtALMT6* mRNA was not detected in roots, all members can be found for instance in rosette leaves, in the stem and in reproductive organs (siliques and flowers). Hence, it is shown that clade II AtALMT members are highly expressed, and co-exist in various tissues and organs, providing the possibility for a heteromeric *in planta* interaction of vacuolar AtALMT channels.

## 3.3. Discussion

We have shown that all members of the clade II of AtALMT proteins reside at the vacuolar membrane. By contrast, members of the other two clades that were characterized (AtALMT1, AtALMT12; Hoekenga et al., 2006, Kobayashi et al., 2007, Meyer et al., 2010b) have been demonstrated to be plasma membrane-spanning proteins. Hence, clade II can be defined as vacuolar subfamily of AtALMTs and shows that more closely related proteins of this family share the same intracellular localization. Besides the intracellular localization, it has been shown in this chapter that vacuolar AtALMTs share similar expression patterns within the plant and throughout the Arabidopsis life cycle. More detailed expression analysis will be required to determine whether the channels are also expressed in the same cell types, for instance in guard cells as AtALMT9 and AtALMT6. For that purpose, I cloned promoter:GUS constructs of all vacuolar AtALMTs and selected transgenic reporter lines (described for AtALMT9 in Baetz et al., submitted; Chapter III). Investigating these lines will enlighten the cell type-specific expression pattern of the vacuolar AtALMT anion channels.

The coinciding expression at the tissue and organ level determined by qRT-PCR raises the questions whether these vacuolar AtALMTs might have a redundant or distinct function, or whether they might form heteromeric channel complexes to increase their

functional diversity. Here, we confirm previous results showing that AtALMT9 forms homomers (Zhang et al., 2013; Chapter I), and we provide evidence that most vacuolar AtALMT channels display the ability to interact when heterologously expressed in a plant expression system (tobacco) as well as when expressed in the native expression system (Arabidopsis protoplast). Interestingly, AtALMT9 does not seem to be capable of interacting with AtALMT6. This result requires confirmation using other protein-protein interaction approaches, e.g. by using blocking agents in patch-clamp analysis (see below). In case AtALMT6 is the only investigated vacuolar AtALMT that does not form multimeric channel complexes with AtALMT9, further bioinformatic analysis and site-directed mutagenesis might enlighten interaction sites and/or amino acid residues that are crucial for multimerization.

Although having several benefits over traditional BiFC approaches, due to the overexpression of the interaction partners, rBiFC only provides evidence that the channel subunits have the potential to interact. Whether this capacity of heteromerization is used *in planta*, and whether the interactions allow building functional channels and have a physiological relevance, remains to be determined. To validate and evaluate the interactions, we have identified AtALMT channel blocking agents as tools to study multimeric channel functionality (Zhang et al., 2013, Zhang et al., 2014; Chapter I). In a previous study, it was shown that free ATP blocks AtALMT9 channels (Zhang et al., 2014). Further characterization of this block identified that AtALMT5 currents are similarly blocked by free ATP, while AtALMT4 currents are insensitive to the blocking agent (Eisenach et al., unpublished). The differences in ATP block sensitivity were used as a tool to investigate the functionality of AtALMT5-AtALMT4 protein interaction. When both channels were co-expressed, a shift in the dissociation constant of free ATP ($K_d^{ATP}$) by nearly one order of magnitude was observed compared to the $K_d^{ATP}$ when the channels were expressed individually. Hence, these results performed by Dr. Cornelia Eisenach confirm that AtALMT5 and AtALMT4 subunits can form functional channels.

Several plant transporters and channels have been found to assemble as homo- and heterooligomers (Ludewig et al., 2003, Reinders et al., 2002, Xuan et al., 2013, Obrdlik et al., 2004, Schulze et al., 2003). Interestingly, intense research on multimeric $K^+$

channels in plants demonstrated that channel heteromerization increases the functional diversity of transport systems by influencing the intracellular localization, electrophysiological properties, channel activity and regulation (Bregante et al., 2008, Duby et al., 2008, Brüggemann et al., 1999, Ivashikina et al., 2005, Reintanz et al., 2002, Xicluna et al., 2007, Lebaudy et al., 2010). To determine the physiological relevance of AtALMT heteromerization and the putative impact on channel properties several approaches can be applied in future research. First, expressing tandem channels linked to each other is a widely used method to study the electrophysiological effects of different subunit combinations on channel properties (e.g. Lebaudy et al., 2010). However, steric hindrance and inappropriate protein folding might tamper with channel expression and activity. A more valuable tool to study electrophysiological channel properties by patch-clamping is the utilization of the rBiFC constructs. The electrophysiological analysis of vacuoles that exhibit an YFP signal might uncover whether heteromerization impacts channel functionality, or for instance also substrate specificity. However, in parallel the characteristics of the homomeric channels AtALMT3, AtALMT4 and AtALMT5 must be studied. Secondly, physiological approaches can be used to understand the relevance of vacuolar anion channel heteromerization. For instance, several vacuolar AtALMTs exhibit (partially opposite) stomatal opening phenotypes (De Angeli et al., 2013b, Eisenach et al., unpublished). The analysis of double knock-out mutants (generated by Dr. Cornelia Eisenach) or an RNAi line that targets all vacuolar AtALMTs for multiple downregulation (generated by Ulrike Baetz and described in Baetz et al., submitted; Chapter III) will contribute to the understanding of the role of multiple AtALMT anion channels and their interaction and physiological connection in the vacuolar membrane.

# 3.4. Material and Methods

Construct Design and Plant Transformation

For subcellular localization, complementary DNA (cDNA) of AtALMT3, AtALMT4 and AtALMT5 was cloned into pART7 and subsequently sub-cloned into pART27 by *NotI* sites (Gleave, 1992). GFP was fused to AtALMT5 at the N-terminus, and to the

C-terminal end of AtALMT4 and AtALMT3. 2in1 BiFC constructs were cloned according to Grefen and Blatt, 2012. The construct that served as positive control (nYFP-AtCBL1 - AtCIPK23-cYFP) was kindly provided by Christopher Grefen.

*Agrobacterium tumefaciens* (GV3101) was transformed with these constructs using electroporation. The *A. tumefaciens*-mediated infiltration of four-weeks-old tobacco (*Nicotiana benthamiana*) leaves was performed as described previously with slight modifications (Yang et al., 2001). After transient transformation, tobacco plants were grown in the greenhouse (16 h light/ 8 h darkness, 25°C/ 23°C, 100 to 200 µmol photons $m^{-2}$ $s^{-1}$, 60% relative humidity) for another 4 to 6 d and then used to isolate protoplasts for subcellular localization and patch-clamping, or for YFP/RFP ratio determination in epidermal cells.

Tobacco protoplasts for confocal microscopy and patch-clamping were obtained by enzymatic digestion as described previously (Zhang et al., 2013; Chapter I). The enzyme solution contained 0.3 % (w/v) cellulase R-10, 0.03 % (w/v) pectolyase Y-23, 1 mM CaCl2, 500 mM sorbitol, and 10 mM MES, pH 5.3, 550 mosmol. Vacuoles were isolated by osmotic shock. Arabidopsis protoplasts were transiently transformed with a PEG-based method as described elsewhere (Yoo et al., 2007). Plasmid DNA used for Arabidopsis protoplast transformation was extracted using the 'Nucleic acid and protein purification kit' (Macherey-Nagel, Oensingen) following manufacturer's instructions.

Patch-Clamp Analysis

Membrane currents from tonoplast patches were recorded with the patch-clamp technique as described before (Zhang et al., 2013; Chapter I). Currents were evoked with voltage pulses ranging from +60 mV to -120 mV for 3 sec with a holding potential of +60 mV. Currents were recorded in the excised cytosolic-side-out configuration in symmetric malate conditions (cytosolic and vacuolar solution contained 100 mM malate, as described in [Zhang et al., 2013; Chapter I]). Liquid junction potentials were measured according to Neher (1992) and corrected when higher than ± 2 mV.

Confocal Laser Scanning Microscopy

Confocal microscopy was conducted using a Leica SP5 laser scanning microscope (www.leica-microsystems.com) that was equipped with a 63x glycerol objective. For intracellular localization of vacuolar AtALMT proteins GFP fluorescence signal was imaged at an excitation wavelength of 488 nm, and the emission was detected between 500 and 530 nm for GFP, and 600 – 650 nm for chlorophyll.

Fluorescence intensity ratios of YFP and RFP and subcellular localization for rBiFC were determined as described in Grefen and Blatt (2012). In brief, the excitation wavelength and emission was set to 514 nm/ 521-553 nm for YFP, and 561 nm/ 580-615 nm for RFP. Laser intensities were kept equal for all pictures and quantifications. Data were obtained from five independent infiltration events in which $n \geq 5$ pictures were acquired and analyzed. The appropriate Leica confocal software (LAS AF LITE) has been used for image acquisition and ratio analysis. The mean grey values of both, YFP and RFP, were calculated over a selected area for each picture. This representative area contained the fluorescent signal of two adjacent cells.

Quantitative Real-Time PCR

For the expression of AtALMTs, Arabidopsis Col-0 plants were grown in a growth chamber with the following conditions: 21 °C, 16 h light /8 h dark. For determination of transcript abundance in various tissues and organs plants were grown on plates (for AtALMT mRNA level determination in seedlings) and in sterile cylinders (for mRNA level determination of all other tissue) that contained ½ MS (Murashige and Skoog), pH5.6, and 1% phytoagar. Seedlings were 7 days old when harvested. All other tissue expression levels were determined in 7-week-old plants. In addition, dry seeds were used for analysis of AtALMT transcript abundance. Two biological replicates were performed, in each of which material of five plants was pooled.

Total RNA was extracted from up to 150 mg of the tissue by using the SV Total RNA Isolation System (Promega) following manufacturer's instructions. 1µg total RNA was reverse transcribed using M-MLV reverse transcriptase (Promega) and oligo (dT) priming. Transcript levels were determined by quantitative real-time PCR (qRT-PCR) using the 7500 Fast Real-Time PCR System (Applied Biosystems) with the 7500 Software version 2.0.4. Reactions were performed in a final volume of 15 µL with 5 µL

cDNA (diluted 1:10), 0.5 µM gene-specific primers and 7.5 µL SYBR Green PCR Master Mix (Applied Biosystems). Reaction conditions for the thermal cycling were as follows: after enzyme activation at 95 °C for 10 min, amplification was carried out in a two-step PCR procedure with 40 cycles of 15 s at 95 °C for denaturation and 1 min at 60C for annealing/extension. Dissociation curves were analyzed to verify the specificity of each amplification reaction; it was obtained by heating the amplicon from 60 to 95 °C. Transcript levels were calculated using the standard curve method as described by Pfaffl (2001) and were normalized against the *AtActin2* (At3g18780.2) gene expression. The primers that were used are the following: *AtActin2* For 5'TGGAATCCACGAGACAACCTA3', Rev 5'TTCTGTGAACGATTCCTGGAC3'; *AtALMT9* For 5'ACCTAATCCGGATCTTAGTCGATACT3', Rev 5'TCACCGAATAAAGTGGAAAGCTCAG3'; *AtALMT6* For 5'CCGTTGCATGATGCTAGTAAATAC3', Rev 5'TGATGATGGTTTGCTCGAAA3'; *AtALMT5* For 5'GAGCCGCTTCAAGATGCTAGTA3', Rev 5'ATGACTTCTTCAAACTCTCCTGCT3'; *AtALMT4* For 5'TGACGCTAGCAAGTATGCTGTT3', Rev 5'CTTCAAATTCTCCAGCTGAAACAGA3'; *AtALMT3* For 5'GGCTTATCCTACAGAGCAGAGGCT3', Rev 5'TCAGAGCCAAACCCATCTTC3'. All reactions were performed in technical triplicates that were averaged to generate one biological replicate.

# 4. Chapter III:

## Vacuolar Chloride Fluxes Impact Whole-Plant Ion Accumulation and Distribution during Early Salinity in Arabidopsis

Ulrike Baetz[1], Cornelia Eisenach[1], Enrico Martinoia[1] and Alexis De Angeli[12]

[1] Department of Plant and Microbial Biology, University of Zurich, 8008 Zurich, Switzerland

[2] Current address: Institut de Biologie Intégrative de la Cellule, CNRS, 91190 Gif-Sur-Yvette, France

Will be submitted to *Plant Physiology*.

Author Contributions:

U.B. performed the major part of the experiments and data analysis. C.E. conducted stomata assays and A.D.A. the patch-clamp study. The research was designed by all authors and the manuscript was written by U.B. and A.D.A.

## Abstract

The ability to control the cytoplasmic environment is a prerequisite for plants to cope with changing environmental conditions. During salt stress, for instance, $Na^+$ and $Cl^-$ are sequestered into the vacuole to help maintain cytosolic ion homeostasis and avoid cellular damage. Vacuolar ion uptake is tied to fluxes across the plasma membrane. The co-ordination of both transport processes and relative contribution to plant adaptation, however, is still poorly understood. To investigate the link between vacuolar anion uptake and whole-plant ion distribution during salinity we used mutants of the only vacuolar $Cl^-$ channel described to date: ALMT9. After 24 h salt treatment, *almt9* knock-out mutants had reduced shoot accumulation of both, $Cl^-$ and $Na^+$. In contrast, *almt9* plants complemented with a mutant variant of ALMT9 that exhibits enhanced channel activity showed higher $Cl^-$ and $Na^+$ accumulation. The altered shoot ion contents were not based on differences in transpiration, pointing to a vacuolar function in regulating xylem loading during salinity. In line with this finding, GUS staining demonstrated that ALMT9 is highly expressed in the vasculature of shoots and roots. RNA-seq analysis of *almt9* mutants under salinity revealed specific expression profiles of transporters involved in long-distance ion translocation. Together, our study uncovers that the capacity of vacuolar $Cl^-$ loading in vascular cells plays a crucial role in controlling whole-plant ion movement rapidly after onset of salinity.

## Introduction

Solute fluxes across the vacuolar membrane are at the center of plant performance and survival in fluctuating environmental conditions. The large central vacuole serves as a storage reservoir that accumulates and releases ions as well as metabolites according to demands. The physical and functional plasticity of the vacuole enables plants to use energy and nutrients efficiently and maintain optimal physiological conditions in the cytosol. Vacuolar storage capacity regulates intracellular ion homeostasis, but influences also whole-plant ion accumulation and distribution. For example, *nhx1 nhx2* mutant plants lack two major $Na^+$, $K^+/H^+$ antiporters at the tonoplast and show lower tissue $K^+$ accumulation (Barragán et al., 2012). Similarly, Arabidopsis (*Arabidopsis thaliana*) mutants deficient in the vacuolar $NO_3^-/H^+$ exchanger CLCa (De Angeli et al., 2006) have diminished nitrate ($NO_3^-$) contents in shoots and roots (Geelen et al., 2000, Monachello et al., 2009). Manipulating ion fluxes through the application of high ionic concentrations (for instance NaCl stress) can reveal the functional role of the vacuole in the co-ordination of ion movement at the whole plant-level.

Salinity has a negative impact on plant development, and this is based on an osmotic and an ion toxicity effect (reviewed in Teakle and Tyerman, 2010, Munns and Tester, 2008). Although salt stress responses and adaptation mechanisms were investigated with a focus on $Na^+$ toxicity and accumulation (Craig Plett and Møller, 2010), $Cl^-$ ions similarly interfere with metabolic processes in particular in photosynthetic tissue (Tavakkoli et al., 2010, Tavakkoli et al., 2011, Geilfus et al., 2015, Genc et al., 2015). To mitigate the damaging effects of salinity the movement of toxic ions across cellular membranes is tightly regulated. At the whole-plant level, plants restrict shoot ion accumulation by controlling net ion uptake and xylem loading (Britto et al., 2004, Møller and Tester, 2007, Brumós et al., 2010, Craig Plett and Møller, 2010, Teakle and Tyerman, 2010). However, recirculation of ions to the roots via the phloem does not significantly contribute to the reduction of $Na^+$ and $Cl^-$ levels in leaf tissue (Munns, 2002, Davenport et al., 2007). The ability of shoot ion exclusion is limited. Therefore, plants allocate toxic ions to specific cells or sites within the shoots to adapt to salinity. Indeed, $Na^+$ and $Cl^-$ accumulate preferentially in old leaves (Sibole et al., 2003, Craig

Plett and Møller, 2010), in the leaf margins (Shapira et al., 2009), and in epidermal cells (Huang and Van Steveninck, 1989, Karley et al., 2000a, Karley et al., 2000b, James et al., 2006) to protect photosynthetically active cells. Consequently, the controlled loading of $Na^+$ and $Cl^-$ into xylem vessels of the vasculature system in roots and shoots majorly determines long-distance ion movement such as root-to-shoot translocation and distribution within the shoots during salinity. Despite the knowledge of these physiological adaptation strategies to salt stress, the core molecular machinery underlying the regulation of ion uptake, xylem loading and partitioning is only slowly being identified.

At the cellular level, plants are capable of sequestering toxic ions into the vacuoles of shoots to minimize harm once ions have accumulated to high concentrations during salt stress (James et al., 2006, Munns and Tester, 2008). Several transport proteins localized at the tonoplast have been suggested to facilitate intracellular ion partitioning and thereby regulate cellular ion homeostasis (Martinoia et al., 2007, Martinoia et al., 2012). However, only few transporters involved in vacuolar uptake of toxic ions during salinity have been studied. The two vacuolar cation/$H^+$ antiporters NHX1 and NHX2 contribute to salinity tolerance in several plant species (Munns and Tester, 2008, and references therein). Subsequently, a role of these NHXs in vacuolar $Na^+$ sequestration has been challenged by findings suggesting their cellular function in $K^+$ compartmentation (Leidi et al., 2010, Jiang et al., 2010). With respect to intracellular $Cl^-$ uptake two members of the channel and transporter protein family CLC (ChLoride Channel), CLCc and CLCg, have been shown to be involved in salinity tolerance (Jossier et al., 2010, Nguyen et al., 2015). Besides the importance of fluxes across the tonoplast, transport proteins localized to other endomembranes such as the *trans*-Golgi network have been implicated in salinity adaptation mechanisms (Krebs et al., 2010, Bassil et al., 2011, Henderson et al., 2015). Yet, the limited knowledge about salt stress-related endomembrane transporters and their functional roles - especially with regards to $Cl^-$ sequestration - restricts our understanding of the contribution of intracellular ion homeostasis to long-distance ion fluxes and salinity adaptation mechanisms.

The ALMT (Aluminum-activated Malate Transporter) protein family is unique to plants and encodes channels able to mediate anion fluxes across cellular membranes (Barbier-Brygoo et al., 2010). In clade II of the Arabidopsis ALMT family, two ion

channels were shown to be localized at the tonoplast and mediate anion fluxes directed to the vacuolar lumen (Kovermann et al., 2007, Meyer et al., 2011, De Angeli et al., 2013). One of them, ALMT6, transports malate ($MA^{2-}$) into guard cell vacuoles in a $Ca^{2+}$- and pH-dependent manner (Meyer et al., 2011). ALMT9, a channel shown to be expressed in mesophyll and guard cells, is permeable for both, $MA^{2-}$and $Cl^-$, whereby its physiological function is linked to the $Cl^-$ conductivity (Kovermann et al., 2007, De Angeli et al., 2013). ALMT9-mediated $Cl^-$ currents across the tonoplast are activated by physiological concentrations of cytosolic $MA^{2-}$, and mesophyll vacuoles of *almt9* knock-out mutants lacking the vacuolar channel exhibit lower overall $Cl^-$ currents (De Angeli et al., 2013). Moreover, *almt9* plants have reduced $Cl^-$ uptake into vacuoles of guard cells resulting in impaired light-dependent stomatal opening and reduced wilting during drought stress.

In the current study, we aimed at uncovering the consequences of impaired intracellular $Cl^-$ fluxes across the tonoplast on whole-plant ion transport during salinity. To address this issue we used knock-out mutants of the only genuine vacuolar $Cl^-$ channel described so far, ALMT9. We found that *almt9* plants show a reduced shoot accumulation of $Cl^-$ as well as $Na^+$ after 24 h salinity, whereas mutants with enhanced ALMT9-mediated $Cl^-$ currents possessed increased ion accumulation. Using transcriptome approaches we demonstrate that genes encoding plasma membrane-localized transport proteins that contribute to long-distance ion transport exhibit an altered transcriptional response in *almt9* during salt stress. In line with this, we show that ALMT9 is highly expressed in the vasculature of shoots and roots. Collectively, the data suggest that vacuolar ion uptake is not only crucial to confer cellular tolerance during long-term salinity, but also to modulate shoot ion accumulation and whole-plant ion distribution during early phases of salinity.

## Results

### *ALMT9* is Expressed in the Vasculature and is Up-Regulated upon NaCl Application.

Gene regulation at the transcriptional level is commonly observed upon salt (NaCl) stress in plants (Tester and Davenport, 2003). To investigate whether ALMT9 is involved in intracellular $Cl^-$ transport during salinity we examined its expression levels by quantitative real-time PCR (qRT-PCR) in shoots and roots of Arabidopsis wild-type plants grown in a hydroponic system in response to 100 mM NaCl for up to 48 h. The up-regulation of expression of the salt stress-inducible gene *SOS1* (Shi et al., 2000, Shi et al., 2002) verified that plants experience salinity stress in our experimental conditions in shoots and roots at the molecular level (Figure 1A). We found that *ALMT9* was transcriptionally up-regulated in response to NaCl application in both tissues after 6 h (Figure 1B). Over 48 h of NaCl treatment, shoot expression of *ALMT9* showed a 3-fold increase when compared to the expression level prior to stress; in roots, the transcription increased 4.2 times. To discriminate whether the stimulation of *ALMT9* transcription is specific to NaCl or depends on a general osmotic effect, we applied 100 mM KCl and 200 mM sorbitol to the plants. Both treatments stimulated the expression of *ALMT9* in shoots (2-fold and 3.5-fold increase after 48 h, respectively), whereas no transcriptional response was detectable in root tissue (Figure 1C and 1D). These findings show that the transcriptional up-regulation of *ALMT9* in roots is specific to the ionic stress of salinity. Subsequently, we used transgenic plants carrying the β-glucuronidase (GUS) reporter gene under the control of the *ALMT9* promoter region ($ALMT9_{pro}$:GUS) to investigate *ALMT9* expression pattern and tissue-specificity during transcriptional up-regulation in response to salinity. As previously shown, *ALMT9* was expressed in leaf mesophyll and guard cells (Figure 1E and 1G; Kovermann et al., 2007, De Angeli et al., 2013). The mesophyll expression was predominantly detected in mature leaves. In contrast, GUS staining was found in the vasculature throughout all developmental stages of the leaf (Figure 1E and 1F). *ALMT9* promoter-driven GUS expression could also be detected in the stele of roots (Figure 1H). A transverse section allowed to locate *ALMT9* expression in vascular and pericycle cells, as well as weakly in the endodermis (Fig. 1J). However, *ALMT9* was not expressed in root cortex or epidermis cells.

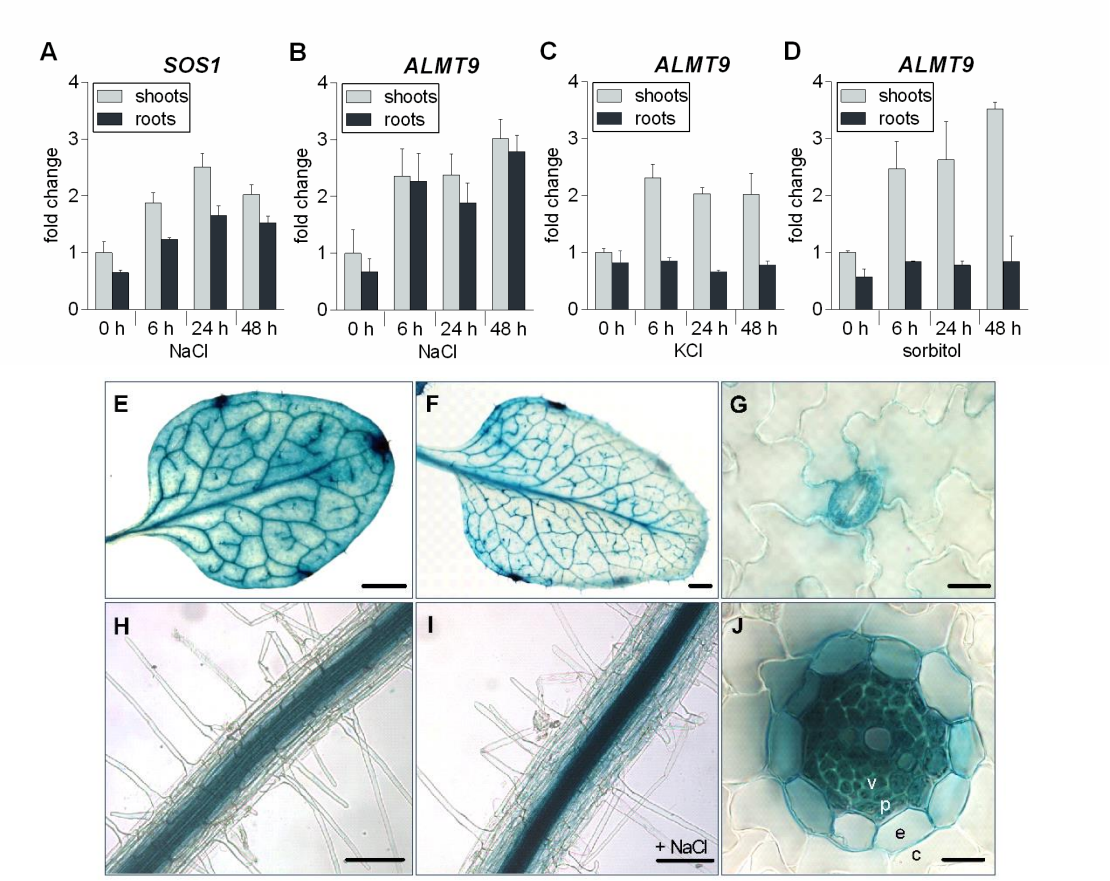


**Figure 1.** *ALMT9* is Expressed in the Vasculature and is Regulated by Salinity.

**(A)** to **(D)** qRT-PCR analysis of *SOS1* **(A)** and *ALMT9* (**[B]** to **[D]**) expression in wild-type shoots and roots after the application of 100 mM NaCl (**[A]** and **[B]**), 100 mM KCl **(C)** and 200 mM sorbitol **(D)** to the hydroponic solution for 0 h, 6 h, 24 h and 48 h. The data was normalized to expression levels in shoots prior to treatment (0 h). *ACT2* served as a reference gene. Data are means ± SD of n = 3 biological replicates.

**(E)** to **(J)** *ALMT9* expression pattern revealed by histochemical localization of GUS activity directed by the *ALMT9* promoter.

**(E)** In the 3rd rosette leaf expression was found in mesophyll cells and the vasculature.

**(F)** In the 6th rosette leaf expression was detected in the vasculature.

**(G)** GUS activity was detected in guard cells.

**(H)** In roots expression was found in stelar cells.

**(I)** In response to 100 mM NaCl for 24 h GUS activity was enhanced but remained restricted to the root stele.

**(J)** In cross sections of roots no expression was detected in cortex cells (c), but in the endodermis (e), the pericycle (p) and the vasculature (v).

Scale bars represent 0.2 mm in **(E)** and **(F)**, 10 µm in **(G)** and **(J)**, and 100 µm in **(H)** and **(I)**.

As observed in the qRT-PCR (Figure 1B), NaCl treatment enhanced the intensity of the GUS staining (Figure 1I), corresponding to a transcriptional up-regulation of *ALMT9*. Nevertheless, the tissue-specific expression pattern did not change upon salt exposure.

**The *almt9* Mutants Have Reduced Shoot $Na^+$ and $Cl^-$ Accumulation during Early Salinity.**

To assess whether the transcriptional up-regulation of *ALMT9* in response to NaCl is associated with a physiological role of ALMT9 during salinity, we conducted ion content measurements in shoots and roots of wild-type and two independent *almt9* knock-out mutant lines (De Angeli et al., 2013). As before, a hydroponic system was used, and roots were exposed to control conditions or salt stress (100 mM NaCl), respectively, for 24 h. Under control conditions, hardly any difference in $Na^+$ and $Cl^-$ contents were detected between *almt9* mutants and wild-types (Figure 2A and 2B; Supplemental Table 1). However, upon 24 h salt stress, $Cl^-$ accumulation was significantly lower in shoots of *almt9* plants compared to the corresponding wild-types (26 ± 4 % in *almt9-1* and 16 ± 3 % in *almt9-2*). Interestingly, $Na^+$ contents in shoots of *almt9* mutants were similarly reduced upon salinity treatment (20 ± 6 % in *almt9-1* and 23 ± 10 % in *almt9-2*), but root ion content was not significantly altered (Figure 2A and 2B; Supplemental Table 1). When plants were treated with 100 mM NaCl for one week differences were no longer significant between wild-type and *almt9* mutants (Supplemental Figure 1). Taken together, these results show that *almt9* knock-out mutants exhibit - besides the reduction in intracellular $Cl^-$ fluxes (De Angeli et al., 2013) - also an altered capacity to accumulate $Na^+$ and $Cl^-$ in shoots during early salinity.

In the following, we elucidated whether reduced $Na^+$ and $Cl^-$ levels in *almt9* mutants during salinity are accompanied by alterations in the accumulation of other ion species. $K^+$ (Figure 2C, Supplemental Table 1), $Mg^{2+}$ (Supplemental Figure 2A), $NO_3^-$ (Figure 2D, Supplemental Table 1), and $MA^{2-}$ (Supplemental Figure 2B) contents showed no significant differences between both genotypes under control and salinity conditions. Also the osmolality of the shoot press sap was indistinguishable between *almt9* and wild-types (Supplemental Figure 2C). This suggests that despite reduced $Na^+$ and $Cl^-$

contents in the shoots of *almt9* mutants, these plant accumulate other solutes that maintain a shoot sap osmolality comparable to that of the wild-type.

ALMT9 has high sequence similarities with several clade II members of the ALMT family (Kovermann et al., 2007). To exclude functional redundancy, we generated a transgenic hairpin-RNA-expressing line in the genetic background of *almt9-1* that simultaneously targets other ALMTs (clade II) for transcriptional down-regulation (Supplemental Figure 3A).

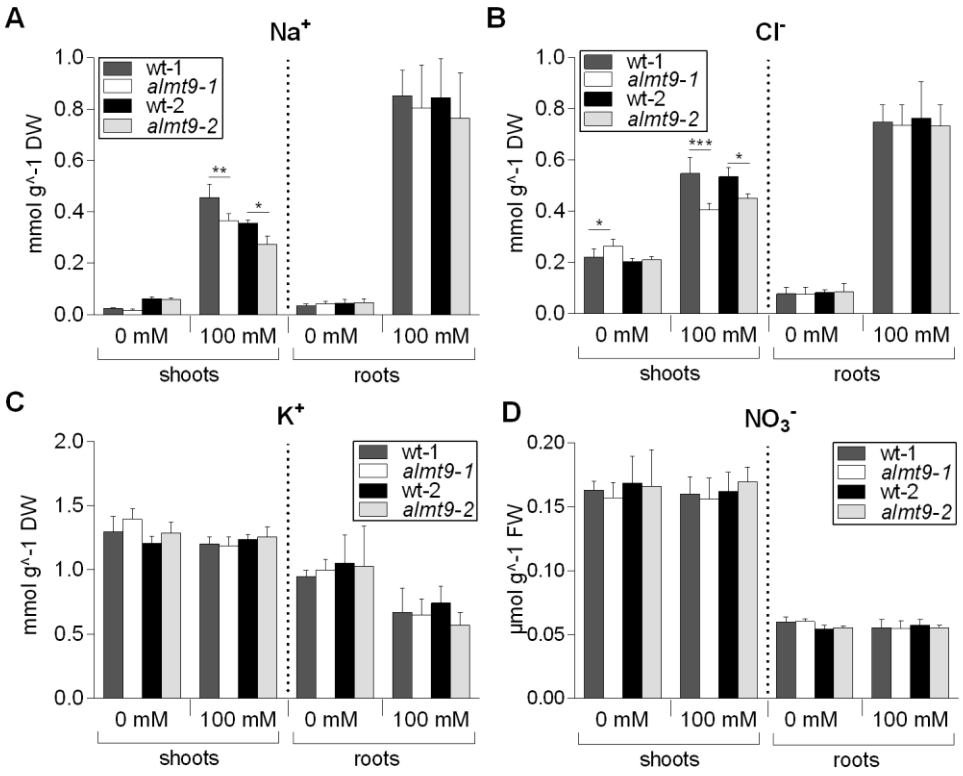


**Figure 2.** *almt9* Mutants Have Reduced Shoot $Na^+$ and $Cl^-$ Contents after 24 h Salt Stress.

Ion content analysis in shoots and roots of the two knock-out alleles *almt9-1 and almt9-2* and the corresponding wild-types (wt-1 and wt-2). Plants were grown in hydroponics and $Na^+$ **(A)**, $Cl^-$ **(B)**, $K^+$ **(C)** and $NO_3^-$ **(D)** contents were determined prior to (0 mM) and after 24 h NaCl treatment (100 mM). Data are means ± SD of $n \geq 5$ biological replicates derived from two independent experiments. One-way ANOVA of each tissue and treatment and a pair-wise comparison was used for statistical analysis. Asterisks indicate significant differences from the corresponding wt (*$P < 0.05$, **$P < 0.01$, ***$P < 0.001$). DW, dry weight; FW, fresh weight.

Shoots of this line did not show further reduction in $Na^+$ or $Cl^-$ accumulation than *almt9-1* (Supplemental Figure 3B and 3C), indicating that other closely related ALMT members do not contribute notably to the modulation of $Na^+$ and $Cl^-$ shoot accumulation upon 24 h salt stress.

**ALMT9-Mediated Vacuolar $Cl^-$ Currents Contribute to the Regulation of Whole-Plant Ion Accumulation.**

Our data show that *almt9* mutants with reduced vacuolar $Cl^-$ currents (De Angeli et al., 2013) accumulate less $Na^+$ and $Cl^-$ during salinity (Figure 2). Hence, we wondered whether enhancing vacuolar $Cl^-$ currents would reverse or complement this effect on whole-plant ion accumulation. When modifying ion fluxes during salinity by transgenic approaches, it is fundamental to maintain cell type-specificity of these transport processes (Møller et al., 2009). Therefore, instead of using ectopic overexpression of ALMT9, we aimed at identifying a mutated channel variant that exhibits increased $Cl^-$ current activity. For this purpose, we took advantage of a collection of point-mutated ALMT9 channels that was previously generated (Zhang et al., 2013). We found that the amino acid exchange E196A induced the desired alterations in ALMT9 channel properties, but did not change the channel localization at the tonoplast (Figure 3A). It has been shown by patch-clamping that the mutation E196A does not affect the $MA^{2-}$ conductivity of ALMT9 (Zhang et al., 2013). Here, we additionally examined the $Cl^-$ conductivity (Figure 3B) and found that both, ALMT9 and $ALMT9_{E196A}$, displayed $Cl^-$ currents and a marked inward rectification (Figure 3C). However, sequential cytosolic-side buffer exchanges (Figure 3B) revealed that the ratio of $Cl^-$ to $MA^{2-}$ currents ($I_{Cl^-}$/ $I_{MA2^-}$) differed between both channel variants (Figure 3D). The $Cl^-$ current amplitude was 5 ± 2 % of the $MA^{2-}$ current amplitude in ALMT9 and 18 ± 4 % in $ALMT9_{E196A}$ (Figure 3D). This shows that $ALMT9_{E196A}$ is approximately three times more permeable for chloride than ALMT9. In addition, by determining $I_{Cl^- + MA2^-}$/ $I_{Cl^-}$ we found that ALMT9 and $ALMT9_{E196A}$ were differently activated by cytosolic $MA^-$ (Figure 3C). ALMT9 showed a 6 ± 1 fold increase of $Cl^-$ conductivity in presence of 1 mM $MA^{2-}$ at -100 mV, whereas $ALMT9_{E196A}$ showed a 2 ± 0.6 fold increase (Figure 3E).

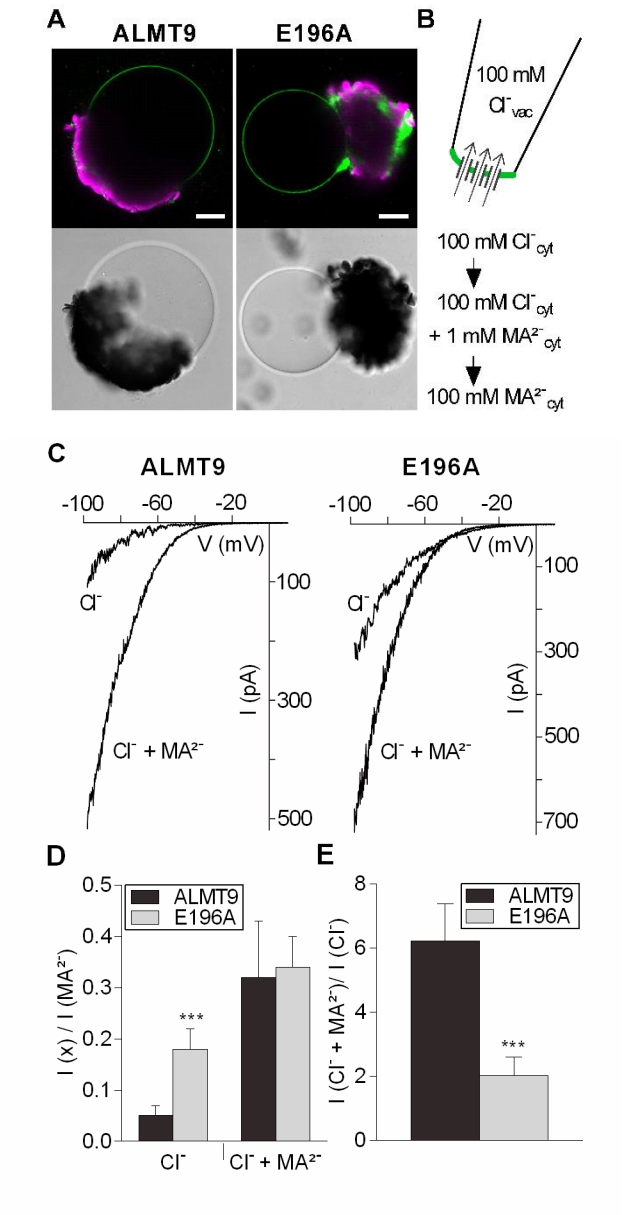


**Figure 3.** The Mutant Channel ALMT9$_{E196A}$ Exhibits Constitutively Higher Vacuolar $Cl^-$ Currents.

**(A)** Fluorescence and transmission images of vacuoles released from lysed tobacco protoplasts that transiently overexpress ALMT9-GFP (left panel) and ALMT9$_{E196A}$-GFP (right panel). Auto-fluorescence of chloroplasts is shown in magenta. Scale bars = 20 µm.

**(B)** Patch-clamp experimental procedure. Vacuoles were patched in excised, cytosolic-side-out configuration under symmetric ionic conditions (100 mM $Cl^-_{vac}$/ 100 mM $Cl^-_{cyt}$). The cytosolic buffer was sequentially exchanged (100 mM $Cl^-$; 100 mM $Cl^-$ + 1 mM $MA^{2-}$; 100 mM $MA^{2-}$) on the same membrane patch.

(Figure legend 3 continued)

**(C)** Representative currents of ALMT9 (left panel) and ALMT9$_{E196A}$ (right panel) in presence of 100 mM $Cl^-$ ($Cl^-$) and 100 mM $Cl^-$ + 1 mM $MA^{2-}$ ($Cl^-$ + $MA^{2-}$) in the cytosolic buffers. Currents were evoked by a 2.5 s voltage ramp ranging from +40 mV to -100 mV.

**(D)** Relative $Cl^-$ and $Cl^-$ + $MA^{2-}$ currents mediated by ALMT9 and ALMT9$_{E196A}$. Currents were normalized to the current amplitude measured at -100 mV in presence of 100 mM $MA^{2-}$ in the cytosolic solution.

**(E)** Level of $MA^-$-activation ($I_{Cl^- + MA2^-}$/ $I_{Cl^-}$) of ALMT9- and ALMT9$_{E196A}$- mediated $Cl^-$ currents at -100 mV.

Data are means ± SD. Asterisks indicate statistically significant differences between ALMT9 (n = 5) and E196A (n = 6) currents (*P < 0.05, **P < 0.01, ***P < 0.001; two-tailed Student's t-test).

However, the ratio $I_{Cl^- + MA2^-}$/ $I_{MA2^-}$ that was 0.32 ± 0.1 and 0.34 ± 0.06 in ALMT9 and ALMT9$_{E196A}$, respectively, was not significantly altered between both cannel variants (Figure 3D). These data demonstrate that the mutation E196A impacts the basal activity of ALMT9 by increasing $Cl^-$ currents across the tonoplast constitutively.

The electrophysiological measurements identified ALMT9$_{E196A}$ as a suitable tool to modify $Cl^-$ fluxes across the tonoplast. To test the physiological consequences of higher vacuolar $Cl^-$ currents, we expressed the mutant channel under the spatial and temporal control of the *ALMT9* promoter (ALMT9$_{pro}$:ALMT9$_{E196A}$) in *almt9-2*; hereafter, this point-mutated complementation line is referred to as *E196A*. Determining the ion content in shoots revealed that *E196A* had slightly higher $Na^+$ and $Cl^-$ concentrations than wild-type-2 and *almt9-2* under control conditions (Figure 4A and 4B). In addition, the reduced shoot ion accumulation phenotype of *almt9-2* was recovered in *E196A* under salt treatment. In roots we found that 24 h salinity treatment induced a significantly higher ion accumulation in *E196A* (1.3 times more $Cl^-$ and 1.7 times more $Na^+$) compared to wild-type-2 (Figure 4A and 4B). To exclude the possibility that differences in ion accumulation occur due to elevated *ALMT9* expression, we analyzed the transcript amounts by qRT-PCR. *ALMT9* expression in *E196A* and wild-type-2 did not differ significantly excluding a transcriptional effect on the measured ion concentrations (Figure 4C). In summary, these results demonstrate that the magnitude

of ALMT9-mediated vacuolar $Cl^-$ uptake alters ion accumulation at the whole-plant level.

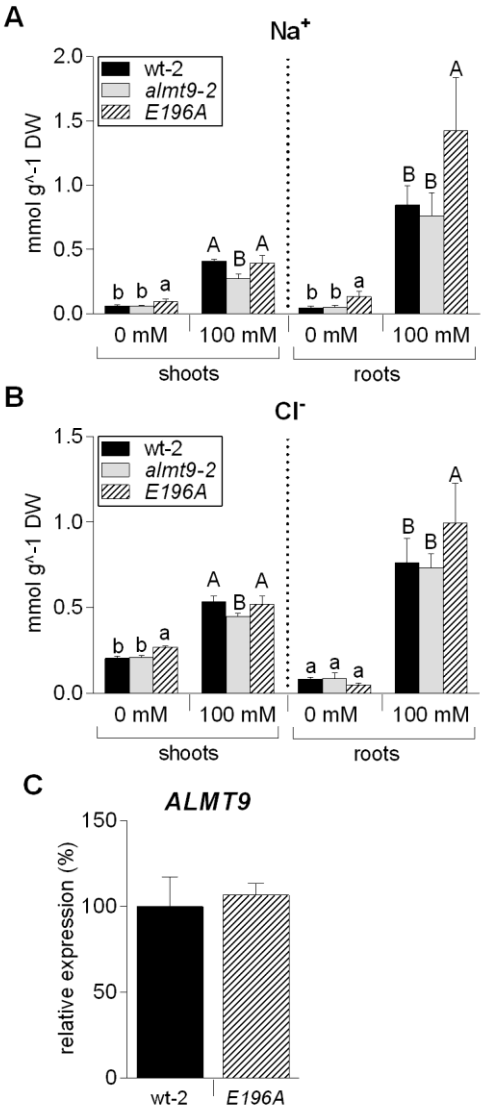


**Figure 4.** Enhanced Vacuolar $Cl^-$ Currents Affect Shoot and Root Ion Contents.

**(A)** and **(B)** Ion contents were analyzed in hydroponically grown plants of wild-type-2 (wt-2), *almt9-2* and the complemented line *E196A* that expresses the point-mutated channel variant $ALMT9_{E196A}$. $Na^+$ **(A)** and $Cl^-$ **(B)** measurements were performed in shoot and root tissue upon treatment with control (0 mM) or NaCl (100 mM) solutions for 24 h. The results are shown as mean ± SD of $n \geq 5$ biological replicates derived from two independent experiments. For statistical analysis, one-way ANOVA of each tissue and treatment and a Tukey-Kramer multiple comparison post-test was used. Different lowercase letters indicate significant

(Figure legend 4 continued)
differences in ion content ($P < 0.05$) under control conditions, capital letters under salinity. DW, dry weight.
**(C)** Expression analysis of *ALMT9* in wt-2 and *E196A* using qRT-PCR. *ACT2* served as a reference gene. The expression levels were normalized to wt-2. Data are means ± SD from n = 2 biological replicates.

## Lower Shoot Ion Accumulation in *almt9* is not Caused by Impaired Stomatal Opening.

Transpiration rates highly impact root-to-shoot translocation of ions. In a previous study, *almt9* has been shown to display impaired light-dependent stomatal opening due to reduced $Cl^-$ fluxes into the vacuoles of guard cells (De Angeli et al., 2013). Therefore, we investigated whether decreased leaf transpiration in *almt9* might be responsible for the observed reduction in shoot ion translocation under salt stress. Previously, stomatal apertures of *almt9* had been analyzed on peeled epidermal strips (De Angeli et al., 2013). In the present study we performed *in situ* stomatal assays using hydroponically grown plants (see Methods) that provide a snapshot of the native stomatal aperture over a time course of NaCl treatment. Indeed, using this method in blind assays the previously reported reduced stomatal aperture of *almt9* mutant plants (De Angeli et al., 2013) was reproduced (Figure 5A). Salinity treatment induced stomatal closure in wild-type-1 and *almt9-1* after 3 h (Supplemental Figure 4A). Upon 24 h salt stress we observed a recovery of the stomatal aperture, which is in accordance with the observation that $Na^+$ can be used as osmotically active solute for stomatal opening (Yu and Assmann, 2015, Zhao et al., 2011). Interestingly, the reduced stomatal opening in *almt9* plants was restored upon salinity (Figure 5A). Similarly, when we conducted the same assay using 100 mM KCl we found no significant difference between the stomatal aperture of wild-type-1 and *almt9-1* (Supplemental Figure 4B), suggesting that this complementation was based on the increased presence of osmotica. This indicated that reduced *almt9* stomatal apertures and transpiration were not responsible for decreased shoot ion accumulation.

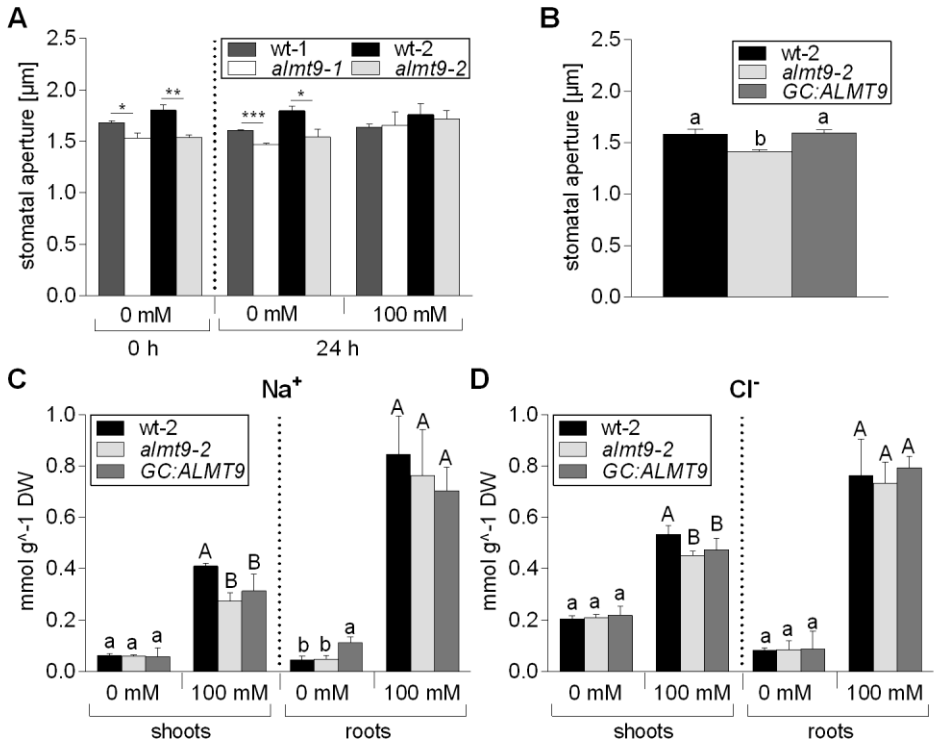


**Figure 5.** Impaired Stomatal Opening of *almt9* does not Account for Differences in Shoot Ion Accumulation.

**(A)** *In situ* assay of native stomatal apertures (see Methods) using hydroponically grown plants of the *almt9-1* and *almt9-2* mutant alleles and the corresponding wild-types (wt-1 and wt-2). Roots were exposed to control (0 mM) or NaCl (100 mM) solutions, and the stomatal aperture was measured before (0 h) and after (24 h) treatment. Error bars correspond to SEM which was calculated from averages of at least four biological replicates. Asterisks indicate statistically significant differences in stomatal aperture from the corresponding wt (*P < 0.05, **P < 0.01, ***P < 0.01; two-tailed Student's t-test).

**(B)** *In situ* assay of native stomatal apertures of wt-2, *almt9-2* and the complemented line *GC:ALMT9* that guard cell-specifically expresses ALMT9 in control conditions. Error bars correspond to SEM which was calculated from n ≥ 4 biological replicates.

**(C)** and **(D)** Contents of $Na^+$ **(C)** and $Cl^-$ **(D)** were measured in shoots and roots of hydroponically grown wt-2, *almt9-2* and *GC:ALMT9* plants after 24 h treatment with control (0 mM) or NaCl (100 mM) solutions. The combined results from two independent experiments are shown as mean ± SD (n ≥ 5). For statistical analysis in **(B)** to **(D)**, one-way ANOVA and a Tukey-Kramer multiple comparison were used. Different letters indicate significant differences

(Figure legend 5 continued)
in ion content ($P < 0.05$) within each tissue (lower case in control conditions; capital letters under NaCl stress). DW, dry weight.

To gain definite evidence that the stomatal conductance of *almt9* does not contribute to lower ion accumulation, we generated an ALMT9 complementation line under the control of the guard cell-specific *MYB60* (Cominelli et al., 2005) promoter ($MYB60_{pro}$:ALMT9) in the genetic background of *almt9-2*, referred to as *GC:ALMT9* (Supplemental Figure 5).
The reduced light-dependent stomatal opening of *almt9-2* was rescued in *GC:ALMT9* (Figure 5B). However, *GC:ALMT9* did not complement the ion accumulation phenotype of *almt9* mutants (Figure 5C and 5D). This result demonstrates that impaired stomatal opening and transpiration of *almt9* does not account for differences in shoot ion accumulation during early salinity.

**Disturbed Intracellular $Cl^-$ Fluxes Induce a Specific Expression Pattern under Salinity.**

In order to unravel the physiological basis of the detected differences in ion accumulation and elucidate the role of vacuolar ion uptake during salinity, we conducted a transcript profile analysis by RNA-seq using wild-type-1 and *almt9-1* shoots and roots under non-saline and saline conditions (0 mM or 100 mM NaCl for 24 h). Data of three biological replicates were analyzed as described in the Methods section. To identify genes with significant differences in expression between wild-type-1 and *almt9-1*, we used a fold change cut-off level of 2 ($\log_2$ ratio $\geq \pm 1$, $P < 0.01$). A total of 352 genes showed a twofold or greater difference in expression in shoots and 52 genes in roots under control conditions, and 144 in shoots and 53 in roots under salinity (Figure 6A; Supplemental Data Set 1 to 4).
Strikingly, under non-saline conditions numerous genes that are suggested to be stress-inducible and/or involved in ABA-mediated signaling, such as the PP2C-type protein phosphatases AIP1 (Lim et al., 2012) and ABI2 ( Merlot et al., 2001, Rubio et al., 2009), were differentially expressed in *almt9-1* (Supplemental Data Set 1 and 2). Besides,

several genes encoding ATP-Binding Cassette (ABC)- transport proteins and genes that belong to the NRT (Nitrate Transporter) family (NRT1.8 (Li et al., 2010) in shoots and NRT2.4 (Kiba et al., 2012) in roots) exhibited changes in expression levels (Supplemental Data Set 1 and 2). The transcriptional modification of stress- and transport-related genes indicate that the reduced vacuolar $Cl^-$ fluxes in *almt9* mutants impact plants at the molecular and physiological level.

We identified only 26 genes in shoots and 10 genes in roots with a significant difference in the expression level under both, control and salinity conditions (Figure 6A). Hence, salt stress evokes distinct changes between the transcriptomes of wild-type-1 plants and *almt9-1* mutants.

Subsequently, we closely analyzed the subset of genes with a significant up- or down-regulation in *almt9-1* exclusively under salt stress (Figure 6B; Supplemental Table 2 and 3; for selection criteria see Method section). We identified 54 genes that were up-regulated in *almt9*-1 shoots and 16 genes that were down-regulated; 13 genes that were up-regulated in *almt9-1* roots and 18 genes that were down-regulated. Several of these genes have functions associated with salt stress (Supplemental Figure 6; Supplemental Table 2 and 3), such as stress signal transduction, e.g. ERF/AP2-type transcription factors, *DDF1* and *DDF2* (Magome et al., 2004, Magome et al., 2008); redox homeostasis, e.g. ascorbate peroxidase, *APX2*; and hormone homeostasis, e.g. *UGT74E2* (Tognetti et al., 2010). The data show that the lack of the vacuolar $Cl^-$ channel ALMT9 has a global impact on the genome-wide transcriptional response under salinity.

Among the genes showing differential transcriptional regulation exclusively upon salinity we examined candidates that code for transporter proteins with a putative role in salinity-related processes in more detail (Figure 6C to 6E). The RNA-seq results were verified by qRT-PCR using the second knock-out allele *almt9-2*. We confirmed that the expression of the *CHX21* gene that encodes for a putative plasma membrane $Na^+$ transporter (Hall et al., 2006) was indistinguishable between both genotypes under control condition in shoots (Figure 6C, Supplemental Table 2). However, upon salinity the transcript levels increased slightly in the wild-type but decreased in *almt9*. Interestingly, we identified three Multidrug and Toxic Compound Extrusion (MATE)-

related transporter genes by RNA-seq whose expression was highly up-regulated in *almt9-1* shoots upon salinity (Supplemental Table 2).

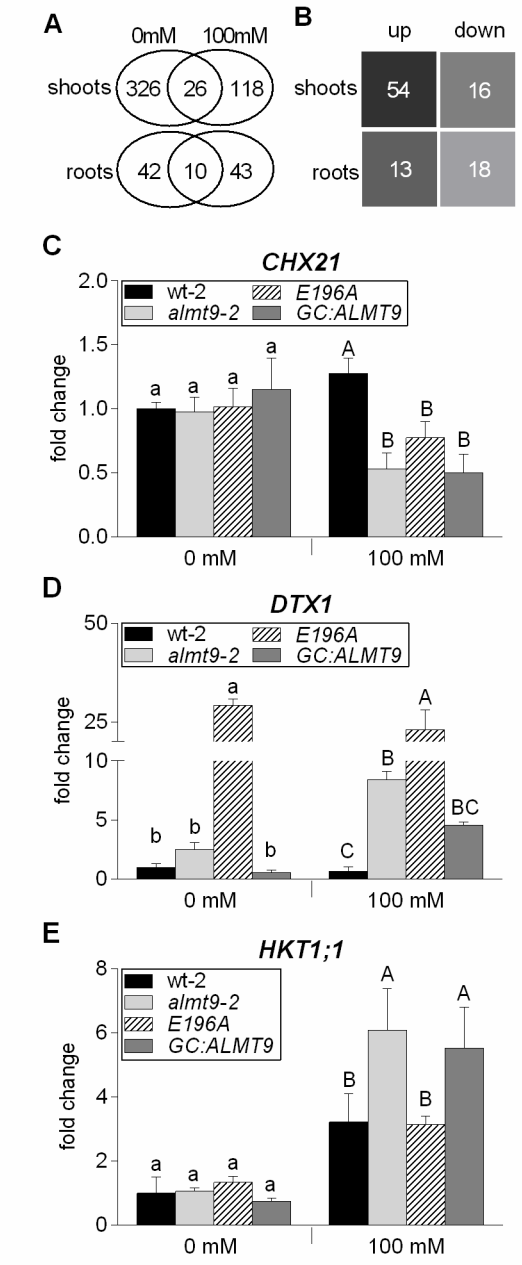


**Figure 6.** Transcriptome Analysis Reveals Distinct Expression Patterns in *almt9* upon Salinity.

**(A)** and **(B)** RNA-seq analysis in shoots and roots of hydroponically grown wild-type-1 (wt-1) and *almt9-1* plants upon exposure to control (0 mM) or NaCl (100 mM) conditions for 24 h. **(A)** Venn diagram showing the number of differentially expressed genes between wt-1 and *almt9-1* within each tissue and treatment. The overlap between the ovals represents genes that have significant changes in gene expression under both treatments.

(Figure legend 6 continued)

**(B)** Number of genes that are significantly differentially expressed between both genotypes exclusively under salinity. For selection requirements see Method section. up, up-regulated genes in *almt9-1*; down, down-regulated genes in *almt9-1*.

**(C)** to **(E)** The expression levels of candidate genes were determined in wt-2, *almt9-2*, and the complemented lines *E196A* and *GC:ALMT9* by qRT-PCR. The same experimental set-up as for the RNA-seq analysis was used. Transcript abundance of *CHX21* **(C)** and *DTX1* **(D)** was determined in shoots, transcript abundance of *HKT1;1* **(E)** in roots. The data were normalized to the expression level of the respective gene in wt-2 under control conditions. *ACT2* served as a reference gene. Each data point was derived from $n \geq 3$ biological replicates and is shown as mean ± SD. In **(C)** to **(E)**, significances at $P < 0.05$ were analyzed by one-way ANOVA and Tukey-Kramer multiple comparison post-test for each treatment and are indicated by lettering (lower case = control conditions; capital letters = salinity).

---

We confirmed this expression pattern using one of them, DTX1 (Figure 6D), a plasma membrane transporter that was suggested to export toxic compounds (Li et al., 2002). In the RNA-seq data of roots, the expression of *HKT1;1*, a well-known gene coding for a $Na^+$-selective transport protein at the plasma membrane of root stelar cells (Davenport et al., 2007), showed high variability between the three biological replicates and was therefore not among the significantly differentially regulated genes. Since HKT1;1 has a crucial role in diminishing long-distance $Na^+$ transport to shoots we further investigated its transcriptional response to salinity in both genotypes by qRT-PCR. The analysis of four biological independent experiments proved that *HKT1;1* expression increased in *almt9-2* roots in response to salinity approximately twice as much as in wild-type-2 roots (Figure 6E).

Our qRT-PCR analysis of *CHX21*, *DTX1* and *HKT1;1* included the complementation lines *E196A* and *GC:ALMT9* to untangle the molecular basis of the transcriptional dis-regulation of the candidate transporter genes. For all three investigated genes *GC:ALMT9* showed similar expression patterns as *almt9-2* (Figure 6C to 6E), consistent with the finding that differences in ion concentration do not arise from differences in stomatal movement between wild-type and *almt9* during salinity (Figure 5). The *E196A* plants, which have enhanced vacuolar $Cl^-$ conductivity in the

vasculature and leaf mesophyll, showed a more complex transcriptional response. Indeed, *E196A* roots displayed the same expression profile of *HKT1;1* as wild-type-2 (Figure 6E), but had a similar expression pattern as *almt9-2* regarding the shoot *CHX21* expression (Figure 6C), and showed an even more pronounced transcriptional up-regulation of *DTX1* in shoots than the *almt9-2* mutant (Figure 6D).

The RNA-seq data identified further transporter genes that show changes in gene expression in *almt9-1* specifically upon salinity (Supplemental Table 2 and 3), namely *ACA12* (Limonta et al., 2014), *ABCB4* (Terasaka et al., 2005), *SUC5* (Baud et al., 2005, Pommerrenig et al., 2013) and *OCT1* (Lelandais-Brière et al., 2007, Strohm et al., 2015). Notably, no member of the ALMT, CLC or NRT family has been identified as differentially regulated in *almt9-1* in response to salinity (Supplemental Table 2 and 3).

## Discussion

During salinity the sequestration of $Na^+$ and $Cl^-$ ions into the vacuole is crucial to maintain optimal metabolic conditions in the cytosol and mitigate cellular damage. Our data provide new insights into the role of intracellular ion partitioning during salt stress. Crucially, we show that $Cl^-$ fluxes across the vacuolar membrane have consequences on fluxes across the plasma membrane and thereby influence global plant ion movement. Firstly, we present evidence that disturbed vacuolar $Cl^-$ uptake has a dramatic effect on shoot ion accumulation during early salt stress. Secondly, the data show a strong correlation between anion and cation fluxes during salinity as not only $Cl^-$ but also $Na^+$ accumulation was affected in *almt9* and *E196A* mutants. And thirdly, our results imply that a disturbed intracellular ion homeostasis acts as a feedback-signal that regulates the expression of genes encoding for plasma membrane-localized transport proteins.

Ions are delivered to the shoot via the transpiration stream. Therefore, differences in shoot ion contents might arise from diminished transpiration rates, or from the modification of transport processes in the root stele that catalyze long-distance ion transport to shoots. Here, we provide comprehensive evidence that stomatal movement and transpiration does not account for the differences in shoot ion accumulation

between *almt9* and wild-type plants during salinity. In contrast, we show that *HKT1;1* shows elevated expression levels in roots of *almt9* mutants in response to salinity. HKT1;1 is a transport protein at the plasma membrane of the root stele involved in xylem retrieval of $Na^+$ from the transpiration stream and reduction of $Na^+$ root-to-shoot transfer (Davenport et al., 2007). Knock-out mutants of HKT1;1 show elevated xylem (Sunarpi et al., 2005) and shoot (Mäser et al., 2002) $Na^+$ levels when exposed to salt stress. In contrast, cell type-specific overexpression of HKT1;1 in stelar root cells reduces shoot $Na^+$ contents (Møller et al., 2009). Thus, the transcriptional up-regulation of *HKT1;1* in *almt9* mutants might contribute to lower shoot $Na^+$ contents. In accordance, *E196A* plants exhibit similar *HKT1;1* expression levels in roots as the wild-type and a similar shoot ion accumulation during salinity.

The coinciding expression pattern of ALMT9 and HKT1;1 (Møller et al., 2009) in the root stele suggests that the lack of the $Cl^-$ channel in these cells modifies the expression of transporters at the plasma membrane. The overall tissue ion content in roots was not altered in *almt9* and wild-type plants. Therefore, we propose a model in which the absence of ALMT9 reduces the loading capacity of $Cl^-$ and presumably also $Na^+$ ions into the vacuole of stelar cells (Figure 7). This disturbed intracellular ion homeostasis in turn might mimic an elevated salt stress that promotes the transcriptional up-regulation of *HKT1;1*. Consistently, *E196A* plants with restored or increased vacuolar $Cl^-$ uptake have a transcriptional response of *HKT1;1* similar to wild-type plants (Figure 7). The importance of intracellular ion homeostasis in regulating cellular events in response to salinity in roots was also demonstrated in the *sos1-1* mutant, which is deficient in cellular $Na^+$ extrusion and showed a magnification of salt stress responses (Oh et al., 2010). A role of ALMT9 in regulating the vacuolar ion uptake in the root stele is in agreement with the fact that *ALMT9* expression in roots is specifically up-regulated in response to NaCl, but not to other ionic or osmotic stresses. Hence, our findings substantiate the suggestion that pericycle and xylem parenchyma cells contribute to the control of net xylem loading of $Na^+$ during salinity (Läuchli et al., 2008). In addition, we propose that the capacity of vacuolar $Cl^-$ uptake in these cells is a factor that regulates root-to-shoot ion transport processes by influencing the expression of plasma membrane-bound ion transporters in response to salt stress. How disturbed intracellular ion homeostasis leads to changes in gene expression is still an

open question. It has to be noted that the vacuolar storage capacity also influences heavy metal long-distance transport. However, the reduced loading of heavy metals in the vacuoles of root stelar cells causes enhanced shoot ion accumulation (Arrivault et al., 2006, Peng and Gong, 2014). Therefore, it seems that an ion-dependent signaling pathway operates downstream the vacuolar ion loading capacity.

The disturbed intracellular ion homeostasis in the vascular system of *almt9* might also affect the regulation of transport proteins in shoots (Figure 7). Interestingly, CHX21 (Hall et al., 2006) and DTX1 (Li et al., 2002), plasma membrane transporters that were identified in the shoot RNA-seq analysis, were also associated with the modulation of xylem loading and long-distance ion transport. CHX21 was previously shown to be expressed in endodermal root cells and suggested to control root-to-shoot translocation of $Na^+$ during salinity (Hall et al., 2006). Although we did not determine the cell type-specific distribution of $Na^+$ ions, the potential role in the regulation of $Na^+$ xylem content (Hall et al., 2006) together with the differential expression in *almt9* mutant shoots leads us to propose that *CHX* genes are likely to contribute to intercellular $Na^+$ partitioning within shoots during salinity.

In our study, the MATE-related transporter gene *DTX1* as well as two further *DTX* members of the same subfamily (Li et al., 2002) were highly up-regulated in shoots of *almt9*. DTX1 has been described as a detoxification efflux carrier that might be required for the export of toxic compounds out of the cell (Li et al., 2002). Since also *E196A* shoots showed a dramatic increase in *DTX1* levels even under control conditions, the transcriptional up-regulation is apparently stimulated by the dis-regulated vacuolar $Cl^-$ fluxes in both mutants. This observation points towards a role of DTX1 in the export of compounds that accumulate in response to impaired intracellular ion homeostasis or to an osmotic imbalance that is probable in mutants with reduced or enhanced vacuolar $Cl^-$ uptake. An implication of ALMT9 in maintaining the osmotic status under salinity is suggested by the transcriptional up-regulation in response to KCl and sorbitol specifically in shoots. Interestingly, *DTX1* and the two other identified *DTX* members are co-expressed (Obayashi et al., 2007, www.atted.jp) with *UGT74E2* (Tognetti et al., 2010) the expression of which was also found to be highly up-regulated in *almt9* shoots in the RNA-seq analysis. The hydrogen peroxide-responsive *UGT74E2* encodes a UDP-glycosyltransferase that contributes to salt stress adaptation mechanisms

(Tognetti et al., 2010). It will be of interest to determine the physiological substrate of these DTX transporters and investigate their functional role during salinity which might be linked to UGT74E2 activity.

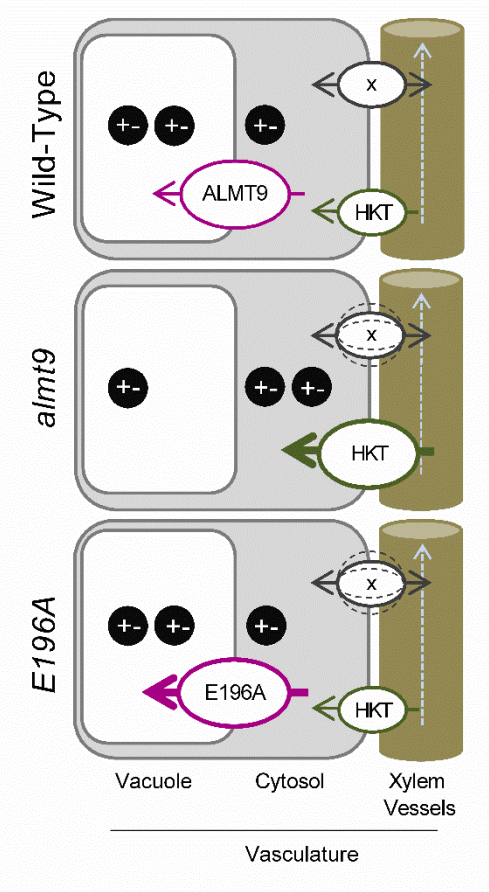


**Figure 7.** Proposed Model for the Transcriptional Regulation of Transporter Genes Involved in Whole-Plant Ion Distribution by Vacuolar Ion Uptake during Early Salinity.

Our data support a model in which the expression of plasma membrane-localized transport proteins involved in long-distance ion transport is tuned by the efficiency of vacuolar $Cl^-$ fluxes in the vasculature at the onset of salinity stress. The reduced $Cl^-$ storage in the vacuoles of *almt9* mutants perturbs the intracellular homeostasis of ions (black circles represent positively and negatively charged ions). This signals an enhanced salinity stress and initiates elevated expression levels of transporters such as the $Na^+$ transporter HKT1;1 (HKT). In accordance, wild-type and *E196A* plants have more efficient vacuolar $Cl^-$ uptake, and exhibit lower salt-induced *HKT1;1* transcript increase. Similarly, transcript levels of other genes encoding for transporters (x) involved in the regulation of long-distance ion translocation in shoots and roots might be up- or down-regulated (dashed lines) in response to the capacity of storing $Cl^-$ in the vacuoles of the vascular system.

The altered expression of $Na^+$ transporters such as HKT1;1 and CHX21 in the $Cl^-$ channel mutants *almt9* and *E196A* substantiates the strong coupling of the transport of both ion species during salinity as also observed in the ion content measurements. Strikingly, among the transporter genes that were differentially regulated in *almt9* under salinity we did not identify genes that encode for putative anion transporters. However, transcription levels of transport-related genes under non-saline conditions might contribute to alterations in tissue ion content during salinity as suggested for different grapevine (*Vitis vinifera*) species (Henderson et al., 2014). For instance, the basal expression of two genes that encode for plasma membrane-localized NRT transporters showed different levels in *almt9*. NRT proteins have been found to mediate transmembrane $NO_3^-$ fluxes, whereby some members were suggested to be implemented in salinity responses (Li et al., 2010, Chen et al., 2012, Taochy et al., 2015). Hence, the expression landscape of transporter genes under control conditions might alter ion fluxes constitutively and contribute potentially to differences in tissue ion accumulation during salinity.

In addition, the activity of several anion channels and transporters has been shown to be stimulated at other levels than the transcriptional, for instance by phosphorylation (Frachisse et al., 2000, Liu and Tsay, 2003, Lee et al., 2009, Wege et al., 2014), or by signals such as the pH (Frachisse et al., 2000, Colcombet et al., 2005, Meyer et al., 2011) and $Ca^{2+}$ concentrations (Gilliham and Tester, 2005, Meyer et al., 2011). If the activity of transporters involved in $Cl^-$ fluxes during salinity are modified by these regulatory mechanisms, RNA-seq experiments will not identify the corresponding genes.

The lower ion contents in *almt9* were detected during early salinity, but not upon extended exposure to salt stress. Transporter proteins that belong to the ALMT or other families might contribute to efficient vacuolar $Cl^-$ uptake in *almt9* during prolonged salinity. For example, members of the CLC family are able to transport $Cl^-$ across the tonoplast (Jossier et al., 2010, Wege et al., 2010, De Angeli et al., 2013, Nguyen et al., 2015). The relative contribution of CLC-mediated $Cl^-$ currents might thereby increase with accumulating $Cl^-$ contents over time, since the slightly negative membrane potential at the tonoplast supports the passive uptake of $Cl^-$ by channels only up to a concentration gradient of three-fold (Teakle and Tyerman, 2010). By contrast,

secondary active transporters such as CLCa can account for up to 50-fold concentration gradients across the tonoplast (De Angeli et al., 2006). Together, this indicates that plants have a set of tonoplast-localized transport proteins that are implicated in intracellular ion uptake at different time-points during salinity.

To conclude, while the role of plasma membrane-localized transport proteins in salt stress adaptation mechanisms has been studied intensively, the importance of vacuolar ion uptake in particular during early salinity remained elusive. In our study we clearly show that the significance of ion movement across the tonoplast during salt stress exceeds a role of vacuolar ion sequestration during long-term salinity to guarantee cellular survival. The differences in shoot ion content in *almt9* and *E196A* mutants and the transcriptional alteration of several plasma membrane-localized transporters with an established or putative role in long-distance ion translocation suggest an interplay between disturbed intracellular ion homeostasis and tissue ion fluxes. Our findings provide strong evidence that the capacity of vacuolar ion uptake in vascular tissue is a pivotal factor that contributes to the modulation of long-distance ion transport at the onset of salinity.

## Methods

### Plant Materials, Growth Conditions and Salinity Treatment

The two independent T-DNA insertion lines of ALMT9 (*almt9-1*: WiscDsLox499H09; *almt9-2*: SALK_055490) were described in a previous study (De Angeli et al., 2013). *Arabidopsis thaliana* wild-type ecotype Columbia (Col-0) and *almt9* plants were grown in a growth chamber (21 °C, 12 h light /12 h dark, 40% relative humidity) in hydroponic culture. ½ MS (Murashige and Skoog) pH 5.6 was used as nutrient solution. Unless otherwise specified, treatment was applied to 5-week old plants by adding control (0 mM supplemental NaCl) or salt stress (100 mM supplemental NaCl) solutions. Treatment was started 6 h after dawn and material was harvested after 24 h.

**Construct Design and Generation of Transgenic Plants**

To generate ALMT9$_{pro}$:GUS, a 548 bp promoter sequence upstream of the start codon of *ALMT9* was cloned into pMDC163 (Curtis and Grossniklaus, 2003). The gene silencing suppressor mutant *rdr-6-11* ( Peragine et al., 2004, Meyer et al., 2011) and Col-0 plants were transformed with the construct and positive transformation events were selected by hygromycin.

The intron-containing hairpin RNA was generated using pKANNIBAL (Wesley et al., 2001). The construct was based on the *ALMT5* nucleotide sequence in order to target ALMT family clade II members (Kovermann et al., 2007) for multiple down-regulation. *NotI* fragments were subcloned into pART27 (Gleave, 1992) for stable transformation into the *almt9-1* knock-out background (transgenic line *hpRNA*). Positive transformation events were selected by kanamycin. The expression of ALMT family clade II members (*ALMT3*, *ALMT4*, *ALMT5*, *ALMT6*) was evaluated by qRT-PCR using 7-day old T3 seedlings grown on plates containing ½ MS pH5.6 and 1% phytoagar. The line *hpRNA* was selected based on the highest degree of transcriptional down-regulation of ALMT clade II members.

To generate the point-mutated complementation line ALMT9$_{pro}$:ALMT9$_{E196A}$ (line *E196A*), *ALMT9* and its upstream promoter region (548 bp) were amplified from wild-type genomic DNA and cloned into pPLV22 (De Rybel et al., 2011). The site-directed mutagenesis was performed as described previously (Zhang et al., 2013). The construct was transformed into *almt9-2* and positive transformation events were selected by BASTA. 7-day old seedlings of the T3 progeny of line *E196A* and wild-type-2 were grown on plates containing ½ MS pH5.6 and 1% phytoagar to determine *ALMT9* expression by qRT-PCR.

To generate a guard cell-specific complementation line of *almt9-2* (line *GC:ALMT9*), *ALMT9* cDNA was amplified and cloned into pMDC32 (Curtis and Grossniklaus, 2003) under the control of the guard cell-specific *MYB60* promoter (Cominelli et al., 2005) as described previously (Nagy et al., 2009). The construct MYB60$_{pro}$:ALMT9 was transformed into *almt9-2*. T3 progeny of hygromycin-resistant transformants of *GC:ALMT9* was used to evaluate *ALMT9* expression by PCR. Mesophyll cell protoplasts of 5-week old soil-grown wild-type-2, *almt9-2*, and *GC:ALMT9* plants were isolated by enzymatic digestion as described in the 'Patch-clamp Measurements'

section. Total RNA of mesophyll cell protoplast, and shoots and roots of plants grown on plates (½ MS pH5.6 and 1% phytoagar), was extracted and cDNA was synthesized as described for qRT-PCR analysis. The PCR conditions were set as follows: 98°C for 2 min in the first cycle; subsequently, multiple amplification cycles consisting of 30 s at 98°C, 30 s at 58°C, and 2.5 min at 72°C; the final extension was 5 min at 72°C. To amplify *ALMT9*, 32 amplification cycles were used, for *KAT1* 35 cycles, and for *ACT2* 27 cycles. *KAT1* served as a control of a guard cell-specific gene (Nakamura et al., 1995) to exclude contamination of mesophyll cell protoplasts with guard cells.
Primers used for amplification and evaluation of the transgenic lines are listed in Supplemental Table 4. Arabidopsis was stable transformed via *Agrobacterium tumefaciens* using the floral dipping method (Clough and Bent, 1998).

**Quantitative Real-Time PCR**

Total RNA was extracted from approximately 30 mg shoot and root tissue (pool of material from 2-3 plants) by using the SV Total RNA Isolation System (Promega) following manufacturer's instructions. 1µg total RNA was reverse transcribed using oligo (dT) priming and M-MLV reverse transcriptase (Promega) according to manufacturer's instructions. Transcript levels were determined by qRT-PCR using the 7500 Fast Real-Time PCR System (Applied Biosystems) and a SYBR Green PCR Master Mix (Applied Biosystems). Transcript levels were calculated with the standard curve method as described by Pfaffl (2001), and were normalized against the expression of the actin gene *ACT2*. All reactions were performed in technical triplicates that were averaged to generate one biological replicate. Primers used for the transcript analysis are listed in Supplemental Table 4.

**Tissue-Specific Expression of *ALMT9***

T3 $ALMT9_{pro}$:GUS reporter plants were grown on plates (½ MS pH5.6 and 1% phytoagar) for 2-3 weeks. For the evaluation of the expression pattern under salinity plants were transferred to plates containing 100 mM supplemental NaCl for 24 h. Shoots and roots were assayed for GUS activity in a staining solution containing 1 mM X-Gluc (5-bromo-4-chloro-3-indolyl-β-D-glucuronide) in 50 mM sodium phosphate buffer pH 7.15, 0.5 mM potassium ferricyanide, 0.5mM potassium ferrocyanide and

0.05 % Triton X-100. After vacuum infiltration, the tissue was incubated for ~4 h (roots) or over-night (shoots) at 37 °C in the staining solution. The reaction was stopped with several washes in 50 mM sodium phosphate buffer pH 7.15 and tissues were cleared with 70 % ethanol over-night. Images were captured with a digital reflex camera from Canon, and with a Leica DMR widefield fluorescence microscope (Leica Microsystems). To obtain transverse sections roots were embedded in a 4 % agarose solution and 150 µm sections were generated by vibratome. Three independent transgenic lines in the *rdr6-11* background and three lines in Col-0 were analyzed for expression of the GUS reporter that each showed similar expression patterns.

**Ion and Osmolality Content Quantification**

$Mg^{2+}$, $K^+$, $Na^+$ and $Cl^-$ ions were extracted and quantified as described in Munns et al., 2010. In brief, shoots and roots of 3-4 plants were pooled for each biological replicate. Dry weight from shoot and root tissue was determined and ions were extracted using 0.5 M nitric acid over-night at 70 °C. Cation content was determined using Atomic Absorption Spectrometry (AAS) and $Cl^-$ was determined using the colorimetric ferricyanide method (Munns et al., 2010). All reactions were performed in technical triplicates that were averaged to generate one biological replicate. The measurements of wt-2, the knock-out mutant *almt9-2* and its complementation lines *GC:ALMT9* and *E196A* were performed in parallel. Hence, the results of the $Na^+$ and $Cl^-$ contents measured in wt-2 and *almt9-2* are presented in Figure 2, Figure 4 and Figure 5.

For nitrate quantification, a colorimetric assay with salicylic acid was used according to Cataldo et al., 1975. In brief, nitrate was extracted from shoots and roots (pool of 2 plants per biological replicate) in 5 ml hot deionized water (90-95 °C) and incubated in an 80 °C waterbath for 30 minutes. Cooled down supernatants and standard solutions were incubated at room temperature with 5 % salicylic acid (w/v) that was dissolved in 96 % sulphuric acid. After 20 minutes 2 M NaOH was added to raise the pH and absorbance was measured at 480 nm. All reactions were performed in technical duplicates that were averaged to generate a biological replicate.

Malate was extracted from shoot tissue as described previously (Hurth et al., 2005). Malate contents were measured with the L-Malic Acid Enzymatic BioAnalysis Kit

(Roche, R-Biopharm) according to manufacturer's instructions. All reactions were performed in technical duplicates that were averaged to generate a biological replicate. Osmolality was determined using the leaf sap extracts of shoots. The material underwent a cycle of freezing and thawing and was subsequently mechanically pressed. After centrifugation the supernatant was collected and used for osmolality measurements with a micro-osmometer (Advanced Instruments, Inc., Model 3320).

**Confocal Microscopy**

The constructs ALMT9-GFP and ALMT9$_{E196A}$-GFP, which have been described previously (Zhang et al., 2013), were transformed into *Agrobacterium tumefaciens* (GV3101) by electroporation. The Agrobacterium-mediated infiltration of four weeks old tobacco leaves was performed as described previously with slight modifications (Yang et al., 2001). After transient transformation tobacco plants were grown in the greenhouse (16h light/ 8h dark, 25 °C/ 23 °C, 100 to 200 µmol photons $m^{-2}$ $s^{-1}$, 60 % relative humidity) for another 2-3 days and then used to extract protoplasts for confocal microscopy and patch-clamp measurements.

Tobacco mesophyll protoplasts transiently overexpressing ALMT9-GFP and ALMT9$_{E196A}$-GFP were extracted by enzymatic digestion as described in the 'Patch-clamp Measurements' section. Vacuoles were isolated by osmotic shock. Images were obtained at the Imagerie-Gif platform (http://www.i2bc.paris-saclay.fr/spip.php?article278) on a Leica SP8 inverted confocal microscope with laser excitation at 488 nm and collection of emitted light at 495 – 550 nm for GFP and 600 – 650 nm for chlorophyll.

**Patch-Clamp Measurements**

Mesophyll protoplasts from ALMT9-GFP and ALMT9$_{E196A}$-GFP overexpressing tobacco leaves were isolated by enzymatic digestion. The enzyme solution contained 0.3 % (w/v) cellulase R-10, 0.03 % (w/v) pectolyase Y-23, 1 mM $CaCl_2$, 500 mM sorbitol and 10 mM MES, pH 5.3, 550 mOsm. Protoplasts were washed twice and resuspended in the same solution without enzymes. Vacuoles were released from mesophyll protoplasts by the addition of 5 mM EDTA and a slight osmotic shock (500 mOsm, see cytosolic solution below). Transformed vacuoles exhibiting an ALMT9-

GFP or ALMT9$_{E196A}$-GFP signal were selected using an epifluorescence microscope. Membrane currents from tonoplast patches were recorded in the excised cytosolic-side out configuration with the patch-clamp technique as described elsewhere (De Angeli et al., 2013). In brief, currents were recorded with an EPC8 patch-clamp amplifier and LIH8+8 AD/DA converter (HEKA electronics, Lambrect/Pflatz, Germany) using the Patchmaster software (HEKA electronics, Lambrect/Pflatz, Germany). Data was analysed with the FitMaster software (HEKA electronics, Lambrect/Pflatz, Germany). For macroscopic current recordings the pipette resistance was 4-5 MΩ. Only patches presenting a seal resistance higher than 2 GΩ were used to perform experiments. Current recordings were filtered at 300 Hz. Currents were evoked with a voltage ramp ranging from +40 to -100 mV in 2.5 s with a holding potential of -40 mV.
The cytosolic solution contained i) 100 mM $Cl^-$ adjusted to pH 7.5 with Bis-Tris-Propane (BTP); ii) 100 mM $Cl^-$, 1mM malic acid adjusted to pH 7.5 with BTP; iii) 100 mM malic acid, adjusted to pH 7.5 with BTP. The osmolality was adjusted to 500 mOsm using sorbitol. The pipette solution contained 100 mM HCl and was adjusted with BTP to pH 6. The osmolality was adjusted to 550 mOsm using sorbitol. All chemicals were purchased from Sigma-Aldrich. Liquid junction potentials were measured according to (Neher, 1992) and corrected when higher than ± 2 mV. Sequential perfusion of cytosolic-side buffer was performed using a custom-built gravity-driven perfusion system.

**Stomata Aperture Measurement**

Before performing *in situ* assays of native stomatal apertures, hydroponically grown plants were transferred to an LED growth chamber and grown for three days at a white light intensity of 250 $\mu mol*m^{-2}*s^{-1}$. Counting from the first true leaf pair, the seventh leaf of each rosette was used to analyse stomata. The leaf was excised and its abaxial side pressed onto a piece of scotch tape. The mesophyll tissue was scrapped off from the adaxial side using a scalpel and the remaining exposed abaxial epidermis was immediately rinsed three times with 10 mM MES-KOH (pH 6.1). The tape containing the epidermal strip was transferred onto a microscope slide and randomly chosen areas covering both sides of the mid-vein were imaged per leaf using an inverted NIKON ECLIPSE TS 100 microscope fitted with a NIKON Plan Fluor 40x/ 0.75 objective and

a NIKON Digital Sight DS-Fi1 camera. Leaves of at least four individual plants per genotype were examined in this way and genotypes were alternated during measurements. The time from leaf excision to completion of imaging was kept at maximally five minutes to ensure that the measured stomatal apertures reflected the native state and were unaffected by the process. Finally, recorded images were blind-analysed using ImageJ (Abramoff et al., 2004) and the apertures of at least 60 stomata were measured across a minimum of six images taken per leaf. Mean apertures of a single leaf were averaged, and the mean of one biological replicate was derived from the averages of at least four leaves per genotype.

**RNA sequencing and Data Processing**

Total RNA was extracted as described in the 'Quantitative Real-Time PCR' section. For each tissue (shoots and roots), genotype (*almt9-1* and wild-type-1) and treatment (0 mM or 100 mM supplemental NaCl for 24 h), three independent biological replicates were produced. RNA library preparation and sequencing was conducted by the Functional Genomics Center Zurich using Illumina HiSeq 2000.

RNA-seq read alignment and expression estimation was performed with RSEM (Li and Dewey, 2011). As a reference we used the TAIR10 genome assembly and the corresponding gene annotations provided by TAIR. Differential expression was computed with the Bioconductor package edgeR (Robinson et al., 2010) using the glm (generalized linear model) fit. A gene was considered as differentially expressed between wild-type-1 and *almt9-1* by applying a threshold of 0.01 for the p-value and ±1 for the $\log_2$ ratio, corresponding to a twofold or greater difference in expression. In addition, we filtered out genes that had very low counts. Specifically, we did not consider a gene as expressed if it did not exceed in at least one condition a read count of 50 in the samples. Positive $\log_2$ ratios correspond to transcriptional up-regulation in *almt9-1*, negative $\log_2$ ratios to transcriptional down-regulation.

Among the differentially expressed genes, we further selected salinity response-specific candidates that are up-regulated in *almt9-1* by requiring that (i) the gene is up- regulated under salinity ($\log_2$ ratio $\geq \pm 1$, $P < 0.01$), and (ii) the gene is not up-regulated under control conditions or the $\log_2$ ratio is at least 1 lower than the $\log_2$ ratio under salinity conditions. The corresponding filtering has been applied for the down-regulated genes.

**Accession Numbers**

The sequence data from this article can be found in the GenBank/EMBL data libraries under the following accession numbers: At3g18440 (*ALMT9*), At2g17470 (*ALMT6*), At1g68600 (*ALMT5*), At1g25480 (*ALMT4*), At1g18420 (*ALMT3*), At2g01980 (*SOS1*), At2g31910 (*CHX21*), At2g04040 (*DTX1*), At4g10310 (*HKT1;1*), At1g08810 (*MYB60*), At5g46240 (*KAT1*), and At3g18780.2 (*ACT2*).

**Supplemental Data**

The following materials are available in the online version of this article.

**Supplemental Figure 1.** Differences in Shoot Ion Contents are not Significant upon Prolonged Exposure to Salinity.

**Supplemental Figure 2.** *almt9* Mutant Plants Exhibit similar $Mg^{2+}$, $MA^{2-}$ and Osmotic Contents as Wild-Type Plants.

**Supplemental Figure 3.** Other ALMT Proteins that Belong to Clade II do not Contribute to the Modulation of $Na^{+}$ and $Cl^{-}$ Shoot Accumulation during Early Salt Stress.

**Supplemental Figure 4.** Stomatal Movement during NaCl and KCl Stress in Wild-Type-1 and *almt9-1*.

**Supplemental Figure 5.** Evaluation of the Guard Cell-Specific Complementation Line of *almt9-2*.

**Supplemental Figure 6.** The RNA-seq Analysis Reveals Distinct Biological Functions of Genes that are Differentially Expressed in *almt9-1* Exclusively under Salinity.

**Supplemental Table 1.** Ion Contents of Wild-Type and *almt9* Mutant Plants upon 24 h Salinity.

**Supplemental Table 2.** Differentially Expressed Genes between Wild-Type-1 and *almt9-1* in Shoots Exclusively under Salinity.

**Supplemental Table 3.** Differentially Expressed Genes between Wild-Type-1 and *almt9-1* in Roots Exclusively under Salinity.

**Supplemental Table 4.** Primers Used in that Study.

**Supplemental Data Set 1.** Differentially Expressed Genes between Wild-Type-1 and *almt9-1* in Shoots under Control Conditions.

**Supplemental Data Set 2.** Differentially Expressed Genes between Wild-Type-1 and *almt9-1* in Roots under Control Conditions.

**Supplemental Data Set 3.** Differentially Expressed Genes between Wild-Type-1 and *almt9-1* in Shoots under Salinity Conditions.

**Supplemental Data Set 4.** Differentially Expressed Genes between Wild-Type-1 and *almt9-1* in Roots under Salinity Conditions.

## Acknowledgment

The authors kindly thank H. Brandl and C. Fabbri for supervising the AAS measurements. Furthermore, we are grateful to S. Aluri and H. Rehrauer from the Functional Genomics Centre Zurich who conducted the RNA sequencing and the data analysis, respectively. We thank Rita Francisco for performing preliminary results on metabolites.

U.B. and A.D.A. were supported by the Swiss National Foundation (31003A_141090/1) and U.B. additionally by a Forschungskredit of the University of Zurich. A.D.A benefits from the support of the LabEx Saclay Plant Sciences-SPS (ANR-10-LABX-0040-SPS). C.E. was supported by the European Union's Seventh Framework Programme for research, technological development and demonstration under grant agreement no GA-2010-267243 – PLANT FELLOWS and a Forschungskredit of the University of Zurich.

## Author Contributions

The research was designed by U.B., C.E., E.M. and A.D.A and performed by U.B., C.E. and A.D.A. The paper was written by U.B., C.E. and A.D.A.

## References

Abramoff, M. D., Magalhaes, P. J. and Ram, S. J. (2004) 'Image Processing with ImageJ', *Biophotonics International*, 11(7), pp. 36-42.

Arrivault, S., Senger, T. and Krämer, U. (2006) 'The Arabidopsis metal tolerance protein AtMTP3 maintains metal homeostasis by mediating Zn exclusion from the shoot under Fe deficiency and Zn oversupply', *Plant J*, 46(5), pp. 861-79.

Barbier-Brygoo, H., De Angeli, A., Filleur, S., Frachisse, J. M., Gambale, F., Thomine, S. and Wege, S. (2010) 'Anion Channels/Transporters in Plants: From Molecular Bases to Regulatory Networks.', *Annu Rev Plant Biol*.

Barragán, V., Leidi, E. O., Andrés, Z., Rubio, L., De Luca, A., Fernández, J. A., Cubero, B. and Pardo, J. M. (2012) 'Ion exchangers NHX1 and NHX2 mediate active potassium uptake into vacuoles to regulate cell turgor and stomatal function in Arabidopsis', *Plant Cell*, 24(3), pp. 1127-42.

Bassil, E., Ohto, M. A., Esumi, T., Tajima, H., Zhu, Z., Cagnac, O., Belmonte, M., Peleg, Z., Yamaguchi, T. and Blumwald, E. (2011) 'The Arabidopsis intracellular Na+/H+ antiporters NHX5 and NHX6 are endosome associated and necessary for plant growth and development', *Plant Cell*, 23(1), pp. 224-39.

Baud, S., Wuillème, S., Lemoine, R., Kronenberger, J., Caboche, M., Lepiniec, L. and Rochat, C. (2005) 'The AtSUC5 sucrose transporter specifically expressed in the endosperm is involved in early seed development in Arabidopsis', *Plant J*, 43(6), pp. 824-36.

Britto, D. T., Ruth, T. J., Lapi, S. and Kronzucker, H. J. (2004) 'Cellular and whole-plant chloride dynamics in barley: insights into chloride-nitrogen interactions and salinity responses', *Planta*, 218(4), pp. 615-22.

Brumós, J., Talón, M., Bouhlal, R. and Colmenero-Flores, J. M. (2010) 'Cl- homeostasis in includer and excluder citrus rootstocks: transport mechanisms and identification of candidate genes', *Plant Cell Environ*, 33(12), pp. 2012-27.

Cataldo, D., Haroon, L., LE, S. and VL, Y. (1975) 'Rapid colorimetric determination of nitrate in plant tissues by nitration of salicylic acid', *Communications in Soil Science and Plant Analysis*, 6(1), pp. 71-80.

Chen, C. Z., Lv, X. F., Li, J. Y., Yi, H. Y. and Gong, J. M. (2012) 'Arabidopsis NRT1.5 is another essential component in the regulation of nitrate reallocation and stress tolerance', *Plant Physiol*, 159(4), pp. 1582-90.

Clough, S. J. and Bent, A. F. (1998) 'Floral dip: a simplified method for Agrobacterium-mediated transformation of Arabidopsis thaliana', *Plant J*, 16(6), pp. 735-43.

Colcombet, J., Lelièvre, F., Thomine, S., Barbier-Brygoo, H. and Frachisse, J. M. (2005) 'Distinct pH regulation of slow and rapid anion channels at the plasma membrane of Arabidopsis thaliana hypocotyl cells', *J Exp Bot*, 56(417), pp. 1897-903.

Cominelli, E., Galbiati, M., Vavasseur, A., Conti, L., Sala, T., Vuylsteke, M., Leonhardt, N., Dellaporta, S. L. and Tonelli, C. (2005) 'A guard-cell-specific MYB transcription factor regulates stomatal movements and plant drought tolerance', *Curr Biol*, 15(13), pp. 1196-200.

Craig Plett, D. and Møller, I. S. (2010) 'Na(+) transport in glycophytic plants: what we know and would like to know', *Plant Cell Environ,* 33(4), pp. 612-26.

Curtis, M. D. and Grossniklaus, U. (2003) 'A gateway cloning vector set for high-throughput functional analysis of genes in planta', *Plant Physiol,* 133(2), pp. 462-9.

Davenport, R. J., Muñoz-Mayor, A., Jha, D., Essah, P. A., Rus, A. and Tester, M. (2007) 'The Na+ transporter AtHKT1;1 controls retrieval of Na+ from the xylem in Arabidopsis', *Plant Cell Environ,* 30(4), pp. 497-507.

De Angeli, A., Monachello, D., Ephritikhine, G., Frachisse, J. M., Thomine, S., Gambale, F. and Barbier-Brygoo, H. (2006) 'The nitrate/proton antiporter AtCLCa mediates nitrate accumulation in plant vacuoles.', *Nature,* 442(7105), pp. 939-42.

De Angeli, A., Zhang, J., Meyer, S. and Martinoia, E. (2013) 'AtALMT9 is a malate-activated vacuolar chloride channel required for stomatal opening in Arabidopsis', *Nat Comm,* 4, pp. 1804.

De Rybel, B., van den Berg, W., Lokerse, A., Liao, C. Y., van Mourik, H., Möller, B., Peris, C. L. and Weijers, D. (2011) 'A versatile set of ligation-independent cloning vectors for functional studies in plants', *Plant Physiol,* 156(3), pp. 1292-9.

Frachisse, J. M., Colcombet, J., Guern, J. and Barbier-Brygoo, H. (2000) 'Characterization of a nitrate-permeable channel able to mediate sustained anion efflux in hypocotyl cells from Arabidopsis thaliana', *Plant J,* 21(4), pp. 361-71.

Geelen, D., Lurin, C., Bouchez, D., Frachisse, J. M., Lelièvre, F., Courtial, B., Barbier-Brygoo, H. and Maurel, C. (2000) 'Disruption of putative anion channel gene AtCLC-a in Arabidopsis suggests a role in the regulation of nitrate content', *Plant J,* 21(3), pp. 259-67.

Geilfus, C. M., Mithöfer, A., Ludwig-Müller, J., Zörb, C. and Muehling, K. H. (2015) 'Chloride-inducible transient apoplastic alkalinizations induce stomata closure by controlling abscisic acid distribution between leaf apoplast and guard cells in salt-stressed Vicia faba', *New Phytol,* 208(3), pp. 803-16.

Genc, Y., Oldach, K., Taylor, J. and Lyons, G. H. (2015) 'Uncoupling of sodium and chloride to assist breeding for salinity tolerance in crops', *New Phytol*, doi: 10.1111/nph.13757.

Gilliham, M. and Tester, M. (2005) 'The regulation of anion loading to the maize root xylem', *Plant Physiol,* 137(3), pp. 819-28.

Gleave, A. P. (1992) 'A versatile binary vector system with a T-DNA organisational structure conducive to efficient integration of cloned DNA into the plant genome.', *Plant Mol Biol,* 20(6), pp. 1203-7.

Hall, D., Evans, A. R., Newbury, H. J. and Pritchard, J. (2006) 'Functional analysis of CHX21: a putative sodium transporter in Arabidopsis', *J Exp Bot,* 57(5), pp. 1201-10.

Henderson, S. W., Baumann, U., Blackmore, D. H., Walker, A. R., Walker, R. R. and Gilliham, M. (2014) 'Shoot chloride exclusion and salt tolerance in grapevine is associated with differential ion transporter expression in roots', *BMC Plant Biol,* 14, pp. 273.

Henderson, S. W., Wege, S., Qiu, J., Blackmore, D. H., Walker, A. R., Tyerman, S. D., Walker, R. R. and Gilliham, M. (2015) 'Grapevine and Arabidopsis

Cation-Chloride Cotransporters Localize to the Golgi and Trans-Golgi Network and Indirectly Influence Long-Distance Ion Transport and Plant Salt Tolerance', *Plant Physiol,* 169(3), pp. 2215-29.

Huang, C. X. and Van Steveninck, R. F. (1989) 'Maintenance of low cl concentrations in mesophyll cells of leaf blades of barley seedlings exposed to salt stress', *Plant Physiol,* 90(4), pp. 1440-3.

Hurth, M. A., Suh, S. J., Kretzschmar, T., Geis, T., Bregante, M., Gambale, F., Martinoia, E. and Neuhaus, H. E. (2005) 'Impaired pH homeostasis in Arabidopsis lacking the vacuolar dicarboxylate transporter and analysis of carboxylic acid transport across the tonoplast', *Plant Physiol,* 137(3), pp. 901-10.

James, R. A., Munns, R., von Caemmerer, S., Trejo, C., Miller, C. and Condon, T. A. (2006) 'Photosynthetic capacity is related to the cellular and subcellular partitioning of Na+, K+ and Cl- in salt-affected barley and durum wheat', *Plant Cell Environ,* 29(12), pp. 2185-97.

Jiang, X., Leidi, E. O. and Pardo, J. M. (2010) 'How do vacuolar NHX exchangers function in plant salt tolerance?', *Plant Signal Behav,* 5(7), pp. 792-5.

Jossier, M., Kroniewicz, L., Dalmas, F., Le Thiec, D., Ephritikhine, G., Thomine, S., Barbier-Brygoo, H., Vavasseur, A., Filleur, S. and Leonhardt, N. (2010) 'The Arabidopsis vacuolar anion transporter, AtCLCc, is involved in the regulation of stomatal movements and contributes to salt tolerance.', *Plant J,* 64(4), pp. 563-76.

Karley, A. J., Leigh, R. A. and Sanders, D. (2000a) 'Differential ion accumulation and ion fluxes in the mesophyll and epidermis of barley', *Plant Physiol,* 122(3), pp. 835-44.

Karley, A. J., Leigh, R. A. and Sanders, D. (2000b) 'Where do all the ions go? The cellular basis of differential ion accumulation in leaf cells', *Trends Plant Sci,* 5(11), pp. 465-70.

Kiba, T., Feria-Bourrellier, A. B., Lafouge, F., Lezhneva, L., Boutet-Mercey, S., Orsel, M., Bréhaut, V., Miller, A., Daniel-Vedele, F., Sakakibara, H. and Krapp, A. (2012) 'The Arabidopsis nitrate transporter NRT2.4 plays a double role in roots and shoots of nitrogen-starved plants', *Plant Cell,* 24(1), pp. 245-58.

Kovermann, P., Meyer, S., Hörtensteiner, S., Picco, C., Scholz-Starke, J., Ravera, S., Lee, Y. and Martinoia, E. (2007) 'The Arabidopsis vacuolar malate channel is a member of the ALMT family', *Plant J,* 52(6), pp. 1169-80.

Krebs, M., Beyhl, D., Görlich, E., Al-Rasheid, K., Marten, I., Stierhof, Y., Hedrich, R. and Schumacher, K. (2010) 'Arabidopsis V-ATPase activity at the tonoplast is required for efficient nutrient storage but not for sodium accumulation.', *Proc Natl Acad Sci U S A,* 107(7), pp. 3251-6.

Lee, S. C., Lan, W., Buchanan, B. B. and Luan, S. (2009) 'A protein kinase-phosphatase pair interacts with an ion channel to regulate ABA signaling in plant guard cells', *Proc Natl Acad Sci U S A,* 106(50), pp. 21419-24.

Leidi, E. O., Barragán, V., Rubio, L., El-Hamdaoui, A., Ruiz, M. T., Cubero, B., Fernández, J. A., Bressan, R. A., Hasegawa, P. M., Quintero, F. J. and Pardo, J. M. (2010) 'The AtNHX1 exchanger mediates potassium compartmentation in vacuoles of transgenic tomato', *Plant J,* 61(3), pp. 495-506.

Lelandais-Brière, C., Jovanovic, M., Torres, G. A., Perrin, Y., Lemoine, R., Corre-Menguy, F. and Hartmann, C. (2007) 'Disruption of AtOCT1, an organic cation transporter gene, affects root development and carnitine-related responses in Arabidopsis', *Plant J,* 51(2), pp. 154-64.

Li, B. and Dewey, C. N. (2011) 'RSEM: accurate transcript quantification from RNA-Seq data with or without a reference genome', *BMC Bioinformatics,* 12, pp. 323.

Li, J. Y., Fu, Y. L., Pike, S. M., Bao, J., Tian, W., Zhang, Y., Chen, C. Z., Li, H. M., Huang, J., Li, L. G., Schroeder, J. I., Gassmann, W. and Gong, J. M. (2010) 'The Arabidopsis nitrate transporter NRT1.8 functions in nitrate removal from the xylem sap and mediates cadmium tolerance', *Plant Cell,* 22(5), pp. 1633-46.

Li, L., He, Z., Pandey, G. K., Tsuchiya, T. and Luan, S. (2002) 'Functional cloning and characterization of a plant efflux carrier for multidrug and heavy metal detoxification', *J Biol Chem,* 277(7), pp. 5360-8.

Lim, C. W., Kim, J. H., Baek, W., Kim, B. S. and Lee, S. C. (2012) 'Functional roles of the protein phosphatase 2C, AtAIP1, in abscisic acid signaling and sugar tolerance in Arabidopsis', *Plant Sci,* 187, pp. 83-8.

Limonta, M., Romanowsky, S., Olivari, C., Bonza, M. C., Luoni, L., Rosenberg, A., Harper, J. F. and De Michelis, M. I. (2014) 'ACA12 is a deregulated isoform of plasma membrane Ca $^{+}$-ATPase of Arabidopsis thaliana', *Plant Mol Biol,* 84(4-5), pp. 387-97.

Liu, K. H. and Tsay, Y. F. (2003) 'Switching between the two action modes of the dual-affinity nitrate transporter CHL1 by phosphorylation', *EMBO J,* 22(5), pp. 1005-13.

Läuchli, A., James, R. A., Huang, C. X., McCully, M. and Munns, R. (2008) 'Cell-specific localization of Na+ in roots of durum wheat and possible control points for salt exclusion', *Plant Cell Environ,* 31(11), pp. 1565-74.

Magome, H., Yamaguchi, S., Hanada, A., Kamiya, Y. and Oda, K. (2004) 'dwarf and delayed-flowering 1, a novel Arabidopsis mutant deficient in gibberellin biosynthesis because of overexpression of a putative AP2 transcription factor', *Plant J,* 37(5), pp. 720-9.

Magome, H., Yamaguchi, S., Hanada, A., Kamiya, Y. and Oda, K. (2008) 'The DDF1 transcriptional activator upregulates expression of a gibberellin-deactivating gene, GA2ox7, under high-salinity stress in Arabidopsis', *Plant J,* 56(4), pp. 613-26.

Martinoia, E., Maeshima, M. and Neuhaus, H. E. (2007) 'Vacuolar transporters and their essential role in plant metabolism', *J Exp Bot,* 58(1), pp. 83-102.

Martinoia, E., Meyer, S., De Angeli, A. and Nagy, R. (2012) 'Vacuolar transporters in their physiological context', *Annu Rev Plant Biol,* 63, pp. 183-213.

Merlot, S., Gosti, F., Guerrier, D., Vavasseur, A. and Giraudat, J. (2001) 'The ABI1 and ABI2 protein phosphatases 2C act in a negative feedback regulatory loop of the abscisic acid signalling pathway', *Plant J,* 25(3), pp. 295-303.

Meyer, S., Scholz-Starke, J., De Angeli, A., Kovermann, P., Burla, B., Gambale, F. and Martinoia, E. (2011) 'Malate transport by the vacuolar AtALMT6 channel in guard cells is subject to multiple regulation.', *Plant J.*, 67(2), pp. 247-57.

Monachello, D., Allot, M., Oliva, S., Krapp, A., Daniel-Vedele, F., Barbier-Brygoo, H. and Ephritikhine, G. (2009) 'Two anion transporters AtClCa and AtClCe

fulfil interconnecting but not redundant roles in nitrate assimilation pathways', *New Phytol*, 183(1), pp. 88-94.
Munns, R. (2002) 'Comparative physiology of salt and water stress', *Plant Cell Environ*, 25(2), pp. 239-250.
Munns, R. and Tester, M. (2008) 'Mechanisms of salinity tolerance', *Annu Rev Plant Biol*, 59, pp. 651-81.
Munns, R., Wallace, P. A., Teakle, N. L. and Colmer, T. D. (2010) 'Measuring soluble ion concentrations (Na(+), K(+), Cl(-)) in salt-treated plants', *Methods Mol Biol*, 639, pp. 371-82.
Mäser, P., Eckelman, B., Vaidyanathan, R., Horie, T., Fairbairn, D., Kubo, M., Yamagami, M., Yamaguchi, K., Nishimura, M., Uozumi, N., Robertson, W., Sussman, M. and Schroeder, J. (2002) 'Altered shoot/root Na+ distribution and bifurcating salt sensitivity in Arabidopsis by genetic disruption of the Na+ transporter AtHKT1.', *FEBS Lett*, 531(2), pp. 157-61.
Møller, I. and Tester, M. (2007) 'Salinity tolerance of Arabidopsis: a good model for cereals?', *Trends Plant Sci*, 12(12), pp. 534-40.
Møller, I. S., Gilliham, M., Jha, D., Mayo, G. M., Roy, S. J., Coates, J. C., Haseloff, J. and Tester, M. (2009) 'Shoot Na+ exclusion and increased salinity tolerance engineered by cell type-specific alteration of Na+ transport in Arabidopsis', *Plant Cell*, 21(7), pp. 2163-78.
Nagy, R., Grob, H., Weder, B., Green, P., Klein, M., Frelet-Barrand, A., Schjoerring, J. K., Brearley, C. and Martinoia, E. (2009) 'The Arabidopsis ATP-binding cassette protein AtMRP5/AtABCC5 is a high affinity inositol hexakisphosphate transporter involved in guard cell signaling and phytate storage', *J Biol Chem*, 284(48), pp. 33614-22.
Nakamura, R. L., McKendree, W. L., Hirsch, R. E., Sedbrook, J. C., Gaber, R. F. and Sussman, M. R. (1995) 'Expression of an Arabidopsis potassium channel gene in guard cells', *Plant Physiol*, 109(2), pp. 371-4.
Neher, E. (1992) 'Correction for liquid junction potentials in patch clamp experiments', *Methods Enzymol*, 207, pp. 123-31.
Nguyen, C. T., Agorio, A., Jossier, M., Depré, S., Thomine, S. and Filleur, S. (2015) 'Characterization of the Chloride Channel-like, AtCLCg, involved in Chloride Tolerance in Arabidopsis thaliana', *Plant Cell Physiol*, doi: 10.1093/pcp/pcv169.
Obayashi, T., Kinoshita, K., Nakai, K., Shibaoka, M., Hayashi, S., Saeki, M., Shibata, D., Saito, K. and Ohta, H. (2007) 'ATTED-II: a database of co-expressed genes and cis elements for identifying co-regulated gene groups in Arabidopsis', *Nucleic Acids Res*, 35(Database issue), pp. D863-9.
Oh, D., Lee, S., Bressan, R., Yun, D. and Bohnert, H. (2010) 'Intracellular consequences of SOS1 deficiency during salt stress', *J Exp Bot*, 61(4), pp. 1205-13.
Peng, J. S. and Gong, J. M. (2014) 'Vacuolar sequestration capacity and long-distance metal transport in plants', *Front Plant Sci*, 5, pp. 19.
Peragine, A., Yoshikawa, M., Wu, G., Albrecht, H. L. and Poethig, R. S. (2004) 'SGS3 and SGS2/SDE1/RDR6 are required for juvenile development and the production of trans-acting siRNAs in Arabidopsis', *Genes Dev*, 18(19), pp. 2368-79.

Pfaffl, M. W. (2001) 'A new mathematical model for relative quantification in real-time RT-PCR', *Nucleic Acids Res*, 29(9), pp. e45.

Pommerrenig, B., Popko, J., Heilmann, M., Schulmeister, S., Dietel, K., Schmitt, B., Stadler, R., Feussner, I. and Sauer, N. (2013) 'SUCROSE TRANSPORTER 5 supplies Arabidopsis embryos with biotin and affects triacylglycerol accumulation', *Plant J*, 73(3), pp. 392-404.

Robinson, M. D., McCarthy, D. J. and Smyth, G. K. (2010) 'edgeR: a Bioconductor package for differential expression analysis of digital gene expression data', *Bioinformatics*, 26(1), pp. 139-40.

Rubio, S., Rodrigues, A., Saez, A., Dizon, M. B., Galle, A., Kim, T. H., Santiago, J., Flexas, J., Schroeder, J. I. and Rodriguez, P. L. (2009) 'Triple loss of function of protein phosphatases type 2C leads to partial constitutive response to endogenous abscisic acid', *Plant Physiol*, 150(3), pp. 1345-55.

Shapira, O., Khadka, S., Israeli, Y., Shani, U. and Schwartz, A. (2009) 'Functional anatomy controls ion distribution in banana leaves: significance of Na+ seclusion at the leaf margins', *Plant Cell Environ*, 32(5), pp. 476-85.

Shi, H., Ishitani, M., Kim, C. and Zhu, J. (2000) 'The Arabidopsis thaliana salt tolerance gene SOS1 encodes a putative Na+/H+ antiporter.', *Proc Natl Acad Sci U S A*, 97(12), pp. 6896-901.

Shi, H., Quintero, F. J., Pardo, J. M. and Zhu, J. K. (2002) 'The putative plasma membrane Na(+)/H(+) antiporter SOS1 controls long-distance Na(+) transport in plants', *Plant Cell*, 14(2), pp. 465-77.

Sibole, J. V., Cabot, C., Poschenrieder, C. and Barceló, J. (2003) 'Efficient leaf ion partitioning, an overriding condition for abscisic acid-controlled stomatal and leaf growth responses to NaCl salinization in two legumes', *J Exp Bot*, 54(390), pp. 2111-9.

Strohm, A. K., Vaughn, L. M. and Masson, P. H. (2015) 'Natural variation in the expression of ORGANIC CATION TRANSPORTER 1 affects root length responses to cadaverine in Arabidopsis', *J Exp Bot*, 66(3), pp. 853-62.

Sunarpi, Horie, T., Motoda, J., Kubo, M., Yang, H., Yoda, K., Horie, R., Chan, W. Y., Leung, H. Y., Hattori, K., Konomi, M., Osumi, M., Yamagami, M., Schroeder, J. I. and Uozumi, N. (2005) 'Enhanced salt tolerance mediated by AtHKT1 transporter-induced Na unloading from xylem vessels to xylem parenchyma cells', *Plant J*, 44(6), pp. 928-38.

Taochy, C., Gaillard, I., Ipotesi, E., Oomen, R., Leonhardt, N., Zimmermann, S., Peltier, J. B., Szponarski, W., Simonneau, T., Sentenac, H., Gibrat, R. and Boyer, J. C. (2015) 'The Arabidopsis root stele transporter NPF2.3 contributes to nitrate translocation to shoots under salt stress', *Plant J*, 83(3), pp. 466-79.

Tavakkoli, E., Fatehi, F., Coventry, S., Rengasamy, P. and McDonald, G. K. (2011) 'Additive effects of Na+ and Cl- ions on barley growth under salinity stress', *J Exp Bot*, 62(6), pp. 2189-203.

Tavakkoli, E., Rengasamy, P. and McDonald, G. K. (2010) 'High concentrations of Na+ and Cl- ions in soil solution have simultaneous detrimental effects on growth of faba bean under salinity stress', *J Exp Bot*, 61(15), pp. 4449-59.

Teakle, N. L. and Tyerman, S. D. (2010) 'Mechanisms of Cl(-) transport contributing to salt tolerance', *Plant Cell Environ*, 33(4), pp. 566-89.

Terasaka, K., Blakeslee, J. J., Titapiwatanakun, B., Peer, W. A., Bandyopadhyay, A., Makam, S. N., Lee, O. R., Richards, E. L., Murphy, A. S., Sato, F. and Yazaki,

K. (2005) 'PGP4, an ATP binding cassette P-glycoprotein, catalyzes auxin transport in Arabidopsis thaliana roots', *Plant Cell,* 17(11), pp. 2922-39.

Tester, M. and Davenport, R. (2003) 'Na+ tolerance and Na+ transport in higher plants.', *Ann Bot,* 91(5), pp. 503-27.

Tognetti, V. B., Van Aken, O., Morreel, K., Vandenbroucke, K., van de Cotte, B., De Clercq, I., Chiwocha, S., Fenske, R., Prinsen, E., Boerjan, W., Genty, B., Stubbs, K. A., Inzé, D. and Van Breusegem, F. (2010) 'Perturbation of indole-3-butyric acid homeostasis by the UDP-glucosyltransferase UGT74E2 modulates Arabidopsis architecture and water stress tolerance', *Plant Cell,* 22(8), pp. 2660-79.

Wege, S., De Angeli, A., Droillard, M. J., Kroniewicz, L., Merlot, S., Cornu, D., Gambale, F., Martinoia, E., Barbier-Brygoo, H., Thomine, S., Leonhardt, N. and Filleur, S. (2014) 'Phosphorylation of the vacuolar anion exchanger AtCLCa is required for the stomatal response to abscisic acid', *Sci Signal,* 7(333), pp. ra65.

Wege, S., Jossier, M., Filleur, S., Thomine, S., Barbier-Brygoo, H., Gambale, F. and De Angeli, A. (2010) 'The proline 160 in the selectivity filter of the Arabidopsis NO(3)(-)/H(+) exchanger AtCLCa is essential for nitrate accumulation in planta', *Plant J,* 63(5), pp. 861-9.

Wesley, S. V., Helliwell, C. A., Smith, N. A., Wang, M. B., Rouse, D. T., Liu, Q., Gooding, P. S., Singh, S. P., Abbott, D., Stoutjesdijk, P. A., Robinson, S. P., Gleave, A. P., Green, A. G. and Waterhouse, P. M. (2001) 'Construct design for efficient, effective and high-throughput gene silencing in plants', *Plant J,* 27(6), pp. 581-90.

Yang, K. Y., Liu, Y. and Zhang, S. (2001) 'Activation of a mitogen-activated protein kinase pathway is involved in disease resistance in tobacco', *Proc Natl Acad Sci U S A,* 98(2), pp. 741-6.

Yu, Y. and Assmann, S. M. (2015) 'The effect of NaCl on stomatal opening in Arabidopsis wild type and agb1 heterotrimeric G-protein mutant plants', *Plant Signal Behav*, doi: 10.1080/15592324.2015.1085275.

Zhang, J., Baetz, U., Krügel, U., Martinoia, E. and De Angeli, A. (2013) 'Identification of a probable pore-forming domain in the multimeric vacuolar anion channel AtALMT9', *Plant Physiol,* 163(2), pp. 830-43.

Zhao, X., Wang, Y. J., Wang, Y. L., Wang, X. L. and Zhang, X. (2011) 'Extracellular Ca + alleviates NaCl-induced stomatal opening through a pathway involving $H_2O_2$-blocked Na+ influx in Vicia guard cells', *J Plant Physiol,* 168(9), pp. 903-10.

## Supplemental Figures

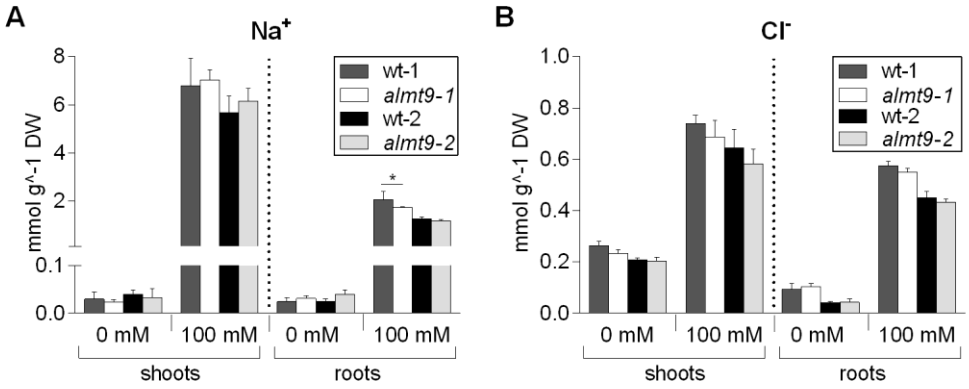


**Supplemental Figure 1.** Differences in Shoot Ion Contents are not Significant upon Prolonged Exposure to Salinity.

**(A)** $Na^+$ and **(B)** $Cl^-$ content analysis in shoots and roots of hydroponically grown *almt9-1 and almt9-2* knock-out mutants and the corresponding wild-types (wt-1 and wt-2) upon 7 days of treatment with control (0 mM) or NaCl (100 mM) solutions. Data are means ± SD of $n \geq 4$ biological replicates. One-way ANOVA of each tissue and treatment and a pair-wise comparison was used for statistical analysis. Asterisks indicate significant differences from the corresponding wt (*$P < 0.05$, **$P < 0.01$, ***$P < 0.001$). DW, dry weight.

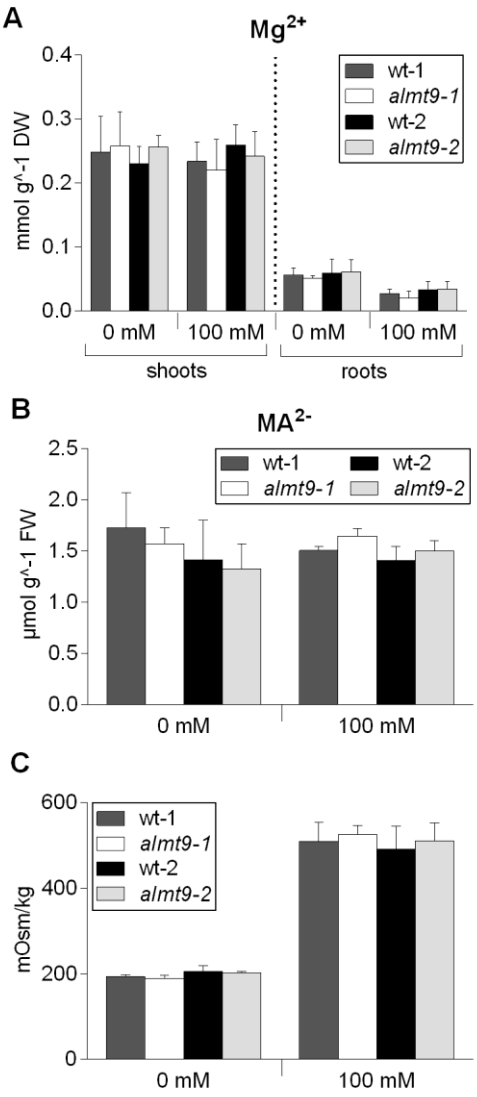


**Supplemental Figure 2.** *almt9* Mutants Exhibit similar $Mg^{2+}$, $MA^{2-}$ and Osmotic Contents as Wild-Type Plants.

**(A)** $Mg^{2+}$ ($n \geq 5$), **(B)** $MA^{2-}$ ($n \geq 4$), and **(C)** osmotic ($n \geq 4$) contents were determined in shoots (and roots **[A]**) of hydroponically grown *almt9-1 and almt9-2* mutants and the corresponding wild-type (wt-1 and wt-2) upon 24 h treatment with control (0 mM) or NaCl (100 mM) solutions. Data are as means ± SD. No statistically significant differences were detected using one-way ANOVA of each tissue and treatment and a pair-wise comparison ($P < 0.05$). DW, dry weight; FW, fresh weight.

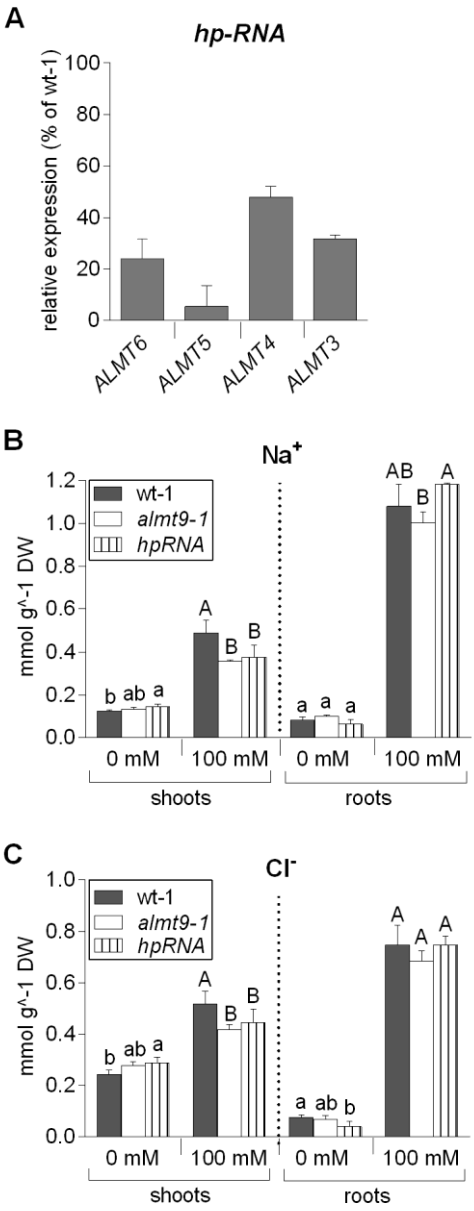


**Supplemental Figure 3.** Other ALMT Proteins that Belong to Clade II do not Contribute to the Modulation of $Na^+$ and $Cl^-$ Shoot Accumulation during Early Salt Stress.

**(A)** qRT-PCR analysis of the transcriptional down-regulation of the ALMT clade II members ALMT6, ALMT5, ALMT4 and ALMT3. Transcript abundance was compared between wild-type-1 (wt-1) and *hpRNA*, an *almt9-1* knock-out line expressing an intron-containing hairpin RNA that targets clade II ALMT members for multiple down-regulation. The data was normalized to expression levels of the target genes in wt-1. *ACT2* served as a reference gene. The SD was calculated from two biological replicates.

(Supplemental Figure legend 3 continued)

**(B)** and **(C)** Ion content analysis of $Na^+$ **(B)** and $Cl^-$ **(C)** in shoots and roots of hydroponically grown wt-1, *almt9-1* and *hpRNA* upon 24 h treatment with control (0 mM) or NaCl (100 mM) solutions. Data are means ± SD of n = 4 biological replicates. One-way ANOVA of each tissue and treatment and a Tukey-Kramer multiple comparison post-test was used for statistical analysis. Different lowercase letters indicate significant differences in ion content ($P < 0.05$) under control conditions, capital letters under salinity. DW, dry weight.

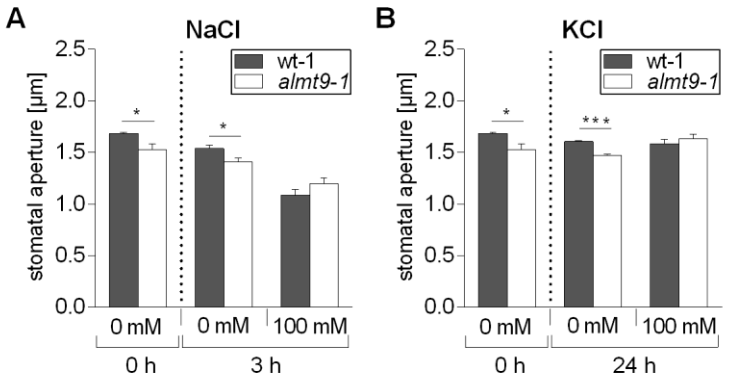


**Supplemental Figure 4.** Stomatal Movement during NaCl and KCl Stress in Wild-Type-1 and *almt9-1*.

*In situ* assay of native stomatal apertures (see Methods) using hydroponically grown wild-type-1 (wt-1) and *almt9-1* plants. Roots were exposed to control (0 mM) or stress solutions, and the stomatal aperture was measured before (0 h) and after treatment.

**(A)** Stomatal movement in response to 100 mM NaCl (100 mM) for 3 h. The measurement was conducted in parallel with the 24 h salinity treatment. Hence, the apertures before treatment are also shown in Figure 5A.

**(B)** Stomatal movement in response to 100 mM KCl (100 mM) for 24 h. The measurement was conducted in parallel with the 24 h salinity treatment. Data of control conditions are also shown in Figure 5A.

The SEM was calculated from averages of $n \geq 4$ biological replicates. Asterisks indicate statistically significant differences from wt-1 (*$P < 0.05$, **$P < 0.01$, ***$P < 0.001$; two-tailed Student's t-test).

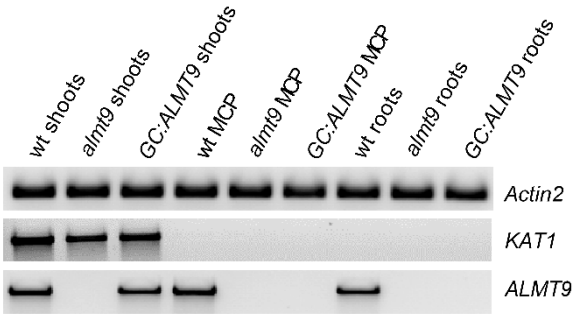


**Supplemental Figure 5.** Evaluation of the Guard Cell-Specific Complementation Line of *almt9-2*.

PCR amplification of *ACT2*, the guard cell-specific *KAT1* and *ALMT9* using cDNA from wild-type-2 (wt), *almt9-2* and *GC:ALMT9*. cDNA was synthesized from mRNA extracted from either shoots, mesophyll cell protoplasts (MCP), or roots.

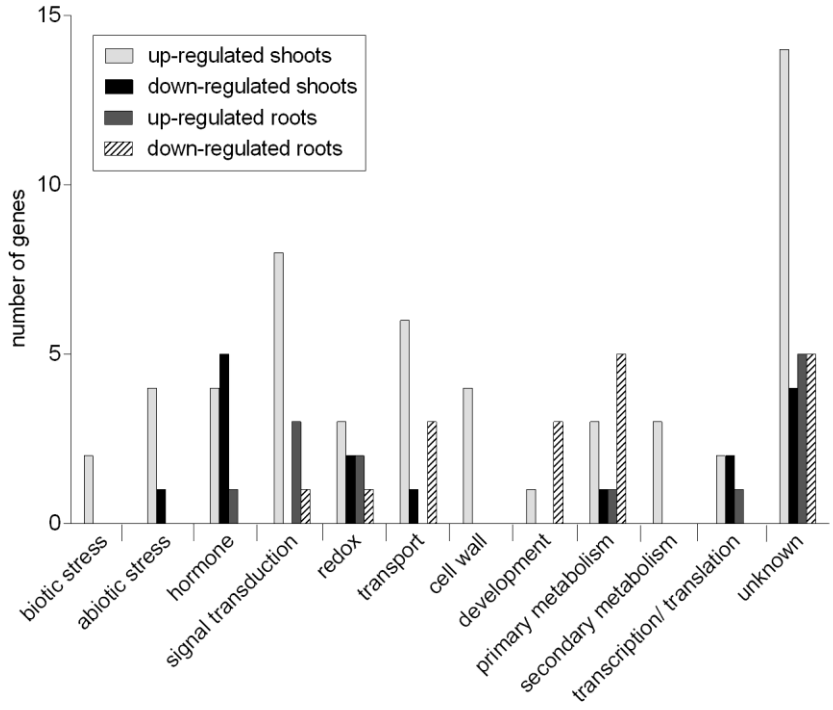


**Supplemental Figure 6.** The RNA-seq Analysis Reveals Distinct Biological Functions of Genes that are Differentially Expressed in *almt9-1* Exclusively under Salinity.

Genes that show a differential expression exclusively under salinity conditions (24 h, 100 mM NaCl) in *almt9-1* shoots and roots (for selection requirements see Method section) were arranged in selected functional categories. Up-regulated, genes with higher expression in *almt9-1* compared to wild-type-1; down-regulated, genes with lower expression in *almt9-1*.

**Supplemental Table 1.** Ion Contents of Wild-Type and *almt9* Mutant Plants upon 24 h Salinity.

| Ion | NaCl [mM] | Tissue | Mean ± SD [a] | | | |
|---|---|---|---|---|---|---|
| | | | wild-type-1 | *almt9-1* | wild-type-2 | *almt9-2* |
| $Na^+$ | 0 | Shoots | 0.023 ± 0.005 | 0.018 ± 0.005 | 0.062 ± 0.009 | 0.059 ± 0.005 |
| | 100 | Shoots | 0.455 ± 0.053 | 0.366 ± 0.028** | 0.355 ± 0.012 | 0.273 ± 0.035* |
| | 0 | Roots | 0.033 ± 0.009 | 0.041 ± 0.012 | 0.045 ± 0.014 | 0.048 ± 0.015 |
| | 100 | Roots | 0.853 ± 0098 | 0.804 ± 0.168 | 0.845 ± 0.150 | 0.763 ± 0.178 |
| $Cl^-$ | 0 | Shoots | 0.221 ± 0.032 | 0.263 ± 0.027* | 0.204 ± 0.122 | 0.209 ± 0.013 |
| | 100 | Shoots | 0.547 ± 0.064 | 0.406 ± 0.023*** | 0.534 ± 0.035 | 0.451 ± 0.017* |
| | 0 | Roots | 0.077 ± 0.026 | 0.075 ± 0.028 | 0.082 ± 0.011 | 0.085 ± 0.034 |
| | 100 | Roots | 0.749 ± 0.067 | 0.737 ± 0.079 | 0.763 ± 0.143 | 0.733 ± 0.083 |
| $K^+$ | 0 | Shoots | 1.295 ± 0.123 | 1.393 ± 0.083 | 1.207 ± 0.052 | 1.287 ± 0.084 |
| | 100 | Shoots | 1.200 ± 0.058 | 1.186 ± 0.069 | 1.238 ± 0.038 | 1.256 ± 0.081 |
| | 0 | Roots | 0.947 ± 0.049 | 0.996 ± 0.085 | 1.052 ± 0.217 | 1.029 ± 0.310 |
| | 100 | Roots | 0.668 ± 0.188 | 0.648 ± 0.124 | 0.740 ± 0.132 | 0.569 ± 0.099 |
| $NO_3^-$ | 0 | Shoots | 0.163 ± 0.007 | 0.157 ± 0.012 | 0.168 ± 0.021 | 0.166 ± 0.028 |
| | 100 | Shoots | 0.160 ± 0.013 | 0.156 ± 0.016 | 0.162 ± 0.015 | 0.170 ± 0.011 |
| | 0 | Roots | 0.060 ± 0.004 | 0.060 ± 0.002 | 0.054 ± 0.003 | 0.055 ± 0.001 |
| | 100 | Roots | 0.055 ± 0.006 | 0.055 ± 0.006 | 0.057 ± 0.004 | 0.055 ± 0.002 |

[a] Concentrations are shown in [mmol/ g dry weight] for $Na^+$, $Cl^-$, and $K^+$. Concentrations are shown in [mmol/ g fresh weight] for $NO_3^-$. The results are illustrated in Figure 2. Data of $n \geq 5$ biological replicates derived from two independent experiments are shown. One-way ANOVA of each tissue and treatment and a pair-wise comparison was used for statistical analysis. Asterisks indicate significant differences from the corresponding wild-type (*$P < 0.05$, **$P < 0.01$, ***$P < 0.001$).

**Supplemental Table 2.** Differentially Expressed Genes between Wild-Type-1 and *almt9-1* in Shoots Exclusively under Salinity.

| Gene ID | Description/ Name | $Log_2$ Ratio | p-value |
|---|---|---|---|
| AT2G18190 | P-loop containing nucleoside triphosphate hydrolases superfamily protein | 4.674 | 1.58E-05 |
| AT3G26830 | Cytochrome P450 enzyme (CYP71B15/ PAD3) | 4.411 | 1.32E-05 |
| **AT2G04040** | **MATE-related detoxification efflux carrier (DTX1)** | **3.998** | **4.70E-05** |
| AT1G29715 | Pseudogene | 3.98 | 5.93E-05 |
| AT1G66390 | MYB DOMAIN PROTEIN 90 (MYB90/ PAP2) | 3.74 | 0.003046 |
| AT1G26380 | FAD-binding Berberine family protein | 3.478 | 7.06E-05 |
| AT4G27140 | Seed storage albumin (SESA1) | -3.441 | 0.001111 |
| AT3G28580 | P-loop containing nucleoside triphosphate hydrolases superfamily protein | 3.371 | 0.0002297 |
| AT1G05680 | **Uridine diphosphate glycosyltransferase (UGT74E2)** | 3.338 | 2.90E-07 |
| AT1G13520 | Protein of unknown function (DUF1262) | 3.313 | 0.0007433 |
| AT3G44300 | Nitrilase (NIT2) | 3.217 | 3.46E-05 |
| **AT2G04070** | **Putative MATE-related efflux carrier** | **3.05** | **0.001947** |
| AT1G62440 | LEUCINE-RICH REPEAT/EXTENSIN 2 (LRX2) | 2.792 | 7.26E-07 |
| AT5G19100 | Eukaryotic aspartyl protease family protein | -2.774 | 0.002622 |
| AT5G01550 | Lectin receptor kinase subfamily A4 (LecRKA4.2) | 2.724 | 0.001441 |
| AT4G04540 | Cysteine-rich receptor like protein kinase (CRK39) | 2.675 | 0.002616 |
| AT2G30750 | Putative cytochrome P450 (CYP71A12) | 2.619 | 0.008339 |
| AT1G17960 | Threonyl-tRNA synthetase | 2.573 | 0.0003076 |
| **AT2G04050** | **Putative MATE-related efflux carrier** | **2.535** | **3.38E-05** |
| AT1G16420 | Metacaspase (MCP2E/ MC8) | 2.497 | 0.001789 |
| **AT1G63030** | **ERF/AP2 transcription factor family (DDF2)** | **-2.258** | **0.0005246** |
| AT2G38240 | 2-oxoglutarate (2OG) and Fe(II)-dependent oxygenase superfamily protein | -2.247 | 2.76E-05 |

| | | | |
|---|---|---|---|
| AT2G12930 | **Gypsy-like retrotransposon family** | **-2.199** | **0.003696** |
| AT3G28740 | Cytochrome P450 family (CYP81D11) | 2.19 | 0.009735 |
| AT1G21240 | Wall-associated kinase (WAK3) | 2.093 | 2.62E-07 |
| AT1G49310 | Unknown protein | 2.079 | 0.00275 |
| AT4G20000 | VQ motif-containing protein | 2.045 | 0.006998 |
| AT5G10970 | C2H2 and C2HC zinc fingers superfamily protein | -2.031 | 0.0006944 |
| AT2G18193 | P-loop containing nucleoside triphosphate hydrolases superfamily protein | 2.007 | 0.0001036 |
| AT5G25260 | SPFH/Band 7/PHB domain-containing membrane-associated protein family | 1.957 | 0.001054 |
| AT1G17170 | Glutathione transferase (GSTU24) | 1.956 | 0.0002155 |
| **AT3G63380** | **AUTO-INHIBITED $CA^{2+}$ ATPASE 12 (ACA12)** | **1.865** | **0.004314** |
| **AT2G31910** | **Putative Na+/H+ antiporter family (CHX21)** | **-1.848** | **0.004987** |
| AT3G13950 | Unknown protein | 1.803 | 0.002431 |
| AT3G29250 | NAD(P)-binding Rossmann-fold superfamily protein (SDR4) | 1.764 | 0.002492 |
| **AT1G12610** | **ERF/AP2 transcription factor family (DDF1)** | **-1.717** | **1.28E-08** |
| **AT3G09640** | **Cytosolic ascorbate peroxidase (APX2/ APX1B)** | **-1.669** | **0.0004518** |
| AT5G51440 | HSP20-like chaperones superfamily protein | 1.664 | 0.007465 |
| **AT2G47000** | **Subfamily B ABC-type auxin efflux transporter (ABCB4/ MDR4/ PGP4)** | **1.636** | **0.001916** |
| AT1G43910 | P-loop containing nucleoside triphosphate hydrolases superfamily protein | 1.597 | 0.005181 |
| AT3G25010 | Receptor like protein (RLP41) | 1.593 | 1.29E-06 |
| AT4G04490 | Cysteine-rich receptor like protein kinase (CRK36) | 1.583 | 0.001103 |
| AT1G61810 | Beta-glucosidase (BGLU45) | 1.58 | 0.003976 |
| AT2G29350 | Senescence-associated gene (SAG13) | 1.564 | 1.40E-07 |
| AT3G57240 | Glycosyl hydrolase family 17 (BG3) | 1.514 | 5.12E-05 |
| AT4G12410 | SAUR-like auxin-responsive protein family (SAUR35) | -1.49 | 0.002346 |

| | | | |
|---|---|---|---|
| AT4G25000 | **ALPHA-AMYLASE-LIKE (AMY1)** | **1.482** | **3.40E-05** |
| AT5G60250 | Zinc finger (C3HC4-type RING finger) family protein | 1.473 | 0.0005328 |
| AT1G57630 | Toll-Interleukin-Resistance (TIR) domain family protein | 1.464 | 0.00685 |
| AT4G34410 | ERF/AP2 transcription factor family (ERF109) | -1.458 | 2.87E-12 |
| AT2G29460 | Glutathione transferase (GSTU4) | 1.415 | 0.007186 |
| AT3G10320 | Glycosyltransferase family 61 protein (MUCI21) | 1.397 | 0.006958 |
| AT5G52020 | ERF/AP2 transcription factor family | -1.396 | 8.35E-06 |
| AT1G53540 | HSP20-like chaperones superfamily protein | -1.386 | 0.002712 |
| AT1G76930 | Extensin (EXT1/EXT4) | 1.38 | 0.0007415 |
| AT4G00700 | C2 calcium/lipid-binding plant phosphoribosyltransferase family protein | 1.378 | 0.004223 |
| AT4G24000 | Cellulose synthase (CSLG2) | 1.324 | 0.002603 |
| AT5G02490 | Heat shock protein 70 (Hsp 70) family protein (HSP70-2) | 1.285 | 9.44E-05 |
| AT4G23140 | Cysteine-rich receptor like protein kinase (CRK6) | 1.229 | 8.88E-17 |
| AT4G37370 | Cytochrome P450 family (CYP81D8) | 1.198 | 0.006318 |
| AT5G18270 | NAC domain containing protein (ANAC087) | 1.184 | 0.002222 |
| AT3G57765 | Small nuclear RNA (U2.3) | -1.149 | 0.00242 |
| AT1G14780 | MAC/Perforin domain-containing protein | 1.125 | 8.42E-05 |
| AT1G15405 | Unknown gene | -1.12 | 0.009702 |
| AT4G27654 | Unknown protein | -1.117 | 2.97E-08 |
| AT3G28890 | Receptor like protein (RLP43) | 1.085 | 0.0001529 |
| AT2G29110 | Ligand-gated ion channel subunit family (GLR2.8) | 1.065 | 0.007163 |
| AT2G03760 | Brassinosteroid sulphotransferase (SOT12/ ST1) | 1.031 | 0.0008528 |
| AT1G58225 | Unknown protein | 1.015 | 0.0008908 |
| AT1G35230 | Arabinogalactan protein (AGP5) | 1.001 | 0.0007468 |

List of genes that are exclusively significantly up- or down-regulated under salinity conditions (24 h, 100 mM NaCl) in *almt9-1* shoots (for selection requirements see Method section). Positive $\log_2$ ratios correspond to transcriptional up-regulation in *almt9-1*, negative $\log_2$ ratios to transcriptional down-regulation. Names and descriptions are according to TAIR. Genes mentioned in the study are highlighted.

**Supplemental Table 3.** Differentially Expressed Genes between Wild-Type-1 and *almt9-1* in Roots Exclusively under Salinity.

| Gene ID | Description/ Name | $Log_2$ Ratio | p-value |
|---|---|---|---|
| AT4G04223 | Unknown gene | -3.337 | 6.03E-22 |
| AT5G24140 | Squalene monooxygenase (SQP2) | -2.981 | 0.0003986 |
| AT5G02330 | Cysteine/Histidine-rich C1 domain family protein | -2.502 | 0.0003037 |
| AT3G01015 | TPX2 (targeting protein for Xklp2) protein family | 2.228 | 0.001345 |
| AT1G19415 | Copia-like retrotransposon family | -2.145 | 0.009452 |
| AT2G30766 | Unknown protein | 2.002 | 3.22E-06 |
| AT1G51030 | Unknown protein | -1.998 | 0.001067 |
| AT4G38590 | Putative beta-galactosidase (BGAL14) | -1.95 | 0.005079 |
| AT4G15690 | Thioredoxin superfamily protein | 1.944 | 0.0003804 |
| AT5G17040 | UDP-Glycosyltransferase superfamily protein | -1.794 | 0.0023 |
| **AT1G71890** | **Sucrose transporter (SUC5)** | **-1.778** | **0.005836** |
| AT4G23320 | Cysteine-rich receptor like protein kinase (CRK24) | 1.777 | 0.003051 |
| AT5G03310 | SAUR-like auxin-responsive protein family (SAUR44) | 1.624 | 0.003661 |
| AT5G11410 | Protein kinase superfamily protein | 1.545 | 0.006612 |
| AT4G23210 | Cysteine-rich receptor like protein kinase (CRK13) | -1.531 | 0.0003196 |
| AT1G14345 | NAD(P)-linked oxidoreductase superfamily protein | -1.5 | 0.003167 |
| AT5G27220 | Frigida-like protein | 1.484 | 0.009174 |
| **AT1G73220** | **Organic cation/carnitine transporter (OCT1)** | **-1.483** | **0.0001871** |
| AT3G53040 | Putative late embryogenesis abundant (LEA) protein | -1.477 | 0.003184 |
| AT2G48121 | Unknown protein | 1.459 | 0.009511 |
| AT1G33320 | Pyridoxal phosphate (PLP)-dependent transferases superfamily protein | -1.441 | 0.0002151 |
| AT2G03710 | SEPALLATA 4 (SEP4/ AGL3) | -1.224 | 0.0006572 |
| AT1G02250 | NAC family of transcription factors (ANAC005) | 1.15 | 0.003483 |

| | | | |
|---|---|---|---|
| AT3G22560 | **Acyl-CoA N-acyltransferases (NAT) superfamily protein** | **-1.146** | **0.00112** |
| AT3G60090 | VQ motif-containing protein | -1.129 | 0.001143 |
| AT2G39510 | Nodulin MtN21-like transporter family protein (UMAMIT14) | -1.112 | 0.003848 |
| AT2G02061 | Nucleotide-diphospho-sugar transferase family protein | 1.069 | 0.00585 |
| AT4G15360 | Cytochrome P450 family (CYP705A3) | 1.031 | 0.0006057 |
| AT1G25150 | F-box family protein | 1.028 | 0.002636 |
| AT4G17660 | Protein kinase superfamily protein | 1.019 | 0.00087 |
| AT5G44565 | Unknown protein | -1.019 | 0.001466 |

List of genes that are exclusively significantly up- or down-regulated under salinity conditions (24 h, 100 mM NaCl) in *almt9-1* roots (for selection requirements see Method section). Positive $\log_2$ ratios correspond to transcriptional up-regulation in *almt9-1*, negative $\log_2$ ratios to transcriptional down-regulation. Names and descriptions are according to TAIR. Genes mentioned in the study are highlighted.

**Supplemental Table 4.** Primers Used in that Study.

| Primer Description | 5' - 3' Sequence |
|---|---|
| qPCR-ACT2-for | TGGAATCCACGAGACAACCTA |
| qPCR-ACT2-rev | TTCTGTGAACGATTCCTGGAC |
| qPCR-SOS1-for | CTCTTCGTCGGAATGTCTCTG |
| qPCR-SOS1-rev | ACGAATTCCATGGCCGATCTTT |
| qPCR-ALMT9-for | ACCTAATCCGGATCTTAGTCGATACT |
| qPCR-ALMT9-rev | TCACCGAATAAAGTGGAAAGCTCAG |
| qPCR-ALMT6-for | CCGTTGCATGATGCTAGTAAATAC |
| qPCR-ALMT6-rev | TGATGATGGTTTGCTCGAAA |
| qPCR-ALMT5-for | GAGCCGCTTCAAGATGCTAGTA |
| qPCR-ALMT5-rev | ATGACTTCTTCAAACTCTCCTGCT |
| qPCR-ALMT4-for | TGACGCTAGCAAGTATGCTGTT |
| qPCR-ALMT4-rev | CTTCAAATTCTCCAGCTGAAACAGA |
| qPCR-ALMT3-for | GGCTTATCCTACAGAGCAGAGGCT |
| qPCR-ALMT3-rev | TCAGAGCCAAACCCATCTTC |
| qPCR-HKT1;1-for | TGGTTGGATCGTTGTTTCAA |
| qPCR-HKT1;1-rev | CGGAATCATCATCTCCTCCT |
| qPCR-CHX21-for | ACGCAACTGTCTGTCGCTAA |
| qPCR-CHX21-rev | CGAGAGCTAAGTTTGCGAATG |
| qPCR-DTX1-for | CCAATACGGAATCCCATCAG |
| qPCR-DTX1-rev | ATTCCCAGCTCCCAAATTGT |
| hpRNA-for | GATCGGATCCCTCGAGGAATACGAGAGAATACC GTCG |
| hpRNA-rev | GATCATCGATGGTACCCAGCTTTCTGAGTTGACAA GAAG |
| ALMT9pro:ALMT9$_{E196A}$-for | TAGTTGGAATGGGTTCGAAAAATTACAATTGTTTC CTCT |

| | |
|---|---|
| ALMT9pro:ALMT9$_{E196A}$-rev | TTATGGAGTTGGGTTCGAACCATCCCAAAACACCT ACGA |
| SDM$_{E196A}$-for | GATGAAAGCTTATGCATACGGGTTCCGGG |
| SDM$_{E196A}$-rev | CCCGGAACCCGTATGCATAAGCTTTCATC |
| ALMT9$_{pro}$-for | GGGGACAAGTTTGTACAAAAAAGCAGGCTTAAA ATTACAATTGTTTCCTCT |
| ALMT9$_{pro}$-rev | GGGGACCACTTTGTACAAGAAAGCTGGGTGTACT AGACGGATTCTCAAAG |
| ALMT9$_{GC}$-for | GGCGCGCCATGGCGGCGAAGCAAGGTTC |
| ALMT9$_{GC}$-rev | GACTAGTCTTACATCCCAAAACACCTAC |
| KAT1-for | ATGTCGATCTCTTGGACTCG |
| KAT1-rev | ATTTGATGAAAAATACAAATGATCACC |

# 5. Chapter IV:

## Role of AtALMT9 during Seed Germination

Unpublished results.

Contributing Researchers:

The complementation lines were cloned by Dr. Jingbo Zhang. The transgenic lines were selected by Ulrike Baetz. Seed germination experiments and qRT-PCR were designed and conducted by Ulrike Baetz.

# 5.1. Introduction

*'... Effect of Salt-Water on the Germination of Seeds. — As you have published notices by Mr. Berkeley and myself on the length of time seeds can withstand immersion in sea-water, you may perhaps like to hear, without minute details, the final results of my experiments. [...] It is remarkable how differently varieties of the same species have withstood the ill effects of the salt water...'* (Darwin, 1855).

Already centuries ago, Darwin made the observation that early seed germination processes are dependent on seed water uptake, and salinity impairs the germination rate. In addition, he described the broad variation between plant species to withstand the presence of salt water during seed germination and seedling establishment.

In many seeds including *Arabidopsis thaliana* (Arabidopsis), the embryo is covered by the maternal seed coat (testa) and a single layer of a triploid endosperm, which are significant barriers to embryo outgrowth (Sánchez et al., 1990, Dahal et al., 1997, Debeaujon and Koornneef, 2000, Debeaujon et al., 2000). The emerging radicle of the embryo thus needs to overcome the dual constrains of this structure to complete germination. Seed germination and embryo outgrowth starts when a dry seed is exposed to water under favorable conditions. Dry seeds have typical average water contents of 10 % and have very low water potentials (Woodstock, 1988, Obroucheva and Antipova, 1997, Weitbrecht et al., 2011). This causes rapid water fluxes into the seed during early germination, a process designated imbibition. The imbibition period is characterized by a rapid swelling, enhanced volume and altered shape of the seed (e.g. Robert et al., 2008, Preston et al., 2009). The imbibition is followed by a stagnated phase (phase II) in which the water content remains stable (Weitbrecht et al., 2011, Daszkowska-Golec, 2011). During imbibition and the subsequent plateau phase of water uptake, the metabolism of the seed re-activates. In addition, water uptake and volume change result in the testa rupture. Subsequently, in water uptake phase III, also the endosperm ruptures, culminating in the emergence of the radicle. Germination is completed by the visible radicle protrusion, and at this point of development the seed is defined as being germinated. Seed germination is followed by seedling development which includes seedling growth and differentiation (Weitbrecht et al., 2011).

Embryo growth during germination is based on the extensibility of the cell wall (Cosgrove, 1996, Cosgrove, 1998a, Cosgrove, 1998b, Cosgrove, 2000, Yan et al., 2014) and is accompanied by a progressive vacuolation during the plateau phase (Bethke et al., 2007). Solute and water uptake across the tonoplast majorly determines the volume of the vacuole and the cells, and therefore presumably the process of testa and endosperm rupture and the resulting radicle emergence. For instance, aquaporin water channels at the tonoplast, so called tonoplast intrinsic proteins (TIPs), that mediate the rapid uptake of water into the vacuole have been implicated in imbibition as well as the timing of the testa rupture (Maurel et al., 1997, Schuurmans et al., 2003, Maurel et al., 2009). $Cl^-$ and malate are crucial osmotically active counter-anions for cations such as $K^+$ and, together, their fluxes largely contribute to solute accumulation, which is driving water uptake through TIPs and volume changes of vacuoles.

The water uptake during imbibition is fundamental for the germination process. Therefore, reducing the surrounding water potential by the addition of high salt concentrations reduces the flow of water into the seed and constitutes a high osmotic stress. Salinity might additionally impose an ionic stress on the seed during early germination. Hence, the application of salt stress to germinating seeds is an established and fast approach to investigate transport mutants that are potentially impaired in solute and water uptake, and/ or $Na^+$ and $Cl^-$ detoxification mechanisms (Shkolnik-Inbar et al., 2013, Yue et al., 2012, Orsini et al., 2010). Of note, although significant advances have been made in understanding such adaptation mechanisms towards salinity during vegetative growth (Munns and Tester, 2008), the molecular events of salinity response during seed germination is barely studied. In addition, the relative contribution of the osmotic and ionic stress component to early germination events upon salinity is not well understood. Yet, extensive natural genetic variation has been documented in seed germination during osmotic and salt stress (Vallejo et al., 2010, Quesada et al., 2002, Clerkx et al., 2004, Joosen et al., 2010). For instance, among worldwide populations of Arabidopsis seeds, the germination ability within a moderately saline environment of 150 mM NaCl varied from > 90 % in the most tolerant lines to complete inability to germinate in the most susceptible lines (DeRose-Wilson and Gaut, 2011). Hence, investigating seed germination during salinity provides an almost unexplored research area for studying stress adaptation and transport mechanisms.

AtALMT9 belongs to the Aluminum-activated Malate Transporter (ALMT) family in Arabidopsis. The anion channel protein is localized at the vacuolar membrane where it is capable of mediating the influx of malate and $Cl^-$ into the vacuole (Kovermann et al., 2007, De Angeli et al., 2013b). AtALMT9 is expressed in guard cells, and mutant plant lacking the channel show reduced stomatal opening (De Angeli et al., 2013b). In this chapter, preliminary results about the contribution of the vacuolar anion channel AtALMT9 on early seed germination will be presented. It will be shown that AtALMT9 is highly expressed in seeds of Arabidopsis. By using two independent knock-out mutants that lack AtALMT9 and that are therefore impaired in vacuolar anion uptake I demonstrate that the anion fluxes mediated by AtALMT9 highly impact on the efficiency of seed germination in the presence of high salt concentrations. The analysis of a transgenic plant line expressing a mutant channel which exhibits exclusively higher constitutive $Cl^-$ currents across the tonoplast provides first evidence that in particular AtALMT9-mediated $Cl^-$ currents are crucial to withstand salinity stress during seed germination.

## 5.2. Results

The vacuolar anion channel AtALMT9 has been shown in previous studies to be expressed in mesophyll cells, guard cells (Kovermann et al., 2007), and the vasculature of shoots and roots (Baetz et. al., submitted; Chapter III). In an attempt to determine other tissues in which AtALMT9 might be expressed, quantitative real-time PCR (qRT-PCR) was conducted using various organs and tissues during different developmental stages of Arabidopsis (Figure 1). Plants were grown on plates and in sterile cylinders to assess the expression during the complete life cycle. *AtALMT9* was found to be ubiquitously expressed in the plant, but besides in the shoots, also particularly high in reproductive organs such as siliques and flowers (Figure 1). Interestingly, the organ in which *AtALMT9* showed highest expression was in dry seeds. Compared to other *AtALMT* members that belong to clade II and that are also located at the tonoplast (see Chapter II), AtALMT9 is by far the predominant member of this vacuolar anion channel subfamily in dry seeds.

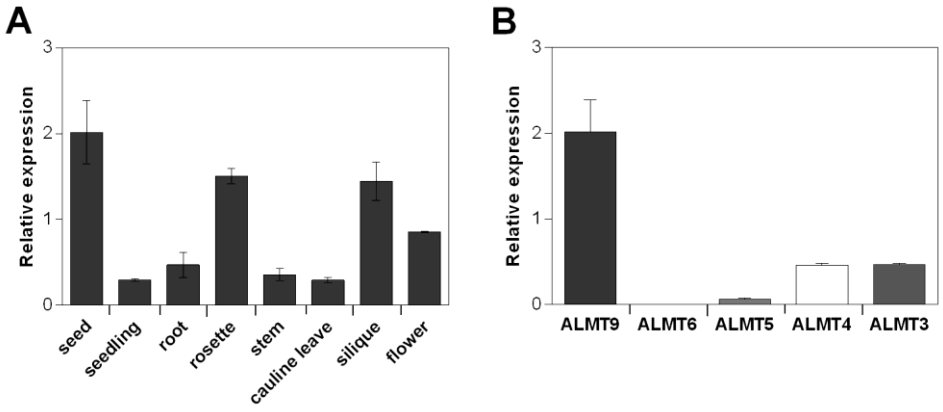


**Figure 1. AtALMT9 is the Major Vacuolar AtALMT Channel in Dry Seeds.**

**(A)** qRT-PCR analysis to determine the expression of *AtALMT9* in different tissues and organs throughout the Arabidopsis life cycle.

**(B)** qRT-PCR analysis to determine the relative expression of all clade II *AtALMTs* in dry seeds. The data was normalized to the expression of *AtACT2* that served as a reference gene. Data are means ± SD of n = 2 biological replicates.

To investigate whether AtALMT9 might have a functional role in vacuolar anion uptake during early germination, two independent knock-out mutants (*atalmt9-1* and *atalmt9-2*) and the corresponding wild-types (wild-type-1 and wild-type-2) that have been selected previously (De Angeli et al., 2013b) were used in germination assays. Both genotypes were grown on the same plates, and seeds of all germination experiments had the same age. Germination was scored as accomplished when the radicle had visibly emerged, and greening when the cotyledons started to get coloured. Seven days after initiation of germination, steady-state germination and greening rates were determined. To challenge water absorption and apply ionic stress to the seeds, the assays were performed under different concentrations of supplemental NaCl ranging from 0 mM NaCl (control conditions) to 200 mM NaCl (Figure 2). As shown in numerous studies, the decrease of external water potential and the increase of toxic ions with increasing salt concentrations results in reduced germination as well as greening rates in wild-type plants after seven days (Figure 2A and 2B). Under control conditions, no significant differences in germination and greening rates between *atalmt9-1* mutant and wild-type seeds were detected.

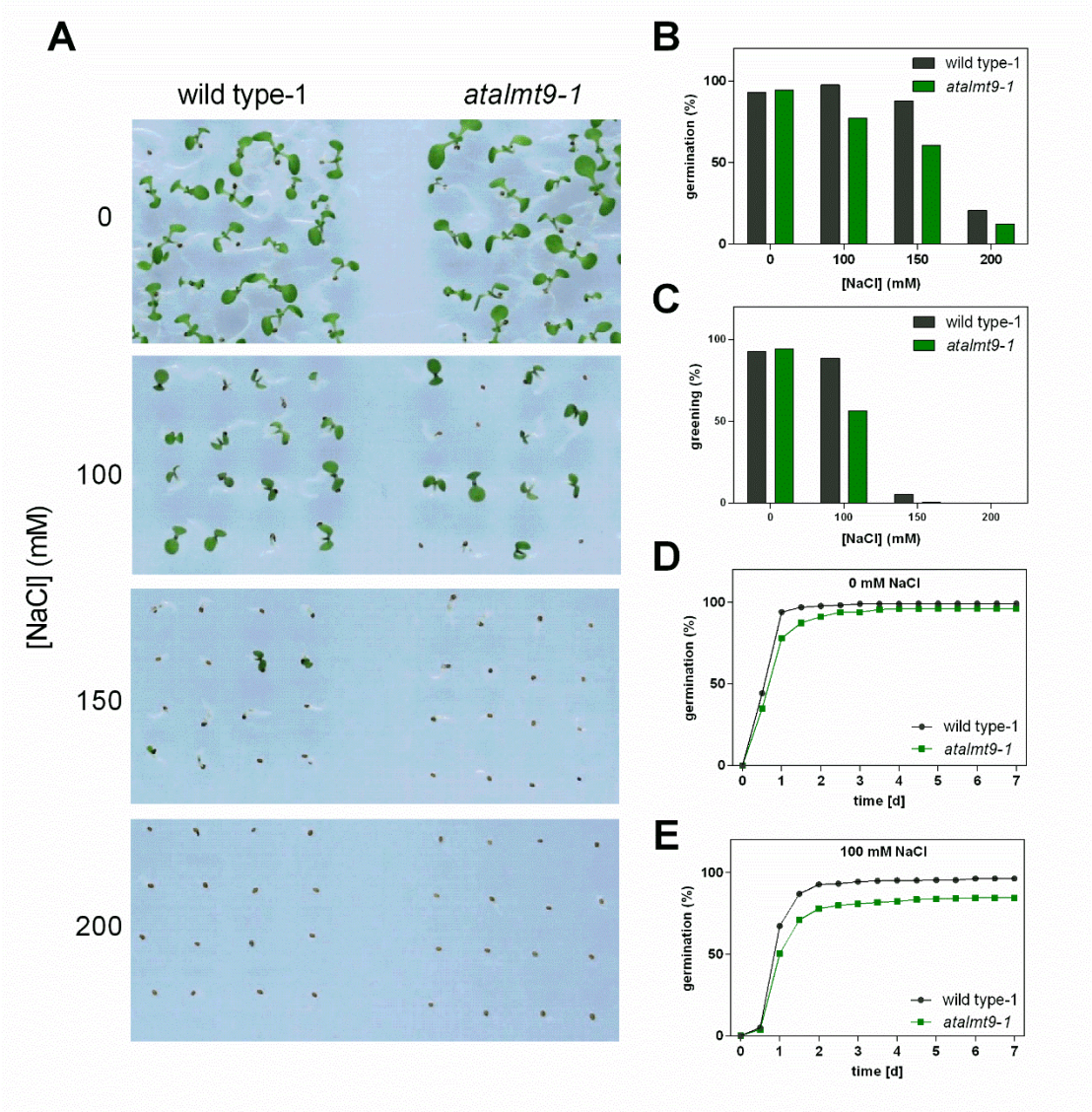


**Figure 2. The *atalmt9* Knock-Out Mutant Shows Reduced Seed Germination and Greening Rates during Salinity.**

Germination assay of *atalmt9-1* and the corresponding wild-type-1 using plates that were supplemented with 0 mM, 100 mM, 150 mM and 200 mM NaCl. On every plate both genotypes were grown in parallel.

**(A)** Picture of representative seeds and seedlings seven days after initiation of germination.

**(B)** and **(C)** Germination (B) and greening rate (C) was scored after seven days. For each condition and genotype, a total of 200 seeds were scored that were distributed on two independent plates.

**(D)** and **(E)** Time course of germination rate during seven days of germination under 0 mM (D) and 100 mM (E) salinity. Germination was scored every 12 hours. For each condition and genotype, a total of 400 seeds were scored that were distributed on two independent plates.

However, germination and greening rates were more reduced in *atalmt9* seeds than the wild-type seeds when challenged on NaCl-containing plates (Figure 2B and 2C). Seed germination appeared to be arrested before the testa ruptured. The difference in salt sensitivity got most apparent under moderate salt stress of 100 mM NaCl (20 % lower germination rate and 32 % lower greening rate in *atalmt9-1* compared to the wild-type-1), since even higher NaCl concentrations restricted germination and greening rates of both genotypes drastically. Therefore, the subsequent 7-d time course conducted to elucidate the kinetics of germination between *atalmt9* and wild-type seeds was examined on plates containing 0 mM and 100 mM NaCl (Figure 2D and 2E). Within the first 24 h the germination rate increased drastically under control conditions. This initial period was followed by a lower germination rate, and after day three a stagnation of germination was observed. Again, after seven days the germination rate of *atalmt9* mutants was significantly reduced (12 %) compared to wild-type-1 exclusively under salinity (Figure 2E). Interestingly, in the knock-out mutants the germination rate was also under control conditions slightly delayed (after 24 h 94 % of wild-type-1 seeds and 78 % of *almt9-1* seeds were germinated; Figure 2D), highlighting the necessity of kinetic germination assays, and demonstrating that the application of abiotic stress is a powerful tool to strengthen and elucidate phenotypes in seed research.

The lower steady-state germination and greening rates of mutants lacking the vacuolar anion channel AtALMT9 specifically under salinity was confirmed using the second allele, *atalmt9-2* and the corresponding wild-type-2 (41 % germination and 32 % greening compared to 64 % germination and 54 % greening, respectively; Figure 3). In this analysis two transgenic complementation lines were included. Firstly, line *comp-5* expresses the genomic DNA of *AtALMT9* under the control of its native promoter region in the genetic background of *atalmt9-2*. The corresponding seeds showed as all other lines almost 100 % germination and greening rates after seven days under control conditions. Moreover, a complementation of the reduced germination and greening phenotype of *atalmt9-2*, and an even slightly more efficient germination and greening (79 % and 73 %, respectively) compared to the wild-type-2 was observed under salinity (Figure 3). Of note, the expression of *AtALMT9* in this line has not yet been compared to the expression levels in the wild-type-2, retaining the possibility that differences might arise from enhanced transcript levels in *comp-5*.

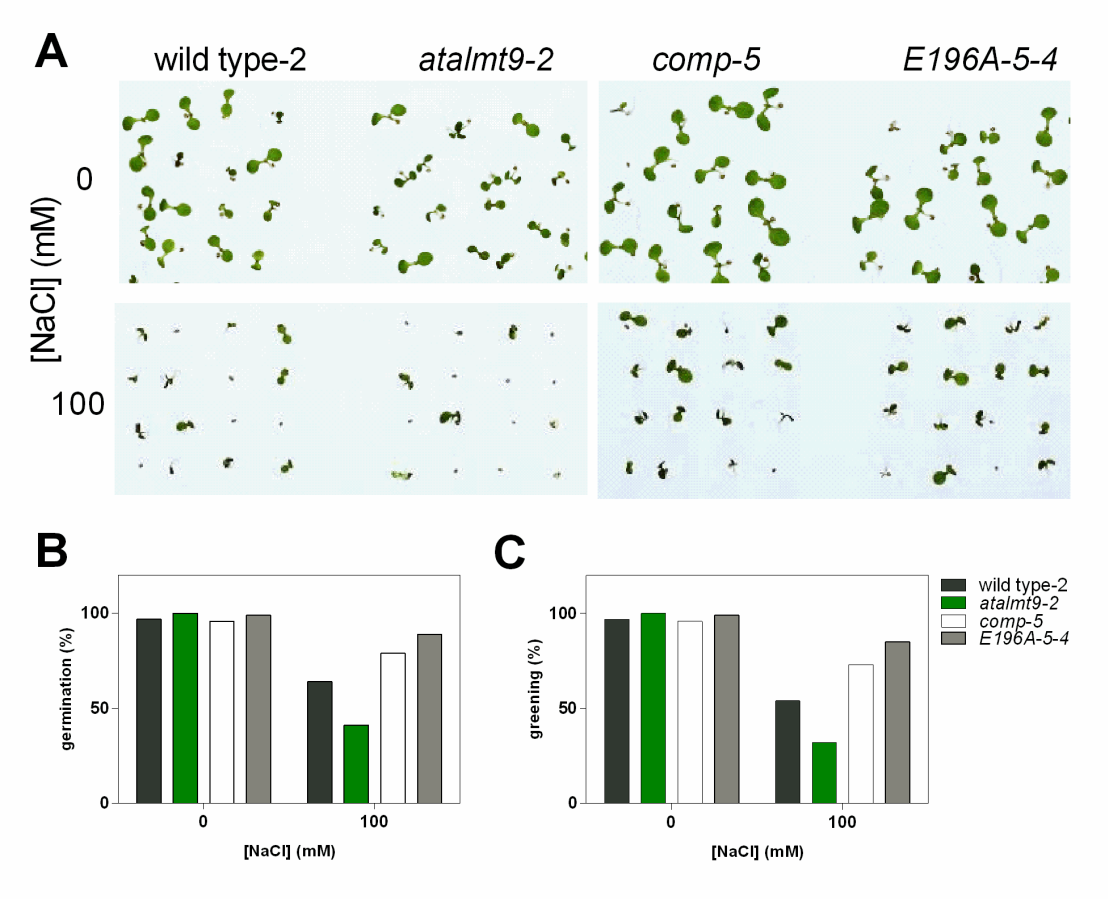


**Figure 3. Enhanced Vacuolar $Cl^-$ Currents Result in more Efficient Seed Germination and Greening upon Exposure to Salinity.**

Germination assay of *atalmt9-2*, the corresponding wild-type-2, and the complementation line *comp-5* as well as a transgenic line that expresses the point-mutated channel variant $AtALMT9_{E196A}$ (*E196A-5-4*). The plates were supplemented with 0 mM or 100 mM NaCl. On every plate all genotypes were grown in parallel.

**(A)** Picture of representative seeds and seedlings seven days after germination was initiated.

**(B)** and **(C)** Germination (B) and greening rate (C) was scored after seven days in one biological replicate. For each condition and genotype, a total of 100 seeds were scored.

---

The second transgenic line, *E196A-5-4*, expresses a point-mutated channel variant ($AtALMT9_{E196A}$) under the control of the native promoter region of *AtALMT9* in the genetic background of *atalmt9-2*. The mutation E196A has been identified in a large-scale site-directed mutagenesis study (Zhang et al., 2013; Chapter I), and the transgenic line has been characterized in a previous work (Baetz et al., submitted; Chapter III).

The transgenic line *E196A-5-4* features constitutively enhanced vacuolar inward rectifying $Cl^-$ currents without changing the expression levels of *AtALMT9*. The magnitude of malate conductivity and the level of malate-activated $Cl^-$ currents is not altered in this mutant line. Interestingly, it was observed that the constitutive increase in vacuolar $Cl^-$ uptake improved the germination and greening rate of *E196A-5-4* (89 % and 85 %, respectively) compared to wild-type-2, featuring an opposite effect as *atalmt9-2* knock-out mutant plants with reduced vacuolar $Cl^-$ fluxes (Figure 3). The *atalmt9-2* complementation by *comp-5* and the enhanced germination and greening rate of *E196A-5-4* was confirmed in a second experiment using more independent lines of the transgenic mutants (*comp-1*, *comp-5*, *E196-4-5* and *E196-11-5*; Figure 4). Another transgenic line of *atalmt9-2* that carries a channel mutation that might influence AtALMT9 activity, *Y197A-1-5* and *Y197A-3-3*, showed in these preliminary experiments no significant differences compared to line *comp-1* and *comp-5* (Figure 4). The expression levels of *AtALMT9* in *Y197A-1-5* and *Y197A-3-3* as well as detailed electrophysiological characterization of this mutant line remains a goal of future research.

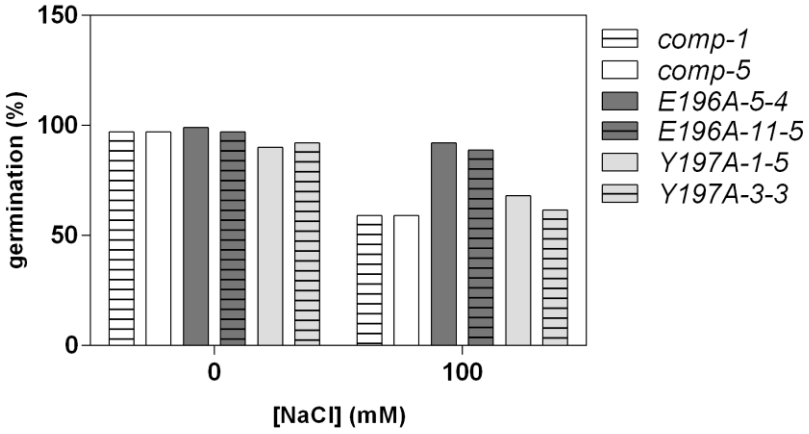


**Figure 4. Germination Rate of Different Complementation Lines.**

Germination assay of the complementation lines *comp-1* and *comp-5*, as well as the transgenic line that expresses the point-mutated channel variant $AtALMT9_{E196A}$ (*E196A-5-4* and *E196A-11-5*) and $AtALMT9_{Y197A}$ (*Y197A-1-5* and *Y197A-3-3*). The plates were supplemented with 0 mM or 100 mM NaCl. On every plate multiple genotypes were grown in parallel. Germination was scored after seven days in one biological replicate. For each condition and genotype, a total of 100 seeds were scored.

# 5.3. Discussion

Seed germination and seedling establishment is the most critical step in a plant's life. Several abiotic constraints such as salt stress result in an arrest of germination to prevent growth under unfavorable environmental conditions. Whether the stress component of salinity during early seed germination is mainly based on osmotic stress or on ionic stress is not well understood. During vegetative growth, early responses to osmotic (drought) and salinity stress have been shown to involve overlapping and distinct signaling components and pathways (Munns and Tester, 2008), indicating that early salt stress is generally not only based on the low water potential surrounding the plant but also on ion-specific triggers.

The present study investigating the function of AtALMT9 during seed germination demonstrates that vacuolar $Cl^-$ uptake is crucial to regulate early germination events that are possibly implemented before or during testa rupture. Seeds of mutant plants that lack the vacuolar anion channel showed reduced germination rates under high NaCl concentrations, whereas seeds of mutant plants that exhibit a constitutively enhanced vacuolar $Cl^-$ uptake, but no differences in malate conductivity, showed less sensitivity to salinity and germinated even more efficiently than the wild-type. Whether this observation is based on the function of AtALMT9 to store $Cl^-$ ions into the vacuole of seeds to counteract toxicity in the cytosol, or whether the accumulation of $Cl^-$ in the vacuoles adds to the maintenance of osmotic balance and guarantees water uptake into the seed cannot be stated clearly with the given results. Also, the implementation of AtALMT9 in both components of salinity stress, the osmotic and the ionic, might be possible. Nevertheless, the results gained so far in this project indicate that the predominant role of AtALMT9 during salinity might be the osmotic balance acquisition in order to allow water uptake. One indication for that comes from the developmental stage at which the germination arrests in *atalmt9* mutant seeds. Before testa rupture, the physiology of seeds is mainly characterized by rapid water uptake (imbibition) in order to allow vacuolation, seed swelling and re-activation of metabolism. The second hint for a role of AtALMT9 in osmotic homeostasis during seed germination comes from kinetic germination rates under control conditions. Under these conditions $Cl^-$

concentrations in the external medium were far from being toxic. Yet, it has been observed that germination rates were delayed in *atalmt9-1* mutants compared to wild-type-1 seeds. The defects in seed germination in the mutant became apparent in steady-state germination rates only when the external water potential was decreased by salinity. Delayed germination under control conditions and amplification of the phenotype under salinity points towards a role of AtALMT9 in osmotic rather than ionic stress tolerance. The importance of AtALMT9 in solute uptake in order to maintain water accumulation and turgor has been shown in guard cells, since a lack of the channel in *atalmt9* mutants resulted in reduced light-dependent stomatal opening (De Angeli et al., 2013b)

Further experiments are required to dissect AtALMT9 function during seed germination. Firstly, more detailed expression analysis could contribute to understand AtALMT9 mode of action. For instance, qRT-PCR investigating *AtALMT9* expression levels could be performed not only on dry seeds, but also using imbibed seeds, or upon radicle emergence. Furthermore, more precise determination of *AtALMT9* cell type expression in seeds will be of interest and can be obtained in further research by transgenic promoter:GUS reporter plants described in another study (Baetz et al., submitted; Chapter III).

Secondly, more germination assays under various ionic and osmotic conditions will add to understand the role of AtALMT9 in seed germination. For instance, the effects of the application of external KCl, $NaNO_3$ or sorbitol on germination rates of *atalmt9* and wild-type seeds will have to be compared. Based on the outcome, several conclusions could be drawn about the nature of stress that AtALMT9 activity counteracts in seeds. The seed germination process is under intense hormonal control (reviewed in Weitbrecht et al., 2011, Daszkowska-Golec, 2011). The phytohormone ABA, for instance, regulates the germination at the stage after the testa has ruptured and targets the endosperm. It plays a key role in integrating environmental information and seed germination. Exposure of seeds to external ABA inhibits endosperm rupture and therefore germination (Müller et al., 2006). Some plant channels have been shown to be regulated by ABA signaling pathways (Geiger et al., 2009, Imes et al., 2013, Geiger et al., 2010, Lee et al., 2009). Differences in germination rate could therefore also point

towards a differential sensitivity to ABA responses (e.g. Gosti et al., 1999, Merlot et al., 2001). Hence, investigating the germination rate under external ABA might contribute to the understanding of the role and putative pathway of AtALMT9 action during germination.

# 5.4. Material and Methods

Construct Design and Plant Transformation

The two independent T-DNA insertion lines of ALMT9 (*almt9-1*: WiscDsLox499H09; *almt9-2*: SALK_055490) were described in a previous study (De Angeli et al., 2013b). To generate complementation lines (*comp*) *ALMT9* and its upstream promoter region (548 bp) were amplified from wild-type genomic DNA and cloned into pPLV22 (De Rybel et al., 2011). The construct was transformed into *almt9-2* and positive transformation events were selected by BASTA. Arabidopsis was stable transformed via *Agrobacterium tumefaciens* using the floral dipping method (Clough and Bent, 1998). Construction and selection of the lines *E196A* have been described previously (Baetz et al., submitted; Chapter III). The lines *Y197A* have been designed and selected accordingly.

Germination Assay

For germination assays, seeds of the same age have been used. Seeds were ethanol-sterilized. Subsequently, seeds were pipetted in a defined distance on plates, and every plate contained each genotype. Seeds were stratified by keeping the plates for 2 d at 4 °C in darkness The plate medium was composed as followed: a final concentration of 1 mM $KNO_3$, 0.15 mM $Ca(NO_3)_2$, 0.7 mM $NaNO_3$, 42.5 µM FeNaEDTA, 0.5 mM $MgSO_4$, 0.625 mM $KH_2PO_4$, 2 mM NaCl, 0.1 µM $CoCl_2$, 0.1 µM $CuSO_4$, 50 µM $H_3BO_3$, 5 µM KI, 24 µM $MnSO_4$, 0.5 µM $Na_2MoO_4$, 30 µM $ZnSO_4$, 3 mM MES-KOH, pH 5.6, and 1 % phytoagar was used. Germination was initiated by illumination in a growth chamber (21 °C, 16 h light /8 h dark) in which seeds remained for seven days until steady-state germination rates were determined under a binocular

(Nikon SMZ1500). For kinetic experiments, germination was evaluated and scored every 12 h. Representative pictures of seeds were captured with a digital reflex camera from Canon.

Quantitative Real-Time PCR

Quantitative Real-Time PCR in different tissues and organs of vacuolar AtALMTs in Arabidopsis was performed as described in Section 3.4 in this thesis.

# 6. Chapter V:

## The vacuolar channel VvALMT9 mediates malate and tartrate accumulation in berries of *Vitis Vinifera*

Alexis De Angeli*[12], Ulrike Baetz*[1], Rita Francisco[1], Jingbo Zhang[13], Maria Manuela[4] Chaves and Ana Regalado[4]

[1] Department of Plant and Microbial Biology, University of Zurich, 8008 Zurich, Switzerland

[2] Current address: Institut de Biologie Intégrative de la Cellule, CNRS, 91190 Gif-Sur-Yvette, France

[3] Current address: Division of Biological Sciences, Cell and Developmental Biology Section, University of California, San Diego, CA 92093-0116, USA

[4] Instituto de Tecnologia Quimica e Biologica, Universidade Nova de Lisboa, 2780-157 Oeiras, Portugal

* These authors contributed equally to this work

Published in *Planta* 2013 Aug; 238 (2):283-91

Author Contributions:

Cloning of VvALMT9 was done by M.M.C. and A.R. Patch-clamp analyses of VvALMT9 and AtALMT9 was performed by A.D.A. and U.B. In addition, A.D.A. conducted bioinformatics analysis and U.B. performed subcellular localization. R.F. did qRT-PCR experiments. J.Z. helped with preliminary transformation of tobacco and intracellular localization. The project was initiated and supervised by A.D.A., M.M.C. and A.R. The manuscript was written by A.D.A. and A.R.

Planta
DOI 10.1007/s00425-013-1888-y

ORIGINAL ARTICLE

# The vacuolar channel VvALMT9 mediates malate and tartrate accumulation in berries of *Vitis vinifera*

**Alexis De Angeli · Ulrike Baetz · Rita Francisco · Jingbo Zhang · Maria Manuela Chaves · Ana Regalado**

Received: 22 January 2013 / Accepted: 21 April 2013


**Abstract** *Vitis vinifera* L. represents an economically important fruit species. Grape and wine flavour is made from a complex set of compounds. The acidity of berries is a major parameter in determining grape berry quality for wine making and fruit consumption. Despite the importance of malic and tartaric acid (TA) storage and transport for grape berry acidity, no vacuolar transporter for malate or tartrate has been identified so far. Some members of the aluminium-activated malate transporter (ALMT) anion channel family from *Arabidopsis thaliana* have been shown to be involved in mediating malate fluxes across the tonoplast. Therefore, we hypothesised that a homologue of these channels could have a similar role in *V. vinifera* grape berries. We identified homologues of the Arabidopsis vacuolar anion channel AtALMT9 through a TBLASTX search on the *V. vinifera* genome database. We cloned the closest homologue of AtALMT9 from grape berry cDNA and designated it VvALMT9. The expression profile revealed that VvALMT9 is constitutively expressed in berry mesocarp tissue and that its transcription level increases during fruit maturation. Moreover, we found that VvALMT9 is targeted to the vacuolar membrane. Using patch-clamp analysis, we could show that, besides malate, VvALMT9 mediates tartrate currents which are higher than in its Arabidopsis homologue. In summary, in the present study we provide evidence that VvALMT9 is a vacuolar malate channel expressed in grape berries. Interestingly, in *V. vinifera*, a tartrate-producing plant, the permeability of the channel is apparently adjusted to TA.

**Keywords** Anion transport · Grape berry ripening · Ion channel · Malic acid · Tartaric acid · Vacuole

**Abbreviations**

| | |
|---|---|
| ALMT | Aluminium-activated malate transporter |
| MA | Malic acid |
| TA | Tartaric acid |
| SUC | Succinic acid |
| AA | L-Ascorbic acid |
| PEPC | Phosphoenolpyruvate carboxylase |
| MDH | Malate dehydrogenase |
| ME | Malic enzyme |
| AttDT | *Arabidopsis thaliana* tonoplast dicarboxylate transporter |
| DAF | Days after flowering |

## Introduction

Grape berries (*Vitis vinifera* L.) exhibit a double-sigmoid growth pattern that results from two successive periods of vacuolar swelling during which the nature of accumulated solutes changes significantly (Coombe 1992). During the first period, called green or herbaceous stage, berries accumulate mainly organic acids in the vacuole [predominantly malic acid (MA) and tartaric acid (TA)] and have a constant vacuolar pH of 2.5 (Terrier et al. 2001). At the onset of ripening (*véraison*), berries often become coloured

A. De Angeli and U. Baetz contributed equally to the work.

A. De Angeli (✉) · U. Baetz · R. Francisco · J. Zhang
Institute of Plant Biology, University of Zurich, Zollikerstr. 107, 8008 Zurich, Switzerland
e-mail: alexis.deangeli@botinst.uzh.ch; deangeli.alexis@gmail.com

R. Francisco · M. M. Chaves · A. Regalado
Instituto de Tecnologia Química e Biológica, Universidade Nova de Lisboa, Av. da República, 2780-157 Oeiras, Portugal

Published online: 05 May 2013

and start to accumulate sugars. At maturity, the concentrations of glucose and fructose may be higher than 1 M (Coombe 1976; Terrier et al. 2001). In parallel, their organic acid content decreases, whereby the vacuolar pH increases to about 3.5 (Terrier et al. 2001). Tartaric and malic acid generally account for 69–92 % of all organic acids in grape berries, and both of them reach maximal concentrations at the end of the green stage (Conde et al. 2007). However during ripening, the content of MA in berries continuously decreases, while that of TA remains constant. The acidity of berries is a major parameter determining their quality. The overall consumer appreciation is more related to the titratable acidity/sugar content than to the soluble sugars alone. Besides flavour and colour, the pH of grapes at harvest is a critical parameter for vinification. Wine pH depends on three major factors: the total amount of acids, the ratio of MA to TA and the concentration of potassium (Conde et al. 2007).

Despite their similar chemical nature, MA and TA synthesis follow different pathways. The biosynthesis of TA starts with L-ascorbic acid (AA) and is still not fully understood (Saito and Kasai 1969). The accumulation of TA resulting in high levels in mature berries suggests a strongly active metabolic pathway that may compete for AA with redox-associated functions more commonly linked to in vivo AA pools (Melino et al. 2009). In contrast, the precursor of MA is sucrose which is translocated from the leaves to the green berries. The main enzymes involved in malate synthesis (phosphoenolpyruvate carboxylase, PEPC and malate dehydrogenase, MDH) have been identified and shown to be active in grape berries (Taureilles-Saurel et al. 1995a, b; Fernie and Martinoia 2009; Sweetman et al. 2009). Instead, the decrease in acid content during grape berry ripening has been mainly associated with mitochondrial malate oxidation, most likely by malic enzyme (ME) (Kanellis and Roubelakis-Angelakis 1993).

Tonoplast transporters of MA and dicarboxylic acids have long been sought given the imperative vacuolar storage of these compounds. Emmerlich et al. (2003) identified the *Arabidopsis thaliana* tonoplast dicarboxylate transporter (*At*tDT) in mesophyll cells at the molecular level. Subsequently, members of the aluminium-activated malate transporter (ALMT) gene family (*A. thaliana* ALMT9 and 6) were identified to encode vacuolar malate channels in mesophyll and guard cells (Kovermann et al. 2007; Meyer et al. 2011).

The amount of MA and TA has a fundamental impact on grape berry quality for the wine-making industry (Conde et al. 2007). Despite the importance of MA and TA transport processes in grape berries, no vacuolar transporter for malate has been identified in *V. vinifera* until now and to the best of our knowledge no tartrate transporter/channel has been reported in plants. Therefore, in the present work we tried to fill this lack of information aiming at identifying a malate/tartrate transporter in *V. vinifera*. We hypothesised that an *At*ALMT9 homologue could code for a vacuolar malate/tartrate channel in grape berries. Here, we describe the cloning and characterisation of a grape berry ALMT (*V. vinifera* ALMT). We identify VvALMT9 and show that it is able to mediate malate and tartrate accumulation in the vacuole of grape berries.

## Materials and methods

### Plant material

Berry samples (*V. vinifera* cv. Aragonez) were collected from an experimental plot at the commercial vineyard Monte dos Seis Reis (South of Portugal, Estremoz, Portugal). Berries were collected during the summer season of 2007 in pre-*véraison* (49DAF), *véraison* (68DAF), maturation (81 DAF) and full maturation stage (97 DAF). Collected berries were immediately frozen in liquid nitrogen and stored at −80 °C before usage.

### Molecular cloning of VvALMT9

Total RNA was extracted from mature mesocarp (pulp) tissues using the method of Reid et al. (2006). Mesocarp tissue was ground in liquid nitrogen to a fine powder and immediately added to pre-warmed RNA extraction buffer. RNA was purified using the RNeasy kit (Qiagen) in the presence of DNaseI according to manufacturer's instructions (RNase-Free DNase Set; Qiagen). Full-length cDNAs were synthesised using RT included in the LongRange 2Step RT-PCR kit (Qiagen) according to the manufacturer's instructions. VvALMT9 full-length cDNA was amplified using the high fidelity DNA polymerase Phusion™ (Finnzymes). The resulting PCR product was cloned into pDONR™ 221 as entry vector and pH7FWG2™ as destination vector (Gateway® Technology, Invitrogen).

### Phylogenetic analysis

The *V.vinifera* genome (http://www.cns.fr/spip/Vitis-vinifera-e.html), phytozome (http://www.phytozome.net) and the National Center for Biotechnology Information (NCBI; http://www.ncbi.nlm.nih.gov/) databases were screened using *At*ALMT9 (At3g18440) as query to find homologous grapevine sequences. Multiple sequence alignments were performed with the ClustalW algorithm (http://align.genome.jp/) using default parameters (Thompson et al. 1994). The phylogenetic analysis was performed with the phylogeny software (http://www.phylogeny.fr).

### Overexpression of VvALMT9-GFP and AtALMT9-GFP in *Nicotiana benthamiana*

For transient overexpression (Kovermann et al. 2007) of VvALMT9-GFP and AtALMT9-GFP, the cDNA was cloned into pH7FWG2™ or the pART27 vector, respectively. The *Agrobacterium*-mediated infiltration of *N. benthamiana* leaves was performed as described with slight modifications (Holsters et al. 1980). After *Agrobacterium*-mediated infiltration, tobacco plants were grown in the greenhouse (16 h light/8 h dark, 25 °C). 2–3 days after the *Agrobacterium*-mediated infiltration, the transformed leaves were used to extract protoplasts and vacuoles for confocal microscopy and patch-clamp experiments. *N. benthamiana* seeds were derived from own stocks.

### Intracellular localisation of VvALMT9-GFP

Protoplasts and vacuoles of *N. benthamiana* leaves overexpressing VvALMT9-GFP were isolated as described for patch-clamp experiments. Microscopy was conducted using a Leica DMIRE2 (http://www.leica-microsystems.com) laser scanning microscope. The microscope was equipped with a 63× glycerol objective. For image acquisition, the appropriate Leica confocal software was used. GFP fluorescence was imaged at an excitation wavelength of 488 nm, and the emission signal was detected between 500 and 530 nm.

### Gene expression of VvALMTs

Total RNA was extracted from 150 mg grape berry pulp (mesocarp) using the RNeasy Plant Mini Kit (Qiagen) following the manufacturer's instructions. An on-column DNase I digestion step was included. Total RNA (1 µg) was reverse transcribed using M-MLV reverse transcriptase (Promega) and oligo (dT) priming. Transcript levels were determined by quantitative real-time PCR using the 7500 Fast Real-Time PCR System (Applied Biosystems) with the 7500 Software version 2.0.4. Reactions were performed in a final volume of 20 µL with 5 µL cDNA (diluted 1:10), 0.25 µM gene-specific primers and 10 µL SYBR Green PCR Master Mix (Applied Biosystems). Reaction conditions for the thermal cycling were as follows: after enzyme activation at 95 °C for 10 min, amplification was carried out in a two-step PCR procedure with 40 cycles of 15 s at 95 °C for denaturation and 1 min at 60 °C for annealing/extension. All reactions were performed in technical triplicates of three biological replicates. Gene primer sequences used in the qRT-PCR analyses were as follows: VvALMT5 forward 5′-GAGT GCCAGCTCCTTGTCTT-3′, VvALMT5 reverse 5′-TTT TGGAGCTGGAAGGTCCG-3′; VvALMT6 forward 5′-G AAACAATCCCCTTGGCCCT-3‘, VvALMT6 reverse 5′-A CATTTTGGAGCCTGGCAAC-3‘; VvALMT9 forward 5′-T GAATTTGTTGCGAGGCTTCA-3′, VvALMT9 reverse 5′-CACCTGCGCAATCTTGTTCC-3′; VvALMT13 forward 5′-CCTTGCCACCTTCACTTCCT-3′, VvALMT13 reverse 5′-CACTGCAAGCTGGTCAACTG-3′. Dissociation curves were analysed to verify the specificity of each amplification reaction; the dissociation curve was obtained by heating the amplicon from 60 to 95 °C. Transcript levels were calculated using the standard curve method and normalised against the VvActin gene (GU585869) as described by (Pfaffl 2001).

### Protoplast preparation and patch-clamp recordings on isolated vacuoles

Tobacco leaves were gently scratched on the abaxial side and floated in the enzymatic solution for 30–45 min at 30 °C. The enzyme solution contained 0.3 % (w/v) cellulase R-10, 0.03 % (w/v) pectolyase Y-23, 1 mM $CaCl_2$, 500 mM sorbitol and 10 mM Mes, pH 5.3. Protoplasts were washed twice and resuspended in solution without enzymes. Vacuoles were isolated by calcium and osmotic shock. Membrane currents were recorded using the patch-clamp technique as described elsewhere (Meyer et al. 2011). Briefly, currents were recorded with an EPC10 patch-clamp amplifier (HEKA electronics) using the Patchmaster software (HEKA Electronics, Lambrecht/Pfalz, Germany). Data were analysed with the FitMaster software (HEKA electronics). Following the formation of giga seals between the patch pipette and the vacuolar membrane, the excised vacuole-side-out patches were obtained after having established the whole-vacuole configuration by pulling the pipette away from the vacuole. Pipette solutions contained 112 mM MA, 5 mM HCl and 3 mM $MgCl_2$ adjusted to pH 6.0 with 100 mM 1,3-bis[tris(hydroxymethyl)methylamino]propane (BTP). The standard bath solution contained 100 mM MA, 160 mM BTP, 3 mM $MgCl_2$ and 0.1 mM $CaCl_2$, pH 7.5. For selectivity studies, MA in the standard bath solution was replaced by equimolar amounts of TA. The osmotic pressure of all solutions was 550 mOsm adjusted with D-sorbitol. Ionic solutions bathing the vacuole were exchanged by a gravity-driven perfusion system coupled to a peristaltic pump. Current–voltage characteristics were either obtained by subtracting the current at $t = 0$ from the quasi-stationary currents (averaging the last 50 ms of the current trace) elicited by main pulses; or from the value of the tail currents (at $t = 0$) fitted by a monoexponential function. Error bars represent standard error throughout the article.

## Results

### Cloning VvALMT9, a homologue of the Arabidopsis vacuolar channel AtALMT9 from *Vitis vinifera*

Since two members of the ALMT family from *A. thaliana* (AtALMT9 and 6; Kovermann et al. 2007; Meyer et al. 2011) have been demonstrated to mediate malate fluxes across the tonoplast, we hypothesised that ALMTs could have a similar role in *V. vinifera* berries. To identify a homologue of the Arabidopsis vacuolar anion channel AtALMT9 (At3g18440; Kovermann et al. 2007), we performed a TBLASTX search on the genome database of *V. vinifera* (http://www.phytozome.net) using the cDNA of this channel as a query. The search identified five sequences displaying a significant similarity to *AtALMT9* ($e$ value $\leq 10^{-30}$). We found that the genomic sequence GSVIVG01008270001 exhibited the highest degree of similarity ($e$ value $= 10^{-161}$). We cloned the grape berry cDNA of the closest homologue of *AtALMT9* from mRNA extracted from the mesocarp of grape berries and designated it *VvALMT9* (Fig. 1). The alignment of the cloned cDNA sequence with the Vitis genome revealed that the *VvALMT9* gene consisted of six exons coding for a protein of 588 amino acids. VvALMT9 displays a high degree of identity with AtALMT9 (64 %). To further analyse the ALMT family in *V. vinifera* we performed additionally a BLAST search on the Vitis proteome (http://www.phytozome.net) using the AtALMT9 amino acid sequence. A dendrogram based on the amino acid similarity indicates that the 13 members of the ALMT family in *V. vinifera* are grouped in three clades as in Arabidopsis (Fig. 1). Notably, even if the total number of ALMTs is similar in Arabidopsis (14 members) and Vitis (13 members), the number of members per clade is different between the two species. Clade I, to which AtALMT1 (Hoekenga et al. 2006) belongs, contains in *V. vinifera* eight members, while it includes five members in *A. thaliana*. Clade II is represented in *V. vinifera* by four members. In contrast, in *A. thaliana* clade II contains five members including AtALMT9 and 6 (Kovermann et al. 2007; Meyer et al. 2011). Interestingly, clade III incorporates only one member in *V. vinifera*, whereas in Arabidopsis there are four members, amongst them AtALMT12 (Meyer et al. 2010).

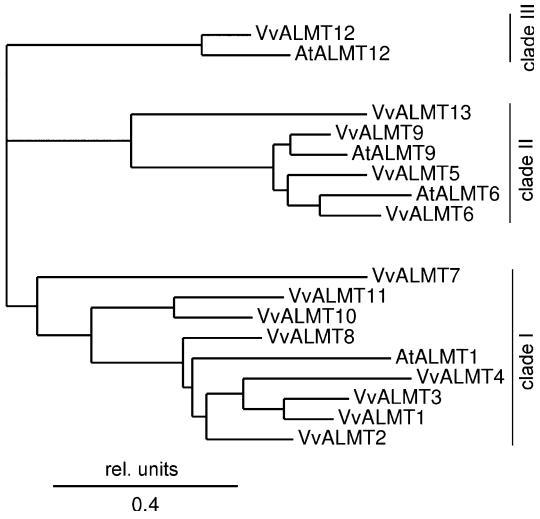


**Fig. 1** Dendrogram of the ALMT protein family in *V. vinifera*. Based on multiple amino acid sequence alignments using ClustalW (Thompson et al. 1994) the 13 members of the VvALMT protein family were classified into three main clades as in *A. thaliana*. Clade I members: VvALMT1, VvALMT2, VvALMT3, VvALMT4, VvALMT7, VvALMT8, VvALMT10 and VvALMT11 (GSVIVT01036162001, GSVIVT01037570001, GSVIVT01037569001, GSVIVT01036157001, GSVIVT01011122001, GSVIVT01011148001, GSVIVT01019627001, GSVIVT01027186001). Clade II members: VvALMT5, VvALMT6, VvALMT9 and VvALMT13 (GSVIVT01011922001, GSVIVT01011922001b, GSVIVT01008270001, GSVIVT01019447001). Clade III: VvALMT12 (GSVIVT01013184001). The ALMTs from *A. thaliana* that have been already characterised are inserted in the dendrogram. Branch lengths are given in relative units illustrating the level of occurred evolutionary change

### VvALMT9 expression levels increase during grape berry development

To elucidate whether the members of VvALMT clade II including VvALMT9 could feature physiological relevance during fruit development and maturation, we conducted expression profile analysis using quantitative real-time PCR. On that purpose, grape berry mesocarp tissue was used to extract RNA at different developmental stages of the fruit. Despite not detecting significant expression levels for VvALMT6 and marginal transcription of VvALMT13 in this tissue, the other clade members VvALMT9 and VvALMT5 were substantially transcribed in berries at all examined stages (Fig. 2). In the green phase (49 days after flowering, DAF) and at the onset of ripening (68 DAF) transcript levels of VvALMT9 were lower relative to the fully developed fruit. After induction of the ripening process (81 and 97 DAF), expression levels rose approximately four times. VvALMT13 showed generally a less pronounced expression magnitude than VvALMT9, but a similar tendency of transcriptional up-regulation during fruit development. In contrast, VvALMT5 was constantly highly expressed throughout maturation, therefore representing the prevalent member of clade II VvALMTs in grape berries. Thus, with the expression profile we demonstrate that VvALMTs are constitutively transcribed in grape mesocarp tissue. Further, VvALMT9 transcript levels experience a marked increase throughout the ripening process. Altogether, these results suggest that clade II VvALMTs might be involved in grape berry maturation.

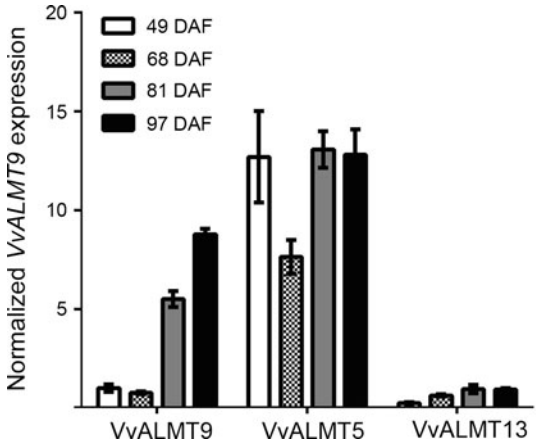


**Fig. 2** Quantitative real-time PCR expression profile of VvALMTs in grape berry mesocarp. Displayed are expression profiles of VvALMT9, VvALMT5 and VvALMT13 in mesocarp tissue during fruit development and ripening (49–97 days after flowering, DAF). VvActin (GU585869) served as a reference gene. Relative expression levels of VvALMTs were normalised to VvALMT9 at 49 DAF. Results represent the mean ± standard deviation (SD) of three biological replicates

## VvALMT9 is localised in the tonoplast

To investigate the subcellular localisation of VvALMT9, we generated a construct encoding the VvALMT9 protein with a C-terminal GFP fusion in pH7FWG2 (Gateway® Technology, Invitrogen). Subsequently, we transiently expressed VvALMT9 in *N. benthamiana* leaves by agro-infiltration (Holsters et al. 1980). Confocal laser scanning microscopy analysis of vacuoles extracted from lysed protoplasts of transiently transformed tobacco leaves allowed localising VvALMT9-GFP in the tonoplast (Fig. 3a). These data indicate that VvALMT9 is targeted to the vacuolar membrane as its counterpart in Arabidopsis.

## VvALMT9 is an ionic channel mediating malate currents

The localisation of VvALMT9 in the tonoplast allowed using the patch-clamp technique to characterise the properties of the putative ion channel. Electrophysiological experiments were conducted on vacuoles obtained from *N. benthamiana* protoplasts transiently transformed with the VvALMT9-GFP construct. Vacuoles expressing VvALMT9-GFP were selected by their fluorescence signal under the microscope and chosen for patch-clamp experiments in excised cytosolic-side-out configuration (i.e. with the cytosolic side of the membrane exposed to the bath solution). As a first step we compared the currents that could be measured in vacuoles from excised patches from non-transformed and transformed cells (Fig. 3b). We found that in symmetric malate concentrations (100 mM $malate^{2-}_{cyt}$ and 100 mM $malate^{2-}_{vac}$), patches from

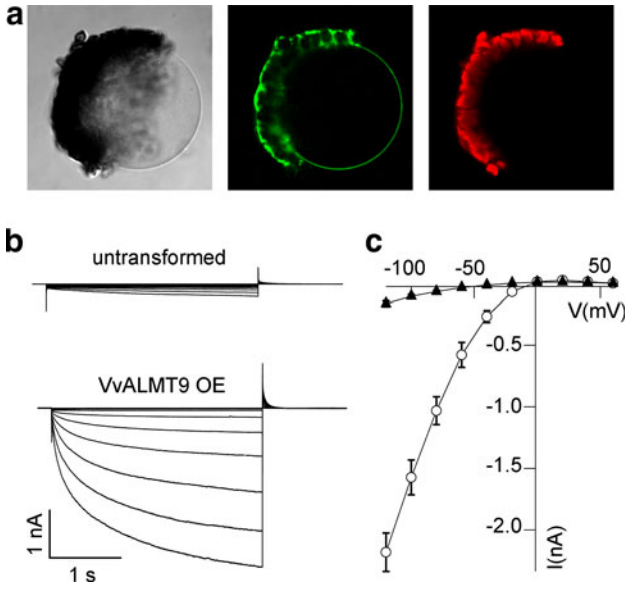


**Fig. 3** Intracellular localisation and anion conductivity of VvALMT9-GFP. **a** Transmission, GFP fluorescence and chlorophyll autofluorescence images showing the tonoplastic localisation of VvALMT9-GFP in an isolated vacuole after lysis of *N. benthamiana* protoplasts which transiently overexpressed VvALMT9-GFP. **b** Representative malate current recordings of non-transformed and VvALMT9-GFP overexpressing vacuoles obtained from patches in excised cytosolic-side-out configuration. Currents were elicited with 3 s voltage pulses ranging from +60 to −120 mV in −20 mV steps followed by a 1.5 s tail pulse at +60 mV. The holding potential was +60 mV. **c** Mean current–voltage relationships of vacuolar patches of non-transformed (*filled triangles*; $n = 4$) and VvALMT9-GFP over-expressing (*open circles*; $n = 7$) protoplasts in symmetrical malate conditions $\left(100\,\text{mM}\ malate^{2-}_{cyt}/100\,\text{mM}\ malate^{2-}_{vac}\right)$. *Error bars* represent ±SE

fluorescent vacuoles displayed a voltage-dependent inward current with a time of half activation of $t_{1/2} = 290 \pm 20$ ms reminiscent of the currents observed in AtALMT9 and AtALMT6 overexpressing vacuoles (Kovermann et al. 2007; Meyer et al. 2011). In patches of transformed vacuoles, we measured current amplitudes of $-1.6 \pm 0.2$ nA, while in patches from non-transformed vacuoles the detected amplitudes were $-0.10 \pm 0.01$ nA at −100 mV (Fig. 3c). The ten times higher currents found in patches from transiently transformed vacuoles indicate that VvALMT9 is able to mediate ionic currents across the tonoplast. To verify whether the currents observed in VvALMT9 transformed vacuoles are mediated by malate, we switched the cytosolic side solution from 100 mM $malate^{2-}_{cyt}$ to 10 mM $malate^{2-}_{cyt}$ and followed the reversal potential and the change in current amplitude (Fig. 4). During the exchange of the cytosolic side solution, the currents mediated by VvALMT9 decreased from $-1.6 \pm 0.2$ nA in 100 mM $malate^{2-}_{cyt}$ to $-0.19 \pm 0.09$ nA in 10 mM $malate^{2-}_{cyt}$ at −100 mV (Fig. 4b). In 100 mM $malate^{2-}_{cyt}$ and

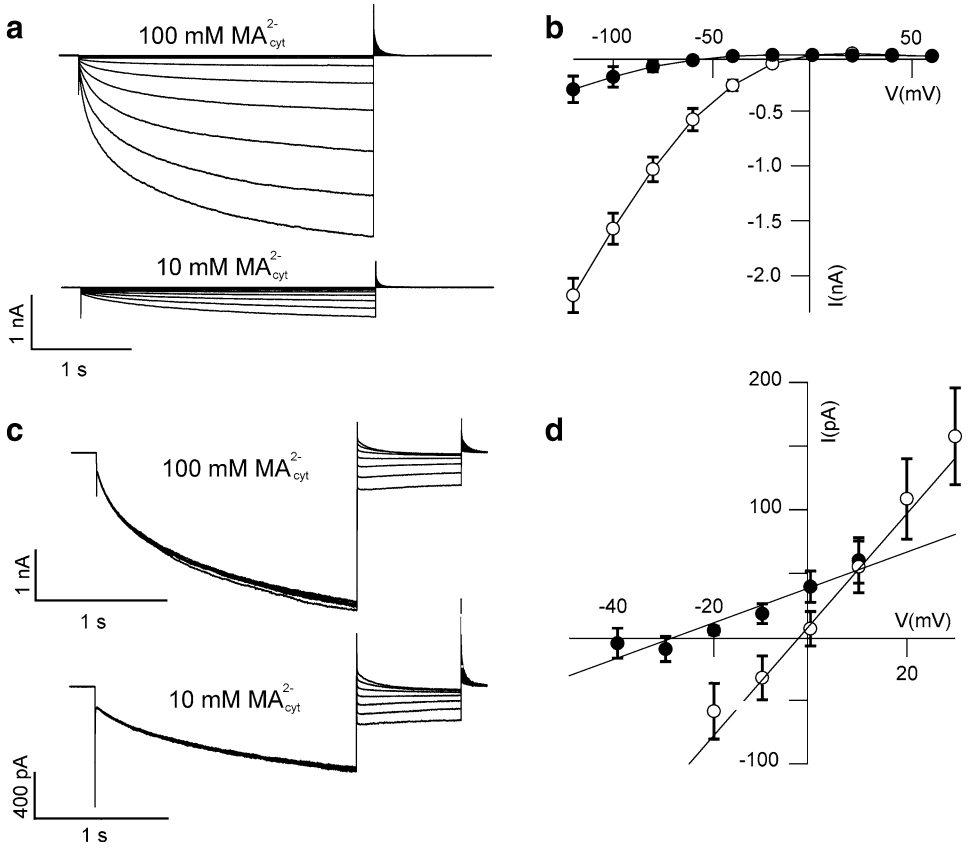


**Fig. 4** Analysis of malate inward fluxes across the tonoplast mediated by VvALMT9. **a** Representative current traces measured in excised cytosolic-side-out patches of VvALMT9-overexpressing vacuoles in the presence of 100 mM cytosolic malate and after the exchange to a 10 mM cytosolic malate solution at different applied membrane potentials. Currents were elicited with 3 s voltage pulses ranging from +60 to −120 mV in −20 mV steps followed by a 1.5 s tail pulse at +60 mV. The holding potential was +60 mV. **b** I–V curves comparing the voltage-dependent inward current of VvALMT9 between 100 mM (*open circles*; $n = 7$) and 10 mM (*filled circles*; $n = 7$) cytosolic malate concentrations. **c** Current traces representing the tail current of patches in 100 and 10 mM malate at the cytosolic side. Currents were elicited by an activating pre-pulse at −100 mV (2 s), followed by a series of test pulses ranging from +30 to −20 mV (100 mM $MA^{2-}_{cyt}$) and +10 to −40 mV (10 mM $MA^{2-}_{cyt}$) in −10 mV steps (1 s). The holding potential was at +60 mV. **d** Corresponding reversal potentials obtained from a linear fit of the mean current–voltage relations of instantaneous tail currents from patches of vacuoles overexpressing VvALMT9 in 100 mM (*open circles*; $n = 4$) and 10 mM malate (*filled circles*; $n = 4$) in the cytosolic bath solution. The values of the instantaneous tail currents derived from a monoexponential fit of the tail current responses. The theoretical Nernst potential of $malate^{2-}$ in 100 mM symmetrical malate conditions is $E_{Nernst}(100\,mM\,MA^{2-}_{cyt}) = 0\,mV$ and in 10 mM cytosolic $malate^{2-}$ concentrations it is $E_{Nernst}(100\,mM\,MA^{2-}_{cyt}) = -28\,mV$. *Error bars* are ±SE

10 mM $malate^{2-}_{cyt}$, the measured reversal potential was +1±1 mV and −29 ± 1 mV, respectively (Fig. 4d). In both cases, these reversal potentials approximate the Nernst potential of $malate^{2-}$ in the investigated conditions ($E_{Nernst}(100\,mM\ malate^{2-}_{cyt} = 0\,mV$ and $E_{Nernst}(100\,mM\ malate^{2-}_{cyt} = -28\,mV$). Therefore, these data show that the current observed in VvALMT9 expressing vacuoles is carried by malate.

## VvALMT9 can transport tartrate better than AtALMT9

During the green stage, grape berries accumulate large amounts of MA and TA in the vacuole. Therefore, we were interested in whether VvALMT9 is able to mediate tartrate currents beside malate currents. We conducted a parallel study of TA permeation in AtALMT9 and VvALMT9 (Fig. 5). By exchanging 100 mM $malate^{2-}_{cyt}$ with 100 mM $tartrate^{2-}_{cyt}$, we observed that both VvALMT9 and AtALMT9 expressing vacuoles could mediate tartrate currents. Referring to the malate currents, the tartrate currents had 61 ± 6 % and 48 ± 4 % of the amplitude at −100 mV in VvALMT9 and AtALMT9, respectively (Fig. 5c). Interestingly, the ratio between the currents of tartrate and malate ($I_{TA}/I_{MA}$) indicates that VvALMT9 is more conductive for tartrate than AtALMT9 (Fig. 5d). Moreover, the current ratio increases with the applied membrane potential (Fig. 5d). This slight voltage

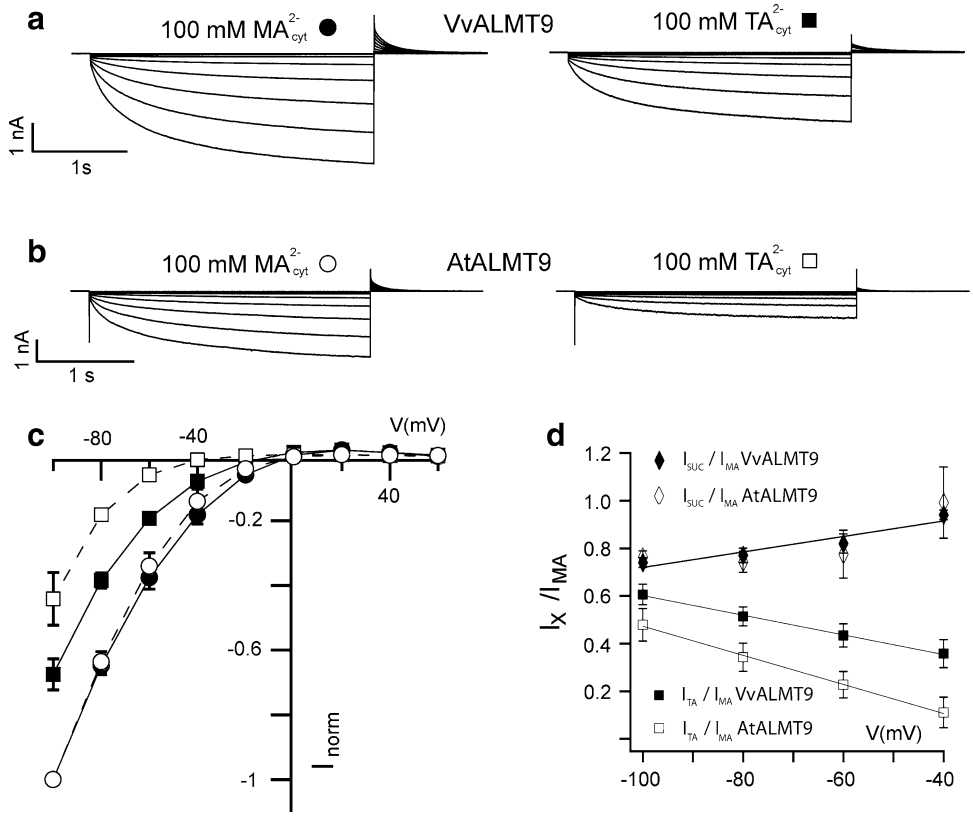


**Fig. 5** Comparison between the ion selectivity of VvALMT9 and AtALMT9 for malate and tartrate. **a, b** Representative currents recorded in the presence of 100 mM malate$^{2-}_{cyt}$ (*left traces*) and 100 mM tartrate$^{2-}_{cyt}$ (*right traces*). The cytosolic malate solution was exchanged with a tartrate solution while keeping the same patches from vacuoles overexpressing VvALMT9 (**a**) and AtALMT9 (**b**). Currents were elicited with 3 s voltage pulses ranging from +60 to −120 mV in −20 mV steps followed by a 1.5 s tail pulse at +60 mV The holding potential was +60 mV. **c** Corresponding current amplitude plots derived from excised cytosolic-side-out patches from VvALMT9 overexpressing vacuoles exposed to 100 mM malate (filled circles) and 100 mM tartrate (*filled squares*, $n = 4$), as well as from AtALMT9 overexpressing vacuoles exposed to 100 mM malate (*open circles*; $n = 4$) and 100 mM tartrate (*open squares*; $n = 4$). **d** Ratio between succinate and malate currents mediated by ALMT9 of *V. vinifera* (*filled diamonds*) and *A. thaliana* (*open diamonds*) and ratio between tartrate and malate currents mediated by ALMT9 of *V. vinifera* (*filled squares*) and *A. thaliana* (*open squares*) plotted as a function of the applied membrane potential. *Error bars* denote ±SE

dependency of the $I_{TA}/I_{MA}$ ratio is more pronounced in AtALMT9 than in VvALMT9 (in Fig. 5d the slope of the fitted line is 0.004 $mV^{-1}$ for VvALMT9 and 0.006 $mV^{-1}$ for AtALMT9). Notably, we illustrate in an equally conducted set of experiments that when exchanging from 100 mM malate$^{2-}_{cyt}$ to 100 mM succinate$^{2-}_{cyt}$ that this dicarboxylic acid is likewise transported by VvALMT9 and AtALMT9 (Fig. 5d). The succinate currents were 76 ± 2 and 74 ± 3 % of the currents in malate in VvALMT9 and AtALMT9 at −100 mV, respectively. This indicates that the permeability of succinic acid is identical between the homologous channels of Arabidopsis and *V. vinifera*. In summary, the data show that both VvALMT9 as well as AtALMT9 are slightly less permeable for tartrate than for malate and succinate. Nonetheless, the ratio $I_{TA}/I_{MA}$ provides evidence that VvALMT9 conducts tartrate ions better than AtALMT9. Taken together, these results indicate that both, MA and TA, can be transported in the vacuoles of *V. vinifera* berries through VvALMT9. Hence, VvAtLMT9 is the first malate and tartrate channel identified so far in grape berries.

## Discussion

In *V. vinifera*, the accumulation of organic acids in the vacuole is involved in berry development and has a great impact on the final quality of grapes from an agronomical point of view. In this species, the data on the vacuolar transporters involved in the accumulation of MA and TA in berry vacuoles are scarce and no information is available concerning their molecular identity. Based on previous studies in *A. thaliana* (Kovermann et al. 2007; Meyer et al. 2011), we hypothesised that members of the ALMT family

could be involved in the vacuolar accumulation of MA and TA in *V. vinifera* berries. In a preliminary phylogenetic analysis, we found that 13 members of the ALMT family can be identified in the *V. vinifera* genome (Fig. 1). The 13 VvALMTs cluster in three clades that correspond to the clades previously described in Arabidopsis (Kovermann et al. 2007). However, the number of members per clade is different between the two species with clade I being overrepresented and clade III harbouring a single member in *V. vinifera* (Fig. 1). Instead, clade II to which VvALMT9 belongs is represented by a similar number of members in grapevine (Kovermann et al. 2007). We found that when transiently expressed in tobacco leaves, VvALMT9-GFP is localised in the tonoplast as AtALMT9-GFP (Fig. 3a). Further electrophysiological analysis on excised cytosolic-side-out patches of vacuoles obtained from transiently transformed tobacco protoplasts allowed us to demonstrate that VvALMT9 was able to mediate an inward rectifying malate and tartrate current facilitating the accumulation of these dicarboxylic acids in the vacuoles of grape berries (Figs. 4, 5). The comparison between the substrate selectivity properties of VvALMT9 and AtALMT9 reveals that VvALMT9, like AtALMT9, transports malate and succinate better than tartrate (Fig. 5). Nonetheless, VvALMT9 is able to catalyse the transport of TA more efficiently than AtALMT9, which is in contrast to the transport of succinic acid, a metabolic intermediate which is not accumulated substantially in grape berries. This functional difference between the two homologous proteins is intriguing since grape berries are one of the few fruits accumulating significant amounts of TA (Saito and Kasai 1968).

The extremely acidic pH values found in grape vacuoles in the green stage ($\sim$2.5) allow the accumulation of MA and TA via a passive transport system like an anion channel. Indeed, at this pH 99 % of MA and TA are in the fully protonated or monovalent form ($pK_A^{1,MA} = 3.40$, $pK_A^{2,MA} = 5.11$, $pK_A^{1,TA} = 2.98$, $pK_A^{2,TA} = 4.34$; Weast and Astle 1982–1983). The ALMTs are known to mediate only the transport of the divalent form of dicarboxylic acids (Meyer et al. 2011). Hence, in grape berries TA and MA can be taken up from the neutral cytosol across the tonoplast as divalent anions ($MA^{2-}$ and $TA^{2-}$). Once in the vacuole at pH 2.5, these acids become neutral or monovalent which prevents the conduction by anion channels back to the cytosol. This mechanism, known as ion trapping (Briggs et al. 1987), facilitates loading of grape berry vacuoles with MA and TA (Fig. 6). The unidirectional acid flux might explain the requirement of less anion channels during the green stage compared to the mature grape berry as represented by lower expression levels of VvALMT9 (Fig. 2). The decline in vacuolar acidity observed

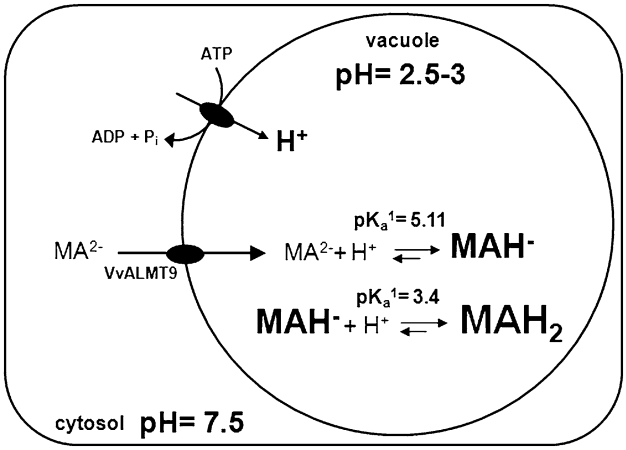


**Fig. 6** The ion-trapping mechanism results in vacuolar malate accumulation in grape berries. In the cytosol at pH 7.5, MA is present in its fully deprotonated divalent form malate$^{2-}$ ($MA^{2-}$). $MA^{2-}$ can be transported by the inward rectifier VvALMT9 into the vacuole. Once in the extremely acidic vacuole of grape berries (pH = 2.5–3), $MA^{2-}$ becomes protonated and accumulates mainly as $MAH_2$ or in the monovalent form, $MAH^-$. Both forms of MA are not permeable through ALMTs and thus they are trapped in the vacuolar lumen. The unidirectional flux of malate forms the basic principle of its vacuolar accumulation to high levels. Tartaric acid can be accumulated in the vacuole by the same ion-trapping mechanism since the acidity constants are $pK_A^{1,TA} = 2.98$ and $pK_A^{2,TA} = 4.34$

systematically during grape berry ripening was shown to be accompanied by an increase in tonoplast passive diffusion (Terrier et al. 2001). The up-regulation of global VvALMT expression could consequently be a counteraction for excessive MA and TA decompartementation through anion leakage. Similarly, the rise of mRNA and protein abundance of both vacuolar proton pumps in grape berries during maturation was suggested to partly compensate for passive permeability of the tonoplast (Terrier et al. 2001). A second explanation for the transcriptional up-regulation of VvALMT9 could be an involvement in releasing organic acids from the vacuole during maturation. In late stages of ripening, the vacuolar pH rises to 3.5–4. Under these conditions, a minor proportion of the vacuolar MA would dissociate into the divalent form ($MA^{2-}$) and be a substrate of VvALMT9. It is therefore possible that the channel catalyses the release of $MA^{2-}$ from the vacuole to the cytosol at this particular phase of development. However, although we cannot exclude this second hypothesis per se, our data demonstrate that anion fluxes mediated by VvALMT9 are directed into the vacuole, thus supporting a role of VvALMT9 in counteracting excessive organic acid decompartementation during maturation.

In conclusion, in the present work we provide evidence that malate and tartrate can be accumulated in the vacuoles of *V. vinifera* berries by VvALMT9. Hence, the present findings represent a step towards understanding

carboxylate metabolism and storage in grapes which are crucial factors impacting wine quality and production.

**Acknowledgments** We would like to thank Prof. Enrico Martinoia (University of Zurich, Switzerland) for his scientific support and helpful discussions, Dr. Stefan Meyer (University of Zurich, Switzerland) for discussions, Dr. Nelson Saibo (Genomics of Plant Stress Laboratory–ITQB, Universidade Nova de Lisboa, Portugal) for kindly providing the cloning vectors and Duarte Figueiredo (Genomics of Plant Stress Laboratory–ITQB, Universidade Nova de Lisboa), Tânia Serra (Genomics of Plant Stress Laboratory–ITQB, Universidade Nova de Lisboa) and André Cordeiro (Genomics of Plant Stress Laboratory–ITQB, Universidade Nova de Lisboa) for technical support with the preliminary *Nicotiana* agroinfiltration experiments. AR and RF acknowledge FCT for the financial support through fellow FRH/BPD/34986/2007 and SFRH/BPD/74210/2010, respectively. AD was supported by a long-term EMBO fellowship (ALTF 87-2009), JZ by the Chinese Scholarship Council and UB by the Swiss National Foundation (31003A_141090/1).

## References

Briggs GG, Rigitano RLO, Bromilow RH (1987) Physico-chemical factors affecting uptake by roots and translocation to shoots of weak acids in barley. Pestic Sci 19:101–112

Conde C, Silva P, Fontes N, Dias ACP, Tavares RM, Sousa MJ, Agasse A, Delrot S, Geros H (2007) Biochemical changes throughout grape berry development and fruit and wine quality. Food 1:1–22

Coombe BG (1976) The development of fleshy fruits. Annu Rev Plant Physiol 27:207–228

Coombe BG (1992) Research on development and ripening on the grape berry. Am J Enol Vitic 43:101–110

Emmerlich V, Linka N, Reinhold T, Hurth MA, Traub M, Martinoia E, Neuhaus HE (2003) The plant homolog to the human sodium/dicarboxylic cotransporter is the vacuolar malate carrier. Proc Natl Acad Sci USA 100:11122–11126

Fernie AR, Martinoia E (2009) Malate: Jack of all trades or master of a few? Phytochemistry 70:828–832

Hoekenga OAL, Maron G, Piñeros MA, Cançado GM, Shaff J, Kobayashi Y, Ryan PR, Dong B, Delhaize E, Sasaki T, Matsumoto H, Yamamoto Y, Koyama H, Kochian LV (2006) *AtALMT1*, which encodes a malate transporter, is identified as one of several genes critical for aluminum tolerance in *Arabidopsis*. Proc Natl Acad Sci USA 103:9738–9743

Holsters M, Silva B, Van Vliet F, Genetello C, De Block M, Dhaese P, Depicker A, Inzé D, Engler G, Villarroel R (1980) The functional organization of the nopaline *A. tumefaciens* plasmid pTiC58. Plasmid 3:212–230

Kanellis AK, Roubelakis-Angelakis KA (1993) Grapes. In: Seymour GI, Taylor J, Tucker GA (eds) Biochemistry of fruit ripening. Chapman & Hall, London, pp 189–234

Kovermann P, Meyer S, Hörtensteiner S, Picco C, Scholz-Starke J, Ravera S, Lee Y, Martinoia E (2007) The Arabidopsis vacuolar malate channel is a member of the ALMT family. Plant J 52:1169–1180

Melino VJ, Soole KL, Ford CM (2009) Ascorbate metabolism and the developmental demand for tartaric and oxalic acids in ripening grape berries. BMC Plant Biol 9:145

Meyer S, Mumm P, Imes D, Endler A, Weder B, Al-Rasheid KA, Geiger D, Marten I, Martinoia E, Hedrich R (2010) *At*ALMT12 represents an R-type anion channel required for stomatal movement in Arabidopsis guard cells. Plant J 63:1054–1062

Meyer S, Scholz-Starke J, De Angeli A, Kovermann P, Burla B, Gambale F, Martinoia E (2011) Malate transport by the vacuolar AtALMT6 channel in guard cells is subject to multiple regulation. Plant J 67:247–257

Pfaffl MW (2001) A new mathematical model for relative quantification in real-time RT-PCR. Nucleic Acids Res 29(9):e45

Reid KE, Olsson N, Schlosser J, Peng F, Lund ST (2006) An optimized grapevine RNA isolation procedure and statistical determination of reference genes for real-time RT-PCR during berry development. BMC Plant Biol 6:27

Saito K, Kasai Z (1968) Accumulation of tartaric acid in the ripening process of grapes. Plant Cell Physiol 9:529–537

Saito K, Kasai Z (1969) Tartaric acid synthesis from l-ascorbic acid-1-$^{14}$C in grape berries. Phytochemistry 8:2177–2182

Sweetman C, Deluc G, Cramer GR, Ford CM, Soole KL (2009) Regulation of malate metabolism in grape berry and other developing fruits. Phytochemistry 70:1329–1344

Taureilles-Saurel C, Romieu CG, Robin JP, Flanzy C (1995a) Grape (*Vitis vinifera* L.) malate dehydrogenase. I. Intracellular compartmentationof the isoforms. Am J Enol Vitic 46:22–28

Taureilles-Saurel C, Romieu CG, Robin JP, Flanzy C (1995b) Grape (*Vitis vinifera* L.) malate dehydrogenase. II. Characterization of the major mitochondrial and cytosolic isoforms and their role in ripening. Am J Enol Vitic 46:29–36

Terrier N, Sauvage FX, Ageorges A, Romieu C (2001) Changes in acidity and in proton transport at the tonoplast of grape berries during development. Planta 213:20–28

Thompson JD, Higgins DG, Gibson TJ (1994) CLUSTAL W: improving the sensitivity of progressive multiple sequence alignment through sequence weighting, position-specific gap penalties and weight matrix choice. Nucleic Acids Res 22:4673–4680

Weast RC, Astle MJ (1982–1983) CRC Handbook of chemistry and physics. CRC Press. Boca Raton

# 7. Conclusion and Outlook

The investigation of vacuolar ALMTs started not even 10 years ago when Kovermann and coworkers showed that the *Arabidopsis thaliana* AtALMT9 is a channel that is localized in the vacuolar membrane and that is capable of mediating malate inward rectifying currents corresponding to anion uptake into the vacuole (Kovermann et al., 2007). Ever since, but in particular in the past few years during which it got for instance apparent that AtALMT9 also mediates $Cl^-$ currents (De Angeli et al., 2013b), our knowledge about this vacuolar anion channel increased rapidly and progressively. Although several studies exist nowadays about the structural organization and function of ALMT9 channels at the tonoplast of Arabidopsis and *Vitis Vinifera* (*inter alia* presented in this thesis), our knowledge is far from being saturated.

As the functions of the vacuole are diverse, also a vacuolar anion channel such as ALMT9 can fulfill multiple roles in plant physiology. In this thesis, the aim was to characterize ALMT9 channels on the molecular, structural and functional level. Taken together, I present several physiological processes in which ALMT9 proteins are involved, such as malate accumulation in grape berries (Chapter V; De Angeli et al., 2013a), and seed germination (Chapter IV) and the regulation of long-distance $Na^+$ and $Cl^-$ transport during salinity in Arabidopsis (Chapter III; Baetz et al., submitted). In addition, it has been shown that AtALMT9 is involved in stomatal opening and drought resistance (De Angeli et al., 2013b). The complexity to study and evaluate ALMT9 channel functions was even more increased with the finding that Arabidopsis AtALMT9 is composed of several subunits (Chapter I; Zhang et al., 2013) and is capable of forming multimeric complexes with other vacuolar AtALMT channels which show partially overlapping expression patterns (Chapter II).

Regarding the structural and compositional organization of AtALMT9, it will be of interest to determine the functional relevance of the capacity of homo- and heteromerization that have been presented in Chapter I and Chapter II. How many subunits contribute to forming a functional channel and what is the stoichiometry? Do

vacuolar AtALMTs interact *in planta*, and does this interaction contribute to increasing the functional diversity of AtALMT9 by changing channel properties (e.g. localization, substrate specificity, activity, regulatory mechanisms)? We have established several tools in the past years which could help to elucidate the uncertainties about vacuolar AtALMT structure and composition in future studies.

(i) Two blocking agents of AtALMT9 have been identified (Zhang et al., 2013, Zhang et al., 2014; Chapter I) that are valuable to understand whether interacting subunits form functional channels: free ATP and citrate. In patch-clamp experiments vacuolar AtALMT channels have been shown to exhibit different sensitivities to these blocking agents (Eisenach et al., unpublished), and for AtALMT9 a point-mutation has been identified that abolishes the reversible citrate inhibition (Zhang et al., 2013; Chapter I). Determining the dissociation constant of free ATP ($K_d^{ATP}$) or citrate ($K_d^{citrate}$) when co-expressing different vacuolar AtALMT channels and mutant variants could proof the functionality of heteromeric channel complexes (Zhang et al., 2013; Chapter I). In addition, these blocking agents can be used to determine the number of subunits that contribute to forming a vacuolar AtALMT channel as well as the stoichiometry by patch-clamping (MacKinnon, 1991).

(ii) The BiFC constructs are a powerful tool to investigate the electrophysiological properties of heteromeric channels in patch-clamping experiments. The BiFC constructs visualize by fluorescence the *in planta* interaction of native channels that are expressed from the same vector backbone but from individual expression cassettes. These constructs have advantages over tandem or chimeric channel constructs in which several subunits are fused in a single open reading frame. For example, in the BiFC constructs there is no need for an artificial linker between two subunits that might interfere with the channel structure and/or activity. Moreover, in order to design tandem constructs, knowing the number of subunits is of advantage, whereas the design of the BiFC constructs is independent of this information.

(iii) We generated a collection of site-directed mutations that exhibited a variety of effects on the channel activity (Zhang et al., 2013; Chapter I), ranging from inactivation, differences in rectification rates, insensitivity to citrate block, and altered malate/$Cl^-$ current ratios (Baetz et al., submitted; Chapter III; Zhang et al., 2013; Chapter I). Not all of these AtALMT9 channel variants have been examined circumstantially, and more

detailed electrophysiological analysis might contribute to further understand structure-function relations and multimerization. Besides the electrophysiological characterization of these mutants, the expression of the channel variants in *atalmt9* knock-out mutants might elucidate certain features that are important for AtALMT9 functionality *in planta*.

(iv) Several transgenic lines have been generated that might contribute to understanding the role of multiple and potentially interacting vacuolar AtALMTs: for instance promoter:GUS reporter plants of all vacuolar AtALMTs to investigate their cell-specific distribution, double knock-out mutants and an RNA interference line that targets all vacuolar AtALMTs for multiple down-regulation (Chapter III; Baetz et al., submitted). In addition, one might consider the usage of further genetic approaches such as the generation of complementation lines of *atalmt9* mutant plants with other AtALMTs (e.g. AtALMT5) in order to determine the redundancy and the capacity to functionally substitute other AtALMT channels.

With respect to the functional role of ALMT9 proteins *in planta* there are several facts that make the interpretation of results difficult, and the design of experiments challenging. First, in Arabidopsis AtALMT9 is capable of mediating malate and $Cl^-$ currents, therefore phenotypes of *atalmt9* knock-out mutants might be correlated to the lack of the one or other (or both) fluxes. Secondly, malate and $Cl^-$ have diverse roles in plants, e.g. they serve as important osmotically active solutes, but $Cl^-$ can be toxic if accumulated to high concentrations in the cytosol (Teakle and Tyerman, 2010). Thus, it is difficult to dissect for instance during salinity whether an anion channel such as ALMT9 is involved in counteracting ion toxicity in the cytosol by vacuolar sequestration of $Cl^-$, or whether it is involved in maintaining $Cl^-$ uptake that is crucial for osmotic adjustment. Thirdly, ALMT9 channels are expressed in different plant species and in a variety of tissues and organs (*inter alia* in guard cells, mesophyll cells, and the vasculature of shoots and roots in Arabidopsis and in fruits of Vitis) in which the function of the anion channel might differ. The three physiological studies presented in this thesis (Chapter III to V) represent this diversity and specificity of the functions of ALMT9 proteins.

(i) The *Vitis Vinifera* homolog, VvALMT9, is expressed in the mesocarp of fruits throughout development, and has been shown to mediate malate and tartrate uptake into the vacuole (Chapter V). Since grape berries accumulate these two organic acids to high concentrations during berry ripening and maturation (Terrier et al., 2001, Conde et al., 2007), the predominant function of the channel is supposedly to catalyze their uptake. Although it has not been investigated whether VvALMT9 is capable of mediating $Cl^-$ uptake, in this developmental stage/ tissue, a putative VvALMT9-mediated vacuolar $Cl^-$ uptake might be less relevant. The accumulation of organic acids does not only have the purpose of maintaining the osmotic homeostasis in fruits. In particular, malate and tartrate accumulation determines the acidity, taste and quality of the berry (Terrier et al., 2001, Conde et al., 2007), pointing towards a substrate-specific transport role of VvALMT9 in fruits of Vitis, and to a lesser extend towards an implementation in osmotic adjustment.

(ii) In Arabidopsis AtALMT9 is highly expressed in seeds, and *atalmt9* knock-out mutants show reduced germination rates during salinity (Chapter IV). The fact that these mutants exhibit slightly delayed germination rates under control conditions in which $Cl^-$ concentrations are low in the external medium, and the fact that the reduced germination rate of *atalmt9* is dramatically magnified when using high NaCl concentrations, suggest a role of AtALMT9 in keeping vacuolar solute uptake that drives water influx into the seed. Hence, in this tissue AtALMT9 could possibly have a crucial function in osmotic homeostasis by mediating $Cl^-$ accumulation. Similarly, in guard cells AtALMT9 has been shown to mediate $Cl^-$ fluxes across the tonoplast that are fundamental for volume control of vacuoles, thereby allowing stomatal movement (De Angeli et al., 2013b).

(iii) In response to salt stress, the role of AtALMT9 in the vascular tissue of Arabidopsis might be the regulation of vacuolar $Cl^-$ uptake in order to modulate ion-specific signals in the cytosol and salinity adaptation mechanisms (Chapter III; Baetz et al., submitted). AtALMT9 is highly expressed in the vascular system of roots and shoots, and *atalmt9* mutants have altered long-distance $Na^+$ and $Cl^-$ transport during salinity. In addition, a plasma-membrane localized $Na^+$ transporter crucial for ionic tolerance through shoot $Na^+$ exclusion exhibits differential expression in *atalmt9* plants in the root vasculature.

The altered expression levels might be initiated by a disturbed intracellular homeostasis of toxic ions during salinity, rather than by an impaired osmotic status in stelar cells.

In summary, the studies on the role of ALMT9 proteins suggest that in Arabidopsis the physiological function of the channel is correlated to *in vivo* $Cl^-$ transport, whereas in berries of Vitis the VvALMT9 homolog might function predominantly as organic acid (malate and tartrate) channel. In addition, the data suggest that dependent on the ALMT homolog, the tissue and the environmental condition, the purpose of vacuolar anion fluxes might be either osmotic adjustment (e.g. rapid solute uptake during seed germination) or specific for the ion species (e.g. malate accumulation by the acid trap mechanism in fruits).

Again, we have established tools that might help in future research to better understand this complex functionality of ALMT9 homologs. Two transgenic complementation lines should be mentioned which have been characterized and successfully used to unravel the physiological basis behind the phenotype of *atalmt9* mutants (Chapter III; Baetz et al., submitted). Firstly, a guard-cell-specific complementation line of *atalmt9* has been generated. This tool can be used to dissect if phenotypes are dependent on the expression of AtALMT9 in guard cells and on stomatal conductance and transpiration. And secondly, a point-mutated AtALMT9 channel variant ($AtALMT9_{E196A}$) has been identified that specifically enhances $Cl^-$ conductivity without altering the permeation of malate. Expressing this mutant channel in the genetic background of *atalmt9* assists to dissect the relative relevance of AtALMT9-mediated malate versus $Cl^-$ fluxes in distinct physiological functions.

Besides genetic approaches, sophisticated experimental designs might unravel the physiological basis of AtALMT9 functions. For instance, using different ion compositions in future germination assays such as KCl, $NaNO_3$ or sorbitol can be valuable to dissect whether the ionic or osmotic stress of salinity impairs seed germination in *atalmt9* mutants. Another set of experiments has been conducted to determine the predominant substrate of AtALMT9 in guard cells. The usage of different KCl concentrations in stomatal opening buffers in epidermal peel assays contributed to conclude that particularly AtALMT9-mediated $Cl^-$ fluxes are crucial for stomatal opening (De Angeli et al., 2013b).

Regarding the preferential substrates of homologous ALMT9 channels in Arabidopsis and Vitis, sequence analysis, site-directed mutagenesis and patch-clamp studies might uncover residues or domains that are crucial for determining the substrate permeability and specificity.

Taken together, the results presented in this thesis provide fundamental insights into the structure and composition of AtALMT9 and demonstrates that the ALMT9 anion channels of Arabidopsis and Vitis are expressed in various tissues and organs in which the proteins fulfill distinct physiological functions. Moreover, in this thesis I provide evidence that vacuolar ion uptake is crucial to regulate tissue ion accumulation and distribution during salt stress, demonstrating that vacuolar channels such as AtALMT9 not just impact ion fluxes at the cellular level, but also whole-plant ion movement. The foundation to further explore these anion channels is given by several electrophysiological and genetic tools that have been established during the period of my PhD. Through the two physiologically relevant substrates (malate and $Cl^-$) as well as based on the broad expression pattern, ALMT9 channels will provide also in future research a rich source for studying vacuolar function in different plant species.

# 8. Appendix

## Vacuolar proton pumping: more than the sum of its parts?

Cornelia Eisenach, Ulrike Baetz and Enrico Martinoia

Department of Plant and Microbial Biology, University of Zurich, 8008 Zurich, Switzerland

Corresponding author: Dr. Cornelia Eisenach

Published in *Trends of Plant Science* 2014 June; 19 (6):344-346

Spotlight

CellPress

# Vacuolar proton pumping: more than the sum of its parts?

**Cornelia Eisenach, Ulrike Baetz, and Enrico Martinoia**

Institute of Plant Biology, University of Zürich, Zollikerstrasse 107, CH-8008 Zürich, Switzerland

**Petunia flower colour is dependent on vacuolar pH and is therefore used to study acidification mechanisms. Recently, it was shown that the concerted action of two tonoplast-localised $P_3$-ATPases is required to hyperacidify vacuoles of petunia petal epidermis cells. Here we discuss how steep cross-tonoplast pH gradients may be established in specific cells.**

The acidity of plant vacuoles varies between plant species, organs, and cell types. In morning glory (*Ipomoea tricolor*), when the slightly acidic vacuoles of flowers become neutral, a shift from a purple to the characteristic blue flower colour can be observed. By contrast, petal epidermis cells of petunia (*Petunia hybrida*) contain acidic vacuoles with a pH around 5, which causes the colour-giving anthocyanins in the vacuoles to appear red. In CAM plants or fruits such as lemon (*Citrus)* or non-ripe grape berries (*Vitis*) the vacuolar pH can reach values as low as 2 or 3. Two types of proton pumps, a $H^+$-ATPase and a $H^+$-PPase have originally been shown to reside at the vacuolar membrane [1]. Besides acidification of the vacuolar lumen, proton pumping also generates a transmembrane gradient in electric potential, $\Delta E_m$. Both gradients, ΔpH and the $\Delta E_m$, are exploited to accumulate solutes within the vacuole. While $\Delta E_m$ regulates channels that mediate vacuolar ion uptake, ΔpH drives cation/proton, anion/proton and sugar/proton antiporters [2]. Besides its role in vacuolar acidification, the V-PPase also functions during postembryonic heterotrophic growth through hydrolysing inorganic pyrophosphate ($PP_i$) to reduce $PP_i$ contents and support gluconeogenesis [3]. Until recently it was thought that V-ATPases and V-PPases at the tonoplast are exclusively responsible for generating the vacuolar pH. However, recent studies comparing the pH of a vacuolar V-ATPase double mutant (*vha-a2*/*vha-a3*) with that of a V-PPase mutant suggested that yet another component was involved in the generation of vacuolar pH [4]. Possibly, the activity of a trans-Golgi network/early endosomes V-ATPase also contributes to vacuolar acidification.

## Petunia flowers can be used to study vacuolar acidification processes

Petunia (*Petunia hybrida*) flowers are an ideal model system to study vacuolar pH and the genes and proteins involved in its generation. Anthocyanins accumulate in the vacuole of flower petal cells, and the colour of these anthocyanins is dependent on–among other factors–vacuolar pH. In petunia a shift in vacuolar pH causes a change in flower colour. Mutants that display a flower colour different to the red-flowering wild type are a useful tool to analyse gene function in vacuolar pH maintenance. Overall, seven pH-mutants defective in petunia flower colour and pH have been identified and termed *ph1* to *ph7* [5].

Within the past decade the team led by Francesca Quattrocchio at Amsterdam University has been successful in identifying several genes that are affected in the respective mutants, using transposon-tagging strategies. Some of the genes such as *PH3*, *PH4* and *PH6* are transcriptional regulators. In 2008 the team identified the mutant *ph5* to be defective in a gene encoding a proton pump [5]. PH5 localises to the tonoplast and belongs to the $H^+$-$P_{3A}$-ATPase subfamily, which finds homologs in the AHA family of *Arabidopsis* (*Arabidopsis thaliana*) plasma membrane $H^+$-ATPases. Three lines of evidence led the researchers to conclude that PH5 is responsible for the transport of protons into the vacuole: (i) PH5 expression was able to rescue a yeast mutant unable to grow on acidic medium; (ii) the difference in flower colour in *ph5* mutants was not caused by altered anthocyanin accumulation; and (iii) over-expression of a PH5 transgene in a *ph5* mutant background rescued the mutants' petal pH and colour phenotype. Interestingly, PH5 overexpression in the background of other pH-mutants such as those of the transcriptional regulators *ph3*, *ph4* and *ph6* could not rescue the pH and flower colour phenotype of those mutants. Considering that *PH5* expression is regulated by *PH3*, *PH4* and *PH6*, the authors reasoned that these regulators may control yet another component, which, in addition to PH5, was necessary for vacuolar acidification.

## The $P_{3B}$-ATPase, PH1, is the second component required to rescue petunia pH-mutants

In a recent study the Quattrocchio group reports the identification of PH1 as an interactor of PH5, necessary for hyperacidification of petal vacuoles [6]. They obtained a transposon-tagged *ph1* mutant line and were able to identify the gene-sequence associated with *ph1* to code for a $P_{3B}$-ATPase. Evidence from procaryots suggests that ATPases of this type are involved in $Mg^{2+}$ uptake.

A first indication that PH1 was the missing component in PH5-driven vacuolar acidification came from gene expression analysis. *PH1* mRNA expression paralleled that of *PH5* in a spatio temporal manner. Like *PH5*, mRNA expression of *PH1* was under the control of the transcription factors *PH3* and *PH4* and the transcriptional regulators *PH6* and *AN11*. While a *35S*-driven *PH5*-GFP

*Corresponding author:* Eisenach, C. (cornelia.eisenach@botinst.uzh.ch).

1360-1385/
 http://dx.doi.org/10.1016/j.tplants.2014.03.008

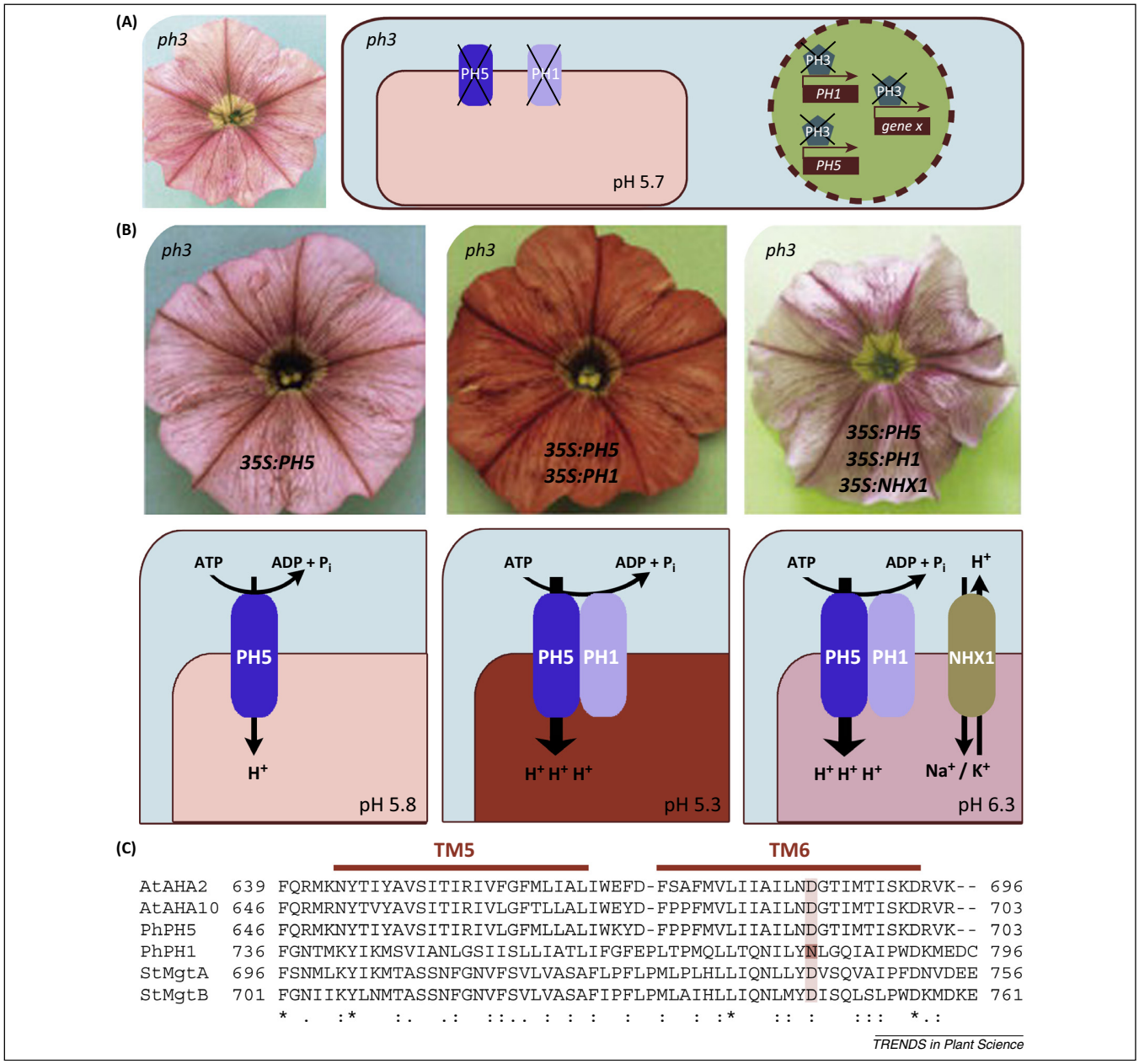


**Figure 1**. Petunia flower colour and pH phenotype of the *ph3* mutant is restored by the constitutive co expression of the P-ATPases PH1 and PH5. **(A)** In the *ph3* mutant PH3-regulated genes such as *PH1* and *PH5* are not expressed, resulting in a pale-rosé flower phenotype and an increase in vacuolar pH compared to wild type petunia flowers. **(B)** The flower and vacuolar pH phenotype of *ph3* mutants is only rescued when 35S:PH1 and 35S:PH5 are co-expressed. The additional introduction of the $Na^+/H^+$ and $K^+/H^+$ antiporter NHX1 restores the *ph3* mutant phenotype. Reproduced, with permission, and modified from [6]. **(C)** Multiple protein sequence alignment of the putative transmembrane domain (TM) 5 and 6 of AtAHA2 according to the UniProt database including the conserved aspartate residue (D684 in AtAHA2) between the *Arabidopsis thaliana* AHA2 and AHA10 (homolog of PH5), PH5 and PH1 of *Petunia hybrida*, and the bacterial $P_{3B}$-ATPases, MgtA and MgtB of *Salmonella typhimurium*. Asterices indicate sequence identity, dots the degree of similarity. The alignment was performed using ClustalW.

construct localised to the tonoplast in the petal epidermis of petunia, only an internally GFP-tagged *35S:PH1-GFPi* construct localised to the tonoplast.

In light of the facts that PH1 and PH5 both encode $P_3$-ATPases, are both under parallel transcriptional control, and overlap in their intracellular localisation, the authors hypothesised that PH1 and PH5 acted in concert in vacuolar petal acidification. In fact, when overexpressed on their own, neither PH5, nor PH1 could rescue the colour and pH phenotype of the *ph3* mutant. Only when PH1 and PH5 were co-expressed the mutant's flower colour reverted back to red, and its petal extract pH decreased from approximately 5.7 to 5.3 (Figure 1). An elegant way to show that this mutant rescue was due to the acidification of petal cell vacuoles was the authors' co-expression of the $Na^+/H^+$ and $K^+/H^+$ antiporter NHX1, which had been shown to reduce cross-tonoplast pH gradients [7]. The PH1/PH5-mediated rescue of the *ph3* mutant colour and petal extract pH was lost when NHX1 was also expressed; as a result the flower colour reverted back from red to the pale-rosé of the *ph3* mutant, even though PH1 and PH5 were expressed.

### Hyperacidification of petunia petal cell vacuoles relies on both $P_3$-ATPases

The final and crucial question addressed in the study was: What constituted the concerted action of PH1 and PH5 in vacuolar acidification on a mechanistic level? To answer this question the authors carried-out two different protein interaction studies using Bimolecular Fluorescence Complementation and Split-Ubiquitin-System assays. Both approaches yielded that PH1 and PH5 were able to interact with one another. Furthermore, the authors applied the patch-clamp technique to whole-vacuoles of petunia leaf cells. Clamping the membrane potential at 0 mV the team could observe ATP-dependent outward currents, arising from proton-transport from the cytosol to the vacuolar lumen. The vast majority of this current was sensitive to bafilomycin, a highly specific inhibitor of V-ATPases. However, in vacuoles expressing PH5, half of the ATP-dependent current was sensitive to bafilomycin, whereas the other half was sensitive to vanadate, an inhibitor of P-ATPases such as PH5. This indicated that PH5 was transporting protons to the vacuolar lumen. Surprisingly, vacuoles expressing PH1 did not display any vanadate-sensitive current, but when PH5 and PH1 were co expressed the vanadate-sensitive current nearly doubled, when compared to vacuoles expressing PH5 only. This indicates that, although PH1 does not seem to have proton-transport activity, it enhances the PH5-mediated current. How such an enhancement may work on a mechanistic level, however, remains elusive.

PH1 displays sequence similarity to bacterial $P_{3B}$-ATPases such as MgtA and MgtB, which are required for $Mg^{2+}$ uptake. Such transporter systems had previously been thought absent in plants but when the researchers carried out phylogenetic analysis they found homologues in other species including *Vitis vinifera*, the berries of which also require vacuolar hyperacidification. Although the authors hypothesised that PH1 might boost PH5-mediated $H^+$ pumping by dissipating $\Delta E_m$ through $Mg^{2+}$ import to the cytosol, they found no evidence for this and reasoned that such an import was energetically unfavourable.

### Concluding remarks and outlook

The authors of this review found that PH1 is lacking an aspartate (D) residue that is conserved in $Mg^{2+}$-, $Ca^{2+}$-, $Na^+/K^+$-, $H^+/K^+$-, and $H^+$-ATPases such as the prokaryotic PH1-homologues and PH5, and which has been proposed to be essential for cation binding and translocation [8]. In PH1 this residue is replaced by an asparagine (N) (Figure 1). When the corresponding Asp 684 of the *Arabidopsis* $H^+$-ATPase AHA2 was mutated to Asn (D684N), the enzyme still displayed ATP hydrolysis activity but did no longer show coupling to $H^+$ transport [8]. The stoichiometry of $H^+$ transported to ATP hydrolysed ($n$) for V-ATPases typically has a value of 2 but depends on vacuolar pH. With steeper cross-tonoplast pH gradients ($\Delta$pH) the value of $n$ decreases [9], because, from a thermodynamic standpoint, transport against a larger concentration gradient requires more energy through ATP hydrolysis. In fact, $H^+$ P-ATPases are essential for the energisation of even steeper gradients as they operate at coupling ratios of $1H^+$/ATP [10]. Early work from the Taiz laboratory uncovered the existence of vanadate-sensitive cross-tonoplast $H^+$ transport in lemon fruit [11]. This vanadate-sensitive transport may indicate the existence of vacuolar P-type ATPases in lemon, which, in light of the findings presented here, may be homologous to that of PH5 or PH1/PH5. Taken together, we speculate that when PH1 and PH5 interact, this might decrease the $H^+$/ATP stoichiometry to hypothetically $0.5H^+$/ATP allowing for hyperacidification. To test this hypothesis, initially one may generate the mutation N782D in PH1 in order to determine if proton-pumping activity is restored. Furthermore, it would be valuable to determine the $H^+$/ATP coupling ratio of the interacting PH1–PH5.

In conclusion, the study described above has not only identified a missing component in petunia flower colour and pH regulation, but it may point to entirely new mechanisms of proton-pumping via P-ATPases.

#### Acknowledgment

We are grateful for funding from the European Union's Seventh Framework Programme for research, technological development, and demonstration under grant agreement no. GA-2010-267243 – PLANT FELLOWS to C.E. and for funding from the Forschungskredit of the University of Zurich to U.B. We thank three anonymous reviewers for valuable suggestions.

#### References

1 Martinoia, E. *et al.* (2007) Vacuolar transporters and their essential role in plant metabolism. *J. Exp. Bot.* 58, 83–102
2 Martinoia, E. *et al.* (2012) Vacuolar transporters in their physiological context. *Annu. Rev. Plant Biol.* 63, 183–213
3 Ferjani, A. *et al.* (2011) Keep an eye on PPi: the vacuolar-type $H^+$-pyrophosphatase regulates postgerminative development in Arabidopsis. *Plant Cell* 23, 2895–2908
4 Krebs, M. *et al.* (2010) *Arabidopsis* V-ATPase activity at the tonoplast is required for efficient nutrient storage but not for sodium accumulation. *Proc. Natl. Acad. Sci. U.S.A.* 107, 3251–3256
5 Verweij, W. *et al.* (2008) An $H^+$ P-ATPase on the tonoplast determines vacuolar pH and flower colour. *Nat. Cell Biol.* 10, 1456–1462
6 Faraco, M. *et al.* (2014) Hyperacidification of vacuoles by the combined action of two different P-ATPases in the tonoplast determines flower color. *Cell Rep.* 6, 32–43
7 Bassil, E. *et al.* (2011) The *Arabidopsis* $Na^+/H^+$ antiporters NHX1 and NHX2 control vacuolar pH and $K^+$ homeostasis to regulate growth, flower development, and reproduction. *Plant Cell* 23, 3482–3497
8 Buch-Pedersen, M.J. *et al.* (2000) Abolishment of proton pumping and accumulation in the E1P conformational state of a plant plasma membrane $H^+$-ATPase by substitution of a conserved aspartyl residue in transmembrane segment 6. *J. Biol. Chem.* 275, 39167–39173
9 Davies, J.M. *et al.* (1994) Vacuolar $H^+$-pumping ATPase variable transport coupling ratio controlled by pH. *Proc. Natl. Acad. Sci. U.S.A.* 91, 8547–8551
10 Briskin, D.P. and Reynolds-Niesman, I. (1991) Determination of $H^+$/ATP stoichiometry for the plasma membrane $H^+$-ATPase from Red Beet (*Beta vulgaris* L.) storage tissue. *Plant Physiol.* 95, 242–250
11 Müller, M.L. *et al.* (1996) On the mechanism of hyperacidification in Lemon. *J. Biol. Chem.* 271, 1916–1924

# Root exudates:
# the hidden part of plant defense

Ulrike Baetz and Enrico Martinoia

Department of Plant and Microbial Biology, University of Zurich, 8008 Zurich, Switzerland

Corresponding author: Ulrike Baetz

Published in *Trends of Plant Science* 2014 Feb; 19 (2):90-98

Note: Both, the review and the book chapter about root exudates were written in periods during which manual lab work was due to a hand fracture not possible.

Review

# Root exudates: the hidden part of plant defense

**Ulrike Baetz and Enrico Martinoia**

Institute of Plant Biology, University of Zurich, Zollikerstrasse 107, CH-8008 Zurich, Switzerland

**The significance of root exudates as belowground defense substances has long been underestimated, presumably due to being buried out of sight. Nevertheless, this chapter of root biology has been progressively addressed within the past decade through the characterization of novel constitutively secreted and inducible phytochemicals that directly repel, inhibit, or kill pathogenic microorganisms in the rhizosphere. In addition, the complex transport machinery involved in their export has been considerably unraveled. It has become evident that the profile of defense root exudates is not only diverse in its composition, but also strikingly dynamic. In this review, we discuss current knowledge of the nature and regulation of root-secreted defense compounds and the role of transport proteins in modulating their release.**

## Root exudates function in belowground plant defense

Plants are constantly exposed to a variety of natural enemies, including pathogenic fungi, oomycetes, bacteria, viruses, nematodes, and root-feeding arthropods. These organisms inhabit the soil surrounding the root system, which is designated the rhizosphere. The fact that roots anchor plants in the soil, account for a substantial storage reservoir, and perform water and nutrient uptake forces plants to defend them efficiently against detrimental microorganisms. To counteract infection and confer tissue-specific resistance, plants release a variety of biologically active compounds into the rhizosphere. Indeed, such root exudates are known to have a multitude of functions in ecological interactions with the microbial soil communities, for example by acting not only as signaling molecules, attractants, and stimulants, but also as inhibitors or repellents. In this review, we focus mainly on compiling the information available on various secreted natural compounds that confer direct defense against soil-borne pathogens. The reader is referred to other recent reviews for detailed information on mutually beneficial interactions between plants and microorganisms, plant–plant communication, and tripartite interactions mediated by root exudates [1–3].

*Corresponding author:* Baetz, U. (baetzu@botinst.uzh.ch).
*Keywords:* ABC transporter; border cells; defense; pathogens; rhizosphere; root exudates.

1360-1385/$ – see front matter
 http://dx.doi.org/10.1016/j.tplants.2013.11.006

The nature and relative abundance of components in root exudate blends have a profound effect on shaping the soil environment, including pathogen levels. Therefore, the root-secreted defense system and its fine-tuned regulation are essential for plant performance and represent a major field of interest in root biology research. The tremendous metabolic diversity of root exudates is gradually being elucidated through the identification and characterization of numerous novel antimicrobial compounds and previously undescribed groups of direct defense chemicals. Concurrently, genes and biosynthetic pathways involved in the production of these phytochemicals are being deciphered. We discuss examples of recently described secreted chemical weapons that contribute to the constitutive and/or targeted local belowground defense of plants. Furthermore, recent advances in the genetic identification and biochemical and physiological characterization of root-expressed transporter proteins result in a deepened understanding of the complex transport machinery that mediates export processes into the rhizosphere. We review current knowledge of the transporters that are involved in the release of defense root exudates, their potential substrates, their regulation, and their direct and indirect effects on the root exudate composition and the soil microbial community.

## Dynamics in the composition of defense root exudates

Photosynthetically fixed carbon that is continuously secreted by plants as root exudates, including antimicrobial compounds, is *prima facie* a significant carbon cost for the plant [2]. To prevent excessive energy loss, the biosynthesis of defense phytochemicals and their rhizodeposition requires tight regulation and adjustment towards necessity in heterogeneous environments. Recently, considerable progress has been made in deciphering regulation processes and stimuli inducing changes in root exudate blends that demonstrate all the more the complexity and accuracy of the belowground defense system in plants.

By definition, low-molecular-weight antimicrobial chemicals that are present in the plant before biotic stress are named phytoanticipins [4]. In a recent study, the diterpene rhizathalene A was found to be constitutively produced and released by non-infected *Arabidopsis* (*Arabidopsis thaliana*) roots [5]. Plants that are deficient in rhizathalene A production were found to be more susceptible to insect herbivory. Therefore, this diterpene was suggested to be part of the constitutive direct defense system of roots. It should be noted that plants secrete a wide array of other

high- and low-molecular-weight defense compounds in the absence of pathogen elicitation [6–14]. Hence, the rhizosphere not only represents the infection court on which pathogens encounter the plant, but is also a preventive microbial buffer zone that protects against infection.

Together with the constitutive root exudation, the synthesis, accumulation, and release of defense-related compounds can be stimulated upon the establishment of pathogen interactions. Inducible, low-molecular-weight antimicrobial compounds that are not detectable in healthy plants are called phytoalexins [4]. When investigating the release of root-derived aromatic exudates in barley (*Hordeum vulgare*) that was attacked by the soil-borne pathogen *Fusarium graminearum*, an induction of five phenylpropanoids exhibiting antifungal activity was found [15]. Among them, labeling experiments highlighted the *de novo* biosynthesis and secretion of *t*-cinnamic acid [15]. Besides this 'phytoalexin prototype', pathogen infection can increase the quantities of certain constitutively exuded phytoanticipins. Momilacton A is an antimicrobial diterpene that is produced and secreted from roots of rice (*Oryza sativa*) seedlings into the rhizosphere [6,7]. In addition, rice that has been challenged with the blast fungus shows targeted leaf-accumulation of momilacton A [16]. Taken together, this indicates that momilacton A and other root exudates feature properties of both constitutively produced and secreted phytoanticipins and pathogen-elicitable phytoalexins [4,17].

An alteration in the defense exudate composition can be stimulated by various factors besides pathogen infection under laboratory conditions. For instance, the ectopic expression of the oomycetal elicitor *β*-cryptogein in hairy roots of the flowering plant *Coleus blumei* mimics pathogen attack, and significantly increases the concentration of rosmarinic acid, which exhibits antimicrobial activity, in the culture medium [18,19]. By contrast, the defense compound is reduced in the root hair tissue when ß-cryptogein is expressed, indicating that this elicitor functions as a regulator of phenolic secretion into the rhizosphere [18]. Furthermore, following exogenous application, the defense signaling molecules salicylic acid (SA), nitric oxide (NO), and methyl jasmonate (MeJA) independently elicit a differential genome-wide transcription profile in roots, resulting in an enhanced rhizosecretion of root exudates [20] in *Arabidopsis* [21] and hairy roots of *Catharanthus roseus* [22].

Compositional shifts in root exudates not only occur in response to exogenous stimuli, such as the above-mentioned pathogenic elicitors or defense signals, but are also controlled by endogenous developmental programs. In maize (*Zea mays*), benzoxazinoids form a class of defense molecules [23] that are released during the emergence of lateral and crown roots [24]. These benzoxazinoids present a genetically regulated, protective chemical barrier, which is thought to prevent pathogen attack at sites that are temporally more susceptible, or in developmental stages at which infection is more deleterious for the plant. Accordingly, the peak of defense-related protein exudation into the rhizosphere can be observed just before flowering [9]. Similarly, plants adopt a tighter defensive strategy towards later stages of their life cycle, as evidenced by an increased amount of putative antimicrobial phenolic compounds in their root exudate profile [11].

Breakthroughs in genome sequencing, extensive collections of mutant lines and tools available for the model plant *A. thaliana*, a combination of '-omics' approaches, new sampling methods, and higher-resolution detection systems have been indispensable in facilitating comparative large-scale analysis of root exudate blends in response to different pathogens. Specifically, the compatible interaction of bacterial or fungal pathogens, or root-feeding insects with *Arabidopsis* roots, but not mechanical wounding, stimulates the rapid secretion of the antimicrobial 1,8-cineole [25]. However, incompatible interactions do not influence the exudation of this monoterpene. In agreement with this result, the secretion of biotic stress-responsive proteins from *Arabidopsis* roots is induced during compatible but not incompatible interaction [26], demonstrating that defense root exudation is influenced by the identity of the microbial neighbor.

Taken together, these results provide circumstantial evidence that the secretion of defense compounds into the rhizosphere is a tightly controlled, temporally dynamic process that is regulated by various endogenous and exogenous stimuli.

## The diverse chemistry of direct defense compounds

Besides the precise regulation of root exudation processes, there is a large chemical diversity of antimicrobial compounds that have been recently identified to protect plants directly against pathogen invasion.

In general, root-secreted compounds belonging to the chemical class of phenolics and terpenoids have strong external antibacterial and antifungal qualities [15,17–19]. Notably, phenolic metabolites also function efficiently in attracting some soil-borne microorganisms and can beneficially influence the native soil microbial community [27]. It was also observed that molecules such as the amino acid canavanine can act as a stimulator for one group of microbes, but as a suppressor for many other soil bacteria [28]. Thus, compounds of the same chemical class can differentially affect the soil environment, and certain substances can be considered as microorganism specific in their biological activity and toxicity. Similarly, a phytoalexin derived from *Arabidopsis* root exudates is required for conferring resistance to *Phytophthora capsici* [29]; however, resistance to *Phytophthora cinnamomi* does not rely on this phytochemical [30]. The finding of differential compound activities may be explained in part by variations in the tolerance to specific defense molecules based on the efficiency of active detoxification and efflux processes between different pathogens.

Phenylpropanoids are ubiquitous plant phenolics that occur in defense root exudates [15]. In line, resistance to *Fusarium graminearum* attack in barley is based on the rapid accumulation and secretion of phenylpropanoids (cinnamic acid derivatives) after fungal infection [15]. Moreover, flavonoids represent one of the largest classes of phenylpropanoid-derived secondary metabolites in plants and constitute a large proportion of root exudates [31]. Derivatives of isoflavonoids, such as the pea (*Pisum sativum*) phytoalexin pisatin, are a crucial class of

compounds with potent antimicrobial properties in legumes [32,33]. The tissue-specific release of pisatin from the root tip can be stimulated by pathogen elicitation [34].

Terpenoids form the largest class of plant defense chemicals above- and belowground and contribute to root exudates [5–7,17,35]. It has been known for some time that nonvolatile terpenoid phytochemicals, such as momilactones, can be secreted into the rhizosphere [6,7]. However, it was only recently that volatile organic compounds (VOCs) were also shown to be emitted from roots as a direct defense mechanism. Plant-derived volatiles have been previously described to function in tritrophic interactions by attracting natural enemies of herbivores upon attack to provide indirect plant defense [36–39]. By contrast, an example of a direct belowground volatile defense compound is the monoterpene 1,8-cineole, which is released from hairy-root cultures of *Arabidopsis* during pathogen interaction [25,40]. Furthermore, a semivolatile diterpene hydrocarbon, rhizathalene A, is implicated in the belowground resistance towards root-feeding insects as a local antiherbivore metabolite of *Arabidopsis* [5]. A new role was discovered for another class of terpenoids, the strigolactones. An extensive body of literature has been published on strigolactones as phytohormones and, when released into the rhizosphere, as a compound involved in plant symbiosis with arbuscular mycorrhizal fungi and in plant infection by root parasitic plants [41]. Intriguingly, the synthetic strigolactone analog GR24 inhibits the growth of an array of phytopathogenic fungi when present in the growth medium [42], indicating that secreted strigolactones can affect natural enemies directly [42] or indirectly by modulating hormonal defense pathways [43] and contribute to belowground plant biotic stress responses.

Other highly potent antifungal or antimicrobial root exudates are tryptophan-derived secondary metabolites, such as some glucosinolates or the indole derivative camalexin, which is the only characterized phytoalexin in *Arabidopsis* [29,44–51]. Several molecular players involved in camalexin biosynthesis have been identified at the genetic level. Their transcriptional activation after infection leads to the intrinsic production, accumulation [44], and exudation [46] of camalexin from *Arabidopsis* roots, whereas their genetic disruption results in lower secretion levels [46], accompanied by enhanced pathogen disease symptoms and fungal growth [44]. In line with these observations, the ectopic overexpression of an *Arabidopsis* gene that modulates camalexin and SA biosynthesis confers disease resistance to soybean (*Glycine max*) against nematodes [52].

Collectively, defense root exudate blends build a diverse and flexible protective layer of chemical compounds in the rhizosphere. In addition to low-molecular-weight metabolites, high-molecular-weight root exudates also contribute to the local belowground resistance. In particular, the repelling and inhibiting role of previously unrecognized molecules, such as secreted proteins and extracellular DNA, has emerged over the past years [8,53]. Below, we discuss these two components of defense root exudates in the context of border cells, because their examination was predominantly conducted using this specialized 'front-line' cell layer.

## Border cells and their exudates act as a defensive barrier of roots

Root tips display local resistance to various infections, whereas more vulnerable parts of roots, such as the elongation zone, are more susceptible [54,55]. This phenomenon of spatially different susceptibility is correlated with the highly controlled, inducible formation and release of metabolically active border cells at the root periphery that originate and detach from the root cap meristem [56–59]. In fact, cap and border cells assist the growing root during the mechanical penetration of the soil by reducing friction at the root–soil interface [58]. In addition, antimicrobial phytochemicals in the rhizosphere largely derive from cap and border cells, hence these cells account for a protective shield against pathogen invasion with a vital impact on plant health [59–61]. Besides developmental and environmental signals, the invasion of pathogenic microorganisms initiates border cell production as a plant defense mechanism [34,59,62]. It was recently shown that the formation of root border cells and exudation of the isoflavonoid phytoalexin pisatin is stimulated in pea when root tips are challenged with a plant pathogen [34]. Moreover, exogenous pisatin, in turn, leads to the upregulation of border cell production *in vitro* [62].

Border cells and their exudates can account for root tip resistance by coping with pathogens via at least three mechanisms that act in concert (Figure 1). First, peripheral border cells can attract pathogenic microorganisms to get infected, a strategy that confers transitory protection to the root tip. In fact, after the removal of the border cell layer, the physiologically independent root tip remains uninfected, defense gene expression is not elicited, and root growth proceeds indistinguishably from nontreated roots [54,63]. Besides providing a sustainable substitute for deleterious pathogenic root tip invasion, border cells can act as chemical and physical barriers towards pathogens by secreting not only antipathogenic low-molecular-weight metabolites, but also a mucilaginous matrix of up to 95% high-molecular-weight polysaccharides and 5% extracellular proteins [53,64]. Proteolytic solubilization of protein exudates derived from progenitor root cap and border cells (referred to as 'root cap secretome') in pea results in the disintegration of the mucilage, the release of bacteria as well as the loss of root tip resistance towards infection by a pea pathogen [53].

Therefore, despite their minor physical fraction, proteins are engaged in the binding, trapping, and aggregation of pathogenic bacteria [53,64]. Moreover, secreted antimicrobial proteins can serve as a direct external defense mechanism by repelling, inhibiting, or killing pathogenic microorganisms. Proteomic analysis of the root exudates of root cap and border cells confirmed that the complex mixture of approximately >100 proteins contains mostly stress and defense-related proteins, besides structural components such as actin [9,10,13,14,26,53]. Upon encountering pathogenic interactions, the protein composition alters dynamically as antimicrobial compounds (e.g., hydrolases, peptidases, and peroxidases) accumulate in the rhizosphere [9,10,26,53].

As well as the presence of antimicrobial enzymes, which have long been known to be associated with plant defense, the root cap secretome contains histone H4 [53].

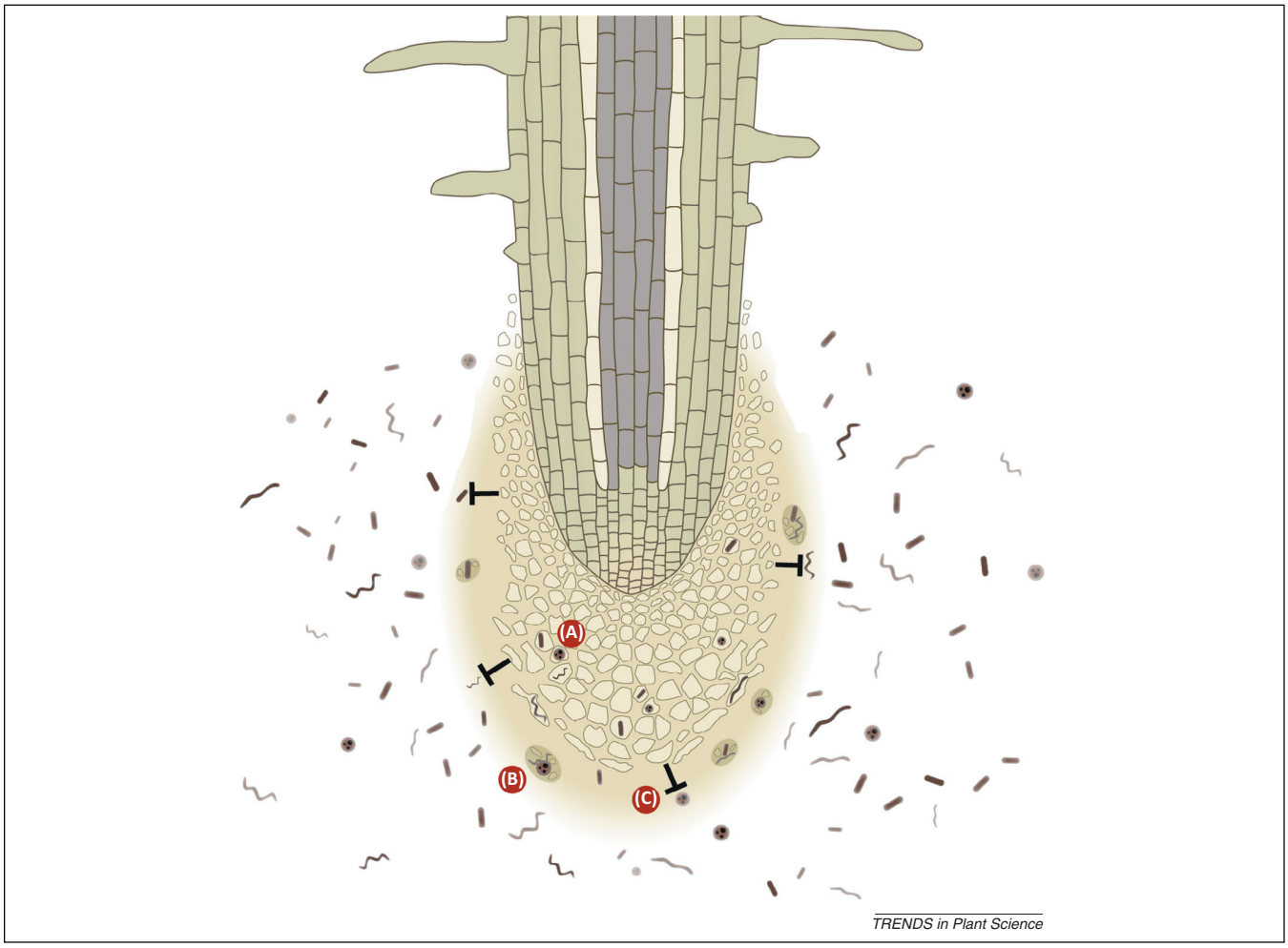


**Figure 1**. Concerted action of root border cells and their exudates in root tip resistance against pathogens. Displayed microorganisms represent pathogenic fungi, oomycetes, bacteria, viruses, nematodes, and root-feeding arthropods. **(A)** Pathogen attraction and penetration of physiologically independent border cells to prevent deleterious root tip infection. **(B)** The mucilage layer comprising mainly polysaccharides, proteins, and extracellular DNA is secreted by border cells and represents a defensive matrix that binds, immobilizes, and aggregates pathogens. **(C)** Depicted is the inhibition or killing of microbes through high-and low-molecular-weight compounds that are released by root border cells and exhibit direct antimicrobial and/or antifungal properties. Copyright University of Zurich, Sarah Steinbacher.

In mammals, histone-linked extracellular DNA (exDNA) is anticipated to have a critical role in defense against microbial pathogens [65–67]. A similar mechanism was suggested in plants when exDNA linked to histone proteins was discovered to be synthetized and exuded from root border cells [8]. The specific mechanism of how exDNA inhibits pathogen growth needs to be determined. However, recent research suggests that exDNA provides, similar to various structural proteins, a fundamental scaffold to trap, immobilize, and subsequently kill root-infecting pathogens in the mucilage matrix, because degradation of either component in root tip exudates using a protease or a nuclease, respectively, results in an abolishment of root tip resistance to fungal infection [8,53]. Given that border cells secrete a mucilage layer that contains proteins and exDNA to protect the root tip by adhesion and aggregation of pathogens, they function analogously to white blood cells in the mammalian innate immune response [8,59,68].

Taken together, the penetration of physiologically independent border cells, the root cap and border cell exudation of the mucilage layer including proteins and exDNA that immobilize pathogens, as well as the secretion of, for instance, antimicrobial enzymes and secondary metabolites, cooperatively provide root tip resistance towards pathogens.

## The transport machinery that modulates the release of defense phytochemicals

As knowledge about the synthesis of defense metabolites and their function in the rhizosphere has improved, the complex mechanisms of regulated rhizosecretion and the critical transport components have also started to be unraveled. Traditionally, root exudation has been suspected to be a passive process mediated by diffusion, channels, and vesicle transport. However, recent studies elucidated a pivotal role of tightly regulated primary and secondary active transport processes across the root plasma membrane in the export and accumulation of defense phytochemicals in the rhizosphere. Two protein families involved in mediating the transport of a wide array of organic substances, namely multidrug and toxic compound extrusion (MATE) and ATP-binding cassette (ABC) transporters [69,70], have attracted particular interest.

Nevertheless, there are a large number of uncharacterized transporters, which might participate in the belowground defense system.

Members of both the MATE and ABC transporter families are capable of releasing constituents of the root phytochemical cocktail into the rhizosphere. In the case of MATE transporter proteins, a subclade that can be found in all plants analyzed so far is implicated in the release of citrate into the rhizosphere to confer aluminum resistance to plants. Citrate is a carbon source for many microorganisms; therefore, this exudation may also have an impact on the microflora at the root tip [71–75]. Recently, a MATE transporter in the stele of rice roots was found to facilitate efflux of phenolic compounds into the xylem [76]. It was speculated that similar transporters might be responsible for phenolic secretion into the soil. In Table 1, we highlight the few genes out of 56 members of the MATE family that are promising candidates to encode transport proteins that are involved in such processes. They exhibit a strong or predominant expression in the outer cell layers of root caps and have not previously been shown to be localized in any membrane other than the plasma membrane (Table 1) [69,77]. However, to our knowledge, to date, no MATE transporter has been identified to export root-derived antimicrobial compounds into the rhizosphere. By contrast, members of the ABC transporter family are fundamentally involved in root exudation and the defense system [78–80] and, recently, putative substrates were attributed to particular transporter proteins [81,82]. Examples of these defense-related ABC transporters and their specific expression profiles that are in agreement with a role in the secretion of compounds into the rhizosphere are shown in Figure 2.

Initially, indirect pharmacological approaches were deployed to demonstrate that the root exudate profile of *Arabidopsis* is quantitatively and qualitatively dependent on ATP hydrolysis [83], indicating that the secretion process of certain phytochemicals is mediated by active transport systems, such as ABC-type proteins [84]. Subsequently, among the >120 genes encoding ABC transporter proteins in *Arabidopsis*, 25 candidates were identified to have a potential role in rhizosecretion, based on their high expression in root cells [85]. Exudate [85,86] and microbial [86] composition differs significantly between knockout lines of several root-expressed ABC transporters and the corresponding wild type, providing evidence that this protein family is involved in root secretion, also of antimicrobial compounds. Furthermore, these studies revealed that multiple ABC transporters can be used for the release of a given phytochemical, and a specific ABC transporter can be capable of mediating the export of several structurally and functionally unrelated substrates. Another example is *At*ABCG37/*At*PDR9, which has been demonstrated to transport not only phenolic compounds into the rhizosphere as an iron acquisition strategy [87,88], but also auxinic compounds [89,90]. Interestingly, to our knowledge, the only direct link between a defined transporter, its substrate, and an effect on soil microorganisms has been demonstrated for *Ph*PDR1, a petunia ABC transporter that catalyzes the release of strigolactones from root cells to initiate mycorrhization [82].

Only a few studies have addressed the connection of transport proteins, defense-related phytochemical rhizosecretion, and soil-borne pathogen susceptibility. Silencing *Nt*ABCG5/*Nt*PDR5 from tobacco (*Nicotiana tabacum*) resulted in enhanced herbivore performance [79]. Similarly, the transporter *Np*PDR1 of *Nicotiana plumbaginifolia* is directly involved in plant defense against pathogen invasion [78,91]. Silencing this ABC transporter resulted in enhanced sensitivity of roots and petals towards various soil-borne pathogens, possibly due to diminished secretion of antifungal compounds, such as the diterpene sclareol [91]. In general, the appearance of a phytochemical in the rhizosphere can be genetically and biochemically regulated by various factors, including not only ABC-type protein abundance, transport activity, substrate availability and specificity, but also pleiotropic effects mediated by ABC transporters. The gene expression of the transporter *Nt*PDR1 positively correlates with export rates of antipathogenic diterpenes into the extracellular medium,

**Table 1. Expression profiles of genes encoding *Arabidopsis* MATE transporters that are predominantly or highly expressed in root caps**

| GO[a] | Gene ID | Root stage I[b] | | | | | | Maximum FC[d] | Tissue of maximum FC |
|---|---|---|---|---|---|---|---|---|---|
| | | Stele[c] | Endo | Endo+cortex | Epi | LRC | FC LRC | | |
| AtDTX5/6 | At2g04090/At2g04100 | 49.16 | 51.52 | 19.98 | 243.55 | 119.49 | 10.62 | 32.06 | Root stage II Epi |
| AtDTX9 | At1g66760 | 110.07 | 216.78 | 235.16 | 55.14 | 157.5 | 3.45 | 29.7 | Mesophyll cells, with 100 μM abscisic acid |
| AtDTX12 | At1g15170 | 40.01 | 53.91 | 61.21 | 220.75 | 184.89 | 5.88 | 7.1 | Bicellular pollen |
| AtDTX33 | At1g47530 | 109.4 | 232.04 | 159.19 | 179.31 | 162.65 | 0.59 | 5.86 | Guard cells, with 100 μM abscisic acid, cordycepin and actinomycin added during protoplasting |
| AtDTX36 | At1g11670 | 437.77 | 568.63 | 734.08 | 958.69 | 1847.14 | 39.76 | 52.16 | Root stage III LRC |
| AtDTX37 | At1g61890 | 882.33 | 745.87 | 1110.85 | 968.94 | 1144.92 | 2.57 | 16.39 | Mesophyll cells |
| AtDTX39 | At4g21910 | 37.86 | 28.42 | 39.09 | 96.92 | 197.76 | 1.88 | 6.56 | Ovary tissue |

[a]Gene ontology.

[b]Root stage I represents cells of the root cap, stage II of the elongation zone, and stage III of the root hair zone.

[c]The stele is the inner-most cell layer of the root and the lateral root cap the outer-most cell layer. Abbreviations: endo, endodermis; endo+cortex, endodermis and cortex; epi, epidermal artrichoblasts; LRC, lateral root cap.

[d]Fold changes (FC) are calculated as the ratio of the gene expression in a given tissue to the mean expression level in the entire plant. Consequently, this value indicates the homogeneity of the gene expression and the maximal fold change occurs in the tissue with the highest absolute expression levels.

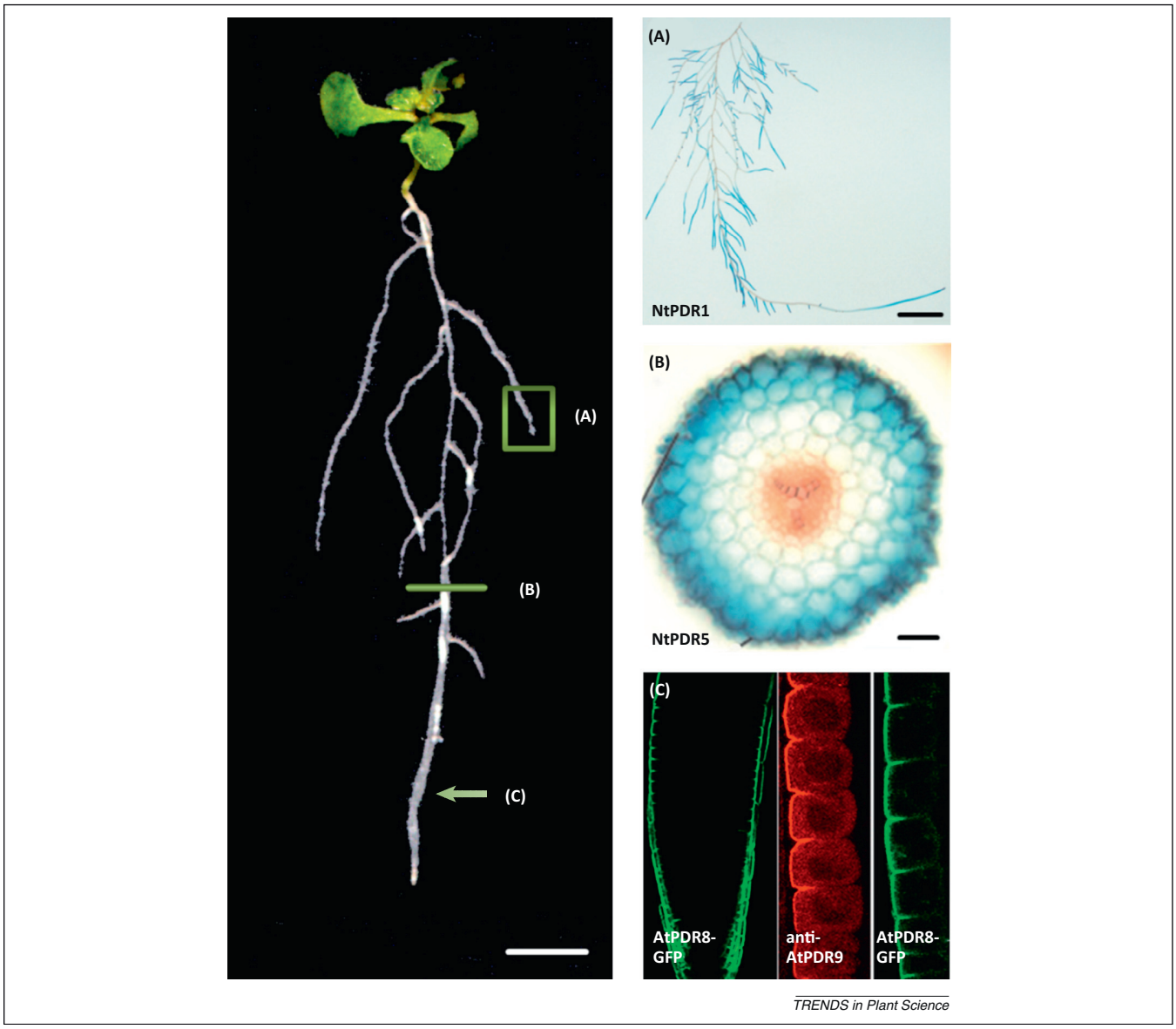


**Figure 2**. Tissue, cell-layer, and subcellular expression profile of transporter proteins that are involved in rhizosecretion and defense processes. Depicted are three representative transport proteins with expression patterns that are likely for transporters exporting root exudates. **(A)** *In situ* expression analysis using β-Glucuronidase (GUS) staining shows that *Nt*PDR1, an ATP-binding cassette (ABC)-type protein in *Nicotiana tabacum* that is implicated in diterpene transport and defense response, is highly expressed in primary and lateral root tip cells [81]. **(B)** Plants expressing *ProPDR5:Gv* are stained for GUS activity. A cross-section of the mature part of the root demonstrates that *Nt*ABCG5/*Nt*PDR5, a transporter that is involved in herbivore resistance, shows a cell layer-specific expression in the epidermis [79]. **(C)** *At*ABCG36/*At*PDR8 and *At*ABCG37/*At*PDR9 transport, among other substrates, auxinic compounds out of the cell and are suggested to be implicated in belowground defense processes [89,90,99,100]. Immunolocalization and live-cell imaging demonstrate that both transport proteins are expressed in the lateral root cap and the epidermis and exhibit outer polar plasma membrane localization. Reproduced, with permission, from [79,81,100]. Scale bars = 0.5 cm (left panel); 1 cm (A); and 50 μm (B).

and the expression can be modified by microbial elicitation [81,92]. By contrast, another study showed that nitrogen deficiency can elicit the increased biosynthesis of the flavonoid signaling molecule, genistein, resulting in its secretion from soybean roots to initiate rhizobium symbiosis [93], whereby the transport machinery involved in genistein export is constitutively active, regardless of the nitrogen availability [84]. A further twist to that story is the fact that ABC transporter proteins themselves exhibit a regulatory function in modulating the synthesis and exudation of defense phytochemicals. For instance, roots of *Medicago truncatula* were rapidly infected by *Fusarium oxysporum* when *MtABCG10*, a gene that encodes a close homolog of *Nt*PDR1 [81,92], was silenced [94]. Concomitantly, this silencing resulted in a reduction of the phenylpropanoid pathway-derived phytoalexin, medicarpin, as well as its precursors in root tissue and exudates. Therefore, it was proposed that *Mt*ABCG10 modulates isoflavonoid levels during the belowground biotic stress response associated with the *de novo* biosynthesis of phytoalexins. Another recent study demonstrated that the *Arabidopsis* mutant *abcg30* exhibited lower levels of several compounds in the rhizosphere, whereas other defense exudates showed higher secretion in the mutant plants [86]. This finding provides evidence that *At*ABCG30 mediates the transport of compounds, and also that the lack of the protein directly and indirectly influences various metabolic processes, such as biosynthesis of secondary metabolites and/or the

expression of other transporters. Hence, in the future, it will be of interest not only to identify the transport machinery of defense compounds and their substrates, but also to examine the distinct pathways that are modified in transporter mutants. This will deepen our understanding of the effects on root exudate patterns mediated by ABC-type proteins.

## Concluding remarks and future perspectives

Despite its importance in ensuring tissue protection and optimizing plant performance, deciphering the belowground defense system has been neglected for a long time, a result of difficulties in accessing the undisturbed, natural rhizosphere communication, which includes symbiotic and pathogenic interactions between plants and microorganisms. Exploring the profiles of secreted metabolites that exhibit a defensive function outside the plant in close proximity to the roots presents a more pronounced technical challenge compared with aboveground or endogenously sequestered antimicrobial compounds. The chemical ensemble released by roots is profoundly shaping native microbial community structures. Notably, alterations of single root exudates in the rhizosphere or single genes in the biosynthetic pathway of phytochemicals or transporters can influence the composition and activity of the soil microbiome [27,48,52,86,95,96]. Hence, the complex network of root exudation and pathogen defense needs to be decoded comprehensively to integrate the regulation of rhizosecretion, with direct and indirect physiological effects on plants and the entire microbial ecosystem. Understanding the ecological impact of valuable defense molecules will provide novel opportunities to engineer a protective rhizosphere. Some studies have aimed to generate roots releasing artificial exogenous bioactive molecules to produce plants with increased resistance to pathogens [18,48,52,97,98]. For instance, pathogen infection is significantly inhibited in tomato roots secreting selected antimicrobial peptides fused to a maize cytokinin–dehydrogenase protein scaffold [97]. Such peptide-delivery agents for plant defense molecules or targeted ectopic expression systems of secondary metabolites or transporters are auspicious candidates for manipulating the formation and secretion of root exudates and enhancing their natural defense properties. However, the potentially large impact at the ecological and environmental level from minor compositional changes in root exudation needs to be taken into account carefully to avoid possible repercussions on microbial communities and nontarget organisms.

## Acknowledgments

We are grateful to the Forschungskredit, UZH, for financial support of U.B. and to Robert Dudler, Hans Lambers, Cornelia Eisenach, and David Seung for critical reading and fruitful discussion on the manuscript. Furthermore, we would like to thank Jiri Friml and Marc Boutry for kindly providing the high-resolution pictures in Figure 2.

## References

1 Bais, H.P. *et al.* (2006) The role of root exudates in rhizosphere interactions with plants and other organisms. *Annu. Rev. Plant Biol.* 57, 233–266
2 Badri, D.V. *et al.* (2009) Rhizosphere chemical dialogues: plant-microbe interactions. *Curr. Opin. Biotechnol.* 20, 642–650
3 Doornbos, R.F. *et al.* (2012) Impact of root exudates and plant defense signaling on bacterial communities in the rhizosphere. A review. *Agron. Sustain. Dev.* 32, 227–243
4 VanEtten, H.D. *et al.* (1994) Two classes of plant antibiotics: phytoalexins versus "phytoanticipins". *Plant Cell* 6, 1191–1192
5 Vaughan, M.M. *et al.* (2013) Formation of the unusual semivolatile diterpene rhizathalene by the *Arabidopsis* class I Terpene Synthase TPS08 in the root stele is involved in defense against belowground herbivory. *Plant Cell* 25, 1108–1125
6 Kato-Noguchi, H. *et al.* (2008) Secretion of momilactone A from rice roots to the rhizosphere. *J. Plant Physiol.* 165, 691–696
7 Toyomasu, T. *et al.* (2008) Diterpene phytoalexins are biosynthesized in and exuded from the roots of rice seedlings. *Biosci. Biotechnol. Biochem.* 72, 562–567
8 Wen, F. *et al.* (2009) Extracellular DNA is required for root tip resistance to fungal infection. *Plant Physiol.* 151, 820–829
9 De-la-Peña, C. *et al.* (2010) Root secretion of defense-related proteins is development-dependent and correlated with flowering time. *J. Biol. Chem.* 285, 30654–30665
10 Shinano, T. *et al.* (2011) Proteomic analysis of secreted proteins from aseptically grown rice. *Phytochemistry* 72, 312–320
11 Chaparro, J.M. *et al.* (2013) Root exudation of phytochemicals in *Arabidopsis* follows specific patterns that are developmentally programmed and correlate with soil microbial functions. *PLoS ONE* 8, e55731
12 Badri, D.V. *et al.* (2010) Root secretion of phytochemicals in *Arabidopsis* is predominantly not influenced by diurnal rhythms. *Mol. Plant* 3, 491–498
13 Liao, C. *et al.* (2012) Comparative analyses of three legume species reveals conserved and unique root extracellular proteins. *Proteomics* 12, 3219–3228
14 Ma, W. *et al.* (2010) The mucilage proteome of maize (*Zea mays* L.) primary roots. *J. Proteome Res.* 9, 2968–2976
15 Lanoue, A. *et al.* (2010) De novo biosynthesis of defense root exudates in response to *Fusarium* attack in barley. *New Phytol.* 185, 577–588
16 Hasegawa, M. *et al.* (2010) Phytoalexin accumulation in the interaction between rice and the blast fungus. *Mol. Plant Microbe Interact.* 23, 1000–1011
17 Wurst, S. *et al.* (2010) Microorganisms and nematodes increase levels of secondary metabolites in roots and root exudates of *Plantago lanceolata*. *Plant Soil* 329, 117–126
18 Vuković, R. *et al.* (2013) Genetic elicitation by inducible expression of β-cryptogein stimulates secretion of phenolics from *Coleus blumei* hairy roots. *Plant Sci.* 199–200, 18–28
19 Bais, H.P. *et al.* (2002) Root specific elicitation and antimicrobial activity of rosmarinic acid in hairy root cultures of *Ocimum basilicum*. *Plant Physiol. Biochem.* 40, 983–995
20 Badri, D.V. and Vivanco, J.M. (2009) Regulation and function of root exudates. *Plant Cell Environ.* 32, 666–681
21 Badri, D.V. *et al.* (2008) Transcriptome analysis of *Arabidopsis* roots treated with signaling compounds: a focus on signal transduction, metabolic regulation and secretion. *New Phytol.* 179, 209–223
22 Ruiz-May, E. *et al.* (2009) Differential secretion and accumulation of terpene indole alkaloids in hairy roots of *Catharanthus roseus* treated with methyl jasmonate. *Mol. Biotechnol.* 41, 278–285
23 Ahmad, S. *et al.* (2011) Benzoxazinoid metabolites regulate innate immunity against aphids and fungi in maize. *Plant Physiol.* 157, 317–327
24 Park, W.J. *et al.* (2004) Release of the benzoxazinoids defense molecules during lateral- and crown root emergence in *Zea mays*. *J. Plant Physiol.* 161, 981–985
25 Steeghs, M. *et al.* (2004) Proton-transfer-reaction mass spectrometry as a new tool for real time analysis of root-secreted volatile organic compounds in *Arabidopsis*. *Plant Physiol.* 135, 47–58
26 De-la-Peña, C. *et al.* (2008) Root-microbe communication through protein secretion. *J. Biol. Chem.* 283, 25247–25255
27 Badri, D.V. *et al.* (2013) Application of natural blends of phytochemicals derived from the root exudates of *Arabidopsis* to the soil reveal that phenolic-related compounds predominantly modulate the soil microbiome. *J. Biol. Chem.* 288, 4502–4512
28 Cai, T. *et al.* (2009) Host legume-exuded antimetabolites optimize the symbiotic rhizosphere. *Mol. Microbiol.* 73, 507–517
29 Wang, Y. *et al.* (2013) A novel *Arabidopsis*-oomycete pathosystem: differential interactions with *Phytophthora capsici* reveal a role for

camalexin, indole glucosinolates and salicylic acid in defence. *Plant Cell Environ.* 36, 1192–1203
30 Rookes, J.E. *et al.* (2008) Elucidation of defence responses and signalling pathways induced in *Arabidopsis thaliana* following challenge with *Phytophthora cinnamomi*. *Physiol. Mol. Plant Pathol.* 72, 151–161
31 Cesco, S. *et al.* (2010) Release of plant-borne flavonoids into the rhizosphere and their role in plant nutrition. *Plant Soil* 329, 1–25
32 Weisskopf, L. *et al.* (2006) White lupin has developed a complex strategy to limit microbial degradation of secreted citrate required for phosphate acquisition. *Plant Cell Environ.* 29, 919–927
33 Wu, Q. and VanEtten, H.D. (2004) Introduction of plant and fungal genes into pea (*Pisum sativum* L.) hairy roots reduces their ability to produce pisatin and affects their response to a fungal pathogen. *Mol. Plant Microbe Interact.* 17, 798–804
34 Cannesan, M.A. *et al.* (2011) Association between border cell responses and localized root infection by pathogenic *Aphanomyces euteiches*. *Ann. Bot. (Lond.)* 108, 459–469
35 Schmelz, E.A. *et al.* (2011) Identity, regulation, and activity of inducible diterpenoid phytoalexins in maize. *Proc. Natl. Acad. Sci. U.S.A.* 108, 5455–5460
36 Hiltpold, I. *et al.* (2011) Systemic root signalling in a belowground, volatile-mediated tritrophic interaction. *Plant Cell Environ.* 34, 1267–1275
37 Hiltpold, I. and Turlings, T.C. (2012) Manipulation of chemically mediated interactions in agricultural soils to enhance the control of crop pests and to improve crop yield. *J. Chem. Ecol.* 38, 641–650
38 Rasmann, S. *et al.* (2005) Recruitment of entomopathogenic nematodes by insect-damaged maize roots. *Nature* 434, 732–737
39 Robert, C.A. *et al.* (2012) Herbivore-induced plant volatiles mediate host selection by a root herbivore. *New Phytol.* 194, 1061–1069
40 Chen, F. *et al.* (2004) Characterization of a root-specific *Arabidopsis* terpene synthase responsible for the formation of the volatile monoterpene 1,8-cineole. *Plant Physiol.* 135, 1956–1966
41 Xie, X. and Yoneyama, K. (2010) The strigolactone story. *Annu. Rev. Phytopathol.* 48, 93–117
42 Dor, E. *et al.* (2011) The synthetic strigolactone GR24 influences the growth pattern of phytopathogenic fungi. *Planta* 234, 419–427
43 Torres-Vera, R. *et al.* (2013) Do strigolactones contribute to plant defence? *Mol. Plant Pathol.* http://dx.doi.org/10.1111/mpp.12074
44 Iven, T. *et al.* (2012) Transcriptional activation and production of tryptophan-derived secondary metabolites in arabidopsis roots contributes to the defense against the fungal vascular pathogen *Verticillium longisporum*. *Mol. Plant* 5, 1389–1402
45 Millet, Y.A. *et al.* (2010) Innate immune responses activated in *Arabidopsis* roots by microbe-associated molecular patterns. *Plant Cell* 22, 973–990
46 Bednarek, P. *et al.* (2005) Structural complexity, differential response to infection, and tissue specificity of indolic and phenylpropanoid secondary metabolism in *Arabidopsis* roots. *Plant Physiol.* 138, 1058–1070
47 Consonni, C. *et al.* (2010) Tryptophan-derived metabolites are required for antifungal defense in the *Arabidopsis* mlo2 mutant. *Plant Physiol.* 152, 1544–1561
48 Bressan, M. *et al.* (2009) Exogenous glucosinolate produced by *Arabidopsis thaliana* has an impact on microbes in the rhizosphere and plant roots. *ISME J.* 3, 1243–1257
49 Schreiner, M. *et al.* (2011) Enhanced glucosinolates in root exudates of *Brassica rapa* ssp. rapa mediated by salicylic acid and methyl jasmonate. *J. Agric. Food Chem.* 59, 1400–1405
50 Schlaeppi, K. *et al.* (2010) Disease resistance of *Arabidopsis* to *Phytophthora brassicae* is established by the sequential action of indole glucosinolates and camalexin. *Plant J.* 62, 840–851
51 Schlaeppi, K. and Mauch, F. (2010) Indolic secondary metabolites protect *Arabidopsis* from the oomycete pathogen *Phytophthora brassicae*. *Plant Signal. Behav.* 5, 1099–1101
52 Youssef, R.M. *et al.* (2013) Ectopic expression of AtPAD4 broadens resistance of soybean to soybean cyst and root-knot nematodes. *BMC Plant Biol.* 13, 67
53 Wen, F. *et al.* (2007) Extracellular proteins in pea root tip and border cell exudates. *Plant Physiol.* 143, 773–783
54 Gunawardena, U. and Hawes, M.C. (2002) Tissue specific localization of root infection by fungal pathogens: role of root border cells. *Mol. Plant Microbe Interact.* 15, 1128–1136
55 Gunawardena, U. *et al.* (2005) Tissue-specific localization of pea root infection by *Nectria haematococca*. Mechanisms and consequences. *Plant Physiol.* 137, 1363–1374
56 Stubbs, V.E. *et al.* (2004) Root border cells take up and release glucose-C. *Ann. Bot. (Lond.)* 93, 221–224
57 Vicré, M. *et al.* (2005) Root border-like cells of *Arabidopsis*. Microscopical characterization and role in the interaction with rhizobacteria. *Plant Physiol.* 138, 998–1008
58 Driouich, A. *et al.* (2007) Formation and separation of root border cells. *Trends Plant Sci.* 12, 14–19
59 Hawes, M.C. *et al.* (2012) Roles of root border cells in plant defense and regulation of rhizosphere microbial populations by extracellular DNA 'trapping'. *Plant Soil* 355, 1–16
60 Griffin, G. *et al.* (1976) Nature and quantity of sloughed organic matter produced by roots of axenic peanut plants. *Soil Biol. Biochem.* 8, 29–32
61 Odell, R.E. *et al.* (2008) Stage-dependent border cell and carbon flow from roots to rhizosphere. *Am. J. Bot.* 95, 441–446
62 Curlango-Rivera, G. *et al.* (2010) Transient exposure of root tips to primary and secondary metabolites: impact on root growth and production of border cells. *Plant Soil* 332, 267–275
63 Hawes, M.C. *et al.* (2000) The role of root border cells in plant defense. *Trends Plant Sci.* 5, 128–133
64 Wen, F. *et al.* (2007) Proteins among the polysaccharides: a new perspective on root cap slime. *Plant Signal. Behav.* 2, 410–412
65 von Köckritz-Blickwede, M. and Nizet, V. (2009) Innate immunity turned inside-out: antimicrobial defense by phagocyte extracellular traps. *J. Mol. Med.* 87, 775–783
66 Brinkmann, V. *et al.* (2004) Neutrophil extracellular traps kill bacteria. *Science* 303, 1532–1535
67 Medina, E. (2009) Neutrophil extracellular traps: a strategic tactic to defeat pathogens with potential consequences for the host. *J. Innate Immun.* 1, 176–180
68 Hawes, M.C. *et al.* (2011) Extracellular DNA: the tip of root defenses? *Plant Sci.* 180, 741–745
69 Yazaki, K. *et al.* (2008) Secondary transport as an efficient Membrane transport mechanism for plant secondary metabolites. *Phytochem. Rev.* 7, 513–524
70 Kang, J. *et al.* (2011) Plant ABC transporters. *Arabidopsis Book* 9, e0153
71 Furukawa, J. *et al.* (2007) An aluminum-activated citrate transporter in barley. *Plant Cell Physiol.* 48, 1081–1091
72 Fujii, M. *et al.* (2012) Acquisition of aluminium tolerance by modification of a single gene in barley. *Nat. Commun.* 3, 713
73 Magalhaes, J.V. *et al.* (2007) A gene in the multidrug and toxic compound extrusion (MATE) family confers aluminum tolerance in sorghum. *Nat. Genet.* 39, 1156–1161
74 Liu, J. *et al.* (2009) Aluminum-activated citrate and malate transporters from the MATE and ALMT families function independently to confer *Arabidopsis* aluminum tolerance. *Plant J.* 57, 389–399
75 Maron, L.G. *et al.* (2010) Two functionally distinct members of the MATE (multi-drug and toxic compound extrusion) family of transporters potentially underlie two major aluminum tolerance QTLs in maize. *Plant J.* 61, 728–740
76 Ishimaru, Y. *et al.* (2011) A rice phenolic efflux transporter is essential for solubilizing precipitated apoplasmic iron in the plant stele. *J. Biol. Chem.* 286, 24649–24655
77 Birnbaum, K. *et al.* (2003) A gene expression map of the *Arabidopsis* root. *Science* 302, 1956–1960
78 Stukkens, Y. *et al.* (2005) NpPDR1, a pleiotropic drug resistance-type ATP-binding cassette transporter from *Nicotiana plumbaginifolia*, plays a major role in plant pathogen defense. *Plant Physiol.* 139, 341–352
79 Bienert, M.D. *et al.* (2012) A pleiotropic drug resistance transporter in *Nicotiana tabacum* is involved in defense against the herbivore *Manduca sexta*. *Plant J.* 72, 745–757
80 Meyer, S. *et al.* (2010) Intra- and extra-cellular excretion of carboxylates. *Trends Plant Sci.* 15, 40–47

81 Crouzet, J. *et al.* (2013) NtPDR1, a plasma membrane ABC transporter from *Nicotiana tabacum*, is involved in diterpene transport. *Plant Mol. Biol.* 82, 181–192
82 Kretzschmar, T. *et al.* (2012) A petunia ABC protein controls strigolactone-dependent symbiotic signalling and branching. *Nature* 483, 341–344
83 Loyola-Vargas, V.M. *et al.* (2007) Effect of transporters on the secretion of phytochemicals by the roots of *Arabidopsis thaliana*. *Planta* 225, 301–310
84 Sugiyama, A. *et al.* (2007) Involvement of a soybean ATP-binding cassette-type transporter in the secretion of genistein, a signal flavonoid in legume-*Rhizobium* symbiosis. *Plant Physiol.* 144, 2000–2008
85 Badri, D.V. *et al.* (2008) Altered profile of secondary metabolites in the root exudates of *Arabidopsis* ATP-binding cassette transporter mutants. *Plant Physiol.* 146, 762–771
86 Badri, D.V. *et al.* (2009) An ABC transporter mutation alters root exudation of phytochemicals that provoke an overhaul of natural soil microbiota. *Plant Physiol.* 151, 2006–2017
87 Rodríguez-Celma, J. *et al.* (2013) Mutually exclusive alterations in secondary metabolism are critical for the uptake of insoluble iron compounds by *Arabidopsis* and *Medicago truncatula*. *Plant Physiol.* 162, 1473–1485
88 Fourcroy, P. *et al.* (2013) Involvement of the ABCG37 transporter in secretion of scopoletin and derivatives by Arabidopsis roots in response to iron deficiency. *New Phytol.* http://dx.doi.org/10.1111/nph.12471
89 Ito, H. and Gray, W.M. (2006) A gain-of-function mutation in the *Arabidopsis* pleiotropic drug resistance transporter PDR9 confers resistance to auxinic herbicides. *Plant Physiol.* 142, 63–74
90 Ruzicka, K. *et al.* (2010) *Arabidopsis* PIS1 encodes the ABCG37 transporter of auxinic compounds including the auxin precursor indole-3-butyric acid. *Proc. Natl. Acad. Sci. U.S.A.* 107, 10749–10753
91 Bultreys, A. *et al.* (2009) *Nicotiana plumbaginifolia* plants silenced for the ATP-binding cassette transporter gene NpPDR1 show increased susceptibility to a group of fungal and oomycete pathogens. *Mol. Plant Pathol.* 10, 651–663
92 Sasabe, M. *et al.* (2002) cDNA cloning and characterization of tobacco ABC transporter: NtPDR1 is a novel elicitor-responsive gene. *FEBS Lett.* 518, 164–168
93 Sugiyama, A. *et al.* (2008) Signaling from soybean roots to rhizobium: an ATP-binding cassette-type transporter mediates genistein secretion. *Plant Signal. Behav.* 3, 38–40
94 Banasiak, J. *et al.* (2013) A *Medicago truncatula* ABC transporter belonging to subfamily G modulates the level of isoflavonoids. *J. Exp. Bot.* 64, 1005–1015
95 Weisskopf, L. *et al.* (2008) Spatio-temporal dynamics of bacterial communities associated with two plant species differing in organic acid secretion: a one-year microcosm study on lupin and wheat. *Soil Biol. Biochem.* 40, 1772–1780
96 Bulgarelli, D. *et al.* (2012) Revealing structure and assembly cues for *Arabidopsis* root-inhabiting bacterial microbiota. *Nature* 488, 91–95
97 Fang, Z.D. *et al.* (2006) Combinatorially selected defense peptides protect plant roots from pathogen infection. *Proc. Natl. Acad. Sci. U.S.A.* 103, 18444–18449
98 Fang, Z.D. *et al.* (2010) Combinatorially selected peptides for protection of soybean against *Phakopsora pachyrhizi*. *Phytopathology* 100, 1111–1117
99 Strader, L.C. and Bartel, B. (2009) The *Arabidopsis* PLEIOTROPIC DRUG RESISTANCE8/ABCG36 ATP binding cassette transporter modulates sensitivity to the auxin precursor indole-3-butyric acid. *Plant Cell* 21, 1992–2007
100 Langowski, L. *et al.* (2010) Trafficking to the outer polar domain defines the root-soil interface. *Curr. Biol.* 20, 904–908

# Root exudates as integral part of belowground plant defense

Ulrike Baetz

Institute of Plant Biology, University of Zurich, Zollikerstrasse 107, CH-8008 Zurich, Switzerland

Book Chapter in 'Belowground defense strategies in plants';

Springer series 'Signaling and communication in plants';

Edited by Christine Vos and Kemal Kazan

**Summary**

Root exudates comprise a heterogeneous group of compounds that display various effects on soil-borne organisms, including stimulation, attraction, but also repellence and inhibition. Therefore, root-secreted chemicals can assist belowground plant defense through direct and/or indirect mechanisms. Direct defense strategies exploited by roots include the secretion of phytochemicals with antimicrobial, insecticide or nematicide properties. In contrast, other root exudates recruit or influence beneficial organisms to serve as biological weapons against plant aggressors, a mechanism termed indirect plant defense. Since rhizosecretion fundamentally shapes the composition of soil-inhabiting organisms and contributes to plant survival, the quality and quantity of defense root exudates is tightly controlled. Various environmental and endogenous factors can stimulate the release of phytochemicals that exhibit precisely targeted bioactivities. On the molecular level, several primary active transport proteins have been demonstrated to affect the composition of defense root exudates in the rhizosphere. In this chapter, we will focus our attention on direct and indirect defense strategies mediated by root exudates. In addition, we will shed light on regulatory mechanisms of defense-related root exudation that prevent belowground disease and ensure optimal plant performance.

**Key Words**

ABC transporter; defense; rhizosphere; root exudates; tripartite interaction

## Introduction

Plants interact with a multitude of soil-borne organisms in complex biological and ecological processes in the narrow zone surrounding the root system, termed the rhizosphere. These beneficial, antagonistic or neutral interactions have a profound effect on plant health and survival, and shape the soil microbiome.

Within the rhizosphere, roots are constantly exposed to biotic stressors, ranging from plant disease-causing pathogens such as bacteria, fungi and oomycetes, to nematodes and insects. Although being sessile organisms anchored to the soil, plants are not just passive victims of these antagonistic microbes and invertebrates that occur in the vicinity of roots. In fact, roots are equipped with an arsenal of defense compounds that can be released into the rhizosphere to counteract plant attackers (Baetz and Martinoia, 2014). However, the significance of root exudates as a direct or indirect belowground protection has long been underestimated, presumably due to literally being out of sight. Secreted substances can be of low or high molecular weight. Low molecular weight root exudates include a variety of defense secondary metabolites such as flavonoids, glucosinolates, and terpenoids. Protective high molecular weight compounds such as antimicrobial proteins and secreted extracellular DNA also contribute to the local belowground resistance. The tremendous metabolic diversity of root exudates has been progressively elucidated in the past decade through the identification and characterization of numerous novel constitutively secreted and inducible compounds, and previously undescribed classes of defense molecules. Equally, genes and biosynthetic pathways involved in the production of these phytochemicals have been gradually deciphered. A deepened knowledge of phytochemical properties, their composition in the rhizosphere and their impact on soil-inhabiting organisms is crucial to understand the diverse nature of root exudate-mediated defense mechanisms that protect plants against pathogens and invaders. It has been demonstrated that some root exudates exhibit antibacterial, antifungal, nematicide or insecticide properties that directly assist the plant in coping with antagonistic organisms. Other root exudates are released from damaged roots to attract natural enemies of the attackers (such as carnivorous nematodes) to indirectly protect plants. Another highly sophisticated indirect defense strategy of plants is to outsource defense compound production. On

that purpose, root exudates attract beneficial microorganisms that release secondary metabolites such as antibiotics with an antagonistic effect on the root-attacking pathogen.
In this chapter, we will compile the roles of root exudates in various direct and indirect, targeted belowground defense processes that protect plants against soil-borne diseases. In addition, we will discuss regulation mechanisms of root exudation, e.g. inducible substance production and controlled secretion, that collectively make root exudate-mediated belowground plant defense a highly efficient process.

## Root exudation as a direct defense strategy against detrimental soil-borne organisms

In the rhizosphere, roots face relentless harmful attack through the presence of plant disease-causing pathogens (e.g. bacteria, fungi and oomycetes), as well as root-damaging animals (in particular nematodes and insects). In the following, we will illustrate with selected examples how aggressors are being repelled, inhibited or killed by certain root-secreted phytochemicals in order to confer direct defense against belowground plant diseases.

**Bacteria.** The bacterial community in the soil is diverse in its composition, ranging from beneficial plant growth-promoting bacteria to bacteria that infect roots and exhibit harmful effects. Plant-derived molecules can act as chemical signals that stimulate or repress microbes. Thereby, root exudates fundamentally drive the selection of bacteria inhabiting the rhizosphere. Shifts in root exudate blends, as observed in an Arabidopsis (*Arabidopsis thaliana*) mutant impaired in root exudation, elicited significant compositional alterations in bacteria that colonize the rhizosphere (Badri et al., 2009). Furthermore, it has been recently reported that merely the application of root exudates collected from Arabidopsis modulated the overall native bacterial community in the soil, even in the absence of the plant (Badri et al., 2013). Conversely, the chemical profile of root-secreted molecules is largely dependent on distinct bacterial members present in the vicinity of roots. For instance, the formation and release of the

antimicrobial monoterpene 1,8-cineole was induced upon compatible interactions between Arabidopsis roots and the bacterial pathogen *Pseudomonas syringae* DC3000 (Steeghs et al., 2004, Kalemba et al., 2002). In another study, Arabidopsis roots that were exposed to *P. syringae* secreted significantly higher amounts of defense-related proteins, whereas the incompatible interaction with a bacterial symbiont did not induce the secretion of these protective proteins (De-la-Peña et al., 2008).

A phytochemical known to feature direct antibacterial activity particularly against *Pseudomonas aeruginosa* is rosmarinic acid (RA) (Bais et al., 2002). This multifunctional caffeic acid ester is produced in hairy root cultures of sweet basil (*Ocimum basilicum* L.), and exuded in response to pathogen attack. However, the compound is absent from exudates of unchallenged root cultures (Bais et al., 2002). Arabidopsis root exudates that were supplemented with exogenous RA prior infection with pathogenic *P. aeruginosa* strains, highly reduced pathogenicity under in *vitro* and in *vivo* conditions (Walker et al., 2004). Without supplementation, Arabidopsis roots displayed a high level of susceptibility to *P. aeruginosa* resulting in mortality. Similarly, the induction of RA secretion by sweet basil roots before infection conferred resistance to *P. aeruginosa* (Walker et al., 2004). Hence, host plants can deliberately release antibacterial molecules into the rhizosphere that directly counteract root colonization of pathogenic bacteria and plant mortality.

**Fungi and oomycetes.** Tremendous yield losses result from fungal root invasion every year, emphasizing the necessity to study the crosstalk between plants and fungi, and to elucidate root exudates that confer direct disease resistance. In fact, oomycetes are phylogenetically distinct organisms, but show high physiological and morphological similarities to fungi. Therefore, fungi and oomycetes will be both covered in this section.

A potent root-secreted antimicrobial compound that is implemented into defense mechanisms against oomycete pathogens is the pea (*Pisum sativum*) isoflavonoid pisatin (Cannesan et al., 2011). Once pea roots were challenged with the oomycete *Aphanomyces euteiches*, the biosynthesis and release of pisatin into the rhizosphere was induced (Cannesan et al., 2011). Interestingly, the inoculation also had a stimulatory effect on border cell production of pea. Border cells are metabolically active cells at the

root periphery that originate and detach from the root cap meristem (Stubbs et al., 2004, Vicré et al., 2005, Driouich et al., 2007). They assist the growing root tip during the mechanical penetration of the soil by decreasing frictional resistance at the root-soil interface (Driouich et al., 2007). In addition, antimicrobial molecules in the rhizosphere largely derive from cap and border cells (Hawes et al., 2012, Griffin et al., 1976, Odell et al., 2008), revealing a link between the *A. euteiches* induced formation of border cells and the increased pisatin exudation (Cannesan et al., 2011). The exposure of pea root tips encompassing border cells to exogenous pisatin, in turn, led to the upregulation of border cell production in *vitro* (Curlango-Rivera et al., 2010). Hence, border cells and their exudates account for a local protective shield that is strengthened in response to pathogen invasion (Cannesan et al., 2011, Hawes et al., 2012, Curlango-Rivera et al., 2010). Because a correlation was observed between border cell separation and the induction of protein secretion, Wen et *al*. (2007) proteolytically degraded the root cap secretome during inoculation with the pea-pathogenic fungus *N. haematococca*. The researcher demonstrated that protease treatment increased the percentage of infected root tips significantly, providing evidence that root-secreted defense proteins from border cells contribute fundamentally to the resistance of pea roots to fungal infection (Wen et al., 2007). Detailed proteome analysis of root exudates of several plant species confirmed the secretion of antimicrobial enzymes and demonstrated dynamic compositional changes during development and upon pathogenic interactions (De-la-Peña et al., 2010, Shinano et al., 2011, Liao et al., 2012, Ma et al., 2010, De-la-Peña et al., 2008, Wen et al., 2007). Unexpectedly, besides defense-related proteins, also the DNA-binding protein histone H4 was detected in border cell exudates of pea (Wen et al., 2007). Histone-linked extracellular DNA (exDNA) is thought to have a critical role in defense against microbial pathogens in mammals (von Köckritz-Blickwede and Nizet, 2009, Brinkmann et al., 2004, Medina, 2009). In plants, exDNA linked to histone proteins has been found to be exuded from root border cells and suggested to be a component of direct belowground defense against fungal invasion (Wen et al., 2009). Similar to proteolytic solubilisation of exuded proteins, nuclease treatment of pea root tips resulted in enhanced susceptibility to fungal infection by *N. haematococca* (Wen et al., 2009). However, the distinct mechanism of how exDNA inhibits pathogen infection awaits elucidation (Hawes et al., 2011, Hawes et al., 2012). In addition to

protective proteins and exDNA, also low-molecular weight antimicrobial root exudates are proven direct chemical weapons against soil-borne diseases of fungal origin. For instance, the phenolic compound *t*-cinnamic acid potently protects barley (*Hordeum vulgare*) against the soil-borne fungus *Fusarium graminearum* (Lanoue et al., 2010a, Lanoue et al., 2010b).

**Nematodes.** Nematodes are worm-like eukaryotic invertebrates that consume bacteria, fungi or other nematodes, and some can parasitize plants. Intense research on root-secreted compounds uncovered attractants that influence the chemotaxis response of beneficial nematodes or assist pathogenic nematodes in host-recognition. Other phytochemicals have been found to exhibit nematode-antagonistic properties (Reynolds et al., 2011, Curtis, 2008, Hiltpold and Turlings, 2012). Lilley et *al*. (2011) investigated the potency of a root-exuded direct defense compound against nematodes. The researchers showed that the root cap targeted expression and release of a nematode-repellent chemo-disruptive peptide in *Arabidopsis thaliana* reduced the establishment of the beet cyst nematode *Heterodera schachtii* (Lilley et al., 2011). In line with this it was found that transgenic *Solanum tuberosum* (potato) that secreted this repellent peptide from their roots suppressed parasitism by the potato cyst nematode *Globodera pallida* (Lilley et al., 2011, Liu et al., 2005). In another study, a genetic approach was used to broaden the resistance of soybean (*Glycine max*) against nematodes. An Arabidopsis gene that modulates synthesis of the antimicrobial camalexin and other defense-related responses was ectopically overexpressed in roots of soybean (Youssef et al., 2013), resulting in enhanced resistance to the parasitic soybean cyst nematode (*Heterodera glycines*) and the root-knot nematode (*Meloidogyne incognita*). Lauric acid, a naturally occurring, highly abundant root exudate from crown daisy (*Chrysanthemum coronarium*) also limited parasitic damage by decreasing the number of *M*. *incognita* and suppressing nematode infection (Dong et al., 2014). Likewise, total root cap exudates from various legumes showed the ability to repel root-knot nematodes in sand assays (Zhao et al., 2000). In summary, root exudates can have direct nematotoxic or repelling effects to ensure protection of the roots. However, in contrast to compounds with antimicrobial activity, examples for nematicide root exudates remain limited.

**Insects.** As plants cannot escape belowground insects and root-feeding causes tremendous tissue damage, roots employ elegant defense strategies to counteract herbivory. For instance, the semi-volatile diterpene hydrocarbon, rhizathalene A, is constitutively produced and released by non-infected Arabidopsis roots (Vaughan et al., 2013). Plants that are deficient in rhizathalene A production were found to be less resistant to herbivory by the fungus gnat (*Bradysia* ss) and suffered considerable removal of peripheral tissue at larval feeding sites. In this study it was comprehensively shown that rhizathalene A is a local antiherbivore metabolite that is implicated in the direct belowground defense against insect herbivory (Vaughan et al., 2013). The monoterpene 1,8-cineole is another volatile compound that exhibits defense activity. It is released from *Arabidopsis thaliana* roots upon compatible interaction with the herbivore *Diuraphis noxia* (Steeghs et al., 2004). However, little is known about root-released volatiles and other root exudates with insecticidal properties that directly defend plants against root-feeding arthropods. Nevertheless, as discussed in the following, belowground volatile compounds and their protective role were extensively studied as an indirect defense trait.

**Root exudates are a tool to establish indirect plant defense**

Direct defense via root exudation is an effective mean of plants to deal with the constant exposure to pathogenic microbes and invertebrates in the rhizosphere. Besides, by root exudation plants can influence the behavior of phytobeneficial soil organisms to serve defensive roles during belowground diseases. For instance, the orientation of rhizospheric nematodes that are predators of insect aggressors can be altered by root released signals, thereby indirectly conferring resistance to the roots against herbivory (Rasmann et al., 2005). Furthermore, some rhizobacteria species are known for their production of toxic compounds targeting plant pathogens, a process that has been hypothesized to be regulated by root exudates upon infection (Jousset et al., 2011, Haas and Défago, 2005). A scenario in which plants recruit defense-assisting organisms to

counteract pathogen attack is considered indirect belowground plant defense. This tripartite interaction is mediated by root exudates.

**Recruitment of 'natural soldiers' by root exudates.** The concept of indirect defense and the corresponding plant-released signaling compounds have been examined thoroughly in the aboveground terrestrial environment. Leaves emit a complex battery of volatile organic compounds to communicate with their environment and attract predators. Intriguingly, when attacked by belowground herbivores, plants can also attract soil-borne mobile predators such as entomopathogenic nematodes (EPN). In fact, EPNs are plant protagonists, but obligate parasites that kill insect hosts. The pivotal role of root-emitted volatile compounds that act as efficient cues to direct natural enemies such as ENPs specifically to the sites where potential hosts are damaging roots has become increasingly evident in the last years (Hiltpold and Turlings, 2008, Hiltpold et al., 2011). The best studied example of a volatile signal that mediates belowground indirect plant defense is the maize (*Zea mays* L.) sesquiterpene olefin (*E*)-β-caryophyllene (EβC) (Rasmann et al., 2005). EβC is completely absent in healthy maize roots but emitted upon feeding by voracious larvae of the western corn rootworm (WCR), *Diabrotica virgifera virgifera*. Herbivore attack induces the expression of the *terpene synthase 23* (*tps23*) gene, which is involved in the biosynthesis of EβC (Capra et al., 2014, Köllner et al., 2008). The released volatile signal strongly attracts the ENP *Heterorhabditis megidis*, a natural enemy of root-feeding herbivores that assists maize defense by killing WCR larvae (Rasmann et al., 2005).

WCR is a severe pest causing tremendous yield losses particularly on maize roots (Miller et al., 2005). Exploiting naturally produced indirect defense compounds against WCR could provide an effective biological control strategy for crop protection. Degenhardt et *al*. (2009) aimed at promoting plant attractiveness to natural enemies of WCR larvae by genetically introducing EβC emission in maize varieties that are not capable of synthesizing the sesquiterpene due to a lack of *tps23* transcript. On that purpose, a non-emitting maize line was transformed with an (*E*)-β-caryophyllene synthase from oregano (*Origanum vulgare*), resulting in a constitutive emission of EβC (Degenhardt et al., 2009). In field experiments, transformed plants attracted ENPs more efficiently and consequently suffered less root feeding by WCR larvae compared to

non-emitting maize plants. In a subsequent study it has been demonstrated that a constitutive emission of the volatile signal generated also physiological costs such as compromised seed germination, plant growth and yield (Robert et al., 2013). This negative effect on plant fitness was possibly due to an increased attraction of herbivores, including aboveground pests. Ali et *al*. (2010, 2012) similarly exercised caution when investigating the complex effects of belowground volatiles on indirect plant defense. Citrus roots release volatile compounds such as pregeijerene (1,5-dimethylcyclodeca-1,5,7-triene) in response to feeding by the larvae of the root weevil, *Diaprepes abbreviates* (Ali et al., 2010, Ali et al., 2012). The herbivore-induced volatile emission recruited naturally occurring ENPs (*Steinernema diaprepesi*), resulting in an increase of root weevil mortality and, hence, the control of herbivore infestation (Ali et al., 2010, Ali et al., 2012). Yet, further research uncovered that besides the recruitment of beneficial nematodes, herbivore-induced volatiles also allowed more efficient host localization by phytopathogenic nematodes (Ali et al., 2011). Collectively these studies illustrate clearly that consequences evoked by the manipulation of belowground volatile emission should be carefully assessed on multitrophic levels and under field conditions, in order to understand their specificity and minimize detrimental physiological or ecological effects for plants or non-target organisms.

Besides targeting volatile emission another elegant approach to enhance the effectiveness of indirect plant defense is selective breeding of natural enemies for increased responsiveness to a volatile host signal in order to obtain a more efficient natural finding and killing of pests. Hiltpold et *al*. (2010) aimed at improving the attraction of *Heterorhabditis bacteriphora*, one of the most virulent nematodes against WCR larvae, towards EβC (Hiltpold et al., 2010a). After few generations of selection, the researchers isolated a *H*. *bacteriphora* strain that was significantly more attracted to the EβC source than the original strain. Consistently, in field experiments WCR populations that attacked EβC-emitting maize roots were more effectively reduced by the selected strain compared to the original strain. Importantly, control experiments showed that this artificial selection for the responsiveness trait of *H*. *bacteriphora* towards the volatile signal has not considerably altered other essential properties for controlling WCR populations such as the infectiveness of *H*. *bacteriphora* (Hiltpold et al., 2010b, Hiltpold et al., 2010a).

Taken together, the research shows that plants can recruit natural enemies of their soil-borne aggressors through root-released volatiles to indirectly defend the root system. Thoroughly exploited manipulation of indirect plant defense has a great potential as an alternative method to traditional broad-spectrum pesticides in controlling root-pests in agroecosystems.

**Root exudates can stimulate the antimicrobial potency of phytobeneficial microbes.** Besides attracting natural predators of their enemies, plants have established dialogues with beneficial root-colonizing bacteria to protect roots against the attack of deleterious rhizosphere microorganisms. Defense-assisting microbes belong to so called plant growth-promoting rhizobacteria (PGPR) (Compant et al., 2005). PGPR primarily stimulate plant growth by e.g. the production of phytohormones or the enhancement of plant nutrition (Vacheron et al., 2013). In contrast, defense-assisting PGPRs can improve plant health either directly by repelling plant aggressors with the production of antibiotics, or indirectly by eliciting induced systemic resistance in host plants (Compant et al., 2005, Haas and Défago, 2005, Doornbos et al., 2012). However, to date only few studies addressed the role and the chemical nature of plant-derived exudates in the suppression of soil-borne diseases via direct bacterial antagonism (Neal et al., 2012, Neal and Ton, 2013, Santos et al., 2014, Jousset et al., 2011, Haas and Défago, 2005, Notz et al., 2001, Baehler et al., 2005, de Werra et al., 2008, de Werra et al., 2011). Jousset et *al*. (2011) made an elaborate experiment providing compelling evidence that plants are able to influence the metabolism of beneficial rhizosphere-colonizing bacteria through root exudates as part of the indirect belowground plant defense against pathogens. In order to prevent physical contact between the microorganisms, barley plants were grown in a split-root system in which one part of the roots was challenged by the pathogenic oomycete *Pythium ultimum*. The other side was inoculated with the biocontrol bacterium *Pseudomonas fluorescens* CHA0, a PGPR known to assist crop plant defense by producing antifungal chemicals against pathogenic fungi (Haas and Défago, 2005). This separation system allowed the investigation of alterations of bacterial gene expression patterns that are induced by pathogens but mediated by systemic signaling of plants and root exudation (Fig. 1). The researchers found that the expression of the bacterial *phlA* gene was considerably

stimulated following pathogen infection at the other side of the root (Jousset et al., 2011). The expression of this gene reflects the production of the antifungal metabolite 2,4-diacetylphloroglucinol (DAPG), a key component of the biocontrol activity of root-associated bacteria acting in disease suppression (Notz et al., 2001, Bangera and Thomashow, 1999, de Souza et al., 2003). Interestingly, also the composition of exudates from the systemic side at which roots were inoculated with *P. fluorescens* changed in response to the presence of the pathogen *Pythium ultimum* at the other side of the root system (Fig. 1), uncovering candidates of signaling root exudates that provoke changes in antifungal gene expression of beneficial bacteria (Jousset et al., 2011). In summary, first insights have been gained on how antifungal activities of rhizobacteria can be adjusted by root exudates to provide service of indirect defense against plant pathogens. It will be of interest to further explore this tripartite interaction, and investigate how and which plant-derived compounds are released under pathogen pressure and subsequently modulate rapidly the activity of plant-growth promoting rhizobacteria.

**Root exudation- a tightly regulated and highly efficient process**

Root exudation enormously impacts plants as well as the rhizosphere habitat. Firstly, photosynthetically fixed carbon is a valuable resource for plants. Since direct and indirect defense root exudates are a significant carbon cost, sensible and deliberate use is of importance to avoid excessive consumption but guarantee efficient plant defense. Secondly, root exudate blends need to be carefully assembled, since the rhizosphere is composed of a diverse variety of inhabitants such as beneficial and pathogenic organisms that can be differentially affected by certain phytochemicals. On the purpose of accurate plant defense and limited damage to other rhizosphere members, plants have established several strategies to optimize root exudation, including elicitation-induced compound production, tightly regulated export processes, and multiple beneficial compound activities, which will be discussed in the following sections.

**Constitutive versus induced exudation of phytochemicals.** Plants are constantly exposed to soil-borne antagonists. To form a protective buffer zone around roots, certain defense root exudates are constitutively released into the rhizosphere. For instance, rhizathalene A, an antifeedant involved in direct plant defense, is synthesized and secreted from Arabidopsis roots even in the absence of root-feeding insects (Vaughan et al., 2013). Plants secrete a wide array of other defense molecules before pathogen elicitation (Kato-Noguchi et al., 2008, Toyomasu et al., 2008, Wen et al., 2009, De-la-Peña et al., 2010, Shinano et al., 2011, Chaparro et al., 2013, Badri et al., 2010, Liao et al., 2012, Ma et al., 2010, McCully et al., 2008, Dong et al., 2014). Besides a constitutive root exudation, the biosynthesis, accumulation and secretion of certain defense molecules can be induced in the presence of aggressors in the rhizosphere. The phenolic compound *t*-cinnamic acid is an antifungal exudate of barley roots (Lanoue et al., 2010a, Lanoue et al., 2010b). Upon attack of a fungal pathogen, labelling experiments demonstrated the *de novo* biosynthesis and secretion of this aromatic defense metabolite into the rhizosphere. Another example is rosmarinic acid, which is constitutively produced in root tissue, but exclusively released into the rhizosphere in response to root infection (Bais et al., 2002). These studies illustrate that the profile of root exudates is not just diverse in its composition, but also strikingly dynamic, to adjust the identity and amount of defense compounds towards necessity in heterogeneous environments.

**Stimuli that control defense root exudation.** As discussed above, the belowground attack by antagonistic organisms can induce the release of a multitude of defense compounds into the rhizosphere. Astonishingly, upon aboveground attack, intra-plant chemical signals can be relayed to influence root exudation (Bezemer and van Dam, 2005, Robert et al., 2012, Pangesti et al., 2013). Secretion of L-malic acid from Arabidopsis roots is stimulated by infection with the bacterial foliar pathogen *Pseudomonas syringae* pv *tomato* Pst DC3000 (Rudrappa et al., 2008, Lakshmanan et al., 2012). Elevated levels of malic acid in the rhizosphere in turn recruit the beneficial *Bacillus subtilis* FB17 and promote rhizobacterial colonization to enhance plant defense (Rudrappa et al., 2008, Lakshmanan et al., 2012).

Under laboratory conditions, the rhizosecretion process can be elicited also by exogenous application of biotic stress-related signaling molecules such as salicylic acid, nitric oxide or methyl jasmonate (Badri et al., 2008b, Badri and Vivanco, 2009, Ruiz-May et al., 2009, Schreiner et al., 2011). Likewise, an ectopic expression of the oomycetal elicitor β-cryptogein in hairy roots of *Coleus blumei* mimics pathogen attack resulting in an enhanced level of secreted antimicrobial rosmarinic acid in the external culture medium (Vuković et al., 2013). Recently it has been reported that the presence of phytobeneficial bacteria can enhance root volatile emission required for indirect plant defense (Santos et al., 2014). Root colonization with *Azospirillum brasilense* induced higher release of (*E*)-β-caryophyllene from maize roots. Furthermore, larvae of the South American corn rootworm, *Diabrotica speciose*, gained less weight when feeding on rhizobacterium-inoculated roots (Santos et al., 2014).

Besides exogenous stimuli that influence the release of compounds implemented in direct and indirect plant defense, root exudation is also under the control of endogenous genetic programs such as the developmental stage of the plant. In maize benzoxazinoids form a class of defense molecules (Ahmad et al., 2011) that are released during the emergence of lateral and crown roots when the plant is locally and temporally more susceptible (Park et al., 2004). Hence, benzoxazinoids secretion presents a genetically regulated, protective process that alleviates damage at local sites or during discrete developmental stages when infection is more deleterious for the plant. In accordance, the peak of defense-related protein exudation into the rhizosphere can be observed just before flowering (De-la-Peña et al., 2010). Towards later stages of the Arabidopsis life cycle, also the level of putatively antimicrobial phenolic compounds increases in the root exudate profile (Chaparro et al., 2013). Again, the recruitment of phytobeneficial microbes that indirectly prevent root infection through the production of antibacterial compounds is dependent on the growth stage of the plant (Picard et al., 2000, Picard et al., 2004).

Taken together, these studies exemplify that the secretion of defense compounds into the rhizosphere is a tightly controlled, spatio-temporal dynamic process that is regulated by various endogenous and exogenous factors.

**The role of transport proteins in root exudation.** Root exudation is in part mediated by diffusion, channels, and vesicle transport. However, a substantial proportion of root exudates is also secreted actively by transport proteins. First indirect evidence of a primary and secondary active secretion process of plant-derived molecules across the root plasma membrane came from comprehensive pharmacological studies. The use of various inhibitors revealed that the secretion of some root-derived phytochemicals was dependent on ATP hydrolysis (Loyola-Vargas et al., 2007), indicating that active transport systems such as ATP-binding cassette (ABC) transporters might be involved in the release of constituents of the root phytochemical cocktail into the rhizosphere. ABC-type proteins constitute a large family of transporters that are involved in mediating the transport of a wide array of organic substances (Yazaki et al., 2009, Kang et al., 2011, Yazaki et al., 2008). More than 120 genes in the *Arabidopsis thaliana* genome encode for ABC transporter proteins, and some of these genes exhibit strikingly high expression in root cells, raising the potential for their involvement in rhizosecretion processes (Badri et al., 2008a). Subsequent studies in which root exudate (Badri et al., 2008a, Badri et al., 2009) and microbial (Badri et al., 2009) compositions of ABC transporter mutants differed significantly from those of corresponding wild-type plants confirmed the essential role of ABC proteins in root exudation. In addition, these studies revealed that multiple ABC transporters can release the same substrate, and that a discrete ABC transporter can have low substrate specificity and export multiple structurally and functionally unrelated substances (Fig. 2a). The role of *At*ABCG37/*At*PDR9 in mediating the rhizosecretion of not only auxinic compounds (Ito and Gray, 2006, Ruzicka et al., 2010) but also of phenolics as an iron acquisition strategy (Rodríguez-Celma et al., 2013, Fourcroy et al., 2013) supports this observation. Likewise, *At*ABCG36/*At*PDR8 is suggested to export cadmium (Kim et al., 2007) as well as indole-3-butyric acid (Strader and Bartel, 2009) into the rhizosphere.

To date, few ABC transport proteins were proposed to be implemented in the export and accumulation of phytochemicals that confer resistance against soil-borne diseases. For example, silencing *Nt*ABCG5/*Nt*PDR5 from tobacco (*Nicotiana tabacum*) improved larval performance of the herbivore *Manduca sexta*, but also increased slightly the susceptibility to the soil-borne fungus *Fusarium oxysporum*, suggesting a role of this transport protein in defense *inter alia* through root exudation (Bienert et al.,

2012). More evidently, the transporter *Np*PDR1 of *Nicotiana plumbaginifolia* was shown to be involved in belowground plant defense against pathogen invasion (Bultreys et al., 2009, Stukkens et al., 2005). Silencing the ABC transporter accounted for enhanced sensitivity of roots and petals towards several fungal and oomycetal pathogens, possibly due to diminished secretion of antimicrobial compounds such as the diterpene sclareol (Bultreys et al., 2009, Stukkens et al., 2005, Jasiński et al., 2001). Besides these obvious connections between a transporter, its substrate and a direct effect on the rhizosphere microbiome, further research on ABC proteins implemented in root exudation uncovered a complex role for transport systems in determining the composition of root exudates (Fig. 2). Certain ABC transporter genes are subject of intense transcriptional regulation. The expression of *Nt*PDR1 from tobacco can be modified by microbial elicitation and positively correlates with export rates of antipathogenic diterpenes into the extracellular medium (Crouzet et al., 2013, Sasabe et al., 2002). In line with this, the transcriptional regulation of ABC transporters in response to their substrates has been reported, e.g. (Kretzschmar et al., 2012). The level of an external phytochemical can be dependent on the transport protein abundance, but also on the substrate availability. For instance, nitrogen deficiency can elicit the increased production of the flavonoid signaling molecule genistein resulting in its secretion from soybean roots to initiate rhizobium symbiosis (Sugiyama et al., 2008). Interestingly, the transport machinery involved in genistein export is constitutively active, regardless of the nitrogen availability (Sugiyama et al., 2007) (Fig. 2b). Yet, other ABC transporters themselves feature regulatory functions influencing biosynthesis and exudation of defense phytochemicals. *Medicago truncatula* roots silenced for *Mt*ABCG10, a close homolog of *Nt*PDR1 (Sasabe et al., 2002, Crouzet et al., 2013) were rapidly infected by *Fusarium oxysporum* (Banasiak et al., 2013). The silencing resulted also in a reduction of the antimicrobial medicarpin as well as its precursors in root tissue and exudates. Thus, during belowground biotic stress response *Mt*ABCG10 supposedly modulates isoflavonoid levels associated with the *de novo* biosynthesis of defense compounds (Banasiak et al., 2013). Another persuasive study showed that the root exudate profile of the Arabidopsis mutant *abcg30* exhibits a decreased secretion of certain compounds whereas other exudates accumulated to higher levels in the mutant plant rhizosphere (Badri et al., 2009). These findings suggest

that ABC transporters have a sophisticated role in mediating substrate export into the rhizosphere, but also in directly or indirectly modifying other physiological processes such as the biosynthesis of secondary metabolites and/or the expression of other transporters involved in root exudation (Fig. 2c).

Besides ABC transporters, members of the multidrug and toxic compound extrusion (MATE) protein family have been demonstrated to actively transport secondary metabolites across plant membranes (Yazaki et al., 2008). A MATE transporter in the stele of rice roots was found to facilitate efflux of phenolic compounds into the xylem (Ishimaru et al., 2011). It has been speculated that similar transporters might be responsible for the secretion of antimicrobial compounds into the soil. A crucial root exudation process that has been shown to be mediated by MATE proteins is the release of citrate into the rhizosphere (Furukawa et al., 2007, Fujii et al., 2012, Magalhaes et al., 2007, Liu et al., 2009, Maron et al., 2010). Since citrate is a carbon source for many microorganisms, this exudation may have a vital impact on microbial soil communities. However, to our knowledge, no evidence has been provided for an implementation of MATE transport proteins in direct or indirect belowground plant defense.

Taken together, active transport systems largely influence the composition of root exudates, and can dynamically adjust the quality and quantity of certain phytochemicals in response to changes in microbial rhizosphere communities. Identification and investigation of transporter proteins implemented in regulated rhizosecretion processes is fundamental to understand belowground direct and indirect plant defense.

**One phytochemical- additive defense functions.** In the previous sections we demonstrated that the release of defense-related root exudates is inducible, how this induction can be elicited, and that regulated secretion is mediated on the molecular level by transport proteins. In this section, we will highlight that single root exudates can target multiple rhizosphere organisms and may elicit dissimilar responses. Belowground plant defense becomes highly efficient if different exudate bioactivities are appropriately fine-tuned to allow an opposite effect on plant mutualists and antagonists.

Some root-secreted defense compounds affect a highly specific spectrum of rhizosphere organisms. For instance, the legume root exudate canavanine exhibits cytotoxic

properties against many soil bacteria, but initiates the detoxification machinery of rhizobacteria, accounting for their resistance to canavanine (Cai et al., 2009). In Arabidopsis, resistance to *Phytophthora capsici* relies on the production of the antimicrobial camalexin (Wang et al., 2013); however, this defense compound does not confer resistance to the oomycetes pathogen *Phytophthora cinnamomi* (Rookes et al., 2008). Notably, this high target specificity of root exudates can be partially explained by variations in the tolerance to specific defense molecules based on the efficiency of active detoxification and efflux processes between different microbes (Cai et al., 2009, Bouarab et al., 2002).

Other root exudates have a broader recipient spectrum and affect various rhizosphere organisms, including beneficial and pathogenic members (Badri et al., 2013). This can be exemplified by the different effects of green pea (*Pisum sativa*) root exudates on the behavior of beneficial and plant-parasitic nematodes (Hiltpold et al., 2015). Low concentrations of root exudates induced loss of mobility and a state of reversible quiescence in antagonistic nematodes, protecting the roots against infection. In sharp contrast, the activity and infectiousness of beneficial entomopathogenic nematodes (EPNs) enhanced markedly under low root exudate concentrations. Dual bioactivity in the rhizosphere was also observed for benzoxazinoids, a class of phytochemicals detected in maize root exudates. Plant-beneficial *Pseudomonas putida* were found to be recruited in response to exudation of a benzoxazinoid metabolite from maize roots during relatively young and vulnerable growth stages (Neal et al., 2012). The root colonization stimulated jasmonic acid-dependent defense pathways in maize entailing a beneficial systemic defense priming in the plant (Neal and Ton, 2013). Conversely, benzoxazinoids were previously shown to exert antimicrobial and insecticidal activities and function in direct above- and belowground plant defense against pests and diseases (Niemeyer, 2009, Park et al., 2004, Ahmad et al., 2011). Hence, released benzoxazinoids provide coupled profitable service for the plant by attracting beneficial microbes (indirect plant defense) and repelling pathogenic organisms in the maize rhizosphere (direct plant defense). Similarly, dimethyl disulphide emitted from cabbage (*Brassica napus*) roots invested by the cabbage root fly *Delia radicum* showed multiple defense bioactivities, the inhibition of ovipostion by cabbage root fly females, and the attraction of natural enemies of *D. radicum* (Ferry et al., 2007, FERRY et al., 2009). In

summary, root exudates with directed dual functions that complement each other enhance the efficiency of belowground plant protection by broadening the spectrum of defense modes and lowering carbon costs for the plant.

## Summary

Interactions between plants and other organisms are as fascinating as they are complex. Plants can, for instance, communicate with arbuscular mycorrhizal fungi to initiate a mutually beneficial symbiosis. However, not all organisms that plants are exposed to have neutral or even advantageous impacts. Negative interactions and defense strategies against antagonistic organisms is an intensively investigated field of biology. Previously, researchers focused on interactions and processes that appear in the visible, more easily accessible half of the plant, the aerial part. However, since tremendous yield losses are caused by root-feeding and infection, it is equally crucial to study plant defense mechanisms belowground.

Root exudates in the rhizosphere serve as chemical mediators of positive interactions between plants and soil-borne organisms, and as defense compounds in negative interactions. During plant attack root exudates are engaged in two types of defense traits, the direct and the indirect defense. Root exudates with direct defense properties act repelling, inhibiting or killing on plant aggressors such as pathogens and feeders. In contrast, root exudates incorporated in indirect plant defense initiate the interaction with beneficial organisms that counteract aggressors. The chemical nature and mode of action of various compounds involved in direct and indirect defense has been progressively elucidated in past years. Interestingly, several compounds were found to exhibit multiple bioactivities in the rhizosphere and influence organisms differently. In other words, a single phytochemical might act synergistically in direct and indirect plant defense. Nevertheless, another compound might recruit beneficial and detrimental organisms. Therefore, it is of importance to carefully assess the targets and effects of root exudates on multitrophic levels. In addition to the discovery of various root-secreted defense compounds and their role in the rhizosphere, the understanding of the stimulation and regulation of root exudation has advanced dramatically. Root exudation

is a dynamic and bidirectional process: root exudates shape the soil inhabitants, and rhizosphere members modulate the root exudate ensemble. Besides the presence of soil-borne organisms, several other exogenous as well as endogenous factors can rapidly and precisely adjust the nature of root-secreted phytochemicals. On the molecular level, transporter proteins have been shown to modulate rhizosecretion processes in a complex manner that goes beyond a role as pure substrate carriers. Consequently, also the stimuli and regulatory mechanisms that modify the quality and quantity of the root exudate cocktail require thorough investigation.

Taken together, root exudates impact the rhizosphere inhabitants markedly. Accordingly, they are a powerful tool that can be exploited to enhance natural defense properties of plants. Deepening our knowledge of the targets and effects of root exudates, as well as the regulation of root secretion processes, will unravel the path for more efficient disease management in the rhizosphere.

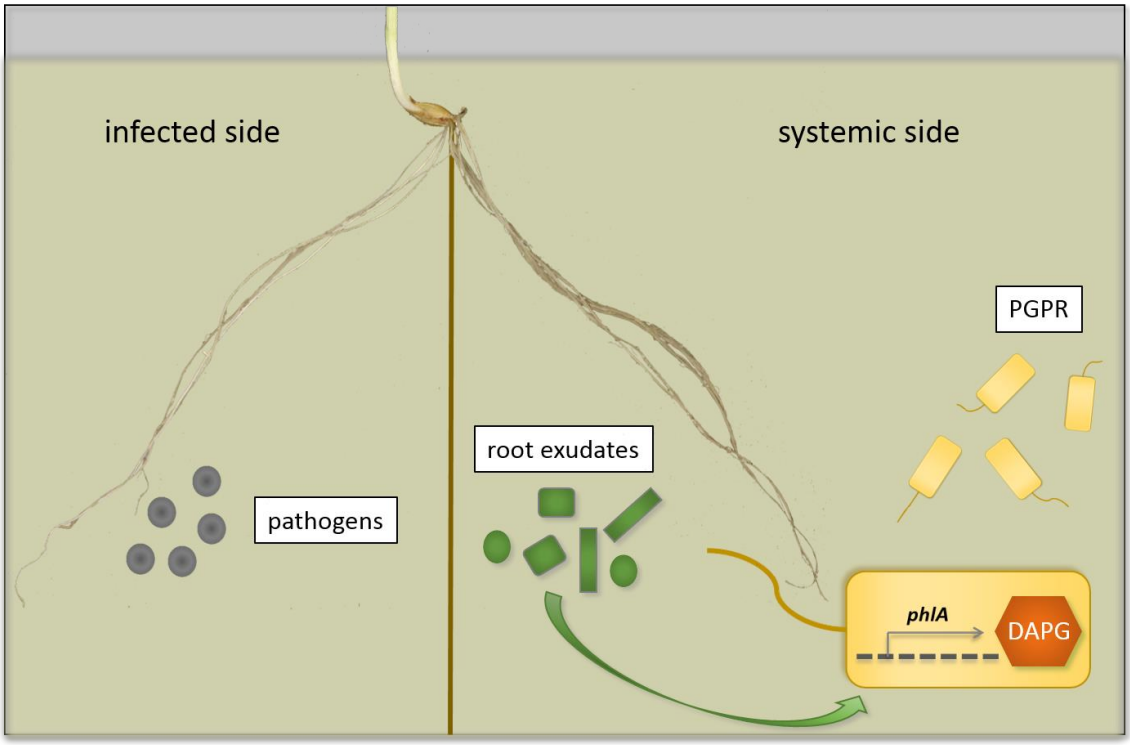


**Figure 1. Relevance of systemic plant signaling and root exudation in a tripartite interaction that confers indirect plant defense.**

To investigate pathogen-induced but plant-mediated modulation of bacterial gene expression and antifungal activity, Jousset et *al*. (2011) grew barley in a split-root system (Jousset et al., 2011). One part of the root (infected side) was challenged with the pathogen *Pythium ultimum*, whereas the other part of the root (systemic side) was exposed to the beneficial plant growth-promoting rhizobacteria (PGPR) *Pseudomonas fluorescens* CHA0. Without physical contact but through systemic plant signaling, pathogen attack induced compositional changes in root exudates on the systemic side. These changes, in turn, stimulated bacterial *phlA* expression. The transcript levels of this gene directly correlate with the production of the antifungal compound 2,4-diacetylphloroglucinol (DAPG).

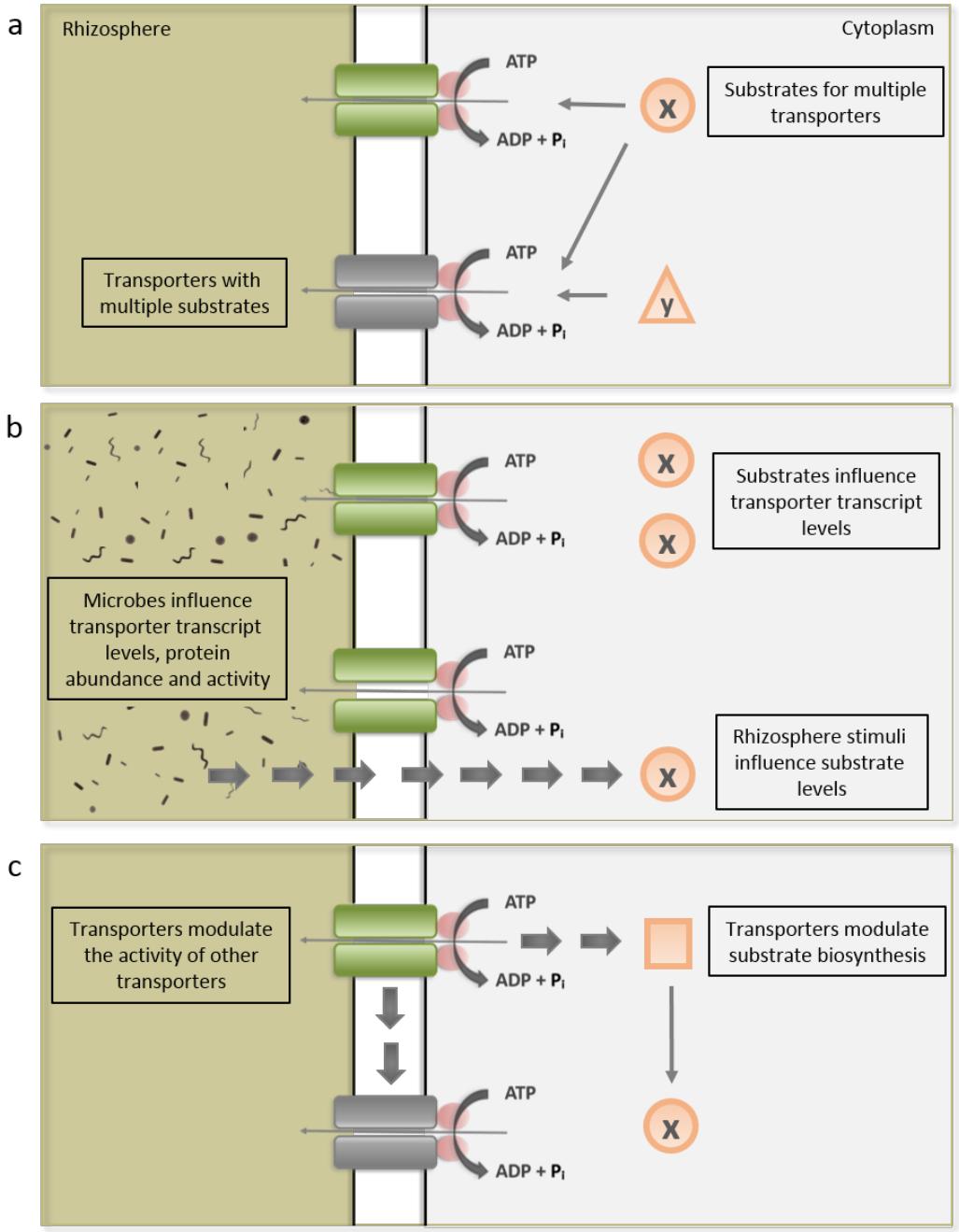


**Figure 2. ABC proteins are complex transport systems that modulate root exudation.**

**(a)** Some ABC proteins transport multiple substrates. Equally, some compounds can be a substrate of several transporters. **(b)** Transporter transcript levels, protein abundance and activity can be dependent on substrate availability, elicitors and microbial presence. In addition, rhizosphere stimuli can influence substrate production. **(c)** ABC transporters can pleiotropically modulate cell physiology, e.g. by influencing substrate biosynthesis or the activity of other transporters.

## References

Ahmad, S., Veyrat, N., Gordon-Weeks, R., Zhang, Y., Martin, J., Smart, L., Glauser, G., Erb, M., Flors, V., Frey, M. and Ton, J. (2011) 'Benzoxazinoid metabolites regulate innate immunity against aphids and fungi in maize', *Plant Physiol,* 157(1), pp. 317-27.

Ali, J. G., Alborn, H. T., Campos-Herrera, R., Kaplan, F., Duncan, L. W., Rodriguez-Saona, C., Koppenhöfer, A. M. and Stelinski, L. L. (2012) 'Subterranean, herbivore-induced plant volatile increases biological control activity of multiple beneficial nematode species in distinct habitats', *PLoS One,* 7(6), pp. e38146.

Ali, J. G., Alborn, H. T. and Stelinski, L. L. (2010) 'Subterranean herbivore-induced volatiles released by citrus roots upon feeding by Diaprepes abbreviatus recruit entomopathogenic nematodes', *J Chem Ecol,* 36(4), pp. 361-8.

Ali, J. G., Alborn, H. T. and Stelinski, L. L. (2011) 'Constitutive and induced subterranean plant volatiles attract both entomopathogenic and plant parasitic nematodes', *Journal of Ecology,* 99(1), pp. 26-35.

Badri, D. V., Chaparro, J. M., Zhang, R., Shen, Q. and Vivanco, J. M. (2013) 'Application of natural blends of phytochemicals derived from the root exudates of Arabidopsis to the soil reveal that phenolic-related compounds predominantly modulate the soil microbiome', *J Biol Chem,* 288(7), pp. 4502-12.

Badri, D. V., Loyola-Vargas, V. M., Broeckling, C. D., De-la-Peña, C., Jasinski, M., Santelia, D., Martinoia, E., Sumner, L. W., Banta, L. M., Stermitz, F. and Vivanco, J. M. (2008a) 'Altered profile of secondary metabolites in the root exudates of Arabidopsis ATP-binding cassette transporter mutants', *Plant Physiol,* 146(2), pp. 762-71.

Badri, D. V., Loyola-Vargas, V. M., Broeckling, C. D. and Vivanco, J. M. (2010) 'Root secretion of phytochemicals in Arabidopsis is predominantly not influenced by diurnal rhythms', *Mol Plant,* 3(3), pp. 491-8.

Badri, D. V., Loyola-Vargas, V. M., Du, J., Stermitz, F. R., Broeckling, C. D., Iglesias-Andreu, L. and Vivanco, J. M. (2008b) 'Transcriptome analysis of Arabidopsis roots treated with signaling compounds: a focus on signal transduction, metabolic regulation and secretion', *New Phytol,* 179(1), pp. 209-23.

Badri, D. V., Quintana, N., El Kassis, E. G., Kim, H. K., Choi, Y. H., Sugiyama, A., Verpoorte, R., Martinoia, E., Manter, D. K. and Vivanco, J. M. (2009) 'An ABC transporter mutation alters root exudation of phytochemicals that provoke an overhaul of natural soil microbiota', *Plant Physiol,* 151(4), pp. 2006-17.

Badri, D. V. and Vivanco, J. M. (2009) 'Regulation and function of root exudates', *Plant Cell Environ,* 32(6), pp. 666-81.

Baehler, E., Bottiglieri, M., Péchy-Tarr, M., Maurhofer, M. and Keel, C. (2005) 'Use of green fluorescent protein-based reporters to monitor balanced production of antifungal compounds in the biocontrol agent Pseudomonas fluorescens CHA0', *J Appl Microbiol,* 99(1), pp. 24-38.

Baetz, U. and Martinoia, E. (2014) 'Root exudates: the hidden part of plant defense', *Trends in Plant Science,* 19(2), pp. 90-98.

Bais, H. P., Walker, T. S., Schweizer, H. P. and Vivanco, J. M. 2002. Root specific elicitation and antimicrobial activity of rosmarinic acid in hairy root cultures of *Ocimum basilicum*. *Plant Physiol Biochem*, 40, pp. 983-95.

Banasiak, J., Biala, W., Staszków, A., Swarcewicz, B., Kepczynska, E., Figlerowicz, M. and Jasinski, M. (2013) 'A Medicago truncatula ABC transporter belonging to subfamily G modulates the level of isoflavonoids', *J Exp Bot,* 64(4), pp. 1005-15.

Bangera, M. G. and Thomashow, L. S. (1999) 'Identification and characterization of a gene cluster for synthesis of the polyketide antibiotic 2,4-diacetylphloroglucinol from Pseudomonas fluorescens Q2-87', *J Bacteriol,* 181(10), pp. 3155-63.

Bezemer, T. M. and van Dam, N. M. (2005) 'Linking aboveground and belowground interactions via induced plant defenses', *Trends Ecol Evol,* 20(11), pp. 617-24.

Bienert, M. D., Siegmund, S. E., Drozak, A., Trombik, T., Bultreys, A., Baldwin, I. T. and Boutry, M. (2012) 'A pleiotropic drug resistance transporter in Nicotiana tabacum is involved in defense against the herbivore Manduca sexta', *Plant J,* 72(5), pp. 745-57.

Bouarab, K., Melton, R., Peart, J., Baulcombe, D. and Osbourn, A. (2002) 'A saponin-detoxifying enzyme mediates suppression of plant defences', *Nature,* 418(6900), pp. 889-92.

Brinkmann, V., Reichard, U., Goosmann, C., Fauler, B., Uhlemann, Y., Weiss, D. S., Weinrauch, Y. and Zychlinsky, A. (2004) 'Neutrophil extracellular traps kill bacteria', *Science,* 303(5663), pp. 1532-5.

Bultreys, A., Trombik, T., Drozak, A. and Boutry, M. (2009) 'Nicotiana plumbaginifolia plants silenced for the ATP-binding cassette transporter gene NpPDR1 show increased susceptibility to a group of fungal and oomycete pathogens', *Mol Plant Pathol,* 10(5), pp. 651-63.

Cai, T., Cai, W., Zhang, J., Zheng, H., Tsou, A. M., Xiao, L., Zhong, Z. and Zhu, J. (2009) 'Host legume-exuded antimetabolites optimize the symbiotic rhizosphere', *Mol Microbiol,* 73(3), pp. 507-17.

Cannesan, M. A., Gangneux, C., Lanoue, A., Giron, D., Laval, K., Hawes, M., Driouich, A. and Vicré-Gibouin, M. (2011) 'Association between border cell responses and localized root infection by pathogenic Aphanomyces euteiches', *Ann Bot*, 108(3), pp. 459-69.

Capra, E., Colombi, C., De Poli, P., Nocito, F. F., Cocucci, M., Vecchietti, A., Marocco, A., Stile, M. R. and Rossini, L. (2014) 'Protein profiling and tps23 induction in different maize lines in response to methyl jasmonate treatment and Diabrotica virgifera infestation', *J Plant Physiol*, 175C, pp. 68-77.

Chaparro, J. M., Badri, D. V., Bakker, M. G., Sugiyama, A., Manter, D. K. and Vivanco, J. M. (2013) 'Root exudation of phytochemicals in Arabidopsis follows specific patterns that are developmentally programmed and correlate with soil microbial functions', *PLoS One*, 8(2), pp. e55731.

Compant, S., Duffy, B., Nowak, J., Clément, C. and Barka, E. A. (2005) 'Use of plant growth-promoting bacteria for biocontrol of plant diseases: principles, mechanisms of action, and future prospects', *Appl Environ Microbiol*, 71(9), pp. 4951-9.

Crouzet, J., Roland, J., Peeters, E., Trombik, T., Ducos, E., Nader, J. and Boutry, M. (2013) 'NtPDR1, a plasma membrane ABC transporter from Nicotiana tabacum, is involved in diterpene transport', *Plant Mol Biol*.

Curlango-Rivera, G., Duclos, D. V., Ebolo, J. J. and Hawes, M. C. (2010) 'Transient exposure of root tips to Primary and secondary metabolites: Impact on root growth and production of border cells', *Plant Soil*, 332, pp. 267-275.

Curtis, R. H. (2008) 'Plant-nematode interactions: environmental signals detected by the nematode's chemosensory organs control changes in the surface cuticle and behaviour', *Parasite*, 15(3), pp. 310-6.

de Souza, J. T., Arnould, C., Deulvot, C., Lemanceau, P., Gianinazzi-Pearson, V. and Raaijmakers, J. M. (2003) 'Effect of 2,4-diacetylphloroglucinol on pythium: cellular responses and variation in sensitivity among propagules and species', *Phytopathology*, 93(8), pp. 966-75.

de Werra, P., Baehler, E., Huser, A., Keel, C. and Maurhofer, M. (2008) 'Detection of plant-modulated alterations in antifungal gene expression in Pseudomonas fluorescens CHA0 on roots by flow cytometry', *Appl Environ Microbiol*, 74(5), pp. 1339-49.

de Werra, P., Huser, A., Tabacchi, R., Keel, C. and Maurhofer, M. (2011) 'Plant- and microbe-derived compounds affect the expression of genes encoding antifungal compounds in a pseudomonad with biocontrol activity', *Appl Environ Microbiol*, 77(8), pp. 2807-12.

De-la-Peña, C., Badri, D. V., Lei, Z., Watson, B. S., Brandão, M. M., Silva-Filho, M. C., Sumner, L. W. and Vivanco, J. M. (2010) 'Root secretion of defense-related proteins is development-dependent and correlated with flowering time', *J Biol Chem*, 285(40), pp. 30654-65.

De-la-Peña, C., Lei, Z., Watson, B. S., Sumner, L. W. and Vivanco, J. M. (2008) 'Root-microbe communication through protein secretion', *J Biol Chem*, 283(37), pp. 25247-55.

Degenhardt, J., Hiltpold, I., Köllner, T. G., Frey, M., Gierl, A., Gershenzon, J., Hibbard, B. E., Ellersieck, M. R. and Turlings, T. C. (2009) 'Restoring a maize root signal that attracts insect-killing nematodes to control a major pest', *Proc Natl Acad Sci U S A*, 106(32), pp. 13213-8.

Dong, L., Li, X., Huang, L., Gao, Y., Zhong, L., Zheng, Y. and Zuo, Y. (2014) 'Lauric acid in crown daisy root exudate potently regulates root-knot nematode chemotaxis and disrupts Mi-flp-18 expression to block infection', *J Exp Bot*, 65(1), pp. 131-41.

Doornbos, R. F., van Loon, L. C. and Bakker, P. A. H. M. (2012) 'Impact of root exudates and plant defense signaling on bacterial communities in the rhizosphere. A review', *Agron. Sustain. Dev.*, 32, pp. 227-243.

Driouich, A., Durand, C. and Vicré-Gibouin, M. (2007) 'Formation and separation of root border cells', *Trends Plant Sci*, 12(1), pp. 14-9.

Ferry, A., Dugravot, S., Delattre, T., Christides, J. P., Auger, J., Bagnères, A. G., Poinsot, D. and Cortesero, A. M. (2007) 'Identification of a widespread monomolecular odor differentially attractive to several Delia radicum ground-dwelling predators in the field', *J Chem Ecol*, 33(11), pp. 2064-77.

Ferry, A., Le Tron, S., Dugravot, S. and Cortesero, A. M. (2009) 'Field evaluation of the combined deterrent and attractive effects of dimethyl disulfide on *Delia radicum* and its natural enemies', *Biological Control*, 49(3), pp. 219–226.

Fourcroy, P., Sisó-Terraza, P., Sudre, D., Savirón, M., Reyt, G., Gaymard, F., Abadía, A., Abadia, J., Alvarez-Fernández, A. and Briat, J. F. (2013) 'Involvement of the ABCG37 transporter in secretion of scopoletin and derivatives by Arabidopsis roots in response to iron deficiency', *New Phytol*.

Fujii, M., Yokosho, K., Yamaji, N., Saisho, D., Yamane, M., Takahashi, H., Sato, K., Nakazono, M. and Ma, J. F. (2012) 'Acquisition of aluminium tolerance by modification of a single gene in barley', *Nat Commun*, 3, pp. 713.

Furukawa, J., Yamaji, N., Wang, H., Mitani, N., Murata, Y., Sato, K., Katsuhara, M., Takeda, K. and Ma, J. F. (2007) 'An aluminum-activated citrate transporter in barley', *Plant Cell Physiol,* 48(8), pp. 1081-91.

Griffin, G., Hale, M. G. and Shay, F. J. 1976. Nature and quantity of sloughed organic matter produced by roots of axenic peanut plants. Soil Biology and Biochemistry.

Haas, D. and Défago, G. (2005) 'Biological control of soil-borne pathogens by fluorescent pseudomonads', *Nat Rev Microbiol,* 3(4), pp. 307-19.

Hawes, M. C., Curlango-Rivera, G., Wen, F., White, G. J., Vanetten, H. D. and Xiong, Z. (2011) 'Extracellular DNA: the tip of root defenses?', *Plant Sci,* 180(6), pp. 741-5.

Hawes, M. C., Curlango-Rivera, G., Xiong, Z. and Kessler, J. O. 2012. Roles of root border cells in plant defense and regulation of rhizosphere microbial populations by extracellular DNA 'trapping'. Plant Soil.

Hiltpold, I., Baroni, M., Toepfer, S., Kuhlmann, U. and Turlings, T. C. (2010a) 'Selection of entomopathogenic nematodes for enhanced responsiveness to a volatile root signal helps to control a major root pest', *J Exp Biol*, 213(Pt 14), pp. 2417-23.

Hiltpold, I., Baroni, M., Toepfer, S., Kuhlmann, U. and Turlings, T. C. (2010b) 'Selective breeding of entomopathogenic nematodes for enhanced attraction to a root signal did not reduce their establishment or persistence after field release', *Plant Signal Behav,* 5(11), pp. 1450-2.

Hiltpold, I., Erb, M., Robert, C. A. and Turlings, T. C. (2011) 'Systemic root signalling in a belowground, volatile-mediated tritrophic interaction', *Plant Cell Environ,* 34(8), pp. 1267-75.

Hiltpold, I., Jaffuel, G. and Turlings, T. C. (2015) 'The dual effects of root-cap exudates on nematodes: from quiescence in plant-parasitic nematodes to frenzy in entomopathogenic nematodes', *J Exp Bot,* 66(2), pp. 603-11.

Hiltpold, I. and Turlings, T. C. (2008) 'Belowground chemical signaling in maize: when simplicity rhymes with efficiency', *J Chem Ecol,* 34(5), pp. 628-35.

Hiltpold, I. and Turlings, T. C. (2012) 'Manipulation of chemically mediated interactions in agricultural soils to enhance the control of crop pests and to improve crop yield', *J Chem Ecol,* 38(6), pp. 641-50.

Ishimaru, Y., Kakei, Y., Shimo, H., Bashir, K., Sato, Y., Uozumi, N., Nakanishi, H. and Nishizawa, N. K. (2011) 'A rice phenolic efflux transporter is essential for solubilizing precipitated apoplasmic iron in the plant stele', *J Biol Chem,* 286(28), pp. 24649-55.

Ito, H. and Gray, W. M. (2006) 'A gain-of-function mutation in the Arabidopsis pleiotropic drug resistance transporter PDR9 confers resistance to auxinic herbicides', *Plant Physiol,* 142(1), pp. 63-74.

Jasiński, M., Stukkens, Y., Degand, H., Purnelle, B., Marchand-Brynaert, J. and Boutry, M. (2001) 'A plant plasma membrane ATP binding cassette-type transporter is involved in antifungal terpenoid secretion', *Plant Cell,* 13(5), pp. 1095-107.

Jousset, A., Rochat, L., Lanoue, A., Bonkowski, M., Keel, C. and Scheu, S. (2011) 'Plants respond to pathogen infection by enhancing the antifungal gene expression of root-associated bacteria', *Mol Plant Microbe Interact,* 24(3), pp. 352-8.

Kalemba, D., Kusewicz, D. and Swiader, K. (2002) 'Antimicrobial properties of the essential oil of Artemisia asiatica Nakai', *Phytother Res,* 16(3), pp. 288-91.

Kang, J., Park, J., Choi, H., Burla, B., Kretzschmar, T., Lee, Y. and Martinoia, E. (2011) 'Plant ABC Transporters', *The Arabidopsis book / American Society of Plant Biologists,* 9, pp. e0153.

Kato-Noguchi, H., Ino, T. and Ota, K. (2008) 'Secretion of momilactone A from rice roots to the rhizosphere', *J Plant Physiol,* 165(7), pp. 691-6.

Kim, D. Y., Bovet, L., Maeshima, M., Martinoia, E. and Lee, Y. (2007) 'The ABC transporter AtPDR8 is a cadmium extrusion pump conferring heavy metal resistance', *Plant J,* 50(2), pp. 207-18.

Kretzschmar, T., Kohlen, W., Sasse, J., Borghi, L., Schlegel, M., Bachelier, J. B., Reinhardt, D., Bours, R., Bouwmeester, H. J. and Martinoia, E. (2012) 'A petunia ABC protein controls strigolactone-dependent symbiotic signalling and branching', *Nature,* 483(7389), pp. 341-4.

Köllner, T. G., Held, M., Lenk, C., Hiltpold, I., Turlings, T. C., Gershenzon, J. and Degenhardt, J. (2008) 'A maize (E)-beta-caryophyllene synthase implicated in indirect defense responses against herbivores is not expressed in most American maize varieties', *Plant Cell,* 20(2), pp. 482-94.

Lakshmanan, V., Kitto, S. L., Caplan, J. L., Hsueh, Y. H., Kearns, D. B., Wu, Y. S. and Bais, H. P. (2012) 'Microbe-associated molecular patterns-triggered root responses mediate beneficial rhizobacterial recruitment in Arabidopsis', *Plant Physiol,* 160(3), pp. 1642-61.

Lanoue, A., Burlat, V., Henkes, G. J., Koch, I., Schurr, U. and Röse, U. S. (2010a) 'De novo biosynthesis of defense root exudates in response to Fusarium attack in barley', *New Phytol,* 185(2), pp. 577-88.

Lanoue, A., Burlat, V., Schurr, U. and Röse, U. S. (2010b) 'Induced root-secreted phenolic compounds as a belowground plant defense', *Plant Signal Behav,* 5(8), pp. 1037-8.

Liao, C., Hochholdinger, F. and Li, C. (2012) 'Comparative analyses of three legume species reveals conserved and unique root extracellular proteins', *Proteomics,* 12(21), pp. 3219-28.

Lilley, C. J., Wang, D., Atkinson, H. J. and Urwin, P. E. (2011) 'Effective delivery of a nematode-repellent peptide using a root-cap-specific promoter', *Plant Biotechnol J,* 9(2), pp. 151-61.

Liu, B., Hibbard, J. K., Urwin, P. E. and Atkinson, H. J. (2005) 'The production of synthetic chemodisruptive peptides in planta disrupts the establishment of cyst nematodes', *Plant Biotechnol J,* 3(5), pp. 487-96.

Liu, J., Magalhaes, J. V., Shaff, J. and Kochian, L. V. (2009) 'Aluminum-activated citrate and malate transporters from the MATE and ALMT families function independently to confer Arabidopsis aluminum tolerance', *Plant J,* 57(3), pp. 389-99.

Loyola-Vargas, V. M., Broeckling, C. D., Badri, D. and Vivanco, J. M. (2007) 'Effect of transporters on the secretion of phytochemicals by the roots of Arabidopsis thaliana', *Planta,* 225(2), pp. 301-10.

Ma, W., Muthreich, N., Liao, C., Franz-Wachtel, M., Schütz, W., Zhang, F., Hochholdinger, F. and Li, C. (2010) 'The mucilage proteome of maize (Zea mays L.) primary roots', *J Proteome Res,* 9(6), pp. 2968-76.

Magalhaes, J. V., Liu, J., Guimarães, C. T., Lana, U. G., Alves, V. M., Wang, Y. H., Schaffert, R. E., Hoekenga, O. A., Piñeros, M. A., Shaff, J. E., Klein, P. E., Carneiro, N. P., Coelho, C. M., Trick, H. N. and Kochian, L. V. (2007) 'A gene in the multidrug and toxic compound extrusion (MATE) family confers aluminum tolerance in sorghum', *Nat Genet,* 39(9), pp. 1156-61.

Maron, L. G., Piñeros, M. A., Guimarães, C. T., Magalhaes, J. V., Pleiman, J. K., Mao, C., Shaff, J., Belicuas, S. N. and Kochian, L. V. (2010) 'Two functionally distinct members of the MATE (multi-drug and toxic compound extrusion) family of transporters potentially underlie two major aluminum tolerance QTLs in maize', *Plant J,* 61(5), pp. 728-40.

McCully, M. E., Miller, C., Sprague, S. J., Huang, C. X. and Kirkegaard, J. A. (2008) 'Distribution of glucosinolates and sulphur-rich cells in roots of field-grown canola (Brassica napus)', *New Phytol,* 180(1), pp. 193-205.

Medina, E. (2009) 'Neutrophil extracellular traps: a strategic tactic to defeat pathogens with potential consequences for the host', *J Innate Immun,* 1(3), pp. 176-80.

Miller, N., Estoup, A., Toepfer, S., Bourguet, D., Lapchin, L., Derridj, S., Kim, K. S., Reynaud, P., Furlan, L. and Guillemaud, T. (2005) 'Multiple transatlantic introductions of the western corn rootworm', *Science,* 310(5750), pp. 992.

Neal, A. L., Ahmad, S., Gordon-Weeks, R. and Ton, J. (2012) 'Benzoxazinoids in root exudates of maize attract Pseudomonas putida to the rhizosphere', *PLoS One,* 7(4), pp. e35498.

Neal, A. L. and Ton, J. (2013) 'Systemic defense priming by Pseudomonas putida KT2440 in maize depends on benzoxazinoid exudation from the roots', *Plant Signal Behav,* 8(1), pp. e22655.

Niemeyer, H. M. (2009) 'Hydroxamic acids derived from 2-hydroxy-2H-1,4-benzoxazin-3(4H)-one: key defense chemicals of cereals', *J Agric Food Chem,* 57(5), pp. 1677-96.

Notz, R., Maurhofer, M., Schnider-Keel, U., Duffy, B., Haas, D. and Défago, G. (2001) 'Biotic Factors Affecting Expression of the 2,4-Diacetylphloroglucinol Biosynthesis Gene phlA in Pseudomonas fluorescens Biocontrol Strain CHA0 in the Rhizosphere', *Phytopathology,* 91(9), pp. 873-81.

Odell, R. E., Dumlao, M. R., Samar, D. and Silk, W. K. (2008) 'Stage-dependent border cell and carbon flow from roots to rhizosphere', *Am J Bot,* 95(4), pp. 441-6.

Pangesti, N., Pineda, A., Pieterse, C. M., Dicke, M. and van Loon, J. J. (2013) 'Two-way plant mediated interactions between root-associated microbes and insects: from ecology to mechanisms', *Front Plant Sci,* 4, pp. 414.

Park, W. J., Hochholdinger, F. and Gierl, A. (2004) 'Release of the benzoxazinoids defense molecules during lateral- and crown root emergence in Zea mays', *J Plant Physiol,* 161(8), pp. 981-5.

Picard, C., Di Cello, F., Ventura, M., Fani, R. and Guckert, A. (2000) 'Frequency and biodiversity of 2,4-diacetylphloroglucinol-producing bacteria isolated from the maize rhizosphere at different stages of plant growth', *Appl Environ Microbiol,* 66(3), pp. 948-55.

Picard, C., Frascaroli, E. and Bosco, M. (2004) 'Frequency and biodiversity of 2,4-diacetylphloroglucinol-producing rhizobacteria are differentially affected by the genotype of two maize inbred lines and their hybrid', *FEMS Microbiol Ecol,* 49(2), pp. 207-15.

Rasmann, S., Köllner, T. G., Degenhardt, J., Hiltpold, I., Toepfer, S., Kuhlmann, U., Gershenzon, J. and Turlings, T. C. (2005) 'Recruitment of entomopathogenic nematodes by insect-damaged maize roots', *Nature,* 434(7034), pp. 732-7.

Reynolds, A. M., Dutta, T. K., Curtis, R. H., Powers, S. J., Gaur, H. S. and Kerry, B. R. (2011) 'Chemotaxis can take plant-parasitic nematodes to the source of a chemo-attractant via the shortest possible routes', *J R Soc Interface*, 8(57), pp. 568-77.

Robert, C. A., Erb, M., Duployer, M., Zwahlen, C., Doyen, G. R. and Turlings, T. C. (2012) 'Herbivore-induced plant volatiles mediate host selection by a root herbivore', *New Phytol*, 194(4), pp. 1061-9.

Robert, C. A., Erb, M., Hiltpold, I., Hibbard, B. E., Gaillard, M. D., Bilat, J., Degenhardt, J., Cambet-Petit-Jean, X., Turlings, T. C. and Zwahlen, C. (2013) 'Genetically engineered maize plants reveal distinct costs and benefits of constitutive volatile emissions in the field', *Plant Biotechnol J*, 11(5), pp. 628-39.

Rodríguez-Celma, J., Lin, W. D., Fu, G. M., Abadia, J., López-Míllán, A. F. and Schmidt, W. (2013) 'Mutually Exclusive Alterations in Secondary Metabolism are Critical for the Uptake of Insoluble Iron Compounds by Arabidopsis and Medicago truncatula', *Plant Physiol*.

Rookes, J. E., Wright, M. L. and Cahill, D. M. 2008. Elucidation of defence responses and signalling pathways induced in *Arabidopsis thaliana* following challenge with *Phytophthora cinnamomi*. *Physiological and Molecular Plant Pathology*.

Rudrappa, T., Czymmek, K. J., Paré, P. W. and Bais, H. P. (2008) 'Root-secreted malic acid recruits beneficial soil bacteria', *Plant Physiol*, 148(3), pp. 1547-56.

Ruiz-May, E., Galaz-Avalos, R. M. and Loyola-Vargas, V. M. (2009) 'Differential secretion and accumulation of terpene indole alkaloids in hairy roots of Catharanthus roseus treated with methyl jasmonate', *Mol Biotechnol*, 41(3), pp. 278-85.

Ruzicka, K., Strader, L. C., Bailly, A., Yang, H., Blakeslee, J., Langowski, L., Nejedlá, E., Fujita, H., Itoh, H., Syono, K., Hejátko, J., Gray, W. M., Martinoia, E., Geisler, M., Bartel, B., Murphy, A. S. and Friml, J. (2010) 'Arabidopsis PIS1 encodes the ABCG37 transporter of auxinic compounds including the auxin precursor indole-3-butyric acid', *Proc Natl Acad Sci U S A*, 107(23), pp. 10749-53.

Santos, F., Peñaflor, M. F., Paré, P. W., Sanches, P. A., Kamiya, A. C., Tonelli, M., Nardi, C. and Bento, J. M. (2014) 'A novel interaction between plant-beneficial rhizobacteria and roots: colonization induces corn resistance against the root herbivore Diabrotica speciosa', *PLoS One*, 9(11), pp. e113280.

Sasabe, M., Toyoda, K., Shiraishi, T., Inagaki, Y. and Ichinose, Y. (2002) 'cDNA cloning and characterization of tobacco ABC transporter: NtPDR1 is a novel elicitor-responsive gene', *FEBS Lett*, 518(1-3), pp. 164-8.

Schreiner, M., Krumbein, A., Knorr, D. and Smetanska, I. (2011) 'Enhanced glucosinolates in root exudates of Brassica rapa ssp. rapa mediated by salicylic acid and methyl jasmonate', *J Agric Food Chem,* 59(4), pp. 1400-5.

Shinano, T., Komatsu, S., Yoshimura, T., Tokutake, S., Kong, F. J., Watanabe, T., Wasaki, J. and Osaki, M. (2011) 'Proteomic analysis of secreted proteins from aseptically grown rice', *Phytochemistry,* 72(4-5), pp. 312-20.

Steeghs, M., Bais, H. P., de Gouw, J., Goldan, P., Kuster, W., Northway, M., Fall, R. and Vivanco, J. M. (2004) 'Proton-transfer-reaction mass spectrometry as a new tool for real time analysis of root-secreted volatile organic compounds in Arabidopsis', *Plant Physiol,* 135(1), pp. 47-58.

Strader, L. C. and Bartel, B. (2009) 'The Arabidopsis PLEIOTROPIC DRUG RESISTANCE8/ABCG36 ATP binding cassette transporter modulates sensitivity to the auxin precursor indole-3-butyric acid', *Plant Cell,* 21(7), pp. 1992-2007.

Stubbs, V. E., Standing, D., Knox, O. G., Killham, K., Bengough, A. G. and Griffiths, B. (2004) 'Root border cells take up and release glucose-C', *Ann Bot,* 93(2), pp. 221-4.

Stukkens, Y., Bultreys, A., Grec, S., Trombik, T., Vanham, D. and Boutry, M. (2005) 'NpPDR1, a pleiotropic drug resistance-type ATP-binding cassette transporter from Nicotiana plumbaginifolia, plays a major role in plant pathogen defense', *Plant Physiol,* 139(1), pp. 341-52.

Sugiyama, A., Shitan, N. and Yazaki, K. (2007) 'Involvement of a soybean ATP-binding cassette-type transporter in the secretion of genistein, a signal flavonoid in legume-Rhizobium symbiosis', *Plant Physiol,* 144(4), pp. 2000-8.

Sugiyama, A., Shitan, N. and Yazaki, K. (2008) 'Signaling from soybean roots to rhizobium: An ATP-binding cassette-type transporter mediates genistein secretion', *Plant Signal Behav,* 3(1), pp. 38-40.

Toyomasu, T., Kagahara, T., Okada, K., Koga, J., Hasegawa, M., Mitsuhashi, W., Sassa, T. and Yamane, H. (2008) 'Diterpene phytoalexins are biosynthesized in and exuded from the roots of rice seedlings', *Biosci Biotechnol Biochem,* 72(2), pp. 562-7.

Vacheron, J., Desbrosses, G., Bouffaud, M. L., Touraine, B., Moënne-Loccoz, Y., Muller, D., Legendre, L., Wisniewski-Dyé, F. and Prigent-Combaret, C. (2013) 'Plant growth-promoting rhizobacteria and root system functioning', *Front Plant Sci,* 4, pp. 356.

Vaughan, M. M., Wang, Q., Webster, F. X., Kiemle, D., Hong, Y. J., Tantillo, D. J., Coates, R. M., Wray, A. T., Askew, W., O'Donnell, C., Tokuhisa, J. G. and Tholl, D. (2013) 'Formation of the Unusual Semivolatile Diterpene Rhizathalene by the Arabidopsis

Class I Terpene Synthase TPS08 in the Root Stele Is Involved in Defense against Belowground Herbivory', *Plant Cell,* 25(3), pp. 1108-25.

Vicré, M., Santaella, C., Blanchet, S., Gateau, A. and Driouich, A. (2005) 'Root border-like cells of Arabidopsis. Microscopical characterization and role in the interaction with rhizobacteria', *Plant Physiol,* 138(2), pp. 998-1008.

von Köckritz-Blickwede, M. and Nizet, V. (2009) 'Innate immunity turned inside-out: antimicrobial defense by phagocyte extracellular traps', *J Mol Med (Berl),* 87(8), pp. 775-83.

Vuković, R., Bauer, N. and Curković-Perica, M. (2013) 'Genetic elicitation by inducible expression of β-cryptogein stimulates secretion of phenolics from Coleus blumei hairy roots', *Plant Sci,* 199-200, pp. 18-28.

Walker, T. S., Bais, H. P., Déziel, E., Schweizer, H. P., Rahme, L. G., Fall, R. and Vivanco, J. M. (2004) 'Pseudomonas aeruginosa-plant root interactions. Pathogenicity, biofilm formation, and root exudation', *Plant Physiol,* 134(1), pp. 320-31.

Wang, Y., Bouwmeester, K., van de Mortel, J. E., Shan, W. and Govers, F. (2013) 'A novel Arabidopsis-oomycete pathosystem: differential interactions with Phytophthora capsici reveal a role for camalexin, indole glucosinolates and salicylic acid in defence', *Plant Cell Environ,* 36(6), pp. 1192-203.

Wen, F., VanEtten, H. D., Tsaprailis, G. and Hawes, M. C. (2007) 'Extracellular proteins in pea root tip and border cell exudates', *Plant Physiol,* 143(2), pp. 773-83.

Wen, F., White, G. J., VanEtten, H. D., Xiong, Z. and Hawes, M. C. (2009) 'Extracellular DNA is required for root tip resistance to fungal infection', *Plant Physiol,* 151(2), pp. 820-9.

Yazaki, K., Shitan, N., Sugiyama, A. and Takanashi, K. (2009) 'Cell and molecular biology of ATP-binding cassette proteins in plants', *Int Rev Cell Mol Biol,* 276, pp. 263-99.

Yazaki, K., Sugiyama, A., Morita, M. and Shitan, N. 2008. Secondary transport as an efficient Membrane transport mechanism for plant secondary metabolites.: Phytochem Rev.

Youssef, R. M., Macdonald, M. H., Brewer, E. P., Bauchan, G. R., Kim, K. H. and Matthews, B. F. (2013) 'Ectopic expression of AtPAD4 broadens resistance of soybean to soybean cyst and root-knot nematodes', *BMC Plant Biol,* 13(1), pp. 67.

Zhao, X., Schmitt, M. and Hawes, M. C. (2000) 'Species-dependent effects of border cell and root tip exudates on nematode behavior', *Phytopathology,* 90(11), pp. 1239-45.

# 9. Literature


Accardi, A. and Miller, C. (2004) 'Secondary active transport mediated by a prokaryotic homologue of ClC Cl- channels', *Nature*, 427(6977), pp. 803-7.

Ache, P., Becker, D., Ivashikina, N., Dietrich, P., Roelfsema, M. R. and Hedrich, R. (2000) 'GORK, a delayed outward rectifier expressed in guard cells of Arabidopsis thaliana, is a K(+)-selective, K(+)-sensing ion channel', *FEBS Lett*, 486(2), pp. 93-8.

Alexander, S. P., Hill, S. J. and Kendall, D. A. (1990) 'Differential effects of elevated calcium ion concentrations on inositol phospholipid responses in mouse and rat cerebral cortical slices', *Biochem Pharmacol*, 40(8), pp. 1793-9.

Allen, G. J., Muir, S. R. and Sanders, D. (1995) 'Release of Ca2+ from individual plant vacuoles by both InsP3 and cyclic ADP-ribose', *Science*, 268(5211), pp. 735-7.

Andrés, Z., Pérez-Hormaeche, J., Leidi, E. O., Schlücking, K., Steinhorst, L., McLachlan, D. H., Schumacher, K., Hetherington, A. M., Kudla, J., Cubero, B. and Pardo, J. M. (2014) 'Control of vacuolar dynamics and regulation of stomatal aperture by tonoplast potassium uptake', *Proc Natl Acad Sci U S A*, 111(17), pp. E1806-14.

Apse, M., Aharon, G., Snedden, W. and Blumwald, E. (1999) 'Salt tolerance conferred by overexpression of a vacuolar Na+/H+ antiport in Arabidopsis.', *Science*, 285(5431), pp. 1256-8.

Apse, M., Sottosanto, J. and Blumwald, E. (2003) 'Vacuolar cation/H+ exchange, ion homeostasis, and leaf development are altered in a T-DNA insertional mutant of AtNHX1, the Arabidopsis vacuolar Na+/H+ antiporter.', *Plant J*, 36(2), pp. 229-39.

Arif, A., Zafar, Y., Arif, M. and Blumwald, E. (2013) 'Improved growth, drought tolerance, and ultrastructural evidence of increased turgidity in tobacco plants overexpressing Arabidopsis vacuolar pyrophosphatase (AVP1)', *Mol Biotechnol*, 54(2), pp. 379-92.

Barbier-Brygoo, H., De Angeli, A., Filleur, S., Frachisse, J. M., Gambale, F., Thomine, S. and Wege, S. (2010) 'Anion Channels/Transporters in Plants: From Molecular Bases to Regulatory Networks.', *Annu Rev Plant Biol*.

Barragán, V., Leidi, E. O., Andrés, Z., Rubio, L., De Luca, A., Fernández, J. A., Cubero, B. and Pardo, J. M. (2012) 'Ion exchangers NHX1 and NHX2 mediate active potassium uptake into vacuoles to regulate cell turgor and stomatal function in Arabidopsis', *Plant Cell*, 24(3), pp. 1127-42.

Bassil, E. and Blumwald, E. (2014) 'The ins and outs of intracellular ion homeostasis: NHX-type cation/H(+) transporters', *Curr Opin Plant Biol*, 22, pp. 1-6.

Bassil, E., Coku, A. and Blumwald, E. (2012) 'Cellular ion homeostasis: emerging roles of intracellular NHX Na+/H+ antiporters in plant growth and development', *J Exp Bot*, 63(16), pp. 5727-40.

Bassil, E., Ohto, M. A., Esumi, T., Tajima, H., Zhu, Z., Cagnac, O., Belmonte, M., Peleg, Z., Yamaguchi, T. and Blumwald, E. (2011a) 'The Arabidopsis intracellular Na+/H+ antiporters NHX5 and NHX6 are endosome associated and necessary for plant growth and development', *Plant Cell*, 23(1), pp. 224-39.

Bassil, E., Tajima, H., Liang, Y. C., Ohto, M. A., Ushijima, K., Nakano, R., Esumi, T., Coku, A., Belmonte, M. and Blumwald, E. (2011b) 'The Arabidopsis Na+/H+ antiporters NHX1 and NHX2 control vacuolar pH and K+ homeostasis to regulate growth, flower development, and reproduction', *Plant Cell*, 23(9), pp. 3482-97.

Beilby, M. and Walker, N. (1981) 'Chloride transport in *Chara*: I. Kinetics and current-voltage curves for a probable proton symporter.', *Journal of Experimental Botany*, 32, pp. 43-54.

Bergsdorf, E. Y., Zdebik, A. A. and Jentsch, T. J. (2009) 'Residues important for nitrate/proton coupling in plant and mammalian CLC transporters', *J Biol Chem*, 284(17), pp. 11184-93.

Berüter, J. (2004) 'Carbohydrate metabolism in two apple genotypes that differ in malate accumulation', *J Plant Physiol*, 161(9), pp. 1011-29.

Bethke, P. C., Libourel, I. G., Aoyama, N., Chung, Y. Y., Still, D. W. and Jones, R. L. (2007) 'The Arabidopsis aleurone layer responds to nitric oxide, gibberellin, and abscisic acid and is sufficient and necessary for seed dormancy', *Plant Physiol*, 143(3), pp. 1173-88.

Bhaskaran, S. and Savithramma, D. L. (2011) 'Co-expression of Pennisetum glaucum vacuolar $Na^+/H^+$ antiporter and Arabidopsis $H^+$-pyrophosphatase enhances salt tolerance in transgenic tomato', *J Exp Bot*, 62(15), pp. 5561-70.

Bienert, G. P., Møller, A. L., Kristiansen, K. A., Schulz, A., Møller, I. M., Schjoerring, J. K. and Jahn, T. P. (2007) 'Specific aquaporins facilitate the diffusion of hydrogen peroxide across membranes', *J Biol Chem*, 282(2), pp. 1183-92.

Black, C. C. and Osmond, C. B. (2003) 'Crassulacean acid metabolism photosynthesis: ;working the night shift'', *Photosynth Res*, 76(1-3), pp. 329-41.

Blatt, M. R. (2000) 'Cellular signaling and volume control in stomatal movements in plants', *Annu Rev Cell Dev Biol*, 16, pp. 221-41.

Blatt, M. R., Wang, Y., Leonhardt, N. and Hills, A. (2014) 'Exploring emergent properties in cellular homeostasis using OnGuard to model K+ and other ion transport in guard cells', *J Plant Physiol*, 171(9), pp. 770-8.

Blumwald, E., Aharon, G. and Apse, M. (2000) 'Sodium transport in plant cells.', *Biochim Biophys Acta*, 1465(1-2), pp. 140-51.

Bracha-Drori, K., Shichrur, K., Katz, A., Oliva, M., Angelovici, R., Yalovsky, S. and Ohad, N. (2004) 'Detection of protein-protein interactions in plants using bimolecular fluorescence complementation', *Plant J*, 40(3), pp. 419-27.

Bregante, M., Yang, Y., Formentin, E., Carpaneto, A., Schroeder, J. I., Gambale, F., Lo Schiavo, F. and Costa, A. (2008) 'KDC1, a carrot Shaker-like potassium channel, reveals its role as a silent regulatory subunit when expressed in plant cells', *Plant Mol Biol*, 66(1-2), pp. 61-72.

Briat, J. F., Curie, C. and Gaymard, F. (2007) 'Iron utilization and metabolism in plants', *Curr Opin Plant Biol*, 10(3), pp. 276-82.

Britto, D. T., Ruth, T. J., Lapi, S. and Kronzucker, H. J. (2004) 'Cellular and whole-plant chloride dynamics in barley: insights into chloride-nitrogen interactions and salinity responses', *Planta*, 218(4), pp. 615-22.

Brumós, J., Colmenero-Flores, J. M., Conesa, A., Izquierdo, P., Sánchez, G., Iglesias, D. J., López-Climent, M. F., Gómez-Cadenas, A. and Talón, M. (2009) 'Membrane transporters and carbon metabolism implicated in chloride homeostasis differentiate salt stress responses in tolerant and sensitive Citrus rootstocks', *Funct Integr Genomics*, 9(3), pp. 293-309.

Brumós, J., Talón, M., Bouhlal, R. and Colmenero-Flores, J. M. (2010) 'Cl- homeostasis in includer and excluder citrus rootstocks: transport mechanisms and identification of candidate genes', *Plant Cell Environ*, 33(12), pp. 2012-27.

Brüggemann, L., Dietrich, P., Dreyer, I. and Hedrich, R. (1999) 'Pronounced differences between the native K+ channels and KAT1 and KST1 alpha-subunit homomers of guard cells', *Planta*, 207(3), pp. 370-6.

Brüx, A., Liu, T., Krebs, M., Stierhof, Y., Lohmann, J., Miersch, O., Wasternack, C. and Schumacher, K. (2008) 'Reduced V-ATPase activity in the trans-Golgi network causes oxylipin-dependent hypocotyl growth Inhibition in Arabidopsis.', *Plant Cell*, 20(4), pp. 1088-100.

Carter, C., Pan, S., Zouhar, J., Avila, E. L., Girke, T. and Raikhel, N. V. (2004) 'The vegetative vacuole proteome of Arabidopsis thaliana reveals predicted and unexpected proteins', *Plant Cell*, 16(12), pp. 3285-303.
Cheffings, C. M., Pantoja, O., Ashcroft, F. M. and Smith, J. A. (1997) 'Malate transport and vacuolar ion channels in CAM plants', *J Exp Bot*, 48 Spec No, pp. 623-31.
Chen, Z. H., Hills, A., Bätz, U., Amtmann, A., Lew, V. L. and Blatt, M. R. (2012) 'Systems dynamic modeling of the stomatal guard cell predicts emergent behaviors in transport, signaling, and volume control', *Plant Physiol*, 159(3), pp. 1235-51.
Chopin, F., Orsel, M., Dorbe, M. F., Chardon, F., Truong, H. N., Miller, A. J., Krapp, A. and Daniel-Vedele, F. (2007) 'The Arabidopsis ATNRT2.7 nitrate transporter controls nitrate content in seeds', *Plant Cell*, 19(5), pp. 1590-602.
Clerkx, E. J., El-Lithy, M. E., Vierling, E., Ruys, G. J., Blankestijn-De Vries, H., Groot, S. P., Vreugdenhil, D. and Koornneef, M. (2004) 'Analysis of natural allelic variation of Arabidopsis seed germination and seed longevity traits between the accessions Landsberg erecta and Shakdara, using a new recombinant inbred line population', *Plant Physiol*, 135(1), pp. 432-43.
Clough, S. J. and Bent, A. F. (1998) 'Floral dip: a simplified method for Agrobacterium-mediated transformation of Arabidopsis thaliana', *Plant J*, 16(6), pp. 735-43.
Cobbett, C. and Goldsbrough, P. (2002) 'Phytochelatins and metallothioneins: roles in heavy metal detoxification and homeostasis', *Annu Rev Plant Biol*, 53, pp. 159-82.
Conde, C., Silva, P., Fontes, N., Dias, A. C. P., Tavares, R. M., Sousa, M. J., Agasse, A., Delrot, S. and Gerós, H. (2007) 'Biochemical Changes throughout Grape Berry Development and Fruit and Wine Quality', *Food*, 1, pp. 1-22.
Conn, S. and Gilliham, M. (2010) 'Comparative physiology of elemental distributions in plants', *Ann Bot*, 105(7), pp. 1081-102.
Cookson, S. J., Williams, L. E. and Miller, A. J. (2005) 'Light-dark changes in cytosolic nitrate pools depend on nitrate reductase activity in Arabidopsis leaf cells', *Plant Physiol*, 138(2), pp. 1097-105.
Cosgrove, D. J. (1996) 'Plant cell enlargement and the action of expansins', *Bioessays*, 18(7), pp. 533-40.
Cosgrove, D. J. (1998a) 'Cell wall loosening by expansins', *Plant Physiol*, 118(2), pp. 333-9.
Cosgrove, D. J. (1998b) 'Molecular regulation of plant cell wall extensibility', *Gravit Space Biol Bull*, 11(2), pp. 61-70.
Cosgrove, D. J. (2000) 'Loosening of plant cell walls by expansins', *Nature*, 407(6802), pp. 321-6.
Craig Plett, D. and Møller, I. S. (2010) 'Na(+) transport in glycophytic plants: what we know and would like to know', *Plant Cell Environ*, 33(4), pp. 612-26.
Curie, C., Cassin, G., Couch, D., Divol, F., Higuchi, K., Le Jean, M., Misson, J., Schikora, A., Czernic, P. and Mari, S. (2009) 'Metal movement within the plant: contribution of nicotianamine and yellow stripe 1-like transporters', *Ann Bot*, 103(1), pp. 1-11.
Cushman, J. C. and Bohnert, H. J. (1999) 'CRASSULACEAN ACID METABOLISM: Molecular Genetics', *Annu Rev Plant Physiol Plant Mol Biol*, 50, pp. 305-332.
Dahal, P., Nevins, D. J. and Bradford, K. J. (1997) 'Relationship of Endo-[beta]-D-Mannanase Activity and Cell Wall Hydrolysis in Tomato Endosperm to Germination Rates', *Plant Physiol*, 113(4), pp. 1243-1252.
Daram, P., Urbach, S., Gaymard, F., Sentenac, H. and Chérel, I. (1997) 'Tetramerization of the AKT1 plant potassium channel involves its C-terminal cytoplasmic domain', *EMBO J*, 16(12), pp. 3455-63.
Darwin, C. (1855) 'Effect of salt-water on the germination of seeds', *Gardeners' Chronicle and Agricultural Gazette*, 47, pp. 773.
Daszkowska-Golec, A. (2011) 'Arabidopsis Seed Germination Under Abiotic Stress as a Concert of Action of Phytohormones.', *OMICS*, 15(11), pp. 763-74.
Davenport, R. J. (2002) 'Glutamate receptors in plants', *Annals of Botany*, 90, pp. 549–557.

Davenport, R. J., Muñoz-Mayor, A., Jha, D., Essah, P. A., Rus, A. and Tester, M. (2007) 'The Na+ transporter AtHKT1;1 controls retrieval of Na+ from the xylem in Arabidopsis', *Plant Cell Environ,* 30(4), pp. 497-507.

De Angeli, A., Baetz, U., Francisco, R., Zhang, J., Chaves, M. M. and Regalado, A. (2013a) 'The vacuolar channel VvALMT9 mediates malate and tartrate accumulation in berries of Vitis vinifera', *Planta,* 238(2), pp. 283-91.

De Angeli, A., Monachello, D., Ephritikhine, G., Frachisse, J. M., Thomine, S., Gambale, F. and Barbier-Brygoo, H. (2006) 'The nitrate/proton antiporter AtCLCa mediates nitrate accumulation in plant vacuoles.', *Nature,* 442(7105), pp. 939-42.

De Angeli, A., Zhang, J., Meyer, S. and Martinoia, E. (2013b) 'AtALMT9 is a malate-activated vacuolar chloride channel required for stomatal opening in Arabidopsis', *Nat Commun,* 4, pp. 1804.

De Rybel, B., van den Berg, W., Lokerse, A., Liao, C. Y., van Mourik, H., Möller, B., Peris, C. L. and Weijers, D. (2011) 'A versatile set of ligation-independent cloning vectors for functional studies in plants', *Plant Physiol,* 156(3), pp. 1292-9.

Debeaujon, I. and Koornneef, M. (2000) 'Gibberellin requirement for Arabidopsis seed germination is determined both by testa characteristics and embryonic abscisic acid', *Plant Physiol,* 122(2), pp. 415-24.

Debeaujon, I., Léon-Kloosterziel, K. M. and Koornneef, M. (2000) 'Influence of the testa on seed dormancy, germination, and longevity in Arabidopsis', *Plant Physiol,* 122(2), pp. 403-14.

Dechorgnat, J., Nguyen, C. T., Armengaud, P., Jossier, M., Diatloff, E., Filleur, S. and Daniel-Vedele, F. (2011) 'From the soil to the seeds: the long journey of nitrate in plants', *J Exp Bot,* 62(4), pp. 1349-59.

Delhaize, E., Craig, S., Beaton, C. D., Bennet, R. J., Jagadish, V. C. and Randall, P. J. (1993a) 'Aluminum Tolerance in Wheat (Triticum aestivum L.) (I. Uptake and Distribution of Aluminum in Root Apices)', *Plant Physiol,* 103(3), pp. 685-693.

Delhaize, E., Ryan, P. R. and Randall, P. J. (1993b) 'Aluminum Tolerance in Wheat (Triticum aestivum L.) (II. Aluminum-Stimulated Excretion of Malic Acid from Root Apices)', *Plant Physiol,* 103(3), pp. 695-702.

Demidchik, V. and Maathuis, F. J. (2007) 'Physiological roles of nonselective cation channels in plants: from salt stress to signalling and development', *New Phytol,* 175(3), pp. 387-404.

DeRose-Wilson, L. and Gaut, B. S. (2011) 'Mapping salinity tolerance during Arabidopsis thaliana germination and seedling growth', *PLoS One,* 6(8), pp. e22832.

Dettmer, J., Hong-Hermesdorf, A., Stierhof, Y. and Schumacher, K. (2006) 'Vacuolar H+-ATPase activity is required for endocytic and secretory trafficking in Arabidopsis.', *Plant Cell,* 18(3), pp. 715-30.

Deyholos, M. K. (2010) 'Making the most of drought and salinity transcriptomics', *Plant Cell Environ,* 33(4), pp. 648-54.

Dietz, K., Tavakoli, N., Kluge, C., Mimura, T., Sharma, S., Harris, G., Chardonnens, A. and Golldack, D. (2001) 'Significance of the V-type ATPase for the adaptation to stressful growth conditions and its regulation on the molecular and biochemical level.', *J Exp Bot,* 52(363), pp. 1969-80.

Ding, L. and Zhu, J. K. (1997) 'Reduced Na+ uptake in the NaCl-hypersensitive sos1 mutant of Arabidopsis thaliana', *Plant Physiol,* 113(3), pp. 795-9.

Dong, Q. L., Liu, D. D., An, X. H., Hu, D. G., Yao, Y. X. and Hao, Y. J. (2011) 'MdVHP1 encodes an apple vacuolar H(+)-PPase and enhances stress tolerance in transgenic apple callus and tomato', *J Plant Physiol,* 168(17), pp. 2124-33.

Dreyer, I., Gomez-Porras, J. L., Riaño-Pachón, D. M., Hedrich, R. and Geiger, D. (2012) 'Molecular Evolution of Slow and Quick Anion Channels (SLACs and QUACs/ALMTs)', *Front Plant Sci,* 3, pp. 263.

Duan, X. G., Yang, A. F., Gao, F., Zhang, S. L. and Zhang, J. R. (2007) 'Heterologous expression of vacuolar H(+)-PPase enhances the electrochemical gradient across the vacuolar membrane and improves tobacco cell salt tolerance', *Protoplasma,* 232(1-2), pp. 87-95.

Duby, G., Hosy, E., Fizames, C., Alcon, C., Costa, A., Sentenac, H. and Thibaud, J. B. (2008) 'AtKC1, a conditionally targeted Shaker-type subunit, regulates the activity of plant K+ channels', *Plant J,* 53(1), pp. 115-23.

Dutzler, R., Campbell, E. B., Cadene, M., Chait, B. T. and MacKinnon, R. (2002) 'X-ray structure of a ClC chloride channel at 3.0 A reveals the molecular basis of anion selectivity', *Nature,* 415(6869), pp. 287-94.

Eisenach, C., Baetz, U. and Martinoia, E. (2014) 'Vacuolar Proton Pumping: More than the sum of ist parts?', *Trends in Plant Science*.

Emmerlich, V., Linka, N., Reinhold, T., Hurth, M. A., Traub, M., Martinoia, E. and Neuhaus, H. E. (2003) 'The plant homolog to the human sodium/dicarboxylic cotransporter is the vacuolar malate carrier', *Proc Natl Acad Sci U S A,* 100(19), pp. 11122-6.

Essah, P. A., Davenport, R. and Tester, M. (2003) 'Sodium influx and accumulation in Arabidopsis', *Plant Physiol,* 133(1), pp. 307-18.

Etienne, A., Génard, M., Lobit, P. and Bugaud, C. (2014) 'Modeling the vacuolar storage of malate shed lights on pre- and post-harvest fruit acidity', *BMC Plant Biol,* 14, pp. 310.

Etienne, A., Génard, M., Lobit, P., Mbeguié-A-Mbéguié, D. and Bugaud, C. (2013) 'What controls fleshy fruit acidity? A review of malate and citrate accumulation in fruit cells', *J Exp Bot,* 64(6), pp. 1451-69.

Etxeberria, E., Pozueta-Romero, J. and Gonzalez, P. (2012) 'In and out of the plant storage vacuole', *Plant Sci,* 190, pp. 52-61.

Faraco, M., Spelt, C., Bliek, M., Verweij, W., Hoshino, A., Espen, L., Prinsi, B., Jaarsma, R., Tarhan, E., de Boer, A. H., Di Sansebastiano, G. P., Koes, R. and Quattrocchio, F. M. (2014) 'Hyperacidification of vacuoles by the combined action of two different P-ATPases in the tonoplast determines flower color', *Cell Rep,* 6(1), pp. 32-43.

Felle, H. H. (1994) 'The H+/Cl- Symporter in Root-Hair Cells of Sinapis alba (An Electrophysiological Study Using Ion-Selective Microelectrodes)', *Plant Physiol,* 106(3), pp. 1131-1136.

Fernie, A. R., Carrari, F. and Sweetlove, L. J. (2004) 'Respiratory metabolism: glycolysis, the TCA cycle and mitochondrial electron transport.', *Curr Opin Plant Biol,* 7(3), pp. 254-61.

Fernie, A. R. and Martinoia, E. (2009) 'Malate. Jack of all trades or master of a few?', *Phytochemistry,* 70(7), pp. 828-32.

Fields, S. and Song, O. (1989) 'A novel genetic system to detect protein-protein interactions', *Nature,* 340(6230), pp. 245-6.

Fischer, R. A. (1968) 'Stomatal opening: role of potassium uptake by guard cells', *Science,* 160(3829), pp. 784-5.

Fontecha, G., Silva-Navas, J., Benito, C., Mestres, M. A., Espino, F. J., Hernández-Riquer, M. V. and Gallego, F. J. (2007) 'Candidate gene identification of an aluminum-activated organic acid transporter gene at the Alt4 locus for aluminum tolerance in rye (Secale cereale L.)', *Theor Appl Genet,* 114(2), pp. 249-60.

Frigerio, L., Hinz, G. and Robinson, D. G. (2008) 'Multiple vacuoles in plant cells: rule or exception?', *Traffic,* 9(10), pp. 1564-70.

Frink, C. R., Waggoner, P. E. and Ausubel, J. H. (1999) 'Nitrogen fertilizer: retrospect and prospect', *Proc Natl Acad Sci U S A,* 96(4), pp. 1175-80.

Gadsby, D. C. (2009) 'Ion channels versus ion pumps: the principal difference, in principle', *Nat Rev Mol Cell Biol,* 10(5), pp. 344-52.

Gambale, F. and Uozumi, N. (2006) 'Properties of shaker-type potassium channels in higher plants', *J Membr Biol,* 210(1), pp. 1-19.

Gamboa, M. C., Baltierra, F., Leon, G. and Krauskopf, E. (2013) 'Drought and salt tolerance enhancement of transgenic Arabidopsis by overexpression of the vacuolar pyrophosphatase 1 (EVP1) gene from Eucalyptus globulus', *Plant Physiol Biochem,* 73, pp. 99-105.

Gao, X. Q., Li, C. G., Wei, P. C., Zhang, X. Y., Chen, J. and Wang, X. C. (2005) 'The dynamic changes of tonoplasts in guard cells are important for stomatal movement in Vicia faba', *Plant Physiol,* 139(3), pp. 1207-16.

Gao, X. Q., Wang, X. L., Ren, F., Chen, J. and Wang, X. C. (2009) 'Dynamics of vacuoles and actin filaments in guard cells and their roles in stomatal movement', *Plant Cell Environ,* 32(8), pp. 1108-16.

Gaxiola, R., Li, J., Undurraga, S., Dang, L., Allen, G., Alper, S. and Fink, G. (2001) 'Drought- and salt-tolerant plants result from overexpression of the AVP1 H+-pump.', *Proc Natl Acad Sci U S A,* 98(20), pp. 11444-9.

Gaxiola, R., Palmgren, M. and Schumacher, K. (2007) 'Plant proton pumps.', *FEBS Lett,* 581(12), pp. 2204-14.

Geelen, D., Lurin, C., Bouchez, D., Frachisse, J. M., Lelièvre, F., Courtial, B., Barbier-Brygoo, H. and Maurel, C. (2000) 'Disruption of putative anion channel gene AtCLC-a in Arabidopsis suggests a role in the regulation of nitrate content', *Plant J,* 21(3), pp. 259-67.

Geiger, D., Scherzer, S., Mumm, P., Marten, I., Ache, P., Matschi, S., Liese, A., Wellmann, C., Al-Rasheid, K. A., Grill, E., Romeis, T. and Hedrich, R. (2010) 'Guard cell anion channel SLAC1 is regulated by CDPK protein kinases with distinct Ca2+ affinities', *Proc Natl Acad Sci U S A,* 107(17), pp. 8023-8.

Geiger, D., Scherzer, S., Mumm, P., Stange, A., Marten, I., Bauer, H., Ache, P., Matschi, S., Liese, A., Al-Rasheid, K. A., Romeis, T. and Hedrich, R. (2009) 'Activity of guard cell anion channel SLAC1 is controlled by drought-stress signaling kinase-phosphatase pair.', *Proc Natl Acad Sci U S A,* 106(50), pp. 21425-30.

Geilfus, C. M., Mithöfer, A., Ludwig-Müller, J., Zörb, C. and Muehling, K. H. (2015) 'Chloride-inducible transient apoplastic alkalinizations induce stomata closure by controlling abscisic acid distribution between leaf apoplast and guard cells in salt-stressed Vicia faba', *New Phytol,* 208(3), pp. 803-16.

Gilliham, M. and Tester, M. (2005) 'The regulation of anion loading to the maize root xylem', *Plant Physiol,* 137(3), pp. 819-28.

Gleave, A. P. (1992) 'A versatile binary vector system with a T-DNA organisational structure conducive to efficient integration of cloned DNA into the plant genome.', *Plant Mol Biol,* 20(6), pp. 1203-7.

Gong, H., Blackmore, D., Clingeleffer, P., Sykes, S., Jha, D., Tester, M. and Walker, R. (2011) 'Contrast in chloride exclusion between two grapevine genotypes and its variation in their hybrid progeny', *J Exp Bot,* 62(3), pp. 989-99.

Gorham, J., Hardy, C., Wyn Jones, R. G., Joppa, L. R. and Law, C. N. (1987) 'Chromosomal location of a K/Na discrimination character in the D genome of wheat', *Theor Appl Genet,* 74(5), pp. 584-8.

Gorham, J., Jones, R. G. and Bristol, A. (1990) 'Partial characterization of the trait for enhanced K(+)-Na (+) discrimination in the D genome of wheat', *Planta,* 180(4), pp. 590-7.

Gosti, F., Beaudoin, N., Serizet, C., Webb, A. A., Vartanian, N. and Giraudat, J. (1999) 'ABI1 protein phosphatase 2C is a negative regulator of abscisic acid signaling', *Plant Cell,* 11(10), pp. 1897-910.

Gouaux, E. and Mackinnon, R. (2005) 'Principles of selective ion transport in channels and pumps', *Science,* 310(5753), pp. 1461-5.

Grefen, C. and Blatt, M. R. (2012) 'A 2in1 cloning system enables ratiometric bimolecular fluorescence complementation (rBiFC)', *Biotechniques,* 53(5), pp. 311-14.

Guo, F. Q., Young, J. and Crawford, N. M. (2003) 'The nitrate transporter AtNRT1.1 (CHL1) functions in stomatal opening and contributes to drought susceptibility in Arabidopsis', *Plant Cell,* 15(1), pp. 107-17.

Hall, D., Evans, A. R., Newbury, H. J. and Pritchard, J. (2006) 'Functional analysis of CHX21: a putative sodium transporter in Arabidopsis', *J Exp Bot,* 57(5), pp. 1201-10.

Hamaji, K., Nagira, M., Yoshida, K., Ohnishi, M., Oda, Y., Uemura, T., Goh, T., Sato, M. H., Morita, M. T., Tasaka, M., Hasezawa, S., Nakano, A., Hara-Nishimura, I., Maeshima, M., Fukaki, H. and Mimura, T. (2009) 'Dynamic aspects of ion accumulation by vesicle traffic under salt stress in Arabidopsis', *Plant Cell Physiol,* 50(12), pp. 2023-33.

Haro, R., Bañuelos, M. A., Senn, M. E., Barrero-Gil, J. and Rodríguez-Navarro, A. (2005) 'HKT1 mediates sodium uniport in roots. Pitfalls in the expression of HKT1 in yeast', *Plant Physiol,* 139(3), pp. 1495-506.

Hedrich, R., Kurkdjian, A., Guern, J. and Flügge, U. I. (1989) 'Comparative studies on the electrical properties of the H+ translocating ATPase and pyrophosphatase of the vacuolar-lysosomal compartment', *EMBO J,* 8(10), pp. 2835-41.

Hedrich, R. and Marten, I. (1993) 'Malate-induced feedback regulation of plasma membrane anion channels could provide a CO2 sensor to guard cells', *EMBO J,* 12(3), pp. 897-901.

Henderson, S. W., Baumann, U., Blackmore, D. H., Walker, A. R., Walker, R. R. and Gilliham, M. (2014) 'Shoot chloride exclusion and salt tolerance in grapevine is associated with differential ion transporter expression in roots', *BMC Plant Biol,* 14, pp. 273.

Henderson, S. W., Wege, S., Qiu, J., Blackmore, D. H., Walker, A. R., Tyerman, S. D., Walker, R. R. and Gilliham, M. (2015) 'Grapevine and Arabidopsis Cation-Chloride Cotransporters Localize to the Golgi and Trans-Golgi Network and Indirectly Influence Long-Distance Ion Transport and Plant Salt Tolerance', *Plant Physiol,* 169(3), pp. 2215-29.

Hetherington, A. and Woodward, F. (2003) 'The role of stomata in sensing and driving environmental change.', *Nature,* 424(6951), pp. 901-8.

Hetherington, A. M. (2001) 'Guard cell signaling', *Cell,* 107(6), pp. 711-4.

Hoekenga, O. A., Maron, L. G., Piñeros, M. A., Cançado, G. M., Shaff, J., Kobayashi, Y., Ryan, P. R., Dong, B., Delhaize, E., Sasaki, T., Matsumoto, H., Yamamoto, Y., Koyama, H. and Kochian, L. V. (2006) 'AtALMT1, which encodes a malate transporter, is identified as one of several genes critical for aluminum tolerance in Arabidopsis.', *Proc Natl Acad Sci U S A,* 103(25), pp. 9738-43.

Hosy, E., Vavasseur, A., Mouline, K., Dreyer, I., Gaymard, F., Porée, F., Boucherez, J., Lebaudy, A., Bouchez, D., Very, A. A., Simonneau, T., Thibaud, J. B. and Sentenac, H. (2003) 'The Arabidopsis outward K+ channel GORK is involved in regulation of stomatal movements and plant transpiration', *Proc Natl Acad Sci U S A,* 100(9), pp. 5549-54.

Hu, C. D., Chinenov, Y. and Kerppola, T. K. (2002) 'Visualization of interactions among bZIP and Rel family proteins in living cells using bimolecular fluorescence complementation', *Mol Cell,* 9(4), pp. 789-98.

Huang, C. X. and Van Steveninck, R. F. (1989) 'Maintenance of low cl concentrations in mesophyll cells of leaf blades of barley seedlings exposed to salt stress', *Plant Physiol,* 90(4), pp. 1440-3.

Hurth, M. A., Suh, S. J., Kretzschmar, T., Geis, T., Bregante, M., Gambale, F., Martinoia, E. and Neuhaus, H. E. (2005) 'Impaired pH homeostasis in Arabidopsis lacking the vacuolar dicarboxylate transporter and analysis of carboxylic acid transport across the tonoplast', *Plant Physiol,* 137(3), pp. 901-10.

Imes, D., Mumm, P., Böhm, J., Al-Rasheid, K. A., Marten, I., Geiger, D. and Hedrich, R. (2013) 'Open stomata 1 (OST1) kinase controls R-type anion channel QUAC1 in Arabidopsis guard cells', *Plant J*, 74(3), pp. 372-82.

Isacoff, E. Y., Jan, Y. N. and Jan, L. Y. (1990) 'Evidence for the formation of heteromultimeric potassium channels in Xenopus oocytes', *Nature*, 345(6275), pp. 530-4.

Isayenkov, S., Isner, J. C. and Maathuis, F. J. (2010) 'Vacuolar ion channels: Roles in plant nutrition and signalling', *FEBS Lett*, 584(10), pp. 1982-8.

Ivashikina, N., Deeken, R., Fischer, S., Ache, P. and Hedrich, R. (2005) 'AKT2/3 subunits render guard cell K+ channels Ca2+ sensitive', *J Gen Physiol*, 125(5), pp. 483-92.

Jacoby, B. and Hanson, J. B. (1985) 'Controls on na influx in corn roots', *Plant Physiol*, 77(4), pp. 930-4.

James, R. A., Munns, R., von Caemmerer, S., Trejo, C., Miller, C. and Condon, T. A. (2006) 'Photosynthetic capacity is related to the cellular and subcellular partitioning of Na+, K+ and Cl- in salt-affected barley and durum wheat', *Plant Cell Environ*, 29(12), pp. 2185-97.

Jaquinod, M., Villiers, F., Kieffer-Jaquinod, S., Hugouvieux, V., Bruley, C., Garin, J. and Bourguignon, J. (2007) 'A proteomics dissection of Arabidopsis thaliana vacuoles isolated from cell culture', *Mol Cell Proteomics*, 6(3), pp. 394-412.

Jentsch, T. J. (2008) 'CLC chloride channels and transporters: from genes to protein structure, pathology and physiology', *Crit Rev Biochem Mol Biol*, 43(1), pp. 3-36.

Jentsch, T. J., Steinmeyer, K. and Schwarz, G. (1990) 'Primary structure of Torpedo marmorata chloride channel isolated by expression cloning in Xenopus oocytes', *Nature*, 348(6301), pp. 510-4.

Jha, D., Shirley, N., Tester, M. and Roy, S. J. (2010) 'Variation in salinity tolerance and shoot sodium accumulation in Arabidopsis ecotypes linked to differences in the natural expression levels of transporters involved in sodium transport', *Plant Cell Environ*, 33(5), pp. 793-804.

Jiang, X., Leidi, E. O. and Pardo, J. M. (2010) 'How do vacuolar NHX exchangers function in plant salt tolerance?', *Plant Signal Behav*, 5(7), pp. 792-5.

Johanson, U., Karlsson, M., Johansson, I., Gustavsson, S., Sjövall, S., Fraysse, L., Weig, A. R. and Kjellbom, P. (2001) 'The complete set of genes encoding major intrinsic proteins in Arabidopsis provides a framework for a new nomenclature for major intrinsic proteins in plants', *Plant Physiol*, 126(4), pp. 1358-69.

Johnson, K. D., Höfte, H. and Chrispeels, M. J. (1990) 'An intrinsic tonoplast protein of protein storage vacuoles in seeds is structurally related to a bacterial solute transporter (GIpF)', *Plant Cell*, 2(6), pp. 525-32.

Johnsson, N. and Varshavsky, A. (1994) 'Split ubiquitin as a sensor of protein interactions in vivo', *Proc Natl Acad Sci U S A*, 91(22), pp. 10340-4.

Joosen, R. V., Kodde, J., Willems, L. A., Ligterink, W., van der Plas, L. H. and Hilhorst, H. W. (2010) 'GERMINATOR: a software package for high-throughput scoring and curve fitting of Arabidopsis seed germination', *Plant J*, 62(1), pp. 148-59.

Joshi-Saha, A., Valon, C. and Leung, J. (2011) 'A brand new START: abscisic acid perception and transduction in the guard cell', *Sci Signal*, 4(201), pp. re4.

Jossier, M., Kroniewicz, L., Dalmas, F., Le Thiec, D., Ephritikhine, G., Thomine, S., Barbier-Brygoo, H., Vavasseur, A., Filleur, S. and Leonhardt, N. (2010) 'The Arabidopsis vacuolar anion transporter, AtCLCc, is involved in the regulation of stomatal movements and contributes to salt tolerance.', *Plant J*, 64(4), pp. 563-76.

Kaldenhoff, R. and Fischer, M. (2006) 'Functional aquaporin diversity in plants', *Biochim Biophys Acta*, 1758(8), pp. 1134-41.

Kaplan, B., Sherman, T. and Fromm, H. (2007) 'Cyclic nucleotide-gated channels in plants', *FEBS Lett*, 581(12), pp. 2237-46.

Karley, A. J., Leigh, R. A. and Sanders, D. (2000) 'Differential ion accumulation and ion fluxes in the mesophyll and epidermis of barley', *Plant Physiol,* 122(3), pp. 835-44.

Kataoka, T., Watanabe-Takahashi, A., Hayashi, N., Ohnishi, M., Mimura, T., Buchner, P., Hawkesford, M. J., Yamaya, T. and Takahashi, H. (2004) 'Vacuolar sulfate transporters are essential determinants controlling internal distribution of sulfate in Arabidopsis', *Plant Cell,* 16(10), pp. 2693-704.

Kawasaki-Nishi, S., Bowers, K., Nishi, T., Forgac, M. and Stevens, T. (2001) 'The amino-terminal domain of the vacuolar proton-translocating ATPase a subunit controls targeting and in vivo dissociation, and the carboxyl-terminal domain affects coupling of proton transport and ATP hydrolysis.', *J Biol Chem,* 276(50), pp. 47411-20.

Kerppola, T. K. (2006) 'Design and implementation of bimolecular fluorescence complementation (BiFC) assays for the visualization of protein interactions in living cells', *Nat Protoc,* 1(3), pp. 1278-86.

Kim, T. H., Böhmer, M., Hu, H., Nishimura, N. and Schroeder, J. I. (2010) 'Guard cell signal transduction network: advances in understanding abscisic acid, CO2, and Ca2+ signaling', *Annu Rev Plant Biol,* 61, pp. 561-91.

Klink, R., Haschke, H., Kramer, D. and Luttge, U. (1990) 'Membrane-particles, proteins and atpase activity of tonoplast vesicles of Mesembryanthemum-Crystallinum in the C-3 and CAM state', *Botanica Acta*, pp. 24-31.

Kluge, C., Lahr, J., Hanitzsch, M., Bolte, S., Golldack, D. and Dietz, K. (2003) 'New insight into the structure and regulation of the plant vacuolar H+-ATPase.', *J Bioenerg Biomembr,* 35(4), pp. 377-88.

Kobayashi, Y., Hoekenga, O. A., Itoh, H., Nakashima, M., Saito, S., Shaff, J. E., Maron, L. G., Piñeros, M. A., Kochian, L. V. and Koyama, H. (2007) 'Characterization of AtALMT1 expression in aluminum-inducible malate release and its role for rhizotoxic stress tolerance in Arabidopsis', *Plant Physiol,* 145(3), pp. 843-52.

Kovermann, P., Meyer, S., Hörtensteiner, S., Picco, C., Scholz-Starke, J., Ravera, S., Lee, Y. and Martinoia, E. (2007) 'The Arabidopsis vacuolar malate channel is a member of the ALMT family', *Plant J,* 52(6), pp. 1169-80.

Krebs, M., Beyhl, D., Görlich, E., Al-Rasheid, K., Marten, I., Stierhof, Y., Hedrich, R. and Schumacher, K. (2010) 'Arabidopsis V-ATPase activity at the tonoplast is required for efficient nutrient storage but not for sodium accumulation.', *Proc Natl Acad Sci U S A,* 107(7), pp. 3251-6.

Kriegel, A., Andrés, Z., Medzihradszky, A., Krüger, F., Scholl, S., Delang, S., Patir-Nebioglu, M. G., Gute, G., Yang, H., Murphy, A. S., Peer, W. A., Pfeiffer, A., Krebs, M., Lohmann, J. U. and Schumacher, K. (2015) 'Job Sharing in the Endomembrane System: Vacuolar Acidification Requires the Combined Activity of V-ATPase and V-PPase', *Plant Cell*.

Kronzucker, H. J. and Britto, D. T. (2011) 'Sodium transport in plants: a critical review', *New Phytol,* 189(1), pp. 54-81.

Kudla, J., Batistic, O. and Hashimoto, K. (2010) 'Calcium signals: the lead currency of plant information processing', *Plant Cell,* 22(3), pp. 541-63.

Kumar, T., Uzma, Khan, M. R., Abbas, Z. and Ali, G. M. (2014) 'Genetic improvement of sugarcane for drought and salinity stress tolerance using Arabidopsis vacuolar pyrophosphatase (AVP1) gene', *Mol Biotechnol,* 56(3), pp. 199-209.

Köhler, B. and Raschke, K. (2000) 'The delivery of salts to the xylem. Three types of anion conductance in the plasmalemma of the xylem parenchyma of roots of barley', *Plant Physiol,* 122(1), pp. 243-54.

Laurie, S., Feeney, K. A., Maathuis, F. J., Heard, P. J., Brown, S. J. and Leigh, R. A. (2002) 'A role for HKT1 in sodium uptake by wheat roots', *Plant J,* 32(2), pp. 139-49.

Lebaudy, A., Hosy, E., Simonneau, T., Sentenac, H., Thibaud, J. B. and Dreyer, I. (2008) 'Heteromeric K+ channels in plants.', *Plant J,* 54(6), pp. 1076-82.

Lebaudy, A., Pascaud, F., Véry, A. A., Alcon, C., Dreyer, I., Thibaud, J. B. and Lacombe, B. (2010) 'Preferential KAT1-KAT2 heteromerization determines inward K+ current properties in Arabidopsis guard cells', *J Biol Chem*, 285(9), pp. 6265-74.

Lee, S. C., Lan, W., Buchanan, B. B. and Luan, S. (2009) 'A protein kinase-phosphatase pair interacts with an ion channel to regulate ABA signaling in plant guard cells', *Proc Natl Acad Sci U S A*, 106(50), pp. 21419-24.

Leidi, E. O., Barragán, V., Rubio, L., El-Hamdaoui, A., Ruiz, M. T., Cubero, B., Fernández, J. A., Bressan, R. A., Hasegawa, P. M., Quintero, F. J. and Pardo, J. M. (2010) 'The AtNHX1 exchanger mediates potassium compartmentation in vacuoles of transgenic tomato', *Plant J*, 61(3), pp. 495-506.

Lemtiri-Chlieh, F., MacRobbie, E. A. and Brearley, C. A. (2000) 'Inositol hexakisphosphate is a physiological signal regulating the K+-inward rectifying conductance in guard cells', *Proc Natl Acad Sci U S A*, 97(15), pp. 8687-92.

Lemtiri-Chlieh, F., MacRobbie, E. A., Webb, A. A., Manison, N. F., Brownlee, C., Skepper, J. N., Chen, J., Prestwich, G. D. and Brearley, C. A. (2003) 'Inositol hexakisphosphate mobilizes an endomembrane store of calcium in guard cells', *Proc Natl Acad Sci U S A*, 100(17), pp. 10091-5.

Leshem, Y., Melamed-Book, N., Cagnac, O., Ronen, G., Nishri, Y., Solomon, M., Cohen, G. and Levine, A. (2006) 'Suppression of Arabidopsis vesicle-SNARE expression inhibited fusion of H2O2-containing vesicles with tonoplast and increased salt tolerance', *Proc Natl Acad Sci U S A*, 103(47), pp. 18008-13.

Li, B., Byrt, C. S., Qiu, J., Baumann, U., Hrmova, M., Evrard, A., Johnson, A. A., Birnbaum, K. D., Mayo, G. M., Jha, D., Henderson, S. W., Tester, M., Gilliham, M. and Roy, S. J. (2015) 'Identification of a stelar-localised transport protein that facilitates root-to-shoot transfer of chloride in Arabidopsis', *Plant Physiol*.

Li, X., Guo, C., Gu, J., Duan, W., Zhao, M., Ma, C., Du, X., Lu, W. and Xiao, K. (2014) 'Overexpression of VP, a vacuolar H+-pyrophosphatase gene in wheat (Triticum aestivum L.), improves tobacco plant growth under Pi and N deprivation, high salinity, and drought', *J Exp Bot*, 65(2), pp. 683-96.

Li, Z., Baldwin, C. M., Hu, Q., Liu, H. and Luo, H. (2010) 'Heterologous expression of Arabidopsis H+-pyrophosphatase enhances salt tolerance in transgenic creeping bentgrass (Agrostis stolonifera L.)', *Plant Cell Environ*, 33(2), pp. 272-89.

Ligaba, A., Katsuhara, M., Ryan, P. R., Shibasaka, M. and Matsumoto, H. (2006) 'The BnALMT1 and BnALMT2 genes from rape encode aluminum-activated malate transporters that enhance the aluminum resistance of plant cells', *Plant Physiol*, 142(3), pp. 1294-303.

Lin, W., Peng, Y., Li, G., Arora, R., Tang, Z., Su, W. and Cai, W. (2007) 'Isolation and functional characterization of PgTIP1, a hormone-autotrophic cells-specific tonoplast aquaporin in ginseng', *J Exp Bot*, 58(5), pp. 947-56.

Liu, L., Wang, Y., Wang, N., Dong, Y. Y., Fan, X. D., Liu, X. M., Yang, J. and Li, H. Y. (2011) 'Cloning of a vacuolar H(+)-pyrophosphatase gene from the halophyte Suaeda corniculata whose heterologous overexpression improves salt, saline-alkali and drought tolerance in Arabidopsis', *J Integr Plant Biol*, 53(9), pp. 731-42.

Lobit, P., Genard, M., Soing, P. and Habib, R. (2006) 'Modelling malic acid accumulation in fruits: relationships with organic acids, potassium, and temperature', *J Exp Bot*, 57(6), pp. 1471-83.

Lorenzen, I., Aberle, T. and Plieth, C. (2004) 'Salt stress-induced chloride flux: a study using transgenic Arabidopsis expressing a fluorescent anion probe', *Plant J*, 38(3), pp. 539-44.

Ludewig, U., Wilken, S., Wu, B., Jost, W., Obrdlik, P., El Bakkoury, M., Marini, A. M., André, B., Hamacher, T., Boles, E., von Wirén, N. and Frommer, W. B. (2003) 'Homo- and hetero-oligomerization of ammonium transporter-1 NH4 uniporters', *J Biol Chem*, 278(46), pp. 45603-10.

Luo, Q., Yu, B. and Liu, Y. (2005) 'Differential sensitivity to chloride and sodium ions in seedlings of Glycine max and G. soja under NaCl stress', *J Plant Physiol*, 162(9), pp. 1003-12.

Lv, Q. D., Tang, R. J., Liu, H., Gao, X. S., Li, Y. Z., Zheng, H. Q. and Zhang, H. X. (2009) 'Cloning and molecular analyses of the *Arabidopsis thaliana c*hloride channel gene family', *Plant Sci*, 176, pp. 650-661.

Läuchli, A., James, R. A., Huang, C. X., McCully, M. and Munns, R. (2008) 'Cell-specific localization of Na+ in roots of durum wheat and possible control points for salt exclusion', *Plant Cell Environ*, 31(11), pp. 1565-74.

Léran, S., Varala, K., Boyer, J. C., Chiurazzi, M., Crawford, N., Daniel-Vedele, F., David, L., Dickstein, R., Fernandez, E., Forde, B., Gassmann, W., Geiger, D., Gojon, A., Gong, J. M., Halkier, B. A., Harris, J. M., Hedrich, R., Limami, A. M., Rentsch, D., Seo, M., Tsay, Y. F., Zhang, M., Coruzzi, G. and Lacombe, B. (2014) 'A unified nomenclature of NITRATE TRANSPORTER 1/PEPTIDE TRANSPORTER family members in plants', *Trends Plant Sci*, 19(1), pp. 5-9.

MacKinnon, R. (1991) 'Determination of the subunit stoichiometry of a voltage-activated potassium channel', *Nature*, 350(6315), pp. 232-5.

MacRobbie, E. A. (1998) 'Signal transduction and ion channels in guard cells', *Philos Trans R Soc Lond B Biol Sci*, 353(1374), pp. 1475-88.

Maeshima, M. (1992) 'Characterization of the major integral protein of vacuolar membrane', *Plant Physiol*, 98(4), pp. 1248-54.

Maeshima, M. (2000) 'Vacuolar H(+)-pyrophosphatase', *Biochim Biophys Acta*, 1465(1-2), pp. 37-51.

Maeshima, M. (2001) 'TONOPLAST TRANSPORTERS: Organization and Function', *Annu Rev Plant Physiol Plant Mol Biol*, 52, pp. 469-497.

Markovich, D. and Murer, H. (2004) 'The SLC13 gene family of sodium sulphate/carboxylate cotransporters', *Pflugers Arch*, 447(5), pp. 594-602.

Marmagne, A., Vinauger-Douard, M., Monachello, D., de Longevialle, A. F., Charon, C., Allot, M., Rappaport, F., Wollman, F. A., Barbier-Brygoo, H. and Ephritikhine, G. (2007) 'Two members of the Arabidopsis CLC (chloride channel) family, AtCLCe and AtCLCf, are associated with thylakoid and Golgi membranes, respectively', *J Exp Bot*, 58(12), pp. 3385-93.

Martinoia, E., Maeshima, M. and Neuhaus, H. E. (2007) 'Vacuolar transporters and their essential role in plant metabolism', *J Exp Bot*, 58(1), pp. 83-102.

Martinoia, E., Massonneau, A. and Frangne, N. (2000) 'Transport processes of solutes across the vacuolar membrane of higher plants', *Plant Cell Physiol*, 41(11), pp. 1175-86.

Martinoia, E., Meyer, S., De Angeli, A. and Nagy, R. (2012) 'Vacuolar transporters in their physiological context', *Annu Rev Plant Biol*, 63, pp. 183-213.

Martinoia, E. and Rentsch, D. (1994) 'Malate compartmentation—responses to a complex metabolism.', *Annu. Rev. Plant Physiol. Plant Mol. Biol.*, 45, pp. 447-67.

Mason, M. G., Jha, D., Salt, D. E., Tester, M., Hill, K., Kieber, J. J. and Schaller, G. E. (2010) 'Type-B response regulators ARR1 and ARR12 regulate expression of AtHKT1;1 and accumulation of sodium in Arabidopsis shoots', *Plant J*, 64(5), pp. 753-63.

Massonneau, A., Martinoia, E., Dietz, K. J. and Mimura, T. (2000) 'Phosphate uptake across the tonoplast of intact vacuoles isolated from suspension-cultured cells of Catharanthus roseus (L.) G. Don', *Planta*, 211(3), pp. 390-5.

Matile, P. (1987) 'The sap of plant cells', *New Phytologist*, 105, pp. 1-26.

Maurel, C. (1997) 'AQUAPORINS AND WATER PERMEABILITY OF PLANT MEMBRANES', *Annu Rev Plant Physiol Plant Mol Biol*, 48, pp. 399-429.

Maurel, C., Chrispeels, M., Lurin, C., Tacnet, F., Geelen, D., Ripoche, P. and Guern, J. (1997) 'Function and regulation of seed aquaporins', *J Exp Bot*, 48 Spec No, pp. 421-30.

Maurel, C., Kado, R. T., Guern, J. and Chrispeels, M. J. (1995) 'Phosphorylation regulates the water channel activity of the seed-specific aquaporin alpha-TIP', *EMBO J*, 14(13), pp. 3028-35.
Maurel, C., Santoni, V., Luu, D. T., Wudick, M. M. and Verdoucq, L. (2009) 'The cellular dynamics of plant aquaporin expression and functions', *Curr Opin Plant Biol*, 12(6), pp. 690-8.
Mazel, A., Leshem, Y., Tiwari, B. S. and Levine, A. (2004) 'Induction of salt and osmotic stress tolerance by overexpression of an intracellular vesicle trafficking protein AtRab7 (AtRabG3e)', *Plant Physiol*, 134(1), pp. 118-28.
Mendoza-Cózatl, D. G., Jobe, T. O., Hauser, F. and Schroeder, J. I. (2011) 'Long-distance transport, vacuolar sequestration, tolerance, and transcriptional responses induced by cadmium and arsenic', *Curr Opin Plant Biol*, 14(5), pp. 554-62.
Merlot, S., Gosti, F., Guerrier, D., Vavasseur, A. and Giraudat, J. (2001) 'The ABI1 and ABI2 protein phosphatases 2C act in a negative feedback regulatory loop of the abscisic acid signalling pathway', *Plant J*, 25(3), pp. 295-303.
Meyer, S., De Angeli, A., Fernie, A. R. and Martinoia, E. (2010a) 'Intra- and extra-cellular excretion of carboxylates.', *Trends Plant Sci*, 15(1), pp. 40-7.
Meyer, S., Mumm, P., Imes, D., Endler, A., Weder, B., Al-Rasheid, K. A., Geiger, D., Marten, I., Martinoia, E. and Hedrich, R. (2010b) 'AtALMT12 represents an R-type anion channel required for stomatal movement in Arabidopsis guard cells.', *Plant J*, 63(6), pp. 1054-62.
Meyer, S., Scholz-Starke, J., De Angeli, A., Kovermann, P., Burla, B., Gambale, F. and Martinoia, E. (2011) 'Malate transport by the vacuolar AtALMT6 channel in guard cells is subject to multiple regulation.', *Plant J*.
Miller, A. J. and Zhen, R. G. (1991) 'Measurement of intracellular nitrate concentrations in Chara using nitrate-selective microelectrodes', *Planta*, 184(1), pp. 47-52.
Miyawaki, A., Griesbeck, O., Heim, R. and Tsien, R. Y. (1999) 'Dynamic and quantitative Ca2+ measurements using improved cameleons', *Proc Natl Acad Sci U S A*, 96(5), pp. 2135-40.
Miyawaki, A., Llopis, J., Heim, R., McCaffery, J. M., Adams, J. A., Ikura, M. and Tsien, R. Y. (1997) 'Fluorescent indicators for Ca2+ based on green fluorescent proteins and calmodulin', *Nature*, 388(6645), pp. 882-7.
Monachello, D., Allot, M., Oliva, S., Krapp, A., Daniel-Vedele, F., Barbier-Brygoo, H. and Ephritikhine, G. (2009) 'Two anion transporters AtClCa and AtClCe fulfil interconnecting but not redundant roles in nitrate assimilation pathways', *New Phytol*, 183(1), pp. 88-94.
Motoda, H., Sasaki, T., Kano, Y., Ryan, P. R., Delhaize, E., Matsumoto, H. and Yamamoto, Y. (2007) 'The Membrane Topology of ALMT1, an Aluminum-Activated Malate Transport Protein in Wheat (Triticum aestivum).', *Plant Signal Behav*, 2(6), pp. 467-72.
Moya, J. L., Gómez-Cadenas, A., Primo-Millo, E. and Talon, M. (2003) 'Chloride absorption in salt-sensitive Carrizo citrange and salt-tolerant Cleopatra mandarin citrus rootstocks is linked to water use', *J Exp Bot*, 54(383), pp. 825-33.
Munemasa, S., Hauser, F., Park, J., Waadt, R., Brandt, B. and Schroeder, J. I. (2015) 'Mechanisms of abscisic acid-mediated control of stomatal aperture', *Curr Opin Plant Biol*, 28, pp. 154-62.
Munns, R. (2002) 'Comparative physiology of salt and water stress', *Plant Cell Environ*, 25(2), pp. 239-250.
Munns, R. and Tester, M. (2008) 'Mechanisms of salinity tolerance', *Annu Rev Plant Biol*, 59, pp. 651-81.
Mäser, P., Eckelman, B., Vaidyanathan, R., Horie, T., Fairbairn, D., Kubo, M., Yamagami, M., Yamaguchi, K., Nishimura, M., Uozumi, N., Robertson, W., Sussman, M. and Schroeder, J. (2002) 'Altered shoot/root Na+ distribution and bifurcating salt

sensitivity in Arabidopsis by genetic disruption of the Na+ transporter AtHKT1.', *FEBS Lett*, 531(2), pp. 157-61.
Møller, I. and Tester, M. (2007) 'Salinity tolerance of Arabidopsis: a good model for cereals?', *Trends Plant Sci*, 12(12), pp. 534-40.
Møller, I. S., Gilliham, M., Jha, D., Mayo, G. M., Roy, S. J., Coates, J. C., Haseloff, J. and Tester, M. (2009) 'Shoot Na+ exclusion and increased salinity tolerance engineered by cell type-specific alteration of Na+ transport in Arabidopsis', *Plant Cell*, 21(7), pp. 2163-78.
Müller, K., Tintelnot, S. and Leubner-Metzger, G. (2006) 'Endosperm-limited Brassicaceae seed germination: abscisic acid inhibits embryo-induced endosperm weakening of Lepidium sativum (cress) and endosperm rupture of cress and Arabidopsis thaliana', *Plant Cell Physiol*, 47(7), pp. 864-77.
Müller, M., Irkens-Kiesecker, U., Rubinstein, B. and Taiz, L. (1996) 'On the mechanism of hyperacidification in lemon. Comparison of the vacuolar H(+)-ATPase activities of fruits and epicotyls', *J Biol Chem*, 271(4), pp. 1916-24.
Neher, E. (1992) 'Correction for liquid junction potentials in patch clamp experiments', *Methods Enzymol*, 207, pp. 123-31.
Neuhaus, H. E. and Trentmann, O. (2014) 'Regulation of transport processes across the tonoplast', *Front Plant Sci*, 5, pp. 460.
Nguyen, C. T., Agorio, A., Jossier, M., Depré, S., Thomine, S. and Filleur, S. (2015) 'Characterization of the Chloride Channel-like, AtCLCg, involved in Chloride Tolerance in Arabidopsis thaliana', *Plant Cell Physiol*.
Nilson, S. E. and Assmann, S. M. (2007) 'The control of transpiration. Insights from Arabidopsis', *Plant Physiol*, 143(1), pp. 19-27.
Nishi, T. and Forgac, M. (2002) 'The vacuolar (H+)-ATPases--nature's most versatile proton pumps.', *Nat Rev Mol Cell Biol*, 3(2), pp. 94-103.
Obrdlik, P., El-Bakkoury, M., Hamacher, T., Cappellaro, C., Vilarino, C., Fleischer, C., Ellerbrok, H., Kamuzinzi, R., Ledent, V., Blaudez, D., Sanders, D., Revuelta, J. L., Boles, E., André, B. and Frommer, W. B. (2004) 'K+ channel interactions detected by a genetic system optimized for systematic studies of membrane protein interactions', *Proc Natl Acad Sci U S A*, 101(33), pp. 12242-7.
Obroucheva, N. and Antipova, O. (1997) 'Physiology of the initiation of seed germination.', *Russian Journal of Plant Physiology*, 44, pp. 250-64.
Orsini, F., D'Urzo, M. P., Inan, G., Serra, S., Oh, D. H., Mickelbart, M. V., Consiglio, F., Li, X., Jeong, J. C., Yun, D. J., Bohnert, H. J., Bressan, R. A. and Maggio, A. (2010) 'A comparative study of salt tolerance parameters in 11 wild relatives of Arabidopsis thaliana', *J Exp Bot*, 61(13), pp. 3787-98.
Pardo, J., Cubero, B., Leidi, E. and Quintero, F. (2006) 'Alkali cation exchangers: roles in cellular homeostasis and stress tolerance.', *J Exp Bot*, 57(5), pp. 1181-99.
Paris, N., Stanley, C. M., Jones, R. L. and Rogers, J. C. (1996) 'Plant cells contain two functionally distinct vacuolar compartments', *Cell*, 85(4), pp. 563-72.
Pasapula, V., Shen, G., Kuppu, S., Paez-Valencia, J., Mendoza, M., Hou, P., Chen, J., Qiu, X., Zhu, L., Zhang, X., Auld, D., Blumwald, E., Zhang, H., Gaxiola, R. and Payton, P. (2011) 'Expression of an Arabidopsis vacuolar H+-pyrophosphatase gene (AVP1) in cotton improves drought- and salt tolerance and increases fibre yield in the field conditions', *Plant Biotechnol J*, 9(1), pp. 88-99.
Peiter, E. (2011) 'The plant vacuole: emitter and receiver of calcium signals', *Cell Calcium*, 50(2), pp. 120-8.
Peng, J. S. and Gong, J. M. (2014) 'Vacuolar sequestration capacity and long-distance metal transport in plants', *Front Plant Sci*, 5, pp. 19.
Pfaffl, M. W. (2001) 'A new mathematical model for relative quantification in real-time RT-PCR', *Nucleic Acids Res*, 29(9), pp. e45.

Pickard, W. (2003) 'The role of cytoplasmic streaming in symplastic transport', *Plant, Cell & Environment*, 26, pp. 1-15.

Picollo, A. and Pusch, M. (2005) 'Chloride/proton antiporter activity of mammalian CLC proteins ClC-4 and ClC-5', *Nature*, 436(7049), pp. 420-3.

Pitman, M. G. (1982) 'Transport across plant roots', *Q Rev Biophys*, 15(3), pp. 481-554.

Piñeros, M. A., Cançado, G. M. and Kochian, L. V. (2008a) 'Novel properties of the wheat aluminum tolerance organic acid transporter (TaALMT1) revealed by electrophysiological characterization in Xenopus Oocytes: functional and structural implications.', *Plant Physiol*, 147(4), pp. 2131-46.

Piñeros, M. A., Cançado, G. M., Maron, L. G., Lyi, S. M., Menossi, M. and Kochian, L. V. (2008b) 'Not all ALMT1-type transporters mediate aluminum-activated organic acid responses: the case of ZmALMT1 - an anion-selective transporter', *Plant J*, 53(2), pp. 352-67.

Poffenroth, M., Green, D. B. and Tallman, G. (1992) 'Sugar Concentrations in Guard Cells of Vicia faba Illuminated with Red or Blue Light : Analysis by High Performance Liquid Chromatography', *Plant Physiol*, 98(4), pp. 1460-71.

Pottosin, I. I. and Schönknecht, G. (2007) 'Vacuolar calcium channels', *J Exp Bot*, 58(7), pp. 1559-69.

Preston, J., Tatematsu, K., Kanno, Y., Hobo, T., Kimura, M., Jikumaru, Y., Yano, R., Kamiya, Y. and Nambara, E. (2009) 'Temporal expression patterns of hormone metabolism genes during imbibition of Arabidopsis thaliana seeds: a comparative study on dormant and non-dormant accessions', *Plant Cell Physiol*, 50(10), pp. 1786-800.

Qiu, Q., Guo, Y., Dietrich, M., Schumaker, K. and Zhu, J. (2002) 'Regulation of SOS1, a plasma membrane Na+/H+ exchanger in Arabidopsis thaliana, by SOS2 and SOS3', *Proceedings of the National Academy of Sciences of the United States of America*, pp. 8436-8441.

Quesada, V., García-Martínez, S., Piqueras, P., Ponce, M. R. and Micol, J. L. (2002) 'Genetic architecture of NaCl tolerance in Arabidopsis', *Plant Physiol*, 130(2), pp. 951-63.

Raman, H., Zhang, K., Cakir, M., Appels, R., Garvin, D. F., Maron, L. G., Kochian, L. V., Moroni, J. S., Raman, R., Imtiaz, M., Drake-Brockman, F., Waters, I., Martin, P., Sasaki, T., Yamamoto, Y., Matsumoto, H., Hebb, D. M., Delhaize, E. and Ryan, P. R. (2005) 'Molecular characterization and mapping of ALMT1, the aluminium-tolerance gene of bread wheat (Triticum aestivum L.)', *Genome*, 48(5), pp. 781-91.

Reguera, M., Bassil, E., Tajima, H., Wimmer, M., Chanoca, A., Otegui, M. S., Paris, N. and Blumwald, E. (2015) 'pH Regulation by NHX-Type Antiporters Is Required for Receptor-Mediated Protein Trafficking to the Vacuole in Arabidopsis', *Plant Cell*, 27(4), pp. 1200-17.

Reinders, A., Schulze, W., Kühn, C., Barker, L., Schulz, A., Ward, J. M. and Frommer, W. B. (2002) 'Protein-protein interactions between sucrose transporters of different affinities colocalized in the same enucleate sieve element', *Plant Cell*, 14(7), pp. 1567-77.

Reintanz, B., Szyroki, A., Ivashikina, N., Ache, P., Godde, M., Becker, D., Palme, K. and Hedrich, R. (2002) 'AtKC1, a silent Arabidopsis potassium channel alpha -subunit modulates root hair K+ influx', *Proc Natl Acad Sci U S A*, 99(6), pp. 4079-84.

Reisen, D., Leborgne-Castel, N., Ozalp, C., Chaumont, F. and Marty, F. (2003) 'Expression of a cauliflower tonoplast aquaporin tagged with GFP in tobacco suspension cells correlates with an increase in cell size', *Plant Mol Biol*, 52(2), pp. 387-400.

Rengasamy, P. (2006) 'World salinization with emphasis on Australia.', *J Exp Bot*, 57(5), pp. 1017-23.

Robert, C., Noriega, A., Tocino, A. and Cervantes, E. (2008) 'Morphological analysis of seed shape in Arabidopsis thaliana reveals altered polarity in mutants of the ethylene signaling pathway', *J Plant Physiol*, 165(9), pp. 911-9.

Rodriguez-Rosales, M. P., Jiang, X., Gálvez, F. J., Aranda, M. N., Cubero, B. and Venema, K. (2008) 'Overexpression of the tomato K+/H+ antiporter LeNHX2 confers salt tolerance by improving potassium compartmentalization', *New Phytol,* 179(2), pp. 366-77.

Roelfsema, M. R. and Hedrich, R. (2005) 'In the light of stomatal opening: new insights into 'the Watergate'', *New Phytol,* 167(3), pp. 665-91.

Rudrappa, T., Czymmek, K. J., Paré, P. W. and Bais, H. P. (2008) 'Root-secreted malic acid recruits beneficial soil bacteria', *Plant Physiol,* 148(3), pp. 1547-56.

Rus, A., Baxter, I., Muthukumar, B., Gustin, J., Lahner, B., Yakubova, E. and Salt, D. E. (2006) 'Natural variants of AtHKT1 enhance Na+ accumulation in two wild populations of Arabidopsis', *PLoS Genet,* 2(12), pp. e210.

Ryan, P. R., Skerrett, M., Findlay, G. P., Delhaize, E. and Tyerman, S. D. (1997) 'Aluminum activates an anion channel in the apical cells of wheat roots', *Proc Natl Acad Sci U S A,* 94(12), pp. 6547-52.

Sanders, D., Pelloux, J., Brownlee, C. and Harper, J. F. (2002) 'Calcium at the crossroads of signaling', *Plant Cell,* 14 Suppl, pp. S401-17.

Sasaki, T., Mori, I. C., Furuichi, T., Munemasa, S., Toyooka, K., Matsuoka, K., Murata, Y. and Yamamoto, Y. (2010) 'Closing plant stomata requires a homolog of an aluminum-activated malate transporter', *Plant Cell Physiol,* 51(3), pp. 354-65.

Sasaki, T., Yamamoto, Y., Ezaki, B., Katsuhara, M., Ahn, S. J., Ryan, P. R., Delhaize, E. and Matsumoto, H. (2004) 'A wheat gene encoding an aluminum-activated malate transporter.', *Plant J,* 37(5), pp. 645-53.

Schauer, N., Semel, Y., Roessner, U., Gur, A., Balbo, I., Carrari, F., Pleban, T., Perez-Melis, A., Bruedigam, C., Kopka, J., Willmitzer, L., Zamir, D. and Fernie, A. R. (2006) 'Comprehensive metabolic profiling and phenotyping of interspecific introgression lines for tomato improvement', *Nat Biotechnol,* 24(4), pp. 447-54.

Schilling, R. K., Marschner, P., Shavrukov, Y., Berger, B., Tester, M., Roy, S. J. and Plett, D. C. (2014) 'Expression of the Arabidopsis vacuolar $H^+$-pyrophosphatase gene (AVP1) improves the shoot biomass of transgenic barley and increases grain yield in a saline field', *Plant Biotechnol J,* 12(3), pp. 378-86.

Schnabl, H. and Raschke, K. (1980) 'Potassium Chloride as Stomatal Osmoticum in Allium cepa L., a Species Devoid of Starch in Guard Cells', *Plant Physiol,* 65(1), pp. 88-93.

Schroeder, J. I. and Keller, B. U. (1992) 'Two types of anion channel currents in guard cells with distinct voltage regulation', *Proc Natl Acad Sci U S A,* 89(11), pp. 5025-9.

Schulze, W. X., Reinders, A., Ward, J., Lalonde, S. and Frommer, W. B. (2003) 'Interactions between co-expressed Arabidopsis sucrose transporters in the split-ubiquitin system', *BMC Biochem,* 4, pp. 3.

Schumacher, K. and Krebs, M. (2010) 'The V-ATPase: small cargo, large effects', *Curr Opin Plant Biol,* 13(6), pp. 724-30.

Schumaker, K. S. and Sze, H. (1986) 'Calcium transport into the vacuole of oat roots. Characterization of H+/Ca2+ exchange activity', *J Biol Chem,* 261(26), pp. 12172-8.

Schuurmans, J. A., van Dongen, J. T., Rutjens, B. P., Boonman, A., Pieterse, C. M. and Borstlap, A. C. (2003) 'Members of the aquaporin family in the developing pea seed coat include representatives of the PIP, TIP, and NIP subfamilies', *Plant Mol Biol,* 53(5), pp. 633-45.

Serrano, R. (1996) 'Salt tolerance in plants and microorganisms: toxicity targets and defense responses.', *Int Rev Cytol,* 165, pp. 1-52.

Shapira, O., Khadka, S., Israeli, Y., Shani, U. and Schwartz, A. (2009) 'Functional anatomy controls ion distribution in banana leaves: significance of Na+ seclusion at the leaf margins', *Plant Cell Environ,* 32(5), pp. 476-85.

Shi, H., Ishitani, M., Kim, C. and Zhu, J. (2000) 'The Arabidopsis thaliana salt tolerance gene SOS1 encodes a putative Na+/H+ antiporter.', *Proc Natl Acad Sci U S A,* 97(12), pp. 6896-901.

Shi, H., Lee, B., Wu, S. and Zhu, J. (2003) 'Overexpression of a plasma membrane Na+/H+ antiporter gene improves salt tolerance in Arabidopsis thaliana.', *Nat Biotechnol,* 21(1), pp. 81-5.

Shi, H., Quintero, F. J., Pardo, J. M. and Zhu, J. K. (2002) 'The putative plasma membrane Na(+)/H(+) antiporter SOS1 controls long-distance Na(+) transport in plants', *Plant Cell,* 14(2), pp. 465-77.

Shigaki, T. and Hirschi, K. (2000) 'Characterization of CAX-like genes in plants: implications for functional diversity', *Gene,* 257(2), pp. 291-8.

Shimaoka, T., Ohnishi, M., Sazuka, T., Mitsuhashi, N., Hara-Nishimura, I., Shimazaki, K., Maeshima, M., Yokota, A., Tomizawa, K. and Mimura, T. (2004) 'Isolation of intact vacuoles and proteomic analysis of tonoplast from suspension-cultured cells of Arabidopsis thaliana', *Plant Cell Physiol,* 45(6), pp. 672-83.

Shimazaki, K., Doi, M., Assmann, S. M. and Kinoshita, T. (2007) 'Light regulation of stomatal movement', *Annu Rev Plant Biol,* 58, pp. 219-47.

Shkolnik-Inbar, D., Adler, G. and Bar-Zvi, D. (2013) 'ABI4 downregulates expression of the sodium transporter HKT1;1 in Arabidopsis roots and affects salt tolerance', *Plant J,* 73(6), pp. 993-1005.

Skerrett, M. and Tyerman, S. (1994) 'A channel that allows inwardly directed fluxes of anions in protoplasts derived from wheat roots.', *Planta,* 192, pp. 295-305.

Stevens, T. and Forgac, M. (1997) 'Structure, function and regulation of the vacuolar (H+)-ATPase.', *Annu Rev Cell Dev Biol,* 13, pp. 779-808.

Storey, R., Schachtmann, D. and Thomas, M. (2003) 'Root structure and cellular chloride, sodium and potassium distribution in salinized grapevines', *Plant Cell Environ,* 26(6), pp. 789-800.

Sun, J., Chen, S., Dai, S., Wang, R., Li, N., Shen, X., Zhou, X., Lu, C., Zheng, X., Hu, Z., Zhang, Z., Song, J. and Xu, Y. (2009) 'NaCl-induced alternations of cellular and tissue ion fluxes in roots of salt-resistant and salt-sensitive poplar species', *Plant Physiol,* 149(2), pp. 1141-53.

Sunarpi, Horie, T., Motoda, J., Kubo, M., Yang, H., Yoda, K., Horie, R., Chan, W. Y., Leung, H. Y., Hattori, K., Konomi, M., Osumi, M., Yamagami, M., Schroeder, J. I. and Uozumi, N. (2005) 'Enhanced salt tolerance mediated by AtHKT1 transporter-induced Na unloading from xylem vessels to xylem parenchyma cells', *Plant J,* 44(6), pp. 928-38.

Sze, H., Li, X. and Palmgren, M. (1999) 'Energization of plant cell membranes by H+-pumping ATPases. Regulation and biosynthesis', *Plant Cell,* 11(4), pp. 677-90.

Sze, H., Schumacher, K., Müller, M., Padmanaban, S. and Taiz, L. (2002) 'A simple nomenclature for a complex proton pump: VHA genes encode the vacuolar H(+)-ATPase.', *Trends Plant Sci,* 7(4), pp. 157-61.

Sánchez, R. A., Sunell, L., Labavitch, J. M. and Bonner, B. A. (1990) 'Changes in the Endosperm Cell Walls of Two Datura Species before Radicle Protrusion', *Plant Physiol,* 93(1), pp. 89-97.

Talbott, L. D. and Zeiger, E. (1996) 'Central Roles for Potassium and Sucrose in Guard-Cell Osmoregulation', *Plant Physiol,* 111(4), pp. 1051-1057.

Tanaka, Y., Kutsuna, N., Kanazawa, Y., Kondo, N., Hasezawa, S. and Sano, T. (2007) 'Intra-vacuolar reserves of membranes during stomatal closure: the possible role of guard cell vacuoles estimated by 3-D reconstruction', *Plant Cell Physiol,* 48(8), pp. 1159-69.

Tavakkoli, E., Fatehi, F., Coventry, S., Rengasamy, P. and McDonald, G. K. (2011) 'Additive effects of Na+ and Cl- ions on barley growth under salinity stress', *J Exp Bot,* 62(6), pp. 2189-203.

Tavakkoli, E., Rengasamy, P. and McDonald, G. K. (2010) 'High concentrations of Na+ and Cl- ions in soil solution have simultaneous detrimental effects on growth of faba bean under salinity stress', *J Exp Bot,* 61(15), pp. 4449-59.

Teakle, N., Flowers, T., Real, D. and Colmer, T. (2007) 'Lotus tenuis tolerates the interactive effects of salinity and waterlogging by 'excluding' Na+ and Cl- from the xylem', *J Exp Bot*, 58(8), pp. 2169-80.

Teakle, N. L. and Tyerman, S. D. (2010) 'Mechanisms of Cl(-) transport contributing to salt tolerance', *Plant Cell Environ*, 33(4), pp. 566-89.

Terrier, N., Sauvage, F. X., Ageorges, A. and Romieu, C. (2001) 'Changes in acidity and in proton transport at the tonoplast of grape berries during development', *Planta*, 213(1), pp. 20-8.

Tester, M. and Davenport, R. (2003) 'Na+ tolerance and Na+ transport in higher plants.', *Ann Bot*, 91(5), pp. 503-27.

Tsay, Y. F., Chiu, C. C., Tsai, C. B., Ho, C. H. and Hsu, P. K. (2007) 'Nitrate transporters and peptide transporters', *FEBS Lett*, 581(12), pp. 2290-300.

Uemura, T., Sato, M. H. and Takeyasu, K. (2005) 'The longin domain regulates subcellular targeting of VAMP7 in Arabidopsis thaliana', *FEBS Lett*, 579(13), pp. 2842-6.

Vallejo, A. J., Yanovsky, M. J. and Botto, J. F. (2010) 'Germination variation in Arabidopsis thaliana accessions under moderate osmotic and salt stresses', *Ann Bot*, 106(5), pp. 833-42.

Vander Willigen, C., Postaire, O., Tournaire-Roux, C., Boursiac, Y. and Maurel, C. (2006) 'Expression and inhibition of aquaporins in germinating Arabidopsis seeds', *Plant Cell Physiol*, 47(9), pp. 1241-50.

Verweij, W., Spelt, C., Di Sansebastiano, G. P., Vermeer, J., Reale, L., Ferranti, F., Koes, R. and Quattrocchio, F. (2008) 'An H+ P-ATPase on the tonoplast determines vacuolar pH and flower colour', *Nat Cell Biol*, 10(12), pp. 1456-62.

von der Fecht-Bartenbach, J., Bogner, M., Dynowski, M. and Ludewig, U. (2010) 'CLC-b-mediated NO-3/H+ exchange across the tonoplast of Arabidopsis vacuoles.', *Plant Cell Physiol*, 51(6), pp. 960-8.

von der Fecht-Bartenbach, J., Bogner, M., Krebs, M., Stierhof, Y. D., Schumacher, K. and Ludewig, U. (2007) 'Function of the anion transporter AtCLC-d in the trans-Golgi network', *Plant J*, 50(3), pp. 466-74.

Waadt, R. and Kudla, J. (2008) 'In Planta Visualization of Protein Interactions Using Bimolecular Fluorescence Complementation (BiFC)', *CSH Protoc*, 2008, pp. pdb.prot4995.

Waadt, R., Schmidt, L. K., Lohse, M., Hashimoto, K., Bock, R. and Kudla, J. (2008) 'Multicolor bimolecular fluorescence complementation reveals simultaneous formation of alternative CBL/CIPK complexes in planta', *Plant J*, 56(3), pp. 505-16.

Walker, D. J., Leigh, R. A. and Miller, A. J. (1996) 'Potassium homeostasis in vacuolate plant cells', *Proc Natl Acad Sci U S A*, 93(19), pp. 10510-4.

Walter, M., Chaban, C., Schütze, K., Batistic, O., Weckermann, K., Näke, C., Blazevic, D., Grefen, C., Schumacher, K., Oecking, C., Harter, K. and Kudla, J. (2004) 'Visualization of protein interactions in living plant cells using bimolecular fluorescence complementation', *Plant J*, 40(3), pp. 428-38.

Wang, Y., Hills, A. and Blatt, M. R. (2014) 'Systems analysis of guard cell membrane transport for enhanced stomatal dynamics and water use efficiency', *Plant Physiol*, 164(4), pp. 1593-9.

Wege, S., De Angeli, A., Droillard, M. J., Kroniewicz, L., Merlot, S., Cornu, D., Gambale, F., Martinoia, E., Barbier-Brygoo, H., Thomine, S., Leonhardt, N. and Filleur, S. (2014) 'Phosphorylation of the vacuolar anion exchanger AtCLCa is required for the stomatal response to abscisic acid', *Sci Signal*, 7(333), pp. ra65.

Wege, S., Jossier, M., Filleur, S., Thomine, S., Barbier-Brygoo, H., Gambale, F. and De Angeli, A. (2010) 'The proline 160 in the selectivity filter of the Arabidopsis NO(3)(-)/H(+) exchanger AtCLCa is essential for nitrate accumulation in planta', *Plant J*, 63(5), pp. 861-9.

Weig, A., Deswarte, C. and Chrispeels, M. J. (1997) 'The major intrinsic protein family of Arabidopsis has 23 members that form three distinct groups with functional aquaporins in each group', *Plant Physiol,* 114(4), pp. 1347-57.

Weitbrecht, K., Müller, K. and Leubner-Metzger, G. (2011) 'First off the mark: early seed germination', *J Exp Bot,* 62(10), pp. 3289-309.

White, M. M. and Miller, C. (1979) 'A voltage-gated anion channel from the electric organ of Torpedo californica', *J Biol Chem,* 254(20), pp. 10161-6.

White, P. J. and Broadley, M. R. (2001) 'Chloride in Soils and ist Uptake and Movement within the Plant: A Review', *Annals of Botany,* 88, pp. 967-988.

Williams, L. E., Pittman, J. K. and Hall, J. L. (2000) 'Emerging mechanisms for heavy metal transport in plants', *Biochim Biophys Acta,* 1465(1-2), pp. 104-26.

Wintz, H., Fox, T., Wu, Y. Y., Feng, V., Chen, W., Chang, H. S., Zhu, T. and Vulpe, C. (2003) 'Expression profiles of Arabidopsis thaliana in mineral deficiencies reveal novel transporters involved in metal homeostasis', *J Biol Chem,* 278(48), pp. 47644-53.

Woodstock, L. (1988) 'Seed imbibition: a critical period for for successful Germination.', *Journal of Seed Technology,* 12, pp. 1-15.

Wu, G. Q., Feng, R. J., Wang, S. M., Wang, C. M., Bao, A. K., Wei, L. and Yuan, H. J. (2015) 'Co-expression of xerophyte Zygophyllum xanthoxylum ZxNHX and ZxVP1-1 confers enhanced salinity tolerance in chimeric sugar beet (Beta vulgaris L.)', *Front Plant Sci,* 6, pp. 581.

Wu, S. J., Ding, L. and Zhu, J. K. (1996) 'SOS1, a Genetic Locus Essential for Salt Tolerance and Potassium Acquisition', *Plant Cell,* 8(4), pp. 617-627.

Xicluna, J., Lacombe, B., Dreyer, I., Alcon, C., Jeanguenin, L., Sentenac, H., Thibaud, J. B. and Chérel, I. (2007) 'Increased functional diversity of plant K+ channels by preferential heteromerization of the shaker-like subunits AKT2 and KAT2', *J Biol Chem,* 282(1), pp. 486-94.

Xu, G., Magen, H., Tarchitzky, J. and Kafkafi, U. (1999) 'Advances in Chloride Nutrition of Plants', *68*, pp. 97–110.

Xuan, Y. H., Hu, Y. B., Chen, L. Q., Sosso, D., Ducat, D. C., Hou, B. H. and Frommer, W. B. (2013) 'Functional role of oligomerization for bacterial and plant SWEET sugar transporter family', *Proc Natl Acad Sci U S A,* 110(39), pp. E3685-94.

Yamaguchi, M., Sasaki, T., Sivaguru, M., Yamamoto, Y., Osawa, H., Ahn, S. J. and Matsumoto, H. (2005) 'Evidence for the plasma membrane localization of Al-activated malate transporter (ALMT1)', *Plant Cell Physiol,* 46(5), pp. 812-6.

Yan, A., Wu, M., Yan, L., Hu, R., Ali, I. and Gan, Y. (2014) 'AtEXP2 is involved in seed germination and abiotic stress response in Arabidopsis', *PLoS One,* 9(1), pp. e85208.

Yang, K. Y., Liu, Y. and Zhang, S. (2001) 'Activation of a mitogen-activated protein kinase pathway is involved in disease resistance in tobacco', *Proc Natl Acad Sci U S A,* 98(2), pp. 741-6.

Yao, M., Zeng, Y., Liu, L., Huang, Y., Zhao, E. and Zhang, F. (2012) 'Overexpression of the halophyte Kalidium foliatum $H^+$-pyrophosphatase gene confers salt and drought tolerance in Arabidopsis thaliana', *Mol Biol Rep,* 39(8), pp. 7989-96.

Yokoi, S., Quintero, F. J., Cubero, B., Ruiz, M. T., Bressan, R. A., Hasegawa, P. M. and Pardo, J. M. (2002) 'Differential expression and function of Arabidopsis thaliana NHX Na+/H+ antiporters in the salt stress response', *Plant J,* 30(5), pp. 529-39.

Yoo, S. D., Cho, Y. H. and Sheen, J. (2007) 'Arabidopsis mesophyll protoplasts: a versatile cell system for transient gene expression analysis', *Nat Protoc,* 2(7), pp. 1565-72.

Yue, Y., Zhang, M., Zhang, J., Duan, L. and Li, Z. (2012) 'SOS1 gene overexpression increased salt tolerance in transgenic tobacco by maintaining a higher K(+)/Na(+) ratio', *J Plant Physiol,* 169(3), pp. 255-61.

Zhang, H., Shen, G., Kuppu, S., Gaxiola, R. and Payton, P. (2011) 'Creating drought- and salt-tolerant cotton by overexpressing a vacuolar pyrophosphatase gene', *Plant Signal Behav,* 6(6), pp. 861-3.

Zhang, J., Baetz, U., Krügel, U., Martinoia, E. and De Angeli, A. (2013) 'Identification of a probable pore-forming domain in the multimeric vacuolar anion channel AtALMT9', *Plant Physiol,* 163(2), pp. 830-43.

Zhang, J., Martinoia, E. and De Angeli, A. (2014) 'Cytosolic nucleotides block and regulate the Arabidopsis vacuolar anion channel AtALMT9', *J Biol Chem,* 289(37), pp. 25581-9.

Zifarelli, G. and Pusch, M. (2010) 'CLC transport proteins in plants', *FEBS Lett,* 584(10), pp. 2122-7.

# 10. Acknowledgment

I look back on almost 4 years I have spent at the Botanic Garden in Zurich as a PhD student. I look back on days, nights, weekends, and holidays in the lab. I look back on happy times, days which were full of excitement and motivation, and certainly also days with setbacks and frustration. During this period I learned a fundamental lesson in life: One has to fight for goals, but hard work pays out!

A big thanks goes to Prof. Enrico Martinoia, Prof. Beat Keller and Prof. Karin Schumacher who belong to my Thesis Committee, and to Dr. Alexis De Angeli and Dr. Cornelia Eisenach who are part of my Examiner Committee. In addition, I would like to thank Prof. Eduardo Blumwald for reading and evaluating this thesis.

A few people accompanied my entire journey, and contributed majorly to the outcome. First of all I would like to thank Enrico for having me in his lab, in the beginning as a Master student and afterwards as a PhD student. Thanks a lot for always having an open door and for all your scientific support as well as your support with any other question or problem I had. I enjoyed the freedom and trust you provided me in daily lab life. And I highly appreciate that you always made clear that there are other important things in life than just science and work!

Alexis, thanks a lot (tremendously) for your constant help and guidance during the past 5 years, for introducing me to the world of patch-clamping and electrophysiology, for keeping me calm and relaxed, for chatting with me for hours and hours, and for giving me this unique nick name ‘URKE’! With your personality and attitude you were always a good example that one does not need to be tense and stressed in research. You influenced my ‘German-ness’ very positively. Thank you for that!

Connie, I’m very happy that we ended up again in the same lab. It’s a luxury situation that I can call my supervisor also my friend! Thanks for spending many many hours with me in the lab, performing experiments with me, designing experiments with me, and enjoying all the ups and cushioning all the downs a PhD student can have. You took over a lot of work, and you always did that as a matter of course: you corrected whatever I wrote, performed short-notice experiments, took over the Studis, to just

name a few. I'm extremely grateful for that, you made my PhD so much easier and better! And, who knows, maybe we meet again in the next job… I would be glad!

Various students were implicated in the research presented in this thesis. Special thanks goes to Kirsten Arens and Marina Maglovski. Both supported me in several experiments, and I was every day happy about and astonished by their accuracy and reliability when performing experimental work.

Many other people contributed to my PhD with their daily support. Unfortunately, here is no space to list everybody, but in particular I'd like to thank Chris, Reto, Kathrin, Dani, Kari and Sascha for their great input and commitment.

Luckily, doing a PhD is not just about science and hard work, but also about finding friends who share sorrows, concerns, but mostly laughs and excitement with you. In particular Daniel and Arianna were these special people for me in the lab! Moreover, I'd like to thank everybody from P1-24, not just the current members, but also former members such as Dr. JZ and Miyoung for bringing so much joy to work. In general, I'm very happy about this friendly and positive atmosphere in P1!

Abschliessend möchte ich gerne noch den wichtigsten Menschen in meinem Leben danken. Zum einen meiner Familie: Man kann gar nicht in Worte fassen wie glücklich ich bin, dass ihr mich all die Jahre in jeder Lebenslage unterstützt habt. Ich ziehe täglich Kraft aus dem Wissen, dass ihr immer für mich da seid. Vielen Dank dafür! Zum anderen Basti: Danke, dass du mir jeden Tag ein Lächeln auf die Lippen zauberst. Egal, wohin uns das Leben verschlagen wird und was die Reise bringen mag, mit dir an meiner Seite werde ich immer glücklich sein!

| | |
|---|---|
| Name | ULRIKE BÄTZ |
| Date/ Place of birth: | 24th September, 1987, in Halle/S. (Germany) |
| Email: | ulrike.baetz@gmx.de |


## EDUCATION

| | |
|---|---|
| June 2012 – March 2016 | **PhD in Science & Policy**<br>*University of Zurich* |
| Sep. 2011 – April 2012 | **Visiting Research Scholar**<br>*University of California, Berkeley/*<br>*United States Department of Agriculture,*<br>*Plant Gene Expression Center* |
| Sep. 2010 – April 2012 | **Master of Science in Biology (Plant Biology) with Distinction**<br>*ETH Zurich* |
| Sep. 2009 – Sep. 2010 | **ERASMUS Exchange Student**<br>Plant Science and Research Project<br>*University of Glasgow* |
| Oct. 2007 – June 2010 | **Bachelor of Science in Biology**<br>*University of Heidelberg* |

## RESEARCH

| | |
|---|---|
| May 2012 – March 2016 | **PhD Thesis**<br>'Structure and Physiological Function of the Vacuolar Anion Channel ALMT9 in *Arabidopsis thaliana* and *Vitis Vinifera;*<br>Supervisor: Prof. Enrico Martinoia, *University of Zurich,* and Dr. Alexis De Angeli, *Institut de Biologie Intégrative de la Cellule, Gif-Sur-Yvette* |
| Sep. 2011 – April 2012 | **Master Thesis**<br>'Identification of transcriptional activation domains in PIF3';<br>Supervisor: Prof. Wilhelm Gruissem, *ETH Zurich*;<br>in collaboration with: Prof. Peter Quail, *University of California, Berkeley/ United States Department of Agriculture, Plant Gene Expression Center* |
| Sep. 2009 – Sep. 2010 | **Bachelor Thesis**<br>'Comparative analysis of the vacuolar $H^+$-ATPase between *Arabidopsis thaliana* and the halophyte *Thellungiella halophila*';<br>Supervisor: Prof. Karin Schumacher, *University of Heidelberg;*<br>in collaboration with: Dr. Anna Amtmann, *University of Glasgow* |

## AWARDS AND SCHOLARSHIPS

| | |
|---|---|
| May 2014 | Travel and Registration Fee Scholarship EMBO/FEBS Lecture Course 'Channels and Transporters', Erice, Italy |
| July 2013- April 2014 | Grant 'Forschungskredit Candoc' University of Zurich; Project: 'Molecular and Structural Analysis of the Vacuolar ALMT Anion Channels in *Arabidopsis thaliana'* |
| Sep. 2010 – April 2012 | Master of Science in Biology at ETH with Distinction |
| Sep. 2009 – Aug. 2010 | Scholarship of the ERASMUS Exchange Service |

## INVITED TALKS

| | |
|---|---|
| August 2015 | Invited Speaker at SYNGENTA Symposium, Stein, Switzerland |
| August 2015 | Talk at 'Institute of Plant and Microbial Biology (University of Zurich) Retreat', Switzerland |
| October 2014 | Invited Keynote Speaker, Top Science International BASF Symposium, Limburgerhof, Germany |

## PUBLICATIONS

U. Baetz, 'Root exudates as integral part of belowground plant defense.' Book Chapter in 'Belowground defense strategies in plants', Springer Series 'Signaling and communication in plants'; under edition.

U. Baetz, C. Eisenach, E. Martinoia, A. De Angeli, 'Vacuolar Chloride Fluxes Impact Whole-Plant Ion Accumulation and Distribution during Early Salinity in Arabidopsis.' Will be submitted to *Plant Physiol*.

C. Eisenach, U. Baetz, E. Martinoia, 'Vacuolar proton pumping: more than the sum of its parts?' *Trends in Plant Science* 19(6), 344-346 (2014).

U. Baetz*, E. Martinoia, 'Root exudates: the hidden part of plant defense.' *Trends in Plant Science* 19, 90-98 (2014); *corresponding author.

J. Zhang*, U. Baetz*, U. Krügel, E. Martinoia, A. De Angeli, 'Identification of a probable pore-forming domain in the multimeric vacuolar anion channel AtALMT9.' *Plant Physiol* 163, 830-843 (2013); *co-first author.

A. De Angeli*, U. Baetz*, R. Francisco, J. Zhang, M. M. Chaves, A. Regalado, 'The vacuolar channel VvALMT9 mediates malate and tartrate accumulation in berries of Vitis vinifera.' *Planta* 238, 283-291 (2013); *co-first author.

Z. H. Chen, A. Hills, U. Bätz, A. Amtmann, V. L. Lew, M. R. Blatt, 'Systems dynamic modeling of the stomatal guard cell predicts emergent behaviors in transport, signaling, and volume control.' *Plant Physiol* 159, 1235-1251 (2012).